FRAGILE X MENTAL RETARDATION PROTEIN INDUCES SYNAPSE LOSS THROUGH ACUTE POSTSYNAPTIC TRANSLATIONAL REGULATION AND GENETIC INTERACTIONS WITH MEF2

APPROVED BY SUPERVISORY COMMITTEE

Kimberly Huber, Ph.D. (Supervisor)

Dean Smith, M.D., Ph.D.

Ilya Bezprozvanny, Ph.D.

Ege Kavalali, Ph.D.

Kristen Lych, Ph.D.

DEDICATION

I would like to thank the members of my Graduate Committee, Dr. Kimberly Huber, and all present and past members of the Huber lab for their friendship and technical assistance. Dr. Huber is an outstanding mentor who has been fundamental in my personal growth as a scientist. I would also like to thank my entire family, especially my wonderful and loving parents who have always supported me in my pursuits. Finally, I would like to thank Lenora Volk for her kindness, patience, and love.

FRAGILE X MENTAL RETARDATION PROTEIN INDUCES SYNAPSE LOSS THROUGH ACUTE POSTSYNAPTIC TRANSLATIONAL REGULATION AND GENETIC INTERACTIONS WITH MEF2

by

BRAD ERICH PFEIFFER

DISSERTATION

Presented to the Faculty of the Graduate School of Biomedical Sciences

The University of Texas Southwestern Medical Center at Dallas

In Partial Fulfillment of the Requirements

For the Degree of

DOCTOR OF PHILOSOPHY

The University of Texas Southwestern Medical Center at Dallas

Dallas, Texas

September, 2008

FRAGILE X MENTAL RETARDATION PROTEIN INDUCES SYNAPSE LOSS THROUGH ACUTE POSTSYNAPTIC TRANSLATIONAL REGULATION AND GENETIC INTERACTIONS WITH MEF2

Brad Erich Pfeiffer, Ph.D.

The University of Texas Southwestern Medical Center at Dallas, 2008

Kimberly M. Huber, Ph.D.

Fragile X Syndrome (FXS) is the most common form of inherited mental retardation. The root cause of FXS is loss of the function of a single protein: the Fragile X Mental Retardation Protein (FMRP). FMRP is an RNA-binding protein that plays a complex role in translational regulation. FMRP may be an important regulator of dendritic protein synthesis, which occurs at or near synapses in response to synaptic activity. Many types of long-term synaptic change require local protein synthesis for their induction and/or maintenance, and several protein synthesis-dependent forms of synaptic plasticity are altered in the absence of FMRP. Both human FXS patients and mice lacking FMRP (*Fmr1*-KO mice) display increased numbers of dendritic spines, the primary sites of excitatory synaptic connections. In addition to increased numbers, the spines of FXS patients and *Fmr1*-KO mice appear morphologically immature. It was unknown whether FMRP plays a direct, cell-autonomous role in the regulation of synapse

number or function. Moreover, the mechanisms through which FMRP might govern neuronal function or number were unclear.

I report that acute postsynaptic expression of FMRP in *Fmr1*-KO neurons results in a decrease in the number of functional and structural synapses without an effect on their synaptic strength or maturational state. Similarly, wild-type neurons endogenously expressing FMRP have fewer synapses than neighboring *Fmr1*-KO neurons, indicating a clear role for FMRP in the regulation of synapse number. An intact K homology 2 (KH2) RNA-binding domain and dephosphorylation of FMRP at S500 are required for the effects of FMRP on synapse number, indicating that FMRP-dependent translation of mRNA targets of FMRP leads to synapse loss. Furthermore, I demonstrate novel phenotypic interactions of FMRP with the transcription factor MEF2. MEF2 activity in wild-type neurons induces robust synapse loss; however, MEF2 fails to decrease synapse number in *Fmr1*-KO neurons. A dominant-negative form of MEF2 increases synapse number in WT, but not *Fmr1*-KO neurons. Finally, when co-expressed with a dominant negative form of MEF2, FMRP fails to induce synapse loss in *Fmr1*-KO neurons. These data represent novel mechanisms through which FMRP regulates neuronal function and suggest novel therapeutic targets and strategies for FXS treatment.

TABLE OF CONTENTS

PRIOR PUBLICATIONS

Waung MW, **Pfeiffer BE**, Nosyreva ED, Ronesi JA, Huber KM (2008) Rapid translation of Arc/Arg3.1 selectively mediates mGluR-dependent LTD through persistent increases in AMPAR endocytosis rate. *Neuron* Jul 10; 59(1): 84-97.

Volk LJ, **Pfeiffer BE**, Gibson JR, Huber KM (2007) Multiple Gq-coupled receptors converge on a common protein synthesis-dependent long-term depression that is affected in fragile X syndrome mental retardation. *J Neurosci* Oct 24; 27(43): 11624-34.

Pfeiffer BE, Huber KM (2007) Fragile X mental retardation protein induces synapse loss through acute postsynaptic translational regulation. *J Neurosci* Mar 21; 27(12): 3120-30.

Pfeiffer BE, Huber KM (2006) Current advances in local protein synthesis and synaptic plasticity. *J Neurosci* Jul 5; 26(27): 7147-50.

Kotti TJ, Ramirez DM, **Pfeiffer BE**, Huber KM, Russell DW (2006) Brain cholesterol turnover required for geranylgernaiol production and learning in mice. *Proc Natl Acad Sci USA* Mar 7; 103(10):3869-74.

Lanford RE, Guerra B, Lee H, Averett DR, **Pfeiffer B**, Chavez D, Notvall L, Bigger C (2003) Antiviral effect and virus-host interactions in response to alpha interferon, gamma interferon, poly(i)-poly(c), tumor necrosis factor alpha, and ribavirin in hepatitis C virus subgenomic replicons. *J Virol* Jan; 77(2): 1092-104.

LIST OF FIGURES

LIST OF TABLES

LIST OF DEFINITIONS

4EBP – eIF4E binding protein
4OHT – 4-hydroxytamoxifen
AChR – acetylcholine receptor
Ago – argonaut
Akt – atypical protein kinase
AMPAR – a-aino-3-hydroxy-5-methylisoxazole-4-propionic acid sensitive glutamate receptor
APP – amyloid precursor protein
Arc – activity-regulated cytoskeletal protein
BDNF – brain-derived neurotrophic factor
CaMK – calcium/calmodulin-mediated kinase
cAMP – cyclic adenosine monophosphate
Cdk5 – cyclin-dependent protein kinase 5
CF – climbing fiber
CKII – casein kinase II
CNS – central nervous system
CPEB – cytoplasmic polyadenylation element binding protein
dFMR1 – *Drosophila melanogaster* Fragile X Mental Retardation protein
DIC – differential interference contrast
DIV – days *in vitro*
DNA – deoxyribonucleic acid
dnPAK – dominant negative p21-activated protein kinase
EF1a – elongation factor 1a
EGFP – enhanced green fluorescent protein
eIF4A/E/F/G – eukaryotic initiation factor 4A/E/F/G
EPSC – excitatory post-synaptic current
ERK – extracellular signal-related kinase
Flox – flanked by *LoxP* sites
Fmr1 – Fragile X mental retardation gene/mRNA
FMRP – Fragile X mental retardation protein
FXR1/2 – Fragile X related protein 1/2
FXS – Fragile X syndrome
GABA – gamma-aminobutyric acid
GAP – GTPase activating protein
GEF – guanine excange factor
GFP – green fluorescent protein
GluR1/2/3/4 – AMPA-type glutamate receptor subunit 1/2/3/4
HAT – histone acetyltransferase
HDAC – histone deacetlyase
IGF-1 – insulin growth factor 1
KH-domain – hnRNP-K homology domain
KO – knock out
LTD – long-term depression

LTP – long-term potentiation
mAChR – muscarinic acetylcholine receptor
MADS – MCM1, Agamous, Deficiens, and Serum response factor
Map1b – microtubule associated protein 1b
MeCP2 – methyl-CpG-binding protein 2
MEF2 – myocyte-enhancer factor 2
MEK – mitogen-activated kinase
mEPSC – miniature excitatory post-synaptic current
miRNA – micro-RNA
mGluR – metabotropic glutamate receptor
mGluR-LTD – metabotropic glutmate receptor-dependent long-term depression
Mnk – MEK interacting kinase
MRE – MEF2 response element
mRNA – messenger RNA
MRX – X-linked mental retardation
mTOR – mammalian target of rapamycin
NDF – N-terminal domain of FMRP
NES – nuclear export signal
NFAT – nuclear factor of activated T-cells
NGF – nerve growth factor
NLS – nucleaer localization signal
NMDAR – N-methyl-D-aspartate sensitive glutamate receptor
NMJ – neuro-muscular junction
NR1/2 – NMDAR subunit 1/2
OHSC – organotypic hippocampal slice culture
PAK – p21-activated protein kinase
PC – Purkinje cell
PF – parallel fiber
PI3K – phospho-inositol-3 kinase
PKA – protein kinase A
PKC – protein kinase C
PLC – phospholipase C
PP2A – protein phosphatase 2A
PPF – paired-pulse facilitation
PSD-95 – post-synaptic density protein of 95 kDa
RGG – arginine/glycine-rich
RISC – RNAi-induced silencing complex
RNA – ribonucleic acid
RNAi – RNA interference
RNP – ribonucleoprotein
S6K – S6 ribosomal subunit kinase
SD – standard deviation
siRNA – short interfering RNA
STDP – spike timing dependent plasticity
SUMO – small ubiquitin-like modifier

TBS – theta burst stimulation
TLS – translocated in liposarcoma
TOP – terminal oligopyrmidine
VP16 – herpes simplex viral protein 16
WT – wild-type
YAC – yeast artificial chromosome
ZBP – zip-code binding protein

CHAPTER ONE

Fragile X Mental Retardation Protein: A Key Regulator of Dendritic Protein Synthesis, Synapse Number, and Synaptic Function

Fragile X Syndrome

In the United States, the prevalence of mental retardation and autism has been estimated at approximately 0.78% of the population (Larson et al., 2001). Although the social impact of these complex diseases is immeasurable, the lifetime economic cost for all mentally retarded individuals born in the U.S. in the year 2000 has been calculated at over $50 billion (Honeycutt et al., 2004), underscoring the importance for scientific research on the root causes of mental retardation and autism.

The most common form of inherited mental retardation is Fragile X Syndrome (FXS), which affects approximately 1:4000 males and 1:8000 females (O'Donnell and Warren, 2002; Turner et al., 1996; Verkerk et al., 1991). Although the severity and manifestation of symptoms varies, FXS has several common phenotypes: in addition to a reduction in intellectual ability or IQ, which ranges from mild to severe, many FXS patients also display hyperactivity, hypersensitivity to sensory stimuli, anxiety, impaired visuo-spatial processing, and developmental delay. Thirty percent of children with FXS are diagnosed with autism and express stereotypic behaviors associated with autism, including repetitive behaviors and impaired social interactions and language skills (Hagerman et al., 2005; Kaufmann et al., 2004). In recent years, a number of human genes have been linked to autism, with the gene responsible for FXS (*FMR1*, see below) being one of the most commonly linked; accordingly, 2-5% of autistic children have FXS (Hagerman et al., 2005; Kaufmann et al., 2004; Persico and Bourgeron, 2006). Furthermore, roughly 25% of FXS patients suffer from epilepsy (Hagerman et al., 2005; Kaufmann et al., 2004), making FXS a leading genetic model of several complex diseases. FXS also has several physical phenotypes, which include connective tissue abnormalities, an elongated face with prominent ears, and macroorchidism (Hagerman, 2002).

Loss of Function of the Fragile X Mental Retardation Gene, *FMR1*, causes Fragile X Syndrome

The molecular cause of FXS arises from loss-of-function mutations in the *FMR1* gene, which resides near the tip of the long arm of the X-chromosome (O'Donnell and Warren, 2002). In nearly all cases, the observed mutation is an expansion of a CGG trinucleotide repeat in the promoter region of the gene, which results in an apparent bend or kink in the chromosome's structure (hence the term "Fragile X"). In unaffected individuals, the CGG region typically has 5-50 repeats. At this size, the CGG repeat region is genetically stable. Individuals harboring between 50-200 CGG repeats are defined as pre-mutation carriers. For reasons that remain unknown, this increased number of CGG repeats causes the region to become genetically unstable, leading to a rapid expansion of this region in subsequent generations (O'Donnell and Warren, 2002). The full mutation state is defined as greater than 200 CGG repeats. At this size, the region becomes subject to hypermethylation, resulting in the transcriptional silencing of the *FMR1* gene and loss of the protein product of *FMR1*, the Fragile X Mental Retardation protein (FMRP). Thus, it is widely accepted that FXS results from the loss or significant reduction of FMRP function. In support of this view, phenotypic variation in IQ and physical features of FXS patients is strongly correlated with protein levels of FMRP (Loesch et al., 2002; Loesch et al., 2003; Loesch et al., 2004; Tassone et al., 1999). In addition, although the majority of FXS cases result from CGG repeat expansion in the non-coding region of the *FMR1* gene, there are rare cases of intragenic loss-of-function point mutations or deletions in the coding region of the gene which also lead to Fragile X Syndrome, suggestive of a primary role for *FMR1* in the disease (De Boulle et al., 1993; Lugenbeel et al., 1995).

A mouse model of FXS was created by inserting a neomycin cassette into exon 5 of the mouse *Fmr1* gene (Bakker, 1994), resulting in a lack of functional FMRP expression. Though it is difficult to model human mental retardation in mice, the *Fmr1* knockout (KO) mouse recapitulates many phenotypes of FXS, including hyperactivity, macroorchidism, anxiety, and learning and memory deficits (Bakker, 1994; Brennan et

al., 2006; Koekkoek et al., 2005; Paradee et al., 1999; Restivo et al., 2005; Spencer et al., 2005; Spencer et al., 2008; Zhao et al., 2005). Thus, the *Fmr1*-KO mouse has been instrumental in expanding our knowledge of the biology of FXS.

Fragile X Syndrome : A Disease of the Synapse

There have been several autopsy and MRI studies demonstrating altered brain structure and size in FXS (Hessl et al., 2004), with FXS patients displaying a slightly larger caudate nucleus and smaller cerebellar vermis. Additionally, there appears to be an age-dependent decrease in the superior temporal gyrus, and an age-dependent increase in the hippocampus (Hessl et al., 2004). Finally, the 4th ventricle has been reported to be larger in FXS patients (Hessl et al., 2004). Although these relatively subtle alterations in gross brain structure may contribute to some of the phenotypes of FXS, it seems unlikely that these minor changes in brain architecture can account for the full range of mental and behavioral symptoms in FXS. Thus, it is reasonable to expect that FXS results, at least in part, from alterations in neuronal function throughout the brain at the level of the synapse.

The first such evidence of altered synaptic structure in FXS came from analysis of post-mortem cortical tissue of FXS patients, which observed that the number of dendritic spines was increased relative to control individuals (Hinton et al., 1991; Irwin et al., 2001). Interestingly, although the specific phenotype varies, alterations in dendritic spine structure are a common finding among many types of mental retardation, including FXS, Rett's Syndrome, and Down Syndrome, suggesting a common synaptic origin in many diverse cognitive disorders (Kaufmann and Moser, 2000; Marin-Padilla, 1972; Purpura, 1975). As dendritic spines are the sites of excitatory synaptic contact, these data suggested that synapse number may be increased in FXS patients and further provided a potential mechanism for the increased rates of epilepsy in FXS. It was additionally noted that a large proportion of the spines of FXS patients appeared abnormally long, thin, and tortuous, a phenotype reminiscent of the immature spine precursors, filopodia, and indicative of alterations in synapse development and/or function (Irwin et al., 2001). It

was therefore unclear from morphological data alone whether the increased numbers of filopodia-like spines reflected an increase in functional synapse number.

Work in the *Fmr1*-KO mouse has largely confirmed the spine phenotype observed in FXS patients (Dolen et al., 2007; Irwin et al., 2002; McKinney et al., 2005; Meredith et al., 2007). However, the magnitude or even the existence of the spine alterations in the *Fmr1*-KO mouse appears to vary across brain region, developmental age, and mouse strain suggesting complex regulation of spine morphology by FMRP.

The most consistent alteration observed across all genotypes and ages of *Fmr1*-KO mice is a shift from mature to immature spine morphology. Spine development follows a stereotyped pattern (Cline, 2001; Fiala et al., 2002). Immature, highly motile filopodia emerge from the dendritic shaft, presumably searching for presynaptic inputs. After establishing a connection with one or more axon terminals, the filopodia retract to become short, stubby, "mushroom-headed" spines. Many studies have examined the effects of FMRP on cortical spine structure, revealing an increased number of long, thin spines and a decreased number of short, stubby spines in *Fmr1*-KO mice relative to wild-type controls (Irwin et al., 2002; McKinney et al., 2005; Meredith et al., 2007; Restivo et al., 2005) . Similarly, a recent study of dendritic spines in the hippocampus demonstrated that the average spine length across all spine categories was increased in the *Fmr1*-KO mouse (Grossman et al., 2006). Surprisingly, however, the authors also report an increase in the number of spines that fall into the category of "stubby spines" and a reduction in the number of "filopodia-like spines" (Grossman et al., 2006), indicating loss of FMRP may affect spine development in the hippocampus differently than in the cortex. The consistency of the immature spine phenotype in the literature is quite striking and strongly suggestive of impairments in the functional maturation of synapses in the absence of FMRP.

The hallmark of the human FXS spine phenotype, that of increased density of dendritic spines, is also present in *Fmr1*-KO mice, although the phenotype appears to be slightly less consistent than alterations in spine shape. Initial reports demonstrated an increase in the number of spines in the visual cortex of *Fmr1*-KO mice of the FVB background strain; however, this data was placed into question when it was revealed that

these mice suffered from retinal degeneration, which may have exacerbated changes in the occipital cortex following loss of FMRP (Comery et al., 1997). A subsequent study in "sighted" FVB *Fmr1*-KO mice found no alteration in spine density in pyramidal neurons of the visual cortex (Irwin et al., 2002). Interestingly, *in vivo* imaging of spines in the somatosensory cortex of FVB *Fmr1*-KO mice showed an elevated number of spines in one-week-old KO mice relative to controls, but not in older, adolescent mice, suggesting an age-dependent effect of FMRP on spine density (Nimchinsky et al., 2001). Investigations of *Fmr1*-KO mice of a different genetic background, C57/Bl6, have also pointed to the possibility of age-dependent affects on spine number. Despite several studies demonstrating that young or adolescent C57/Bl6 *Fmr1*-KO mice have no alterations in spine density in visual or medial prefrontal cortex, work on adult mice has consistently revealed an increase in the number of spines of mature *Fmr1*-KO cortical neurons relative to wild-type controls (Dolen et al., 2007; Galvez and Greenough, 2005; Hayashi et al., 2007; McKinney et al., 2005; Meredith et al., 2007; Restivo et al., 2005). Thus, current evidence suggests that alterations in the density of dendritic spines in *Fmr1*-KO mice may be dependent upon both background strain and age, indicative of complex regulation of spine number by FMRP. However, the bulk of the data demonstrate an increase in spine density in *Fmr1*-KO mice. In Chapter 4, I directly examine the effects of both developmental age and genetic background on FMRP regulation of synapse number.

FMRP and Synapse Pruning

The cumulative data on alterations in spine number and morphology in FXS patients and *Fmr1*-KO mice indicate that FMRP plays an important role in the regulation of synapse number and/or maturation. Early neuronal development is characterized by the excess production of synaptic connections; during maturation, competition between synapses results in the activity-dependent elimination, or pruning, of inappropriate connections.

The mechanisms of synaptogenesis have largely been elucidated by studies investigating these processes at the neuro-muscular junction (NMJ) (Goda and Davis,

2003). At the NMJ, a rudimentary postsynaptic structure termed prepatterning is observed prior to presynaptic contact, indicating that the most basic level of NMJ postsynaptic development occurs independent of synaptic activity (Lin et al., 2001). As the presynaptic motoneuron terminal draws near the prepatterning, it releases the proteoglycan agrin, which induces further development of the postsynaptic structure and clustering of postsynaptic acetylcholine receptors (AChR) (Sanes and Lichtman, 1999). The postsynapse then reciprocally induces presynaptic maturation, likely through laminin, the principle component of the basal lamina (Goda and Davis, 2003). Mutant mice which demonstrate improper postsynaptic development also fail to differentiate the presynaptic motoneuron terminals, implicating reciprocal induction as a necessary step in NMJ formation (Nguyen et al., 2000).

In comparison, significantly less is known regarding synaptogenesis in the central nervous system (CNS), due in part to the wide array of synapse types and developmental timecourses encountered in the CNS (Ziv and Garner, 2004). The prevailing model of brain development holds that neuronal projections are targeted to their general final destinations through attractive or repulsive interactions with gradients of cell surface proteins or secreted molecules. Once they have arrived at the proper location, both axonal growth cones and dendrites extend highly motile filopodia, which appear to sample their local environment, searching for a synaptic partner (Knott et al., 2006; Nagerl et al., 2007). The mobility of filopodia is dependent upon the actin cytoskeleton and perturbations in actin-regulating proteins can affect filopodial extensions, thereby affecting synapse formation (see Chapter 5). In addition, many extracellular proteins, including the neurotrophins brain-derived neurotrophic factor (BDNF) and nerve growth factor (NGF), secreted signaling proteins such as Wnt, and the neurotransmitter glutamate, can regulate both axonal and dendritic filopodial movement and subsequent synaptogenesis (Goda and Davis, 2003; Ziv and Garner, 2004).

Once an appropriate synaptic partner has been found, interactions between cell adhesion molecules initiate synapse formation (Ziv and Garner, 2004). The incredible diversity of synaptic adhesion molecules found throughout the CNS is thought to provide specificity for pre- and post-synaptic connections between distinct neuron types in

specific brain regions. In particular, homophilic interaction of SynCAM, a member of the Ig superfamily, and heterophilic associations between presynaptic neurexins and postsynaptic neuroligins appear to mediate synapse formation (Biederer et al., 2002; Sara et al., 2005; Scheiffele et al., 2000). Expression of either SynCAM or neuroligin in non-neuronal cells is sufficient to induce axonal attachment and presynaptic assembly from neighboring neurons in culture, reminiscent of reciprocal induction observed at the NMJ (Sara et al., 2005; Scheiffele et al., 2000).

Association of synaptic adhesion molecules is thought to initiate synapse formation through extensive intracellular interactions with synaptic scaffolding molecules, which serve to cluster both pre- and postsynaptic components such as synaptic vesicles and neurotransmitter receptors (Ziv and Garner, 2004). Interestingly, there is evidence that many components of the presynaptic active zone may be pre-assembled in large vesicles that can be rapidly inserted into the presynaptic specialty (Goda and Davis, 2003). During the early stages of synaptogenesis, pre-synaptic terminals are characterized by a small number of docked vesicles and a poorly-defined active zone (Kraszewski et al., 1995). Insertion of pre-assembled active zones may therefore be a critical step in converting the nascent presynaptic specialty into a fully-functional axon terminal. Furthermore, pre-packaged terminals likely facilitate the rapid rate of synapse assembly, which can be completed in as little as one to two hours after initial filopodial contact.

Some components of the postsynapse may also be pre-packaged prior to synaptic insertion (Goda and Davis, 2003). However, postsynaptic development occurs at a slower pace than its presynaptic partner. Along with the postsynaptic scaffolding molecules, functional NMDA-type receptors (NMDARs), but not AMPA-type receptors (AMPARs), are initially observed at nascent synapses; NMDARs typically conduct little current when the neuron is not depolarized, so these nascent synapses are referred to as "silent synapses" (Friedman et al., 2000; McGee and Bredt, 2003). As the synaptic connection matures, NMDAR activity drives the insertion of AMPARs into the synapse, "unsilencing" them (Friedman et al., 2000). In addition, NMDARs undergo a maturational change in their subunit composition as the neuron develops. NR2B-

containing NMDARs are gradually, but not completely, replaced by NR2A-containing NMDARs, leading to a decreased current decay constant and less total calcium influx (Cull-Candy et al., 2001).

Reports demonstrating that postsynaptic expression of synaptic adhesion proteins can induce presynaptic differentiation, coupled with the timecourse of both pre- and postsynaptic development, support a model whereby initial filopodial contact with the nascent postsynapse causes reciprocal induction of the presynaptic terminal, which in turn leads to the differentiation of the postsynaptic terminal. Continued synaptic activity causes calcium influx through NMDARs, which leads to the insertion of AMPARs and the functional maturation of the postsynapse.

As with synaptogenesis, a majority of the data on synapse elimination comes from work on the mammalian NMJ (Goda and Davis, 2003). Muscle fibers are originally multiply innervated by several motoneurons. During the development of the organism, activity-dependent competition between these inputs results in the elimination of all but one, leaving each muscle fiber innervated by a single motoneuron (Sanes and Lichtman, 1999). Current evidence suggests that weaker synaptic connections are selectively eliminated and stronger connections are solidified, likely through retrograde signals originating from the post-synaptic muscle fiber. Importantly, however, the process of elimination is reversible, as demonstrated by recent imaging studies of green fluorescent protein (GFP)-expressing motoneurons (Walsh and Lichtman, 2003). Even after beginning the process of elimination, a synapse can re-establish itself as the dominant synaptic connection, leading to the pruning of other, initially stronger synapses (Walsh and Lichtman, 2003). These data indicate that synapse elimination is likely a long-term process requiring continued signaling between the pre- and postsynapse rather than a pre-programmed pattern that is triggered by a single event.

Current data suggests that synapse elimination occurs throughout the mammalian CNS across the lifetime of the organism; however, there appear to be developmentally programmed periods of intense synapse removal in particular brain regions (Goda and Davis, 2003). Unfortunately, the specific mechanistic processes underlying synapse elimination in the CNS are only now beginning to be elucidated and the picture is far

from clear. Much work has focused on the elimination of climbing fiber inputs to Purkinje cells in the cerebellum, which has provided researchers a platform with which to study the molecular mechanisms of synapse pruning.

In the cerebellum of adult rodents, Purkinje cells (PC) are innervated by a single presynaptic climbing fiber (CF), which originates in the inferior olivary nucleus; however, at birth, PCs are innervated by multiple CFs (Hashimoto and Kano, 2005). PCs also receive input from parallel fibers (PFs) originating from cerebellar granule cells, which preferentially form distal synapses on PCs, while CF synapses in mature PCs are found at more proximal sites. During maturation of the cerebellum, all but one of the CF inputs are eliminated on each PC, a process reminiscent of synapse elimination at the NMJ (Hashimoto and Kano, 2005; Sanes and Lichtman, 1999). The mechanism of this synapse pruning is unknown, although several genetic mouse models have shed light on the underlying process. Mice with impaired PF synapses display an expansion in the CF innervation to more distal synapses, indicating that PF inputs may compete with CF synapses for distal locations, aiding in the pruning process (Kashiwabuchi et al., 1995). In addition, mice lacking expression of either metabotropic glutamate receptor 1 (mGluR1), G_{aq}, phospholipase C (PLC), or protein kinase C (PKC) demonstrate impaired CF-PC synapse elimination, as well as various locomotor defects (Aiba et al., 1994; Chen et al., 1995; Conquet et al., 1994; Ichise et al., 2000; Kano et al., 1995; Kim et al., 1997; Offermanns et al., 1997). Importantly, it is believed that activation of PF inputs is primarily responsible for activating the mGluR1 ? G_{aq} ? PLC ? PKC pathway, suggesting that PF synapses play an active role in CF pruning. Re-expression of mGluR1 exclusively in PCs of mGluR-KO mice rescued the impairment in CF pruning, strongly implicating post-synaptic signaling mechanisms mediated by mGluR1 as necessary for this process (Ichise et al., 2000).

As described below, activation of the group I mGluRs, mGluR1 and mGluR5, induce a form of long-term synaptic depression (LTD; mGluR-LTD) in the hippocampus and cerebellum that requires rapid, local protein synthesis (Huber et al., 2000; Koekkoek et al., 2005). mGluR1 is the predominant group I mGluR expressed in the cerebellum and genetic removal of mGluR1 results in not only impairments in CF elimination, but

also mGluR-LTD (Ichise et al., 2000). There is evidence indicating that repeated mGluR-LTD can initiate synapse elimination (Shinoda et al., 2005). These data provide a compelling argument that mGluR-LTD may be a particularly important process in synapse elimination. Combining this argument with the strong biochemical link between mGluR activity and FMRP function (see below) and the increased numbers of synapses in FXS patients and *Fmr1*-KO mice, suggests that FMRP may play a key role in synapse elimination through its effects on mGluR-LTD. Interestingly, CF elimination is enhanced in the *Fmr1*-KO mouse (Koekkoek et al., 2005). My data strongly suggests that synapse number is elevated in the absence of FMRP. Thus, it may be expected that PF inputs to PCs are also elevated. As decreased PF synapses or PF-mediated signaling impairs CF pruning, it stands to reason that increased PF synapse may enhance the elimination of CF synapses, as reported in *Fmr1*-KO mice (Koekkoek et al., 2005). To my knowledge, an in-depth examination of PF synapse number in wild-type vs. *Fmr1*-KO mice has not been undertaken, although PC dendritic spine number appears to be normal in *Fmr1*-KO mice (Koekkoek et al., 2005).

It has been hypothesized that the absence of FMRP results in an overabundance of synapses through a deficit in synaptic pruning, as opposed to an enhancement in synaptogenesis. Several independent studies lend credence to a role for FMRP in dendritic pruning. In the mouse somatosensory barrel cortex, immature spiny stellate cells extend their dendrites into both the hollow and septa of the cortical "barrels." During development, septal-oriented protrusions are normally eliminated; however, *Fmr1*-KO mice display a failure to prune these septal-oriented dendrites (Galvez et al., 2003). In addition, work on several *Drosophila* lines has also revealed changes in synaptic development and function following alterations in the expression of the *Drosophila* homolog of FMRP, dFmr1. Consistent with the phenotype in mouse somatosensory cortex, neurons of dFmr1 null larvae and flies have an increased number of dendritic protrusions and a highly elaborate dendritic arborization (Lee et al., 2003; Pan et al., 2004). Finally, as described in detail in Chapter 2, post-synaptic expression of FMRP results in the elimination of synaptic connections at both the structural and functional level. It is important to note, however, that the developmental pruning of

multiply-innervated climbing fiber/Purkinje cell connections to singly-innervated connections appears to be normal or even slightly accelerated in *Fmr1*-KO mice (Koekkoek et al., 2005). It is therefore possible that FMRP may have a region- or cell type-specific role in postsynaptic pruning mechanisms. However, prior to the work described in Chapter 2, there had been no reports which directly examined the effects of FMRP expression on functional synapse number or synaptic development.

Surprisingly, despite the fact that FMRP is canonically believed to function at the post-synapse, multiple studies report presynaptic changes in dFmr1 mutant flies, with increased axonal branching and altered pathfinding/targeting of axon fibers in the absence of dFmr1 (Michel et al., 2004; Morales et al., 2002; Pan et al., 2004). It was initially believed that the presynaptic alterations seen in *Drosophila* dFmr1 mutants result from the fact that dFmr1 fills the role of three mammalian proteins: FMRP, FXR1, and FXR2. However, recent work has revealed presynaptic abnormalities in *Fmr1*-KO mice as well. Though FMRP is primarily found in the soma and dendrites and is canonically believed to function at the post-synapse, it has been observed presynaptically in both axonal growth cones and mature axons, where it appears to negatively regulate the number of growth cone filopodia, as well as filopodia retraction in response to semaphorin (Antar et al., 2006). Because loss of FMRP results in increased growth of axons in both mice and *Drosophila*, it therefore seems likely that *Fmr1*-KO mice would have increased numbers of presynaptic connections. However, an electrophysiological study on a "mosaic" mouse line, in which wild-type and *Fmr1*-KO neurons exist side-by-side, reported that presynaptic loss of FMRP led to a reduction of synaptically connected neurons in hippocampal area CA3, with no demonstrated effect of postsynaptic FMRP loss (Hanson and Madison, 2007). Consistent with this finding, axonal filopodia of *Fmr1*-KO mice were less motile than those of wild-type mice (Antar et al., 2006). These data cumulatively highlight a role for presynaptic FMRP in synapse formation and/or maintenance, although the precise mechanisms remain unresolved.

While a large portion of research on the synaptic function of FMRP has focused on glutamatergic synapses, several important alterations in inhibitory, GABA-ergic synapses have also been observed in the brains of *Fmr1*-KO mice. Examination of

cortical synapses in *Fmr1*-KO mice revealed an increase in presynaptic release probability of GABA-ergic synapses onto striatal spiny neurons, with no change in postsynaptic GABA-ergic properties (Centonze et al., 2008). In addition, *Fmr1*-KO mice appear to have alterations in the number of parvalbumin-positive interneurons, a sub-population of inhibitory neurons, in nearly all layers of somatosensory cortex (Selby et al., 2007). Finally, a recent study demonstrates a reduction of functional excitatory inputs onto GABA-ergic neurons in Layer IV of somatosensory cortex of *Fmr1*-KO mice (Gibson et al., 2008, in preparation). These data reveal clear, if somewhat inconsistent, changes in inhibitory neural function in the absence of FMRP.

The cumulative data suggests that FMRP acts as a negative regulator of synapse number, possibly through stimulation of synaptic pruning. Axonal growth and targeting might also be affected by FMRP function.

FMRP is an RNA-binding Protein

To understand the molecular and biological alterations that underlie FXS, it is important to clarify the role that FMRP plays in normal cellular function. The *fmr1* transcript is roughly 4.4 kb and houses 17 exons; due to extensive alternate splicing, FMRP is observed as several isoforms ranging from 65-80 kDa (Ashley et al., 1993; Eichler et al., 1993; Verkerk et al., 1993).

FMRP has two homologs in humans and rodents, Fragile X Related Proteins 1 and 2 (FXR1 and FXR2), which share roughly 60% amino acid identity with FMRP (Kaufmann et al., 2002). The FXRs likely function similarly to FMRP, as they have similar RNA-binding motifs (see below) and are co-localized with FMRP (Bakker et al., 2000; De Diego Otero et al., 2002; Kanai et al., 2004). In addition, a double-knockout mouse of *Fmr1* and *Fxr2* displays exaggerated behavioral phenotypes in comparison to the *Fmr1*-KO alone (Spencer et al., 2006). Interestingly, loss of *Fxr1* results in early post-natal lethality due to cardiac or respiratory failure (Mientjes et al., 2004), indicating a critical role for this protein. In *Drosophila melanogaster*, a single gene, *Drosophila* Fragile X Related Protein (*dFmr1*), is thought to serve the function of the three mammalian genes (Zarnescu et al., 2005). *dFmr1* shares roughly 35% amino acid

identity with FMRP (Gao, 2002; Zhang et al., 2001) and does not seem to be crucial for survival, although the phenotypes observed in the *dFmr1*-mutant *Drosophila* lines are typically exaggerated or distinct from the mouse and human phenotypes.

FMRP has several well-characterized domains, including four RNA-binding domains (described below) as well as a functional nuclear localization signal (NLS) and nuclear export signal (NES) (Bardoni et al., 1997; O'Donnell and Warren, 2002; Tamanini et al., 1999a; Tamanini et al., 1999b). In addition, exon 7 of FMRP contains a dimerization domain that is important for homodimerization as well as oligomerization with the FXR proteins (Adinolfi et al., 2003; Siomi et al., 1996). The N-terminus of FMRP also forms a large protein-protein interaction domain termed the NDF (N-terminal domain of FMRP) that likely associates with binding partners through a helix-loop-helix motif (Adinolfi et al., 2003). Finally, FMRP harbors a conserved, 38-residue region near its C-terminus that is capable of being multiply phosphorylated (Ceman et al., 2003). Within this phosphorylation domain, a serine at residue 500 (S500) appears to be the primary phosphorylation site – mutation of this serine to an alanine largely eliminates phosphorylation of the other residues (Ceman et al., 2003).

FMRP is found in most cell types of the body, though it is expressed particularly strongly in the testes and the adult brain, where it is found predominantly in neurons, with minimal expression in astrocytes or oligodendrocytes (Feng et al., 1997b). Although present in all regions of the brain, FMRP immunoreactivity is most intense in the cell body layers of the hippocampus and the pyriform cortex, likely due to increased density of the neuronal population in those regions (Feng et al., 1997b). FMRP has functional nuclear localization and export elements; however, FMRP is primarily (~95%) found in the cytoplasm where it is largely restricted to the soma, dendrites, and post-synapse (Antar et al., 2004; Bakker et al., 2000; Feng et al., 1997b). It is important to note, however, that FMRP has been observed in both axonal growth cones and some mature axons (Antar et al., 2006; Feng et al., 1997b; Price et al., 2006).

FMRP is an RNA-binding protein and it is widely believed that its primary cellular function is to regulate mRNA translation (reviewed by (Feng, 2002; Garber et al., 2006)). FMRP interacts with RNA through several RNA-binding regions: an

arginine/glycine-rich RNA-binding motif (RGG box), two hnRNP-K homology domains (KH domains, KH1 and KH2), and a recently discovered N-terminal domain of FMRP (NDF) (Adinolfi et al., 2003; Ashley et al., 1993; Gibson et al., 1993; Siomi et al., 1993; Zalfa et al., 2005). The RGG box appears to represent the highest-affinity RNA-binding region, showing a preference for G-rich stretches and an RNA tertiary structure known as a G-quartet (Darnell et al., 2001; Schaeffer et al., 2001). FMRP can be methylated within the RGG box, which appears to decrease association of FMRP with mRNA targets, thus providing a means for regulation of FMRP-RNA interactions (Denman, 2002; Stetler et al., 2006). The KH domains associate with a specific RNA tertiary structure termed a "kissing complex" (Darnell et al., 2005), whereas NDF has been reported to interact with a small non-coding RNA, termed BC1 (Zalfa et al., 2003). BC1, in turn, has been proposed to base pair with neuronal target mRNAs of FMRP, thus mediating FMRP-mRNA interactions (Adinolfi et al., 2003; Zalfa et al., 2005; Zalfa et al., 2003). However, a specific interaction of FMRP with BC1 RNA has recently been disputed (Wang et al., 2005a). The KH2 domain is particularly interesting because a point mutation in the KH2 domain (an isoleucine to asparagine substitution at residue 304; I304N) in FMRP results in a severe form of Fragile X Syndrome in a single patient (De Boulle et al., 1993). In addition to disrupting interaction with "kissing complex" RNA structures, I304N-FMRP also no longer associates with polyribosomes or regulates translation of its normal mRNA targets (see below) (Darnell et al., 2005; Feng et al., 1997a; Laggerbauer et al., 2001).

FMRP is thought to bind to as many as 400 different brain mRNAs, including its own message (Brown et al., 2001; Brown et al., 1998; O'Donnell and Warren, 2002). Although many studies have attempted to identify the complete mRNA target list for FMRP, there is little consensus between studies, likely due to the distinct methods used to identify FMRP-interacting mRNAs (Brown et al., 2001; Darnell et al., 2001; Dolzhanskaya et al., 2003; Miyashiro et al., 2003; Sung et al., 2000; Zalfa et al., 2003). However, a handful of mRNAs have been validated as confirmed FMRP targets or shown to be misregulated in *Fmr1*-KO mice, including the mRNA for FMRP itself, microtubule associated protein 1b (MAP1b), postsynaptic density protein 95kDa (PSD-95), activity-

regulated cytoskeletal protein (Arc), amyloid precursor protein (APP), elongation factor 1a (EF1a), a Ca^{2+}/Calmodulin-dependent kinase II (a-CaMKII), and glucocorticoid receptor (Brown et al., 2001; Darnell et al., 2001; Hou et al., 2006; Lu et al., 2004; Sung et al., 2003; Todd et al., 2003a; Zalfa et al., 2007). Although yet to be validated, numerous mRNAs for both pre- and post-synaptic proteins have been identified as putative mRNA targets, suggesting that FMRP may regulate synaptic structure and function through processing, localization, or translational regulation of synaptic mRNAs (Brown et al., 2001; Darnell et al., 2001; Miyashiro et al., 2003).

Interestingly, all of the confirmed FMRP target mRNAs are dendritically localized, suggesting that FMRP functions in either dendritic mRNA transport or the regulation of dendritic, "local" translation (see below). FMRP is observed in ribonucleoprotein particles (RNPs), which are large complexes of protein synthesis machinery, RNA-binding proteins, and translationally arrested mRNAs that are transported to dendrites on microtubules (Antar et al., 2005; Kanai et al., 2004), consistent with a role for FMRP in localization of its target mRNAs. To date, however, there is no evidence that FMRP is required for dendritic mRNA transport, as the localization of mRNA targets of FMRP appears normal in the *Fmr1*-KO mouse (Muddashetty et al., 2007; Steward et al., 1998; Zalfa et al., 2007). However, both FMRP and its associated mRNAs are co-transported into dendrites under basal conditions and in response to neuronal activity, indicating that association with additional factors is likely important in the spatial and temporal localization of FMRP and its target mRNAs (Antar et al., 2004; Antar et al., 2005). Additionally, there is evidence that FMRP may function to stabilize some mRNA targets (Li et al., 2001; Zalfa et al., 2007), although the mechanism of this protection is unknown.

A majority of FMRP is associated with either polyribosome clusters or large RNPs (sometimes referred to as "RNA granules") (Darnell et al., 2001; Feng et al., 1997a; Khandjian et al., 1996; Khandjian et al., 2004; Tamanini et al., 1996). Both FMRP-polyribosome and FMRP-RNP interactions are RNA-dependent and occur throughout neurons, including dendrites and spines (Antar et al., 2004; Corbin et al., 1997; Stefani et al., 2004; Wang et al., 2008). Interestingly, recent evidence suggests that

FMRP can shuttle between polyribosomes and the translationally silent RNPs depending upon the translational state of the cell (Vasudevan et al., 2007; Wang et al., 2008). It is therefore believed that FMRP functions in the regulation of dendritic protein synthesis.

Dendritic Translation

Many forms of long-term synaptic change, from bidirectional synaptic plasticity to the growth or retraction of dendritic spines, require precise alterations in the protein complement of individual synapses for their induction and/or maintenance (Bramham and Wells, 2007). Since the discovery of dendritically localized ribosomes near synapses over twenty-five years ago (Steward and Levy, 1982), it has been hypothesized that the neuron is capable of tightly controlling individual synaptic function through temporal and spatial regulation of mRNA translation. The observation of ribosomes near synapses was soon followed by the discovery of many other dendritically localized components of the protein synthesis machinery, including select mRNAs, initiation and elongation factors, chaperone proteins, and even endoplasmic reticulum (Bramham and Wells, 2007). It is now widely accepted that local, dendritic translation can and does occur in neurons, and that dendritic protein synthesis is critically important for many synaptic functions.

The mechanism through which a subset of mRNA species is selectively transported to dendrites, while others remain restricted to the soma, remains an area of intense study. Although the precise pathways of transport remain unclear, recent investigations have revealed several key steps in the sequence from mRNA transcription in the nucleus to localized translation near synapses (Bramham and Wells, 2007). mRNAs which are destined for dendritic localization are likely designated as such with short *cis*-acting sequences that act as a molecular zip-code (Bramham and Wells, 2007). This localization sequence, which usually lies in the untranslated region of the transcript, is recognized by specific RNA-binding proteins, such as zip-code binding protein (ZBP), heterogenous nuclear ribonucleoprotein A2 (hnRNP A2), purine-rich-element-binding protein a (Pur-a), and Staufen1/2, which then help to shuttle the mRNA to its final destination. Shortly after being transcribed, such mRNAs are rapidly associated with RNA-binding proteins, typically in the nucleus, and assembled into RNPs in the soma.

The RNPs are, in turn, linked to the microtubule cytoskeleton and actively transported to their final locations via the kinesin family of proteins. Although the specific composition of RNPs appears to be quite heterogenous, each RNP has similar components: a number of mRNAs, RNA-binding proteins, some elements of the translation machinery (typically translation initiation proteins), and proteins which link the RNP with the microtubule cytoskeleton. It is thought that mRNAs are held in a translationally dormant state inside the RNP, as translation initiation proteins such as eIF4AIII, which would be removed during the first round of translation, are still found associated with mRNA within the RNP. Upon reaching their final destinations, mRNAs are likely kept translationally suppressed until the appropriate cellular signal is received, at which point the transcripts are transported, with their accompanying translation initiation proteins, from RNPs to ribosomes.

RNP transport is, at least in part, regulated by neuronal activity. Under basal conditions, it appears that a majority of RNPs are stationary. However, synaptic activation of either NMDA receptors or metabotropic glutamate receptors (mGluRs) stimulates the movement of RNPs and increases the synaptic localization of dendritically targeted mRNAs. Interestingly, the transcript for the activity-regulated cytoskeletal protein (Arc) is preferentially targeted only to synapses that have been recently activated, indicating that RNPs can be specifically trafficked to sites of synaptic activity. Current evidence suggests that once mRNAs have arrived near synapses on microtubules, they are transported from RNPs into dendritic spines via the actin cytoskeleton, providing an additional step of regulation.

The final stage of dendritic protein synthesis involves the formation of the translation complex itself. A majority of proteins are synthesized through cap-dependent translation, which involves the formation of a large pre-initiation complex on the 5' 7-methyl-guanosine cap of the transcript. The construction of this initiation complex is highly regulated, involving the precise association of a large number of individual proteins. Recent studies have pointed to eukaryotic initiation factor 4E (eIF4E) as a principle site of dendritic regulation of cap-dependent protein synthesis. eIF4E is a necessary component of the pre-initiation complex, associating with eIF4G and eIF4A to

form the eIF4F complex, which promotes initiation. Phosphorylation of eIF4E is crucial in the formation of the eIF4F complex, and is regulated by the mitogen-activated protein kinase (MEK) ? extracellular activity-regulated kinase (ERK) ? MAPK-interacting kinase (Mnk) signaling pathway. eIF4E can also be sequestered by eIF4E-binding protein (4E-BP), thus preventing the formation of the initiation complex and subsequent protein synthesis. The affinity of 4E-BP for eIF4E is greatly reduced by phosphorylation of 4E-BP, which is regulated by the phosphoinositol 3-kinase (PI3K) ? Akt ? mammalian target of rapamycin (mTOR) pathway.

Both the MEK? ERK? Mnk and PI3K? Akt? mTOR pathways also regulate the phosphorylation of S6 kinase (S6K), which in turn phosphorylates the ribosomal protein S6 and thereby stimulates the translation of mRNAs containing a terminal oligopyrimidine (TOP) tract at their 5' end. TOP-containing mRNAs largely code for elements of the protein synthesis machinery. Thus, activation of the MEK? ERK? Mnk and PI3K? Akt? mTOR pathways would increase the translational capacity of neuron as well as stimulate cap-dependent translation through phosphorylation of S6K, eIF4E, and 4E-BP.

Interestingly, both of these signal transduction pathways are themselves regulated by synaptic activity. In particular, activation of the group I metabotropic glutamate receptors (mGluRs) stimulates both pathways and leads to increased rates of dendritic protein synthesis. In addition, activation of mGluRs induces long-term depression (mGluR-LTD) of synaptic responses and facilitation of NMDAR-dependent long-term potentiation (LTP), both of which require the rapid, local translation of pre-existing mRNA. Importantly, many of the mRNAs that are translated in response to mGluR activation are known FMRP targets. Furthermore, mGluR-LTD is abnormal and mGluR-stimulated protein synthesis is absent in the *Fmr1*-KO mouse (described in more detail below), strongly implicating FMRP in regulation of synaptic function through control dendritic protein synthesis, particularly in relation to mGluR activity.

FMRP Regulates Translation

It is currently widely accepted that FMRP plays an important role in regulating local, dendritic translation of its mRNA targets. Among the earliest evidence implicating FMRP in the regulation of protein synthesis came from experiments demonstrating that recombinant FMRP inhibits the translation of RNA in a dose-dependent fashion *in vitro* (Laggerbauer et al., 2001; Li et al., 2001). The inhibition of translation requires FMRP-mRNA interactions, as overexpression of a small RNA target of FMRP sequesters FMRP, preventing it from regulating the translation of additional targets (Li et al., 2001). Furthermore, deletion of the putative FMRP-binding sequence in a target mRNA impaired the ability of FMRP to affect its translation (Li et al., 2001), while a mutant form of FMRP harboring the I304N mutation, which fails to associate with polyribosomes, has no effect on translation (Laggerbauer et al., 2001). It is important to note that very high levels of FMRP, roughly 10 times the molar concentration of mRNA, were required to observe inhibition of translation in these two reports. Regardless, FMRP was initially viewed as an inhibitor of translation.

Subsequent studies have largely supported these initial findings. FMRP inhibits the translation of co-transfected RNAs when expressed in oocytes (Laggerbauer et al., 2001), non-neuronal cell culture (Mazroui et al., 2002), and oligodendrocyte precursors (Wang et al., 2004). Furthermore, general *in vivo* protein synthesis rates are elevated throughout the *Fmr1*-KO mouse brain, while several known mRNA targets of FMRP, including PSD-95, Arc, and GluR1 (a subunit of the AMPA type of glutamate receptors), display increased association with translating polyribosomes in *Fmr1*-KO mice, consistent with a role for FMRP in translational inhibition (Hou et al., 2006; Muddashetty et al., 2007; Qin et al., 2005; Zalfa et al., 2007). Additionally, a confirmed mRNA target of FMRP, *Map1B*, displays elevated translation rates *in vivo* in the hippocampi of *Fmr1*-KO mice (Lu et al., 2004), although this increase is only observed in 10-day-old mice, and not in 5- or 15-day-old mice.

Interestingly, there is also considerable evidence that FMRP may be required for the translation of its mRNA targets, indicating that the protein may not function exclusively as an inhibitor of translation. FMRP has been demonstrated repeatedly to

associate with actively translating polyribosomes (Corbin et al., 1997; Feng et al., 1997a; Stefani et al., 2004), clearly at odds with a view of FMRP as a translational inhibitor. As described above, activation of group I mGluRs results in rapid dendritic synthesis; however, global mGluR-dependent protein synthesis is absent in synaptoneurosomes prepared from *Fmr1*-KO mice (Weiler et al., 2004). The mRNA for both PSD-95 and a-CaMKII are known targets for FMRP and are both rapidly translated in response to mGluR activation (Muddashetty et al., 2007; Todd et al., 2003a). In *Fmr1*-KO neurons, however, mGluR activation fails to induce synthesis of these two proteins (Muddashetty et al., 2007; Todd et al., 2003a).

Mechanisms of FMRP Regulation of Translation

Thus, it is possible that FMRP may bi-directionally regulate the translation of its mRNA targets. Consistent with this hypothesis, recent evidence suggests that the phosphorylation status of FMRP may act as a molecular switch to regulate the translation of FMRP-bound mRNAs. As described previously, FMRP contains a phosphorylation domain which is largely governed by a key serine at residue 500 (S500) (Ceman et al., 2003). When this serine is converted to an aspartic acid to mimic the phosphorylated state, FMRP is observed to associate with stalled polyribosomes, while an alanine substitution at this site, mimicking the dephosphorylated state and inhibiting phosphorylation throughout the domain, causes FMRP to associate more strongly with actively translating ribosomes (Ceman et al., 2003). Thus, phosphorylation of FMRP may lead to the translational suppression of its target mRNAs, while dephosphorylation would allow their translation.

Further supporting the above model of FMRP function, mGluR stimulation, which induces a rapid burst of protein synthesis, also leads to the rapid (<1 minute) dephosphorylation of FMRP, followed shortly (5-10 minutes) by hyperphosphorylation of FMRP (Narayanan et al., 2007; Narayanan et al., 2008), providing a narrow temporal window during which FMRP-dependent translation may occur. There are two reported kinases for FMRP: the non-specific casein kinase II (CKII) and S6K (Narayanan et al., 2008; Siomi et al., 2002), while the phosphatase responsible for dephosphorylating

FMRP is protein phosphatase 2A (PP2A) (Narayanan et al., 2007). Interestingly, PP2A and S6K are both activated by mGluR stimulation on a time scale consistent with FMRP phosphorylational regulation: PP2A is activated within seconds of mGluR stimulation, while S6K is not activated until approximately 10 minutes later.

This data has led to the following simplified model of FMRP regulation of translation (Fig 1.1). Under basal conditions, a majority of FMRP exists in a phosphorylated state due to the combined activity of CKII and S6K, maintaining its target mRNAs in a translationally dormant state while they are trafficked from the soma to their final dendritic destinations via RNPs. Upon activation of mGluRs, PP2A is rapidly activated, which dephosphorylates FMRP, allowing translation of its target mRNAs to occur. Shortly thereafter, S6K becomes strongly activated, which re-phosphorylates FMRP, shutting down translation.

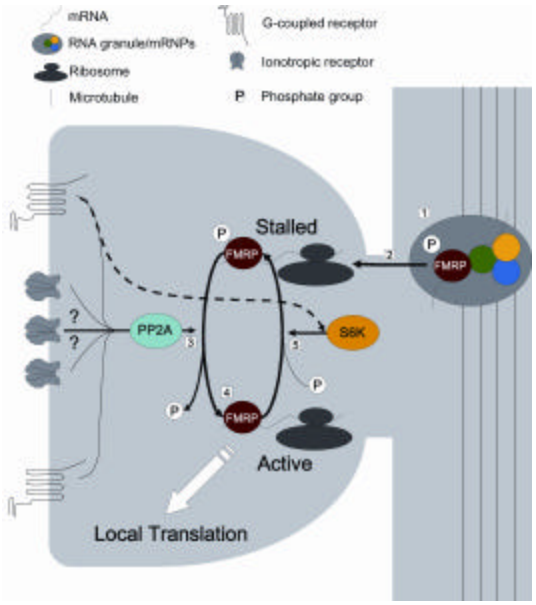

Figure 1.1. Simplified model of FMRP regulation of protein synthesis via phosphorylation/dephosphorylation. ***1***, FMRP is bound to mRNA in RNPs at or near dendritic spines. The mRNA targets of FMRP are held translationally dormant. FMRP is likely maintained in a phosphorylated state by persistent activity of CKII and S6K. ***2***, Cellular signals promote the movement of FMRP-bound mRNAs to polyribosomes at or near dendritic spines. Phosphorylated FMRP associates with mRNA-polyribosome complexes and holds them in a translationally arrested state. ***3***, Cellular signals, presumably from group I mGluRs, rapidly activate PP2A, which dephosphorylates FMRP. ***4***, Dephosphorylated FMRP allows or stimulates the translation of its bound mRNA targets, leading to a rapid burst of local, dendritic translation. ***5***, Activation of group I mGluRs lead to the slower activation of S6K, which re-phosphorylates FMRP and ends the period of local translation.

Cellular control of FMRP expression and localization may provide an additional step of regulation for FMRP-dependent translation. FMRP is rapidly synthesized in response to synaptic stimulation or mGluR activation (Gabel et al., 2004; Hou et al., 2006; Todd and Mack, 2000; Todd et al., 2003a; Todd et al., 2003b; Weiler et al., 1997). However, although mGluRs stimulate *Fmr1* translation, they also initiate the degradation of FMRP through the ubiquitin-proteasome pathway, resulting in only a brief elevation of FMRP levels (Hou et al., 2006). The purpose for the rapid synthesis and subsequent degradation of FMRP following mGluR activation remains unresolved; however, it may provide a mechanism for mRNA targets of FMRP to be shuttled from translationally silent mRNPs to active polyribosomes.

In support of this hypothesis, recent studies suggest that FMRP and its target mRNAs may be differentially localized following synaptic activity. Synaptic depolarization or mGluR stimulation induces the rapid mobility of both FMRP and *Fmr1* mRNA into dendrites (Antar et al., 2004; Antar et al., 2005). However, although *Fmr1* mRNA remains synaptically localized following mGluR activation, FMRP association with synapses is reduced, either through degradation of synaptic FMRP or trafficking of FMRP away from synapses into nearby dendritic shafts (Antar et al., 2004). These data suggest that following synaptic stimulation, FMRP may release its bound mRNA targets, which are then targeted to synaptically localized polyribosomes for translation.

This model is somewhat incongruent with the strong association of FMRP with polyribosomes. In fact, a majority of FMRP is reported to be incorporated into actively translating polyribosomes, with only small fraction retained in RNP complexes (Wang et al., 2008). Indeed, the data suggests that FMRP does not release its mRNA targets, but rather remains associated with them throughout translation. A recent study demonstrated that FMRP is rapidly sequestered into translationally dormant RNPs after being released from elongating polyribosomes (Wang et al., 2008). These data imply that FMRP may shuttle its mRNA targets between actively translating ribosomes and translationally dormant RNPs.

Finally, an additional report observes that synaptic FMRP levels are actually increased following mGluR stimulation (Ferrari et al., 2007). The increase in FMRP at

the synapse appears to be, at least in part, due to *de novo* synthesis of FMRP (Ferrari et al., 2007). It is possible, therefore, that synaptic FMRP is rapidly shuttled away from synaptically localized polyribosomes following mGluR activation (Antar et al., 2004), carrying its mRNA targets with it back to RNPs (Wang et al., 2008), only to be replaced at the synapse by newly synthesized FMRP (Ferrari et al., 2007).

Thus, the precise mechanisms through which FMRP controls dendritic translation remain unclear. However, a working model states that FMRP first associates with its target mRNAs when bound within a RNP, likely as the RNP forms within the nucleus or soma. While associated with the RNP, FMRP-polyribosome interactions are inhibited, thus preventing translation of its mRNA targets. Upon mGluR stimulation, FMRP-containing RNPs are trafficked along the microtubule cytoskeleton, likely to a location near the site of synaptic activity. Once there, FMRP may release its mRNA targets from the RNP, where they can be bound by newly-synthesized, polyribosome-associated FMRP; alternatively, FMRP may directly shuttle its mRNA targets to translationally competent polyribosomes. Following association with a polyribosome, phosphorylated FMRP likely holds the polyribosome in a "stalled" state, waiting for the appropriate cellular signal to dephosphorylate FMRP, resulting in the rapid translation of the transcript.

It is unknown exactly how phosphorylated FMRP may inhibit or stall polyribosomes, but one proposed mechanism for FMRP-dependent translational inhibition is through association with microRNAs (miRNAs), which are short, 20-25 nucleotide, noncoding RNAs. miRNAs are thought to suppress translation through association with the Argonaut proteins, members of the RNA-induced silencing complex (RISC), which in turn guide miRNAs to mRNA targets containing complementary sequences (Bartel, 2004). Near-perfect complementarity results in the RISC-dependent degradation of the targeted mRNA, while imperfect complementarity leads to inhibition of translation through an as-of-yet indeterminate mechanism (Bartel, 2004). One member of the Argonaut family, Argonaut 2 (AGO2), has been shown to interact with the *Drosophila* homolog of FMRP, dFmr1 (Caudy et al., 2002; Ishizuka et al., 2002; Jin et al., 2004a; Jin et al., 2004b). In addition, mammalian FMRP associates with eIF2C2, a

mammalian Argonaut protein, although this interaction was not shown to be direct (Jin et al., 2004b). Importantly, down-regulation of another *Drosophila* Argonaut protein, AGO1, suppressed some of the phenotypes associated with dFmr1 overexpression, implicating the Argonaut proteins as necessary components of dFmr1 function (Jin et al., 2004b). It is therefore intriguing to consider the possibility that FMRP may regulate translation of its mRNA ligands via interactions with components of the RISC complex. In fact, there is biochemical evidence that FMRP associates with a small, non-coding RNA termed BC1, which is predicted to base-pair with known FMRP target mRNAs (Rozhdestvensky et al., 2001; Zalfa et al., 2003). This data is particularly interesting considering that BC1 RNA has recently been shown to inhibit translation in a dose-dependent fashion, similar to FMRP (Wang et al., 2002). The interaction between FMRP and BC1 may facilitate translational suppression of mRNA targets, although recent data has emerged challenging a specific interaction of FMRP with BC1 (Iacoangeli et al., 2008; Wang et al., 2005a). If FMRP does, in fact, control translation through association with the RISC complex, it is possible that this interaction is dependent upon the phosphorylation state of FMRP, although this hypothesis has yet to be tested.

Finally, methylation of FMRP may provide an additional step of translational regulation. Methylation of arginine residues is a common cellular process executed by arginine methyl transferases, and has been implicated in the regulation of transcription, protein-protein interactions, and protein-RNA interactions (Lukong and Richard, 2004). It was recently demonstrated that FMRP can be post-translationally methylated on four critical arginine residues within the RGG-box domain (Denman, 2002; Denman et al., 2004; Stetler et al., 2006). Methylation of these residues reduced the ability of FMRP to associate with mRNA, particularly mRNAs containing G-quartet tertiary structures, the canonical target of the RGG-box (Denman, 2002; Stetler et al., 2006). Moreover, while homodimerization is unaffected by the methylation status of FMRP, methylation is necessary for heterodimerization with the FXR proteins and greatly increases the association of FMRP into dense, RNP-like, ribosome-lacking granules (Dolzhanskaya et al., 2006). It is likely, therefore, that methylation of FMRP decreases its effect on translation by decreasing its association with its mRNA ligands and by sequestering it

away from polyribosomes in RNPs. In addition, methylation of FMRP may serve to alter the mRNA targets of FMRP, from G-quartet containing mRNAs which interact with the RGG-box to kissing-complex containing mRNAs that interact with the KH domains (Stetler et al., 2006). It remains to be seen whether the methylation status of dendritically targeted FMRP can be regulated through synaptic activity and what effect, if any, this might have on synaptic function.

Thus, like many proteins which control critical cellular processes such as translation, FMRP appears to be highly regulated by multiple pathways, allowing tight temporal and spatial control over the translation of FMRP target mRNAs.

Changes in Synaptic Plasticity in FXS

The most common mental phenotype associated with FXS is a loss of cognitive ability. A prevailing view in neuroscience is that the phenomenon of synaptic plasticity – the ability of neurons to persistently strengthen (long-term potentiation, LTP) or weaken (long-term depression, LTD) individual synaptic connections in response to activity patterns – is a molecular mechanism underlying memory and cognition. Recently, several studies have investigated whether the loss of mental function in the absence of FMRP may result from impairments or alterations in synaptic plasticity. Two principle findings have emerged from this work: enhanced Gq-protein receptor-dependent LTD and impaired cortical LTP in *Fmr1*-KO mice.

Activation of multiple Gq-coupled neurotransmitter receptors induces LTD in several regions of the brain (Huber et al., 2000; Pfeiffer and Huber, 2006; Volk et al., 2007; Zhang and Linden, 2003). The most well-characterized of these are the group I metabotropic glutamate receptors (mGluRs), mGluR1 and mGluR5, which mediate persistent changes in neurons and synaptic function and are important for many cognitive processes, including learning and memory, drug addiction, and chronic pain (Balschun and Wetzel, 2002; Chiamulera et al., 2001; Huber et al., 2000; Huber et al., 2001; Swanson et al., 2005). Although Gq proteins canonically couple to the PLC? IP3? PKC? Ca^{++} biochemical pathway, there is little evidence suggesting that this pathway plays a role in mGluR-dependent LTD (mGluR-LTD). Instead, mGluR-

dependent activation of the MEK? ERK? Mnk and PI3K? Akt? mTOR pathways mediate mGluR-LTD (for review, see (Ronesi and Huber, 2008b)). Most importantly for FXS research, mGluR-LTD requires rapid dendritic synthesis of pre-existing mRNAs (Huber et al., 2000). In fact, many mRNAs that have been shown to be translated following mGluR activation are known targets of FMRP. In addition, the signaling pathways that induce mGluR-LTD also regulate FMRP (described above).

mGluR-LTD is enhanced in both the hippocampus and cerebellum of *Fmr1*-KO mice (Hou et al., 2006; Huber et al., 2002; Koekkoek et al., 2005), while mGluR-LTD is abolished in mice that overexpress FMRP (Hou et al., 2006). Importantly, a distinct form of LTD, which is induced by activation of NMDA receptors (NMDAR) and does not require protein synthesis for its induction, is unaffected in *Fmr1*-KO mice (Huber et al., 2002). The initial interpretation of these data was that FMRP acted to inhibit translation of mRNAs that were required for mGluR-LTD. It was proposed that in the absence of FMRP there would be increased levels of mGluR-stimulated protein synthesis, leading to enhanced mGluR-LTD. One of the proteins synthesized in response to mGluR activation is FMRP itself, suggesting that it may normally function as a negative feedback mechanism to limit mGluR-stimulated translation. Recent data, however, have suggested an alternate explanation. Rather than enhanced protein synthesis following mGluR activation, *Fmr1*-KO mice display a near-complete absence of mGluR-stimulated translation (Hou et al., 2006; Ronesi and Huber, 2008a). Instead, *Fmr1*-KO mice have elevated basal protein synthesis and increased baseline levels of several proteins known to be synthesized by mGluR activation (Hou et al., 2006; Lu et al., 2004; Qin et al., 2005). This led to the current model of mGluR-LTD in *Fmr1*-KO mice, which states that in the absence of FMRP control of translation, there are increased basal levels of proteins necessary for mGluR-LTD (termed "LTD proteins"), which causes an enhancement of the synaptic depression following mGluR stimulation (Fig 1.2). A direct prediction from this hypothesis is that mGluR-LTD, which is normally blocked by administration of protein synthesis inhibitors, should be insensitive to acute blockade of translation in *Fmr1*-KO mice because the proteins necessary for mGluR-LTD expression have already been produced. Indeed, it was recently demonstrated that in the absence of FMRP,

mGluR-LTD persists following acute application of protein synthesis inhibitors (Hou et al., 2006; Nosyreva and Huber, 2006).

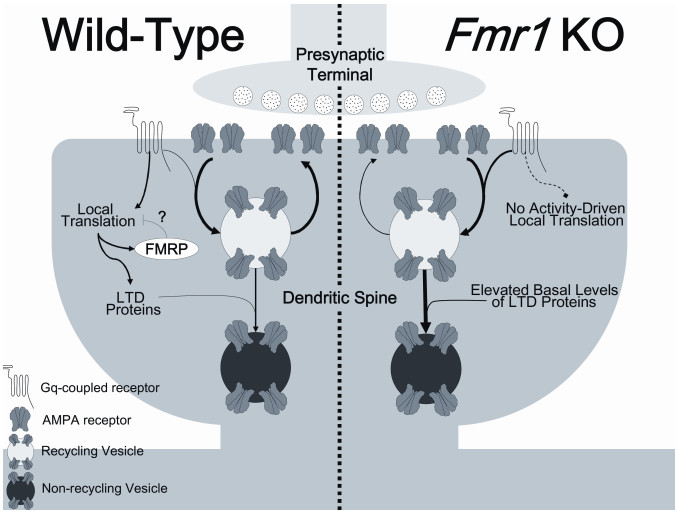

Figure 1.2. Simplified model of altered mGluR-LTD in *Fmr1*-KO mice. **Wild-Type**, In wild-type neurons, act ivation of mGluRs induces the internalization of AMPARs and simulatenously induces local translation of several dendritically localized mRNAs. This local translation is likely limited to a short burst of protein synthesis through the inhibitory effects of FMRP (see Figure 1.1). The newly synthesized proteins ("LTD proteins") are necessary to maintain the internalized AMPARs in the cytoplasm. In the presence of protein synthesis inhibitors, "LTD proteins" are not synthesized and the internalized AMPARs are rapidly returned to the postsynaptic surface. ***Fmr1*-KO**, In *Fmr1*-KO neurons, mGluR activation fails to induce local translation. This may be because in the absence of FMRP, local translation of these proteins is already at a maximum level, as evidenced by the presence of elevated basal levels of "LTD proteins." Alternatively, FMRP may be necessary for both the initiation and suppression of local translation (see Figure 1.1) and in the absence of the protein, translation of mRNA targets of FMRP is globally misregulated. The persistant increase in "LTD proteins" leads to increased maintenance of internalized AMPARs, resulting in enhanced mGluR-LTD. Thus, acute application of protein synthesis inhibitors fails to block mGluR-LTD in *Fmr1*-KO neurons.

The mechanisms responsible for enhanced mGluR-LTD remain elusive. In *Fmr1*-KO mice, there is a reduced association of one subtype of the mGluR family, mGluR5, with the protein Homer, which serves as both a synaptic scaffold and a signaling protein (Giuffrida et al., 2005; Ronesi and Huber, 2008a). The reduction in mGluR5 association with Homer in *Fmr1*-KO mice suggests that mGluR5 may not be anchored to the post-synapse. Indeed, there is a reduced synaptic localization of mGluR5 in the KO mouse (Giuffrida et al., 2005). mGluR-Homer interactions are normally required for mGluR-LTD, as they link mGluR stimulation with activation of the PI3K? Akt? mTOR pathway (Ronesi and Huber, 2008a). However, in hippocampal slices prepared from *Fmr1*-KO mice, inhibition of mGluR-Homer interaction fails to affect mGluR-LTD (Ronesi and Huber, 2008a). It is unclear whether the uncoupling of

mGluR5 from Homer, and the subsequent removal of mGluR5 from synapses, is a direct effect of FMRP loss or whether it might be caused by compensatory changes.

Recent data also implicate FMRP in the regulation of LTD induced by other Gq-coupled receptors (Volk et al., 2007). Specifically, activation of Gq-coupled muscarinic acetylcholine receptors induces a protein synthesis-dependent LTD (mAChR-LTD) which relies upon some of the same signaling pathways as mGluR-LTD and is similarly enhanced in *Fmr1*-KO mice (Volk et al., 2007). As with mGluR-LTD, mAChR-LTD is insensitive to protein synthesis inhibitors in *Fmr1*-KO mice, and activation of mAChRs fails to stimulate the translation of FMRP mRNA targets in *Fmr1*-KO mice (Volk et al., 2007). Thus, the plasticity induced by multiple Gq-coupled receptors is similarly altered in *Fmr1*-KO mice, suggesting a convergent point of misregulation in the absence of FMRP.

Transient activation of group I mGluRs can also elicit prolonged synchronized discharges in hippocampal slices, which resemble the synchronized neuronal activity observed during epileptic seizures (Chuang et al., 2005; Taylor et al., 1995). This form of mGluR-dependent synaptic plasticity, like mGluR-LTD, relies on new protein synthesis for its induction (Merlin et al., 1998). Such epileptiform discharges require strong activation of mGluRs with pharmacological agonists in WT hippocampal slices – synaptic activity alone is not sufficient to induce their expression (Lee et al., 2002). However, in *Fmr1*-KO mice, increased synaptic activity caused by the GABA receptor antagonist bicuculline induced robust epileptiform discharges that were blocked by acute administration of mGluR antagonists (Chuang et al., 2005). These data strongly imply that synaptic activity induces a much higher level of mGluR activation or function in *Fmr1*-KO neurons, and that this increased mGluR function can result in persistent epileptiform discharges. This finding was particularly intriguing considering that roughly 25% of FXS patients suffer from epilepsy and that *Fmr1*-KO mice are particularly susceptible to audiogenic seizures (Chen and Toth, 2001; Musumeci et al., 2000; Musumeci et al., 1999; Sabaratnam et al., 2001; Yan et al., 2004).

In addition to altered mGluR-dependent epileptiform bursts and Gq-dependent-LTD in the hippocampus and cerebellum, cortical LTP is also affected in *Fmr1*-KO mice.

Multiple studies have reported a complete absence of LTP in Layer V of the visual, anterior cingulate, and somatosensory cortices of *Fmr1*-KO mice using a variety of induction paradigms. Although many forms of LTP in the hippocampus and cortex are canonically believed to require NMDAR function, there is a report demonstrating that LTP induced by theta-burst stimulation (TBS) in neocortical layers V and VI may instead rely upon mGluR activation (Wang and Daw, 2003). Thus, while mGluR-LTD in the hippocampus and cerebellum appears to be enhanced in *Fmr1*-KO mice, mGluR-dependent LTP may be impaired.

Additional data pointing to a loss of mGluR-dependent LTP comes from studies in the lateral amygdala, a brain region known to be important in fear-related memory (Dityatev and Bolshakov, 2005; Rodrigues et al., 2004). LTP in the lateral amygdala has been demonstrated to be dependent upon the activity of mGluR5, as a specific antagonist of mGluR5, MPEP, completely abolishes amygdalar LTP (Rodrigues et al., 2002). In *Fmr1*-KO mice, LTP in the lateral amygdala is absent, indicating impaired mGluR function in this brain region (Zhao et al., 2005). As might be expected in a mouse model with reduced synaptic plasticity in the amygdala, *Fmr1*-KO mice display impaired fear memory (Zhao et al., 2005).

Alterations in cortical LTP in the absence of FMRP may also be dependent upon the age of the mouse. A recent study demonstrated that LTP induced by TBS in the anterior piriform cortex is normal in young, 3-6 month old *Fmr1*-KO mice, partially impaired in 6-12 month old *Fmr1*-KO mice, and greatly impaired (but not abolished) in 12-18 month old *Fmr1*-KO mice (Larson et al., 2005). Interestingly, no changes were observed in hippocampal LTP at any age.

In fact, nearly every study examining hippocampal LTP, which has been repeatedly shown to rely upon NMDAR activity and is largely insensitive to blockade of mGluRs, has demonstrated normal LTP in the hippocampus of *Fmr1*-KO mice using a variety of induction paradigms. However, a recent report observes a deficit in hippocampal LTP induced by a specific TBS protocol (Lauterborn et al., 2007). When 10 theta bursts were used to induce LTP, no difference was observed between WT and *Fmr1*-KO hippocampal slices, consistent with previous reports. When only 5 theta bursts

were applied, however, *Fmr1*-KO hippocampal slices failed to demonstrate LTP, while WT hippocampal slices displayed robust LTP. The interpretation of these data was that the mechanisms necessary for inducing LTP remain intact in the *Fmr1*-KO mouse, but the threshold for initiating hippocampal LTP in *Fmr1*-KO mice is increased.

Further evidence supporting the hypothesis that the threshold for inducing LTP is increased in the absence of FMRP comes from a study investigating spike-timing dependent plasticity (STDP) in the neocortex of *Fmr1*-KO mice (Desai et al., 2006) . STDP, which is considered to be one of the most physiologically relevant paradigms for inducing long-term synaptic plasticity, is evoked by repeated pairings of a presynaptic input and a postsynaptic depolarization. The order of the pre- vs. post-synaptic stimulation and the length of time between the two (?t) determines the direction (LTP vs. LTD) and magnitude, respectively, of the resulting plasticity. While STD-LTD was normal in *Fmr1*-KO mice, STD-LTP was absent under the standard induction paradigm (Meredith et al., 2007). Investigations into the mechanism underlying this impairment revealed a reduction of L-type Ca^{++} channels and a partial loss of external Ca^{++} influx in the spines of *Fmr1*-KO mice. Prolonged induction paradigms, which increased postsynaptic Ca^{++} entry, restored STD-LTP in *Fmr1*-KO mice, strongly suggesting that the underlying mechanisms for LTP remain intact in the absence of FMRP. This work attributed the altered Ca^{++} dynamics to elongated spine structure, thereby linking altered spine morphology with a functional plasticity deficit.

Importantly, despite the above studies demonstrating altered synaptic plasticity in the *Fmr1*-KO mouse, there appear to be no changes in basal synaptic function. Input/output curves, a gross measure of general synaptic strength, appear normal in the absence of FMRP (Huber et al., 2002; Larson et al., 2005; Li et al., 2002; Zhao et al., 2005). In addition, both pre-synaptic release probability and post-synaptic strength, as measured by paired-pulse facilitation and miniature event amplitude, respectively, are unchanged in *Fmr1*-KO mice (Centonze et al., 2008; Desai et al., 2006; Hou et al., 2006; Koekkoek et al., 2005; Larson et al., 2005; Pfeiffer and Huber, 2007; Zhao et al., 2005). Finally, the expression and function of NMDARs, which are necessary for most forms of synaptic plasticity, appears normal in *Fmr1*-KO mice (Desai et al., 2006; Li et al., 2002;

Zhao et al., 2005). Thus, global synaptic function appears normal following the loss of FMRP expression, even though several important forms of synaptic plasticity are absent or significantly altered. This is somewhat perplexing, as impaired LTP coupled with enhanced LTD should result in significantly weaker synaptic function, which is not what has been observed. This inconsistency remains to be resolved in the literature.

The mGluR Theory of Fragile X

There is considerable evidence in the literature indicating a link between mGluR activity and FXS. As described in detail above, mGluR-LTD in both the hippocampus and the cerebellum is enhanced in mice lacking FMRP expression (Hou et al., 2006; Huber et al., 2002; Koekkoek et al., 2005). In addition, mGluR-LTD in *Fmr1*-KO mice is no longer blocked by acute administration of protein synthesis inhibitors (Hou et al., 2006; Nosyreva and Huber, 2005; Nosyreva and Huber, 2006). mGluR-induced epileptiform bursts are also enhanced in *Fmr1*-KO mice (Chuang et al., 2005) LTP in cortex and amygdala, which is dependent upon mGluR activity, is absent or significantly impaired in *Fmr1*-KO mice (Desai et al., 2006; Larson et al., 2005; Li et al., 2002; Meredith et al., 2007; Wilson and Cox, 2007; Zhao et al., 2005). mGluR-mediated protein synthesis is absent in *Fmr1*-KO mice and many proteins that are synthesized in response to mGluR activation have elevated expression levels in the absence of FMRP (Hou et al., 2006; Lu et al., 2004; Ronesi and Huber, 2008a; Zalfa et al., 2007). Finally, FMRP expression, dendritic localization, and phosphorylation status are regulated by mGluR activity (Antar et al., 2004; Ferrari et al., 2007; Hou et al., 2006; Narayanan et al., 2007; Narayanan et al., 2008; Todd and Mack, 2000; Wang et al., 2008; Weiler et al., 1997).

There is additional indirect evidence suggesting that mGluR function may play a role in the expression of many phenotypes observed in FXS. Roughly 25% of FXS patients suffer from epilepsy and *Fmr1*-KO mice are particularly susceptible to audiogenic seizures; inhibition of mGluR activity reduces the occurrence of audiogenic seizures in mice (Chapman et al., 2000; Chen and Toth, 2001). A key phenotype of FXS is increased sensitivity to sensory stimuli; mGluR activation results in enhanced neuronal

excitability (Castren et al., 2003; Sourdet et al., 2003)(Sourdet 2003, Castren 2003). FXS is characterized by heightened anxiety and obsessive-compulsive disorder, and *Fmr1*-KO mice display altered fear-based memory and repetitive behaviors; mGluR-dependent LTP in the amygdala and corticostriatal synapse are important for fear-based memory formation and habitual activity, respectively (Graybiel, 1998; Gubellini et al., 2003; Rodrigues et al., 2002; Tatarczynska et al., 2001). Finally, FXS patients and *Fmr1*-KO mice display impaired eyeblink conditioning; cerebellar LTD, which is induced by mGluR activity, mediates eyeblink conditioning (Koekkoek et al., 2005).

The findings of enhanced mGluR-LTD in *Fmr1*-KO mice, alterations in mGluR-mediated protein synthesis in *Fmr1*-KO mice, clear biochemical pathways connecting mGluR activation to FMRP regulation, and multiple links between FXS symptoms and mGluR-mediated neural functions led to a novel view of the disease: the mGluR theory of FXS (Bear et al., 2004). This theory postulates that many of the symptoms of FXS stem from increased and unregulated activity of group I mGluRs, particularly those that rely upon protein synthesis for their induction or maintenance.

The mGluR theory is supported by literature in the FXS field, specifically those studies demonstrating enhanced mGluR-LTD in *Fmr1*-KO mice. However, the mGluR theory, in its most basic form, seems at odds with several key pieces of data. Firstly, mGluR-mediated protein synthesis is absent in *Fmr1*-KO mice, suggesting impaired mGluR activity. However, the mGluR theory accounts for this by asserting that the normal neuronal function of FMRP is to inhibit mGluR-mediated translation, such that in the absence of FMRP (in either *Fmr1*-KO mice or FXS patients), mGluR-mediated translation is persistently and maximally activated so that further mGluR activation fails to induce additional protein synthesis. Additional data seemingly inconsistent with the notion of enhanced mGluR activity in FXS are studies demonstrating abolished mGluR-mediated LTP in the amygdala and Layer V of the neocortex of *Fmr1*-KO mice. The mGluR theory would explain this data by predicting that these forms of plasticity are induced and maintained by mGluR-mediated protein synthesis, and in the absence of FMRP, maximal synthesis of these proteins leads to a saturation of the LTP such that no more can be elicited.

The mGluR theory predicts that inhibition of mGluR activity should reduce or abolish phenotypes associated with the loss of FMRP. Several key studies have largely confirmed this prediction. Suppression of GABA-ergic transmission in hippocampal area CA3 causes epileptiform discharges which are prolonged in *Fmr1*-KO mice (Chuang et al., 2005). In agreement with the mGluR theory, application of an mGluR antagonist rescues this phenotype completely. Similarly, treatment with the mGluR5 antagonist MPEP reduced the prevalence of audiogenic seizures in *Fmr1*-KO mice (Yan et al., 2005). Furthermore, multiple physiological and behavioral alterations in dFmr1-null *Drosophila* are also rescued following treatment with MPEP (McBride et al., 2005). In addition, neuronal growth and craniofacial alterations following FMRP deletion in zebrafish is reversed by exposure to MPEP during embryonic development (Tucker et al., 2006). Finally, genetically decreasing the levels of mGluR5 in an *Fmr1*-KO mouse completely rescues multiple phenotypes, including increased spine number, increased basal protein synthesis, increased susceptibility to audiogenic seizures, and impaired inhibitory avoidance extinction memory (Dolen et al., 2007). Thus, the mGluR theory has led to the promise of a pharmacological treatment for FXS, a situation that would have been unthinking less than a decade ago.

Recent data demonstrating that *Fmr1*-KO mice display altered translation-dependent synaptic plasticity following activation of a second Gq-coupled receptor (mAChR) (Volk et al., 2007) indicate that multiple Gq-coupled receptors may converge upon FMRP-regulated translation. This finding strongly argues for both an expansion of the mGluR theory to encompass multiple Gq-associated proteins and a broadening of the search for pharmaceutical and therapeutic targets for FXS treatment, as multiple Gq-coupled receptors appear to converge upon many similar pathways which are misregulated in the absence of FMRP. Altering the function of just one Gq-coupled receptor may ameliorate some of the symptoms of FXS, allowing the selective use of pharmaceutical agents to prevent unwanted side effects.

Motivation for Studies and Summary of Research

Fragile X Syndrome, the most common form of inherited mental retardation, is caused by the loss of FMRP function. FMRP is a selective mRNA-binding protein, and likely functions to regulate the translation of its mRNA targets, particularly in response to mGluR stimulation. Loss of FMRP expression in both FXS patients and *Fmr1*-KO mice results in an increase in the numbers of dendritic spines. Furthermore, the dendritic spines observed in *Fmr1*-KO mice and FXS patients display a clear structural shift toward an immature morphology. *Fmr1*-KO mice also display altered synaptic plasticity and aberrant mGluR-mediated protein synthesis.

Before the experiments described in Chapter 2 were performed, it was unknown whether FMRP loss caused the above changes in neuronal morphology and function through a deficit in neuronal development or through a loss of immediate, acute FMRP activity in mature neurons. Previous studies had relied upon comparison of WT mice and *Fmr1*-KO mice, in which FMRP had been eliminated from the onset of development, and thus could not differentiate between these two possibilities. In addition, although the increased numbers of dendritic spines observed in *Fmr1*-KO mice and FXS patients suggests an increase in the number of functional synapses, the fact that these spines appear to be morphologically immature raises the possibility that the number of functional synapses may not be different or may even be reduced following loss of FMRP. Thus, the question of whether FMRP directly regulates synapse number had not been previously addressed. Furthermore, the precise mechanisms through which loss of FMRP results in the phenotypes observed in FXS patients and *FMR1*-KO mice was unclear. Finally, the role that FMRP plays in translation had largely been determined through *in vitro* assays in which FMRP and a single mRNA target were both massively overexpressed. There had been few studies which investigated the role of FMRP-dependent protein synthesis *in vivo*, and a systematic, detailed analysis of how FMRP association with target mRNAs or regulation of translation affected the phenotypes observed in *Fmr1*-KO mice had not been performed. At the time the experiments described in Chapter 2 were conducted, the mGluR theory of FXS had not yet been developed, and no rescue of an *Fmr1*-KO phenotype had been reported.

Considering the importance of understanding the mechanisms underlying FMRP-related changes in neuronal function, I sought to examine the role that FMRP may play in regulating synaptic function in mature neurons. Toward this end, I expressed wild-type FMRP at near-endogenous levels in hippocampal slices and dissociated neurons derived from *Fmr1*-KO mice. My experimental paradigms allowed me to make side-by-side electrophysiological and immunocytochemical comparisons between neurons expressing FMRP and *Fmr1*-KO neurons. Based upon the prevailing evidence in the field, we hypothesized that FMRP expression would reduce synapse number and that this effect would require association of FMRP with its target mRNAs through RGG-box interactions and through translational inhibition of its mRNA ligands.

I observed that acute FMRP expression induced rapid loss of synaptic connections, with no apparent change in the function of the remaining synapses, consistent with our hypothesis. I was further able to express several mutant forms of FMRP to determine regions important for regulation of synapse number. I identified the KH2 RNA-binding domain as critically important for FMRP function in this assay, as a point mutation in this region abolished the ability of FMRP to alter synapse number. Interestingly, in disagreement with our hypothesis, I observed no effect of deletion of the RGG-box domain, suggesting that RGG-box–mRNA interactions are unnecessary for FMRP-dependent synapse elimination. Furthermore, I determined that while a mutant form of FMRP that cannot be phosphorylated induced synapse loss similarly to wild-type FMRP, a phospho-mimic form of FMRP failed to alter synapse number. As phosphorylated FMRP is believed to inhibit translation of its mRNA targets, while dephosphorylated FMRP is believed to allow or possibly even stimulate translation, this result indicated that FMRP may regulate synapse number through actively inducing the translation of select mRNAs. This finding was at odds with the canonical view of FMRP function at the time, which held that FMRP acted solely as a translational inhibitor.

My data strongly suggests that FMRP regulates synapse number by actively inducing the translation of target mRNAs. I wished to identify which mRNA targets were necessary for FMRP-dependent synapse loss. The transcription factor myocyte-enhancer factor 2 (MEF2) induces the transcription of several mRNA targets of FMRP

and negatively regulates synapse number in a manner similar to FMRP (as described in detail in Chapter 4). Based upon these data, I hypothesized that there might be a genetic interaction between FMRP and MEF2. I observed that while MEF2 activity induced robust synapse loss in WT neurons, it failed to alter synapse number or function in *Fmr1*-KO neurons. In addition, FMRP-induced synapse loss was completely prevented by expression of a dominant-negative form of MEF2. These data implicate FMRP translational regulation of MEF2-derived transcripts in regulation of synapse number.

I further sought to investigate the molecular mechanisms and signal transduction pathways through which FMRP might control synapse number. Using a variety of pharmacological inhibitors, I performed several experiments examining whether synaptic activity or specific signaling molecules or proteins were important for FMRP-dependent synapse loss. Although largely preliminary, these studies never-the-less provide useful information and launch points for future studies on FMRP-mediated synapse elimination.

The data presented in this work detail novel effects of FMRP on neuronal function and development, and further describe specific molecular mechanisms through which FMRP functions to affect synapse number. In addition, these experiments describe a previously unreported, fundamental genetic interaction of FMRP with MEF2, providing additional insight into how FMRP may alter not only synapse number, but also other aspects of neuronal function, including synaptic plasticity. These data provide unique avenues for FXS therapies suggest novel strategies for FXS treatment.

CHAPTER TWO

Fragile X Mental Retardation Protein Induces Synapse Loss through Acute Postsynaptic Translational Regulation

Summary

Fragile X syndrome, as well as other forms of mental retardation and autism, is associated with altered dendritic spine number and structure. Fragile X syndrome is caused by loss-of-function mutations in Fragile X mental retardation protein (FMRP), an RNA-binding protein that regulates protein synthesis *in vivo*. It is unknown whether FMRP plays a direct, cell-autonomous role in regulation of synapse number, function, or maturation. Here, I report that acute postsynaptic expression of FMRP in *Fmr1* knock-out (KO) neurons results in a decrease in the number of functional and structural synapses without an effect on their synaptic strength or maturational state. Similarly, neurons endogenously expressing FMRP (wild-type) have fewer synapses than neighboring *Fmr1*-KO neurons. An intact K homology domain 2 (KH2) RNA-binding domain and dephosphorylation of FMRP at S500 were required for the effects of FMRP on synapse number, indicating that FMRP interaction with RNA and translating polyribosomes leads to synapse loss.

Introduction

Altered dendritic spine number and structure is associated with mental retardation and autism (Bagni and Greenough, 2005; Kaufmann and Moser, 2000; Pickett and London, 2005), suggesting that deficits in synaptic connectivity and function contributes to the etiology of these prevalent diseases. Fragile X syndrome (FXS) is the most common inherited form of mental retardation and is caused by loss of function mutations in the Fragile X mental retardation gene (*FMR1*). FXS affects ~1/4000 males and 1/8000 females and is characterized by several physical, behavioral, and cognitive abnormalities, including mild to severe mental retardation, hyperactivity, and autism (O'Donnell and Warren, 2002). Cortical neurons in patients with FXS and *Fmr1* knock-out (*Fmr1*-KO)

mice have increased dendritic spine density, as well as longer spines, reminiscent of immature filopodia (Irwin et al., 2001; Nimchinsky et al., 2001; Bagni and Greenough, 2005; Antar et al., 2006; Grossman et al., 2006a,b). From these findings, it has been suggested that the protein product of *Fmr1*, Fragile X mental retardation protein (FMRP), facilitates synapse elimination or pruning and regulates synapse maturation (Weiler and Greenough, 1999; Bagni and Greenough, 2005; Antar et al., 2006). FMRP is an RNA-binding protein and functions to regulate mRNA translation in neurons and synapses (Feng, 2002; O'Donnell and Warren, 2002; Weiler et al., 2004; Bagni and Greenough, 2005; Grossman et al., 2006a). Although the lifelong loss of FMRP in humans and mice results in altered dendritic spines, it is unknown whether FMRP directly regulates synapse number, function, or maturation in a cell autonomous manner or whether these changes can be reversed with postnatal expression of FMRP. Furthermore, no role for FMRP regulated translation in mammalian synapse development has been established.

Determining the function of FMRP in neurons is critical to understanding deficits in neuronal function that result from its absence, as in FXS. In the present study, I investigate the role of FMRP in synaptic function and synapse maturation *in vitro* by acutely expressing FMRP in *Fmr1*-KO neurons and directly comparing them to neighboring *Fmr1*-KO neurons using both electrophysiological and immunocytochemical techniques. I find that acute postsynaptic expression of FMRP in *Fmr1*-KO neurons in culture reduces the number of functional and structural synaptic connections without altering the strength or maturational state of the remaining synapses. As observed with acute exogenous expression of FMRP, wild-type (WT) neurons have fewer synapses than their *Fmr1*-KO neighbors in dissociated cocultures. Mutations of FMRP in the K homology domain 2 (KH2) RNA-binding region or that mimic phosphorylated FMRP are unable to affect synapse number or function. These results support the idea that FMRP directly regulates synapse number postnatally through postsynaptic interactions with RNA and regulation of translation.

Materials and Methods

Hippocampal slice cultures and FMRP transfection

Organotypic hippocampal slice cultures were prepared from postnatalday 6 (P6) WT or *Fmr1*-KO mice bred from the congenic C57BL/6 mouse strain (Jackson Laboratories, Bar Harbor, ME) using previously published protocols (Stoppini et al., 1991). Biolistic transfection and gold bullet preparation were performed with the Helios Gene Gun system (Bio-Rad, Hercules, CA) according to the manufacturer's protocols (McAllister, 2004). All FMRP-green fluorescent protein (GFP) constructs were obtained from Dr. Jennifer Darnell at Rockefeller University and are driven by the human *FMR1* promoter. Construction of the GFP-tagged FMRP (wtFMRP-GFP) as well as I304N FMRP and arginine/glycine-rich box (RGG) deletion (ΔRGG) FMRP have been described previously (Darnell et al., 2005). The S500A and S500D mutations were introduced into wtFMRP-GFP by QuikChange site-directed mutagenesis (Stratagene, La Jolla, CA) of the *Kpn*I-fragment, which was subcloned into pBluescript for mutagenesis and then replaced in the WT construct.

Dissociated culture and immunocytochemistry

Dissociated CA3–CA1 hippocampal cultures (dentate gyrus was cutoff) were prepared from P0–P1 WT and *Fmr1*-KO mice using modified, previously published protocols (Brewer et al., 1993). Neurons were plated at a density of 250 neurons/mm^2 on poly-D-lysine/laminin or matrigel coated coverslips. At 7 days *in vitro* (DIV), cultures were transfected with either calcium phosphate or Lipofectamine 2000 (Invitrogen, Eugene, OR). At 12 DIV, cells were fixed in 4% paraformaldehyde (PFA)/4% sucrose for 15 min at 37°C, blocked in PBS/10% goat serum and labeled with 1° antibody against the extracellular N terminus of glutamate receptor 1 (GluR1; 1:50; Calbiochem, La Jolla, CA). For the postsynaptic marker 95 kDa postsynaptic density protein (PSD-95) and synapsin, neurons were permeabilized with 0.2% Triton-X for 1 h before treatment with 1° antibodies to PSD-95 (1:800; Affinity Bioreagents, Golden, CO), synapsin (1:1,000; provided by Dr. Thomas Sudhof, University of Texas Southwestern Medical Center), or 2F5 monoclonal FMRP antibody (1:400) (Gabel et al., 2004) (provided by Dr. Justin

Fallon, Brown University, Providence, RI, and Dr. Jennifer Darnell, Rockefeller University, New York, NY) for 1 h and AlexaFluor-conjugated 2° antibodies (1:300, 1 h; Invitrogen). Hippocampal slice cultures were fixed in 4% PFA (4°C, overnight) permeabilized with 0.7% Triton-X (4°C, overnight). The slices were treated with 2F5 FMRP antibody (1:400) and AlexaFluor 2° antibody (1:300 both overnight at 4°C).

Fluorescence was detected using a Nikon (Tokyo, Japan) TE2000 inverted microscope equipped with a cooled CCD camera (dissociated neuron culture) or a Zeiss (Oberkochen, Germany) LSM 510 Meta confocal microscope (slice sections). Images were analyzed and quantitated using MetaMorph software (Universal Imaging, Downingtown, PA). Healthy neurons are first identified by their smooth soma and multiple processes under differential interference contrast (DIC) microscopy. For synaptic staining, immunoreactive puncta are defined as discrete points along a dendrite (within 50 μm from the soma) with fluorescence intensity at least twice the background staining of a region adjacent to the dendrite. Significant differences between *Fmr1*-KO neurons and WT or FMRP-transfected neurons were determined with an unpaired *t* test. For all group data, averages +SEM are plotted and *n* (number of cells) is on each bar (*$p < 0.05$; **$p < 0.01$; ***$p < 0.001$).

Electrophysiology

Simultaneous whole-cell recordings were obtained from CA1 pyramidal neurons in slice cultures visualized using infrared-DIC and GFP fluorescence to identify transfected and nontransfected neurons. Recordings were made at 30°C in a submersion chamber perfused at 3 ml/min with artificial CSF (ACSF) containing the following (in mM): 119 NaCl, 2.5 KCl, 26 NaHCO3, 1 NaH_2PO_4, 11 D-Glucose, 3 CaCl2, 2 MgCl2, 0.1 picrotoxin, 0.002 2-chloro-adenosine, 0.1% DMSO, pH 7.28, 320 mOsm and saturated with 95% O_2/5%CO_2. For all intracellular recordings, the neuron was clamped at –60 mV through whole-cell recording pipettes (~3–7 MΩ) filled with an intracellular solution containing the following (in mM): 2.5 BAPTA, 125 Cs-Meth, 6 CsCl, 3 NaCl, 10 HEPES, 10 sucrose, 2 QX-314, 10 tetraethylammonium-Cl, 4 ATP-Mg, 0.4 GTP-Na, 14 phosphocreatine-Tris, pH 7.2, 285 mOsm. For isolated NMDA receptor (NMDAR)

measurements, the ASCF was supplemented with 20 µM DNQX and 20 µM glycine and the neuron was clamped at +50 mV. For mEPSC measurements, the ACSF was supplemented with 1 µM TTX. Synaptic responses were evoked by single bipolar electrode placed in stratum radiatum of area CA1 (along the Schaeffer collaterals) 50–200 µm from the recorded neurons with monophasic current pulses (5–40 µA, 200 µs). For minimal stimulation experiments, a glass theta-tube electrode was filled with ACSF and positioned in the stratum radiatum along the Schaeffer collaterals ~20–50 µm from the recorded neurons. Once a synaptic response was obtained, the stimulation intensity was gradually decreased until synaptic failures and synaptic successes could be clearly distinguished in both neurons (typically 0.5–5 µA). Capacitance, series resistance, and input resistance were measured in voltage clamp with a 400 ms, –10 mV step from a –60 mV holding potential (filtered at 30 kHz, sampled at 50 kHz). The capacitance was calculated by first obtaining the decay time constant of a current transient induced by a voltage step (the faster time constant of a double-exponential decay fitted to the first 20 ms) and then dividing this by the series resistance. Cells were only used for analysis if the series resistance was <30 M? and was stable throughout the experiment. Input resistance ranged from 75 to 350 M? . Data were not corrected for junction potential.

Synaptic potentials were filtered at 2 kHz, acquired and digitized at 10 kHz on a personal computer using custom software (Labview; National Instruments, Austin, TX). Time constants (t) of the decay of isolated NMDAR EPSCs were determined by fitting the decay of the maximum amplitude of NMDAR EPSC with a double exponential in LabView using the Levenberg-Marquardt algorithm to determine the least-squares set of coefficients that best fit the set of input data points (X,Y) as expressed by a nonlinear function $y = f(x,a)$, where a is the set of coefficients. Miniature EPSCs (mEPSCs) were detected off-line using an automatic detection program (MiniAnalysis; Synaptosoft, Decatur, GA) with a detection threshold set at a value greater than at least 2 SD of the noise values, followed by a subsequent round of visual confirmation. The detection threshold remained constant for the duration of each experiment. Failures and successes were defined as responses with amplitudes less than or >10 pA, respectively, followed by a subsequent round of visual confirmation for each qualification without knowledge of

the transfection state of the neuron. The percentage of silent synapses calculated as 1 – ln(failure rate at –60 mV)/ln(failure rate at +50), as described previously (Liao et al., 1995). Significant differences between transfected and nontransfected neurons were determined using a paired *t* test.

Results

Acute expression of FMRP reduces evoked excitatory synaptic transmission

To determine whether FMRP acutely regulates evoked excitatory synaptic transmission, I acutely expressed a GFP-tagged human FMRP (wtFMRP-GFP) in organotypic hippocampal slice cultures prepared from P6 *Fmr1*-KO mice. Neurons were biolistically transfected at 3 DIV with wtFMRP-GFP driven via the endogenous human *FMR1* promoter to avoid strong overexpression. wtFMRP-GFP displays similar polyribosome association and localization as endogenous FMRP, suggesting that addition of the N-terminal GFP does not affect the protein's function (Antar et al., 2004, 2006; Darnell et al., 2005). Consistent with the pattern of endogenous FMRP expression, wtFMRP-GFP was punctate throughout the soma and dendritic arborization (Fig. 2.1*A*) (Antar et al., 2004). To quantify the levels of wtFMRP-GFP expression after transfection, immunocytochemistry for FMRP in untransfected wild-type and transfected *Fmr1* KO slice cultures was performed (Fig. 2.7*A*). Somatic wtFMRP-GFP expression in transfected *Fmr1* KO neurons was ~180% of that observed in WT neurons (Fig. 2.7*B*). Although transfected FMRP levels are greater than endogenous FMRP levels in unstimulated WT neurons, these levels are within the physiological range of FMRP induced by experience or neuronal activity (Weiler et al., 1997; Todd and Mack, 2000; Hou et al., 2006).

Three to seven days posttransfection (equivalent postnatal day 12–16), simultaneous whole-cell patch-clamp recordings were obtained from untransfected *Fmr1*-KO and neighboring transfected wtFMRP-GFP-expressing CA1 pyramidal neurons (hereafter referred to as "neuron pairs"). AMPA receptor (AMPAR)-mediated EPSCs were evoked with extracellular stimulation of Schaffer collateral axons and were measured in the neuron pairs held at –60 mV. I observed an ~20% reduction in the

amplitude of EPSCs in neurons transfected with wtFMRP-GFP (Fig. 2.1*B,D*). No significant difference was observed between transfected and untransfected neurons in resting membrane potential, input resistance, or whole-cell capacitance (Table 2.1), indicating that overall neuronal health, subthreshold membrane conductances, and size were unaffected by transfection of wtFMRP-GFP.

Although AMPA and NMDA receptors typically colocalize at excitatory synapses, they can be differentially regulated (Petralia et al., 1999; Groc and Choquet, 2006). To determine whether wtFMRP-GFP expression affects NMDAR-mediated EPSCs, I measured the peak amplitude of isolated NMDAR-mediated EPSCs in neuron pairs, by voltage clamping neurons at +50 mV in the presence of the AMPAR antagonist, DNQX. Like AMPAR-mediated EPSCs, isolated NMDAR-mediated EPSCs were reduced by ~20% after FMRP expression (Fig. 2.1*C,D*). Although the amplitude of NMDAR-mediated EPSCs was reduced in wtFMRP-GFP-expressing neurons, there was no change in the time constants of decay of the isolated NMDAR-mediated currents (Table 2.1). Because the decay rate of NMDAR-mediated currents declines over the course of synapse maturation and is regulated by the NMDAR subunit composition (Cull-Candy et al., 2001), these results indicate that wtFMRP-GFP does not alter NMDAR subunit composition or functional synapse maturation. Transfection of GFP alone in *Fmr1* KO slice cultures had no effect on AMPAR- or NMDAR-mediated EPSCs (Fig. 2.1*E–H*). These data indicate that acute, postnatal expression of FMRP reduces evoked synaptic transmission.

FMRP reduces the frequency of miniature EPSCs

An FMRP-induced decrease in evoked EPSCs may occur through a decrease in synapse number, strength of individual synapses, or presynaptic release probability. To begin to differentiate between these possibilities, I measured the effects of FMRP on spontaneous (action-potential independent) mEPSCs in neuron pairs in the presence of TTX (1 μM) (Fig. 2.2*A*). mEPSC amplitude is indicative of the strength of individual functional synapses, whereas mEPSC frequency is dependent on synapse number as well as presynaptic release probability. The frequency of mEPSCs was reduced by ~35% in

wtFMRP-GFP-expressing cells as compared with untransfected *Fmr1*-KO neurons, whereas the amplitude of mEPSCs was unchanged (Fig. 2.2*B–D*). Neither the frequency nor the amplitude of mEPSCs was altered after GFP expression (Fig. 2.2*E–H*). Therefore, postsynaptic FMRP expression reduces synaptic transmission not by reducing the strength of individual synapses, but by either decreasing presynaptic glutamate release probability or the number of synapses.

Acute expression of FMRP increases synaptic failures, but does not affect short-term plasticity or the percentage of silent synapses

To determine effects of postsynaptic wtFMRP-GFP expression on glutamate release probability, I measured paired-pulse facilitation of EPSCs after rapid, successive stimuli (Fig. 2.3*A*) in neuron pairs. Paired-pulse facilitation is inversely proportional to presynaptic release probability and provides a relative indicator of this measure (Manabe et al., 1993). Although wtFMRP-GFP expression reduced the amplitude of the first EPSC (Fig. 2.3*C*,*D*, 2.7), similar to my previous results (Fig. 21*B*), there was no effect on paired-pulse facilitation at a range of interstimulus intervals (Fig. 2.3*B*). These results indicate that postsynaptic expression of FMRP does not affect the presynaptic release probabilities of axons providing input to that neuron.

One explanation that can account for the observed reduction in evoked synaptic responses and mEPSC frequency in FMRP expressing neurons, without a change in mEPSC amplitude or presynaptic release probability, is a reduction in the number of functional synaptic connections. To examine this idea, I used a "minimal stimulation" protocol to stimulate a small number of axons, allowing me to compare the relative number of functional synaptic connections one axon makes onto both an *Fmr1*-KO untransfected and wtFMRP-GFP-expressing neuron. Because of the probabilistic nature of glutamate release, I observed both failures and successes of synaptic transmission (Fig. 2.3*E*). Simultaneous voltage-clamp recordings of neuron pairs revealed a ~60% increase in synaptic failures in neurons expressing wtFMRP-GFP (Fig. 2.3*F*). Furthermore, the amplitude of successes, or synaptic potency, was reduced by ~35% in neurons expressing wtFMRP-GFP (Fig. 2.3*F*). Because mEPSC amplitude is unchanged (Fig. 2.2*C*,*D*), the

decrease in synaptic potency is likely caused by a decrease in the number of synaptic contacts per axon. It is important to note that the failure rate is also representative of the presynaptic release probability of a synaptic bouton. Therefore, it is possible that the changes I observe in failure rate with wtFMRP-GFP expression could be presynaptic in nature. However, based on the findings that FMRP does not alter paired-pulse facilitation, I hypothesize that FMRP results in a decrease in functional synapse number.

A hallmark of excitatory synapse maturation is the insertion of postsynaptic of AMPARs, which occurs after NMDARs (Petralia et al., 1999; Wu et al., 1996). As a result, there is a developmental decline in the number of "silent synapses," synapses that contain NMDARs, but not AMPARs (Durand et al., 1996). To determine whether FMRP regulated functional synapse maturation, I measured silent synapses in simultaneous recordings of neuron pairs. Synaptic failures and successes in response to minimal stimulation of presynaptic axons were measured at holding potentials of –60 mV and +50 mV. Expression of wtFMRP-GFP increased synaptic failures measured at both –60 mV and +50 mV, but did not affect the percentage of silent synapses (Fig. 2.3*F*). Thus, FMRP expression appears to reduce the number of synaptic connections without altering the function or maturational state of the remaining synapses.

Exogenous and endogenous postnatal expression of FMRP reduces structural synapse number

To examine whether acute FMRP expression resulted in a decrease in the number of structural synapses, I acutely expressed wtFMRP-GFP into dissociated hippocampal cultures prepared from *Fmr1*-KO mice. After transfection of wtFMRP-GFP, neurons were stained for the AMPAR subunit GluR1 (surface), the postsynaptic marker PSD-95, or the presynaptic marker synapsin. Synapsin puncta were quantified at synapses on dendrites expressing or not expressing FMRP. wtFMRP-GFP expression reduced the number of synapses as measured with all three synaptic markers by 30–40% as compared with neighboring untransfected KO neurons (Fig. 2.4*A–C*). wtFMRP did not affect the fluorescent intensity of remaining synaptic puncta, but did reduce PSD-95 puncta size (Table 2.2). As a control for transfection and GFP expression, exogenous expression of

two different FMRP-GFP mutants with single site mutations had no effect on synapse number (Figs. 2.4*A–C*, 2.6*M,N*). These results, together with my functional synapse measurements in slice culture, indicate that acute postsynaptic FMRP expression reduces the number of structural and functional synapses.

In the above experiments, I have used exogenous, acute expression of FMRP to evaluate its effects on synapses. To determine whether WT neurons expressed fewer synapses than *Fmr1*-KO neurons, I prepared dissociated cocultures containing both WT and *Fmr1*-KO neurons. This allowed me to make side-by-side comparisons of synapse number on FMRP-expressing (WT) and KO neurons on the same coverslip as performed with wtFMRP-GFP transfected neurons (Fig. 2.4*D*). Immunocytochemistry for both FMRP and synaptic markers was performed on these cocultures at 11–12 DIV to identify synapses on WT and *Fmr1*-KO neurons. As observed with acute FMRP expression, WT neurons displayed 20–35% fewer synapses as measured with all synaptic markers compared with neighboring *Fmr1* KO neurons (Fig. 2.4*D–G*). WT neurons also displayed smaller PSD-95 puncta similar to wtFMRP-GFP transfected neurons (Table 2.2). Importantly, the number of synaptic puncta in WT neurons is not different from *Fmr1*-KO neurons transfected with wtFMRP-GFP, indicating that the increased synapse number in *Fmr1*-KO neurons can be rescued by acute, postnatal, exogenous FMRP expression (Table 2.2). These data further indicate that decreases in synapse number are not merely a result of acute, exogenous FMRP expression, but reflect the function of endogenous FMRP.

Synaptic function in WT versus Fmr1 KO mice

My findings of reduced synapse number and function after FMRP expression suggest that WT neurons may have reduced synaptic function compared with *Fmr1*-KO neurons. I measured evoked AMPAR-mediated EPSCs and mEPSCs in single neurons of WT organotypic slice cultures and compared these values with those obtained from untransfected *Fmr1*-KO neurons in previous experiments. I failed to detect any differences in synaptic function between WT and *Fmr1*-KO slice cultures (AMPAR-mediated EPSCs: WT, 109.6 ± 10.3 pA, $n = 72$; *Fmr1*-KO, 100.4 ± 5.4 pA, $n = 126$; $p =$

0.4; mEPSC frequency: WT, 1.89 ± 0.23 Hz, n = 34; *Fmr1*-KO, 1.60 ± 0.14 Hz, n = 95; p = 0.3; mEPSC amplitude: WT, 28.2 ± 0.8 pA, n = 34; *Fmr1*-KO, 25.9 ± 0.6 pA, n = 95; p = 0.1). However, there is a high level of variability in evoked EPSCs and mEPSCs between slice cultures, even between slices prepared from the same animal. Specifically, the mathematical variance and SD were greater (~40%) between neurons on different slices than between neurons within the same slice. These data suggest that side-by-side comparisons of FMRP expressing and *Fmr1*-KO neurons are required to detect the 20–35% differences in synaptic function which I observe after acute FMRP transfection. In support of this view, when I minimize variability by coculturing wild-type and *Fmr1*-KO neurons, I observe a difference in the number of synapses between neighboring neurons (Fig. 2.4*D–G*).

The KH2 RNA-binding domain, but not the RGG box is required for FMRP regulation of synapse number and function

FMRP is an RNA-binding protein that binds to as many as 400 brain mRNAs and associates with large polyribosome complexes in brain and synaptoneurosomes (Feng et al., 1997a; O'Donnell and Warren, 2002; Khandjian et al., 2004; Stefani et al., 2004). FMRP interacts with RNA through several RNA-binding motifs, including two heterogeneous nuclear ribonucleoprotein (hnRNP)-KH domains (KH1 and KH2) and an arginine/glycine-rich RNA-binding motif (RGG box) (Darnell et al., 2001, 2005a; Schaeffer et al., 2001). The KH_2 domain associates with a specific RNA structure termed a "kissing complex" (Darnell et al., 2005). A single point mutation in the KH_2 domain of FMRP (an Ile to Asn switch at residue 304, originally found in a patient with a particularly severe form of FXS) abolishes FMRP interactions with kissing complex RNAs, but also reduces dimerization with other FMRP molecules and polyribosome association (Feng et al., 1997; Laggerbauer et al., 2001; Darnell et al., 2005). To test whether the FMRP-dependent reduction in synaptic function required interaction with kissing complex RNAs or polyribosomes, I expressed the I304N-FMRP-GFP construct in *Fmr1*-KO slice cultures and examined synaptic function. Although the total level of expression of this construct was not different, the expression pattern of I304N-FMRP-

GFP in dendrites was more diffuse than wtFMRP-GFP (Figs. 2.4*A–C*, 2.5*A*, Table 2.1). The diffuse expression pattern of I304N-FMRP-GFP in neurons is consistent with previous reports that I304N-FMRP associates with a smaller messenger RNP and is diffusely distributed in cultured cell lines (Feng et al., 1997; Schrier et al., 2004; Darnell et al., 2005). Transfection of I304N-FMRP-GFP into *Fmr1*-KO neurons had no effect on evoked synaptic transmission, mEPSC frequency, or amplitude (Fig. 2.5*B–F*). Similarly, I304N-FMRP-GFP expressed in *Fmr1*-KO dissociated hippocampal cultures did not affect the number, size, or intensity of synapse marker puncta (Fig. 2.4*A–C*, Table 2.2). These results indicate that postsynaptic interactions of FMRP with polyribosomes or kissing complex mRNAs are required for regulation of synapse number.

The RNA-binding domain of FMRP with the highest reported affinity for RNA is the RGG-box, which associates with a tertiary RNA structure termed a "G-quartet" (Darnell et al., 2001; Schaeffer et al., 2001). To examine whether association of FMRP with G-quartet containing mRNAs is important for the regulation of synapse function by FMRP, a mutant construct was used in which the entire RGG-box was deleted (?RGG-FMRP-GFP) (Fig. 2.5*G–L*) (Darnell et al., 2005). When this construct was introduced into *Fmr1*-KO neurons, the expression level and pattern was similar to wtFMRP-GFP (Fig. 2.5*G*, Table 2.1). Expression of ?RGG-FMRP-GFP reduced both the amplitude of evoked AMPAR-mediated responses and the frequency of mEPSCs without altering the amplitude of mEPSCs (Fig. 2.5*H–L*), implying that, like wild-type FMRP, this mutant construct reduced the number of functional synaptic connections. These results suggest that postsynaptic FMRP interactions with G-quartet containing RNAs are not required to regulate synapse number.

A nonphosphorylatable form of FMRP at S500 mimics wild-type FMRP and induces synapse loss

My data suggest that acute expression of FMRP in *Fmr1*-KO neurons decreases synapse number through the ability of FMRP to regulate translation, as expression of the I304N-FMRP-GFP construct, which is unable to regulate translation, has no effect on synapse number. In mammalian neurons, FMRP is associated with translating

polyribosomes and is required for glutamate stimulated translation at synapses, suggesting FMRP functions to allow or stimulate translation (Todd et al., 2003; Stefani et al., 2004; Weiler et al., 2004; Hou et al., 2006). However, *in vitro* FMRP suppresses translation of its target mRNAs (Laggerbauer et al., 2001; Li et al., 2001; Sung et al., 2003), and the brains of *Fmr1*-KO mice have elevated protein synthesis rates *in vivo*, and increased levels of specific proteins (Sung et al., 2003; Zalfa et al., 2003; Qin et al., 2005; Hou et al., 2006). These results are more consistent with a role for FMRP as a translational suppressor. Furthermore, translational suppression of target mRNAs by the *Drosophila* homolog of FMRP, dFmr1, is implicated in regulation of axonal and dendritic development (Zhang et al., 2001; Lee et al., 2003). Previously, it has been proposed that phosphorylation of FMRP on a conserved serine residue (Ser500 in human FMRP) switches FMRP from a translational activator to a suppressor (Ceman et al., 2003). An FMRP mutant, S500A-FMRP, which cannot be phosphorylated (mimicking the dephosphorylated state), is largely associated with actively translating polyribosomes, whereas a phosphorylation site mimic of FMRP, S500D-FMRP, is more strongly associated with stalled polyribosomes. To determine whether FMRP association with stalled or translating polysomes resulted in synapse loss, I transfected either of the phosphorylation site FMRP mutants (S500A-FMRP-GFP or S500D-FMRP-GFP) into *Fmr1*-KO slice cultures. Both S500A-FMRP-GFP and S500D-FMRP-GFP displayed a similar expression level and punctate expression pattern to wtFMRP-GFP (Fig. 2.6*A*,*G*, Table 2.1). S500A-FMRP-GFP expression resulted in a 35–40% decrease in both evoked AMPAR EPSCs and mEPSC frequency, similar to wtFMRP-GFP, with no change in mEPSC amplitude (Fig. 2.6*B–F*) or paired-pulse facilitation (Table 2.1). Consistent with its effects on synapse function in slice cultures, transfection of S500A-FMRP-GFP into dissociated *Fmr1*-KO neuron cultures reduced synapse number by 25–30% as measured with immunocytochemistry for presynaptic and postsynaptic markers, similar to wtFMRP-GFP (Fig. 2.6*M*,*N*). In contrast, S500D-FMRP-GFP had no effect on any measure of synaptic function or number (Fig. 2.6*G–N*, Table 2.1). Therefore, S500A-FMRP-GFP mimics wtFMRP-GFP with regard to synapse loss and suggests that at least some of wtFMRP-GFP exists in a dephosphorylated state which leads to a reduction in

synapse number. Furthermore, these data imply that FMRP association with translating polyribosomes leads to synapse loss.

Discussion

FMRP negatively regulates synapse number

Changes in dendritic spine number and shape have been observed in FXS patients and *Fmr1*-KO mice, both *in vivo* and in cultures (Braun and Segal, 2000; Irwin et al., 2001; Nimchinsky et al., 2001; Bagni and Greenough, 2005; Antar et al., 2006; Grossman et al., 2006a,b). How these morphological changes relate to functional synapses and whether FMRP plays a direct role in determining synapse number or function was unknown. Here, I demonstrate that acute expression of FMRP in *Fmr1*-KO neurons at near-endogenous levels reduces synapse number without changing the function or maturational state of the remaining synapses. Furthermore, *Fmr1*-KO neurons have more synapses compared with their wild-type neighbors in dissociated culture and acute postnatal expression of FMRP is sufficient to reverse this overabundance. My results are supported by observations of increased dendritic spine number on cortical neurons of FXS patients and *Fmr1*-KO mice that have developed *in vivo* (Irwin et al., 2001; Nimchinsky et al., 2001; Bagni and Greenough, 2005; Grossman et al., 2006b). My results extend on these structural studies and find that postsynaptic FMRP directly regulates functional synapse number.

Does FMRP regulate synapse formation, maturation, or pruning?

The abundance of filopodial-like spines in FXS patients and *Fmr1*-KO mice have prompted the idea that synapses in *Fmr1*-KO are more immature (Braun and Segal, 2000; Irwin et al., 2001, 2002; Nimchinsky et al., 2001; Antar et al., 2006; Grossman et al., 2006b). Acute FMRP expression did not effect short-term plasticity, mEPSC amplitude, the decay of NMDAR EPSCs, or percentage of silent synapses (Figs. 2.1–2.3), indicating that FMRP is not regulating presynaptic release probability, the strength of individual synapses, or their functional maturation. FMRP may play a role in the earliest stages of synapse development that occur before glutamate receptor insertion, making it less likely

that a synapse is created (Waites et al., 2005). Alternatively, FMRP may facilitate elimination or pruning synapses after they are formed. *Drosophila* FMRP (dFmr1) reduces synaptic bouton number at the neuromuscular junction as well as dendritic arborization in the CNS (Zhang et al., 2001; Pan et al., 2004), which could also be attributable to either inhibition of growth or pruning. In support of a role for FMRP in dendritic pruning, spiny stellate cells in the barrel cortex of *Fmr1*-KO mice fail to prune their dendrites from the barrel septa (Galvez and Greenough, 2005). More experiments are needed to determine the roles for FMRP in synapse formation and elimination.

Here, I observed that acute postsynaptic FMRP expression resulted in a reduction in synapse function and number compared with neighboring untransfected *Fmr1*-KO neurons (Figs. 2.1–2.4). Similarly, fewer synapses were observed in WT neurons in dissociated neuron cultures compared with their *Fmr1*-KO neighbors, indicating that my results with acute expression of FMRP reflect endogenous FMRP function (Fig. 2.4). Because the effects of acute FMRP expression on synapse function are moderate (20–35%), the large variability across slice culture preparations may make it difficult to detect differences in evoked EPSCs and mEPSCs between WT and *Fmr1*-KO cultures. It may be necessary to make comparisons between neighboring neurons in the same culture. Alternatively, or in addition, there may be intercellular interactions between FMRP-expressing and *Fmr1*-KO neurons, which result in *Fmr1*-KO neurons having more synapses. This would be relevant to females with FXS who have a mosaic expression of FMRP.

FMRP regulates synapse number through postsynaptic KH2 domain interactions

Previous work has focused on two RNA tertiary structures that are important for FMRP-RNA interactions. The RGG box of FMRP binds with high specificity and affinity to mRNAs containing a G-quartet structure and is implicated in their translational suppression (Brown et al., 2001; Darnell et al., 2001; Schaeffer et al., 2001), whereas the KH domains KH1 and KH2 interact with kissing complex RNA structures (Darnell et al., 2005a). FMRP with a deleted RGG box (ΔRGG-FMRP) functioned just as well as wtFMRP in reduction of synapse number (Fig. 2.5). This result suggests that interactions

of FMRP with postsynaptic G-quartet-containing mRNAs such as microtubule-associated protein 1b (MAP1b), or the PSD-95-associated protein SAPAP4 are not required for FMRP regulation of synapse number in mammals (Brown et al., 2001; Darnell et al., 2001). In contrast to the RGG box deletion, a single point mutation in the KH2 domain (I304N-FMRP) abolished the effects of FMRP on synapse number. I304N-FMRP, which was first discovered in a patient with a particularly severe form of FXS (De Boulle et al., 1993), fails to dimerize and associate with large translating polyribosomes (Feng et al., 1997b; Laggerbauer et al., 2001; Darnell et al., 2005b). I304N-FMRP abolishes binding to kissing complex RNAs and no longer acts as a translational suppressor (Laggerbauer et al., 2001; Darnell et al., 2005a). Thus, it is likely that FMRP regulation of translation, either through interaction with kissing-complex-containing mRNAs or polyribosomes, is critically important for the ability of FMRP to reduce synapse number. In addition, whereas wild-type FMRP and all other mutant constructs of FMRP displayed a punctate expression pattern, the I304N-FMRP mutant construct was much more diffuse (Figs. 2.4, 2.5), as observed in cultured cell lines (Schrier et al., 2004; Darnell et al., 2005b). These puncta observed with endogenous or wtFMRP-GFP may be polyribosomes or RNA granules because they contain RNA and move via microtubules in dendrites (Antar et al., 2004, 2005; Kanai et al., 2004). This result indicates that FMRP association with polyribosomes and/or RNA granules is required to induce synapse loss and implicates translational regulation of FMRP target mRNAs in this process.

FMRP mutant that associates with translating polyribosomes leads to synapse loss

FMRP has been implicated in both translational suppression and activation. Such dual translational regulation by RNA-binding proteins is important to mediate specific and localized protein expression (Huang and Richter, 2004; Kindler et al., 2005; Wells, 2006). Phosphorylation of RNA-binding proteins such as cytoplasmic polyadenylation-binding protein (CPEB) and zip code-binding protein (ZBP) is a mechanism by which the switch from repression to activation (or derepression) occurs (Huang and Richter, 2004; Huttelmaier et al., 2005; Wells, 2006). Like CPEB and ZBP, phosphorylation of FMRP on a conserved serine (406 in *Drosophila*, 499 in mouse, and 500 in human) has been

suggested to be a mechanism to regulate translational suppression and activation by FMRP. In vitro phosphorylation of *Drosophila* dFmr1 affected binding to poly(U), but not poly(G) RNA (Siomi et al., 2002). However, mimicking phosphorylation of murine FMRP at Ser499 with Asp does not affect binding to known target mRNAs, but rather increases association of FMRP with stalled polysomes in vivo. Substitution of Ala for Ser, thereby mimicking the dephosphorylated form, recruited FMRP to translating polysomes (Ceman et al., 2003). From these findings, it was suggested that in the phosphorylated state, FMRP binds mRNAs that are initiated but not actively elongating (stalled polysomes); FMRP dephosphorylation results in a conformational change to facilitate elongation (Ceman et al., 2003). A dephosphomimic of FMRP (S500A) reduces synapse function and number in the same manner as wild-type FMRP, whereas the phosphomimic of FMRP (S500D) had no effect (Fig. 2.6). These results suggest that the ability of FMRP to regulate synapse number requires association with translating polyribosomes, whereas suppression of protein synthesis prevents synaptic regulation. Although I cannot rule out the possibility that the S500 mutation affects other aspects of FMRP function, I propose a model in which FMRP dephosphorylation and stimulation of translation of mRNA target(s) leads to synapse loss. This idea is in contrast to conclusions in the dFmr1-null fly that translational suppression of MAP1b or Rac1 is thought to lead to a reduction in presynaptic and postsynaptic structures, respectively (Zhang et al., 2001; Lee et al., 2003). However, it is likely in both species that FMRP-mediated translational suppression and activation are important for proper synapse development. Determining how FMRP phosphorylation is regulated and, in turn, how FMRP phosphorylation regulates translation in neurons and dendrites will provide more detailed insight into how FMRP controls synapse number.

Translational regulation by FMRP is also implicated in acute long-term synaptic depression (LTD) in mature neurons (>P21) (Huber et al., 2002; Koekkoek et al., 2005; Hou et al., 2006; Nosyreva and Huber, 2006). Therefore, FMRP may regulate translation of the same or different proteins to coordinate rapid changes in function with long-term changes in synapse structure. Because FMRP binds to as many as 4% of brain mRNAs, the challenge now lies in determining which mRNAs of postsynaptically expressed

proteins are regulated by FMRP and lead to LTD and synapse loss (Sung et al., 2000; Brown et al., 2001; Miyashiro et al., 2003). I would anticipate that these mRNA targets are dendritically expressed and require an intact KH2 domain of FMRP for translational regulation.

Figure 2.1. Acute postsynaptic FMRP expression reduces evoked AMPAR and NMDAR mediated EPSCs.

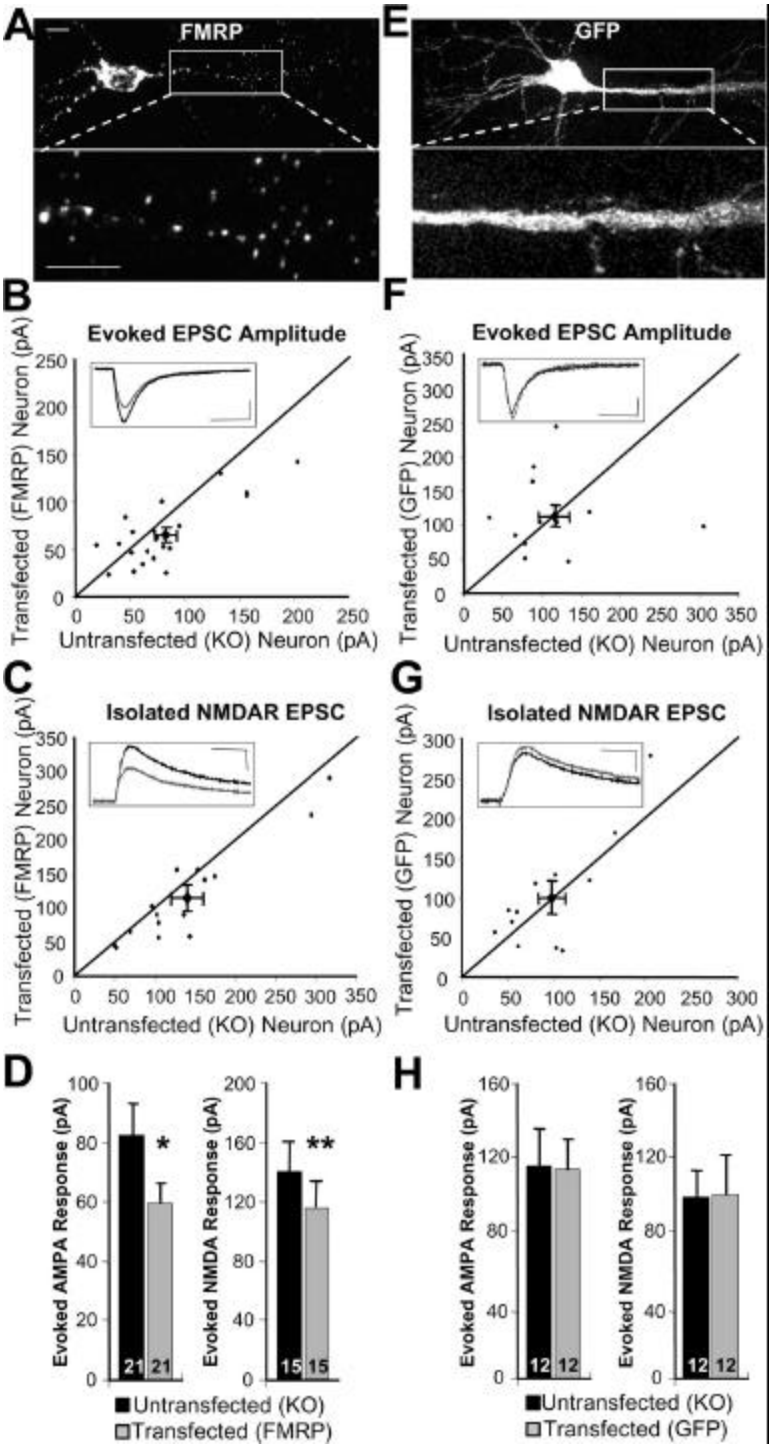

Figure 2.1. Acute postsynaptic FMRP expression reduces evoked AMPAR and NMDAR mediated EPSCs. ***A***, Expression pattern of FMRP-GFP fusion protein in a CA1 pyramidal neuron in hippocampal slice culture. Scale bars, 10 µm. ***B***, ***C***, Dot plot of the peak amplitude of the evoked AMPAR- (***B***) or NMDAR-mediated EPSCs (***C***) of paired recordings from an untransfected *Fmr1* KO versus a neighboring FMRP transfected neuron. In this and all figures, the diagonal line represents the values where the EPSC amplitudes from transfected and untransfected cells are equal. The large diamond represents mean ± SEM. Inset, Average of 25 consecutive traces from a representative experiment. Black trace is the untransfected neuron, gray trace is the transfected neuron. Scale bar is 20 pA and 20 ms. Stimulation artifact has been digitally removed for clarity. ***D***, Average AMPAR and NMDAR EPSC amplitude from untransfected KO and FMRP transfected cells. ***E***, As in ***A***, but image shows GFP expression pattern. ***F***, ***G***, As in ***B*** and ***C***, but dot plots represent peak evoked AMPAR-mediated (***F***) and NMDAR-mediated (***G***) EPSCs from neighboring untransfected and GFP-expressing *Fmr1* KO neurons. ***H***, Average AMPAR and NMDAR EPSC amplitude from untransfected KO and GFP transfected cells. In this and all figures, averages are plotted + SEM and *n* is plotted on each bar. $*p < 0.05$; $**p < 0.01$, $***p < 0.001$.

Figure 2.2. Postsynaptic FMRP reduces the frequency, but not amplitude of miniature EPSCs.

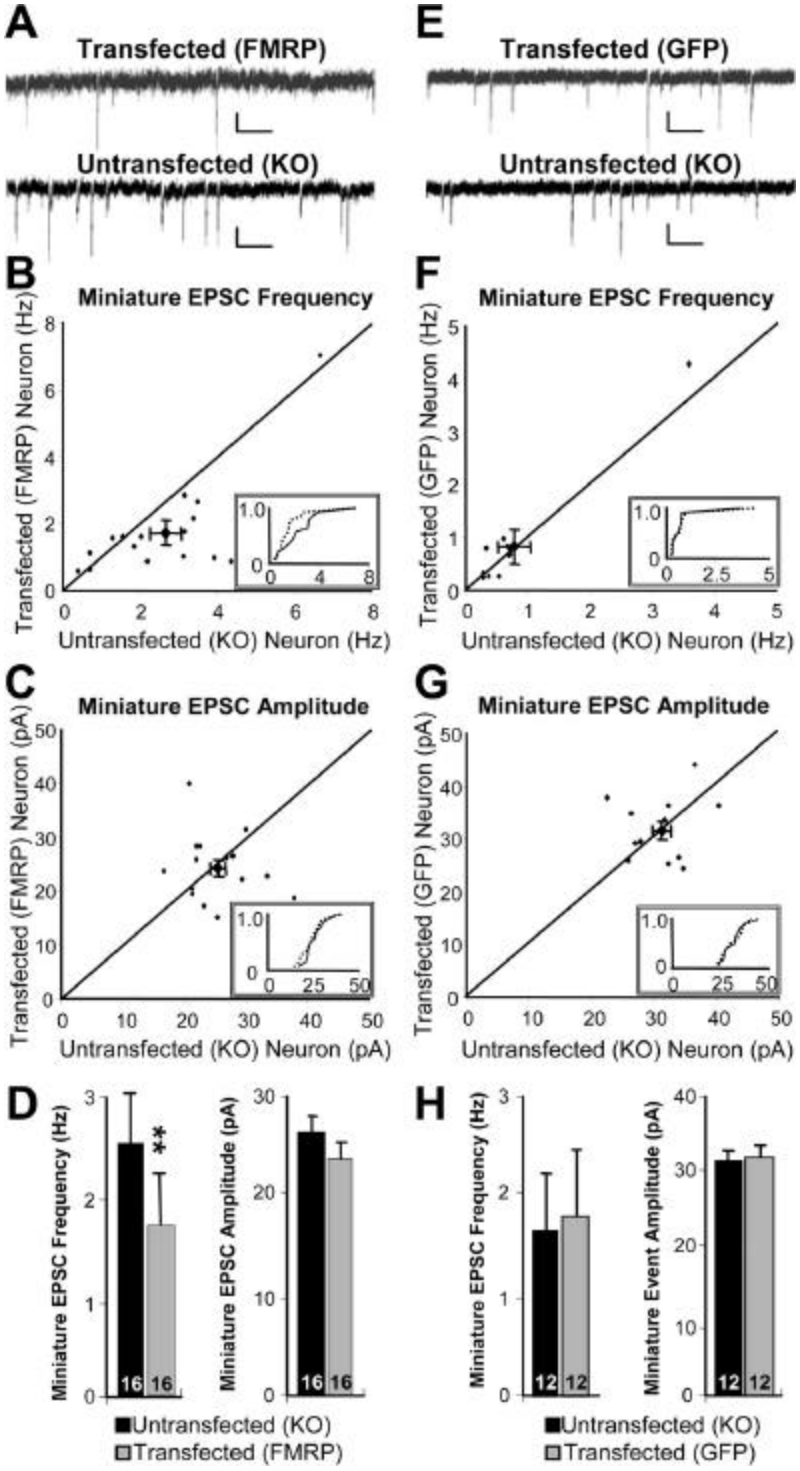

Figure 2.2. Postsynaptic FMRP reduces the frequency, but not amplitude of miniature EPSCs. ***A***, Representative traces of mEPSCs simultaneously recorded from an untransfected *Fmr1* KO and a neighboring FMRP transfected neuron. Calibration: 10 pA, 500 ms. ***B***, ***C***, Dot plot representation of the frequency (***B***) and amplitude (***C***) of mEPSCs in paired recordings. Inset, Cumulative probability distributions for both untransfected neurons (solid black line) and transfected, FMRP-expressing neurons (dotted line). Each point on the curve represents the average mEPSC frequency and amplitude from an individual neuron. The *x*-axis is the mEPSC frequency (***B***) or amplitude (***C***). The *y*-axis is the cumulative probability. ***D***, Average mEPSC frequency and amplitude in untransfected KO and FMRP transfected cells. ***E***, Representative traces from untransfected and neighboring GFP-expressing *Fmr1* KO neurons. Calibration: 20 pA, 500 ms. ***F***, ***G***, Dot plots of mEPSC frequency (***F***) and amplitude (***G***) from neighboring untransfected and GFP-expressing *Fmr1* KO CA1 pyramidal neurons. Inset, Cumulative probability distribution for both untransfected neurons (solid black line) and transfected, GFP-expressing neurons (dotted line). ***H***, Average mEPSC frequency and amplitude in untransfected KO and GFP transfected cells. $^{**}p < 0.01$.

Figure 2.3. Postsynaptic FMRP increases synaptic failures, but does not affect paired-pulse facilitation or silent synapses.

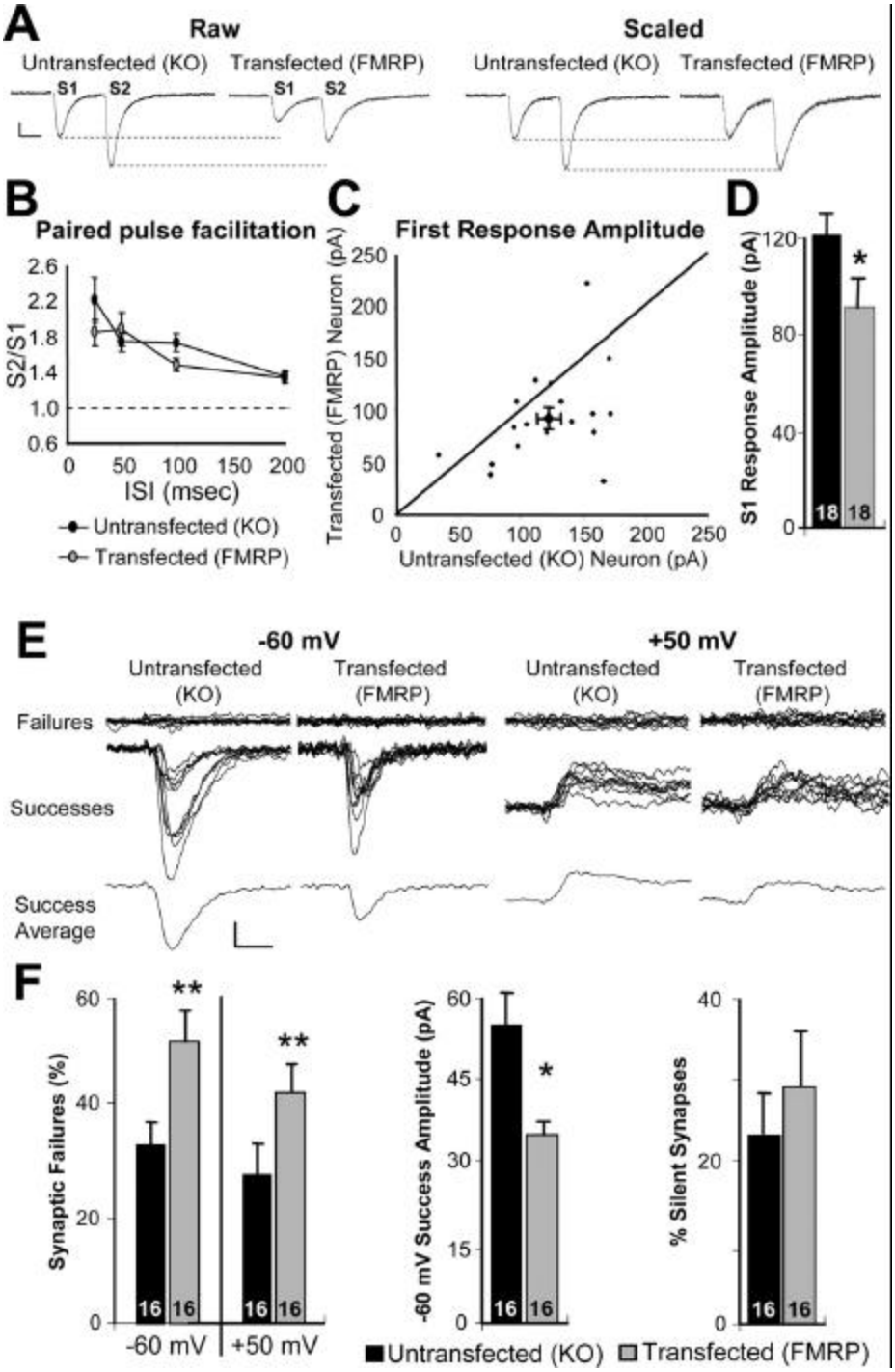

Figure 2.3. Postsynaptic FMRP increases synaptic failures, but does not affect paired-pulse facilitation or silent synapses. ***A***, Representative experiment. Raw, Average of 25 consecutive traces simultaneously recorded from an untransfected *Fmr1* KO and a neighboring FMRP transfected neuron. Calibration: 20 pA, 20 ms. Scaled, Traces from Raw have been scaled so that the S1 EPSC amplitude of the transfected neuron is equal to that of the untransfected neuron. ***B***, Paired-pulse facilitation values (mean ± SEM) at a range of interstimulus intervals is not different between FMRP transfected and untransfected KO neurons as determined with a repeated measures ANOVA ($F_{(1,30)}$ = 0.642; p = 0.42). ***C***, Dot plot representation of the peak amplitude of the first response (S1) in paired recordings from an untransfected *Fmr1* KO neuron and FMRP-transfected neuron (n = 18). ***D***, Average EPSC amplitude for S1. ***E***, Representative minimal stimulation experiment. Evoked responses were obtained in simultaneous recordings from an untransfected *Fmr1* KO neuron and FMRP transfected neuron using minimal stimulation. Shown are 25 consecutive traces separated into failures and successes for an FMRP-transfected and untransfected neuron held at –60 mV (left) and +50 mV (right) and an average of the successes. Calibration: 20 pA, 10 ms. ***F***, Average percentage of synaptic failures at –60 mV and +50 mV, the peak amplitude of synaptic successes at –60 mV (synaptic potency), and the percentage of silent synapses in FMRP transfected and untransfected neurons. *p < 0.05; **p < 0.01.

Figure 2.4. Acute exogenous and endogenous FMRP reduce the number of synapses as measured with immunocytochemical markers.

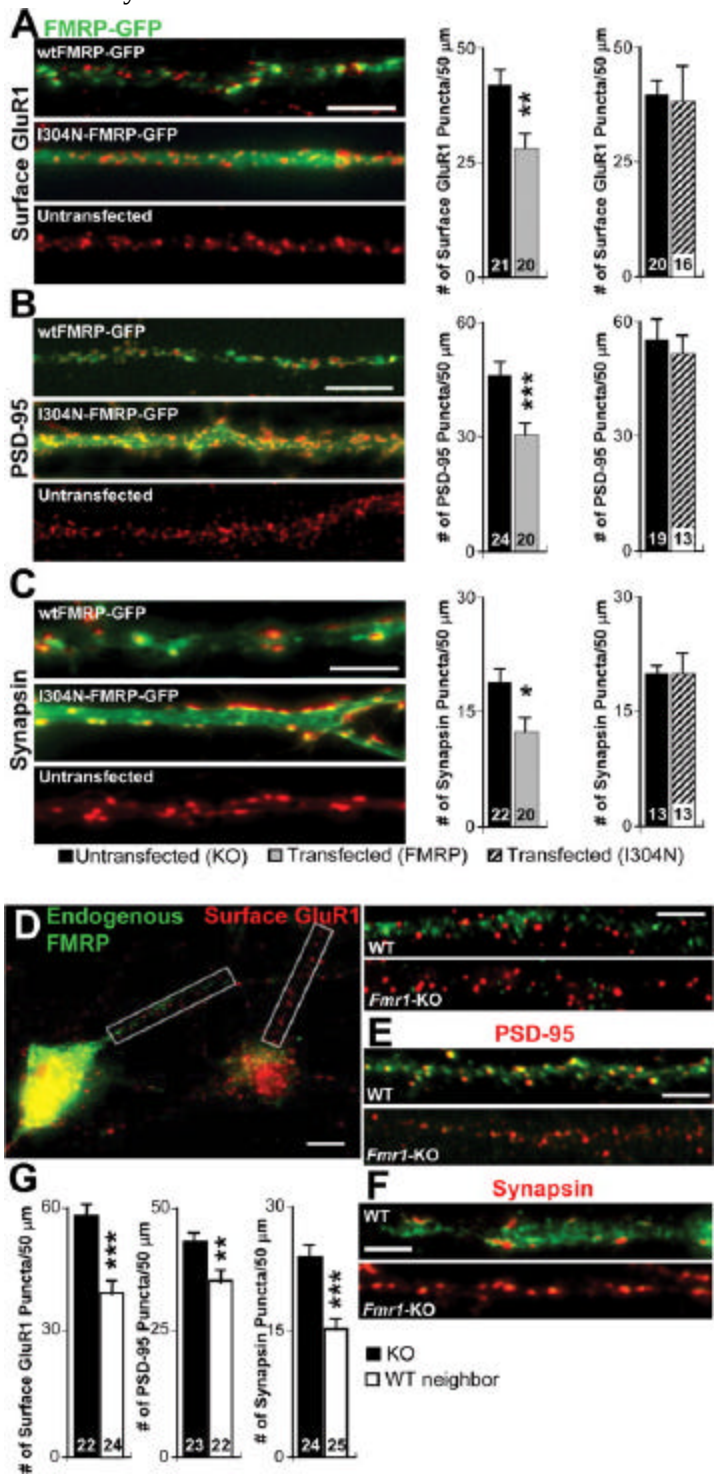

Figure 2.4. Acute exogenous and endogenous FMRP reduce the number of synapses as measured with immunocytochemical markers. ***A***, Left, Representative dendrites of *Fmr1* KO dissociated hippocampal cultures transfected with either wtFMRP-GFP or I304N-FMRP-GFP (green) and labeled for surface GluR1 (red). Right, Average number of surface GluR1 puncta in neurons transfected with either wtFMRP-GFP or I304N-FMRP-GFP and neighboring untransfected KO neurons. ***B***, Left, As in ***A***, except red is PSD-95 immunofluorescence. Right, Average number of PSD-95 puncta. ***C***, Left, As in ***A***, except red is synapsin immunofluorescence. Right, Average number of synapsin puncta. ***D***, Left, Representative image of side-by-side wild-type and *Fmr1* KO neurons in culture. Green is endogenous FMRP immunofluorescence. Red is surface GluR1 immunofluorescence. Right, Dendrites of the wild-type and *Fmr1* KO neuron. ***E***, As in ***A***, except red is PSD-95 immunofluorescence. ***F***, As ***A***, except red is synapsin immunofluorescence. ***G***, Average number of surface GluR1, PSD-95, and synapsin puncta in wild-type neurons and neighboring *Fmr1* KO neurons. $*p < 0.05$; $**p < 0.01$; $***p < 0.001$. Scale bars: ***A–C***, 10 μm; ***D***, left, 10 μm; ***D***, right, 5 μm; ***E***, ***F***, 10 μm

Figure 2.5. An intact KH2 RNA-binding domain of FMRP, but not an RGG box, is required to reduce synapse function.

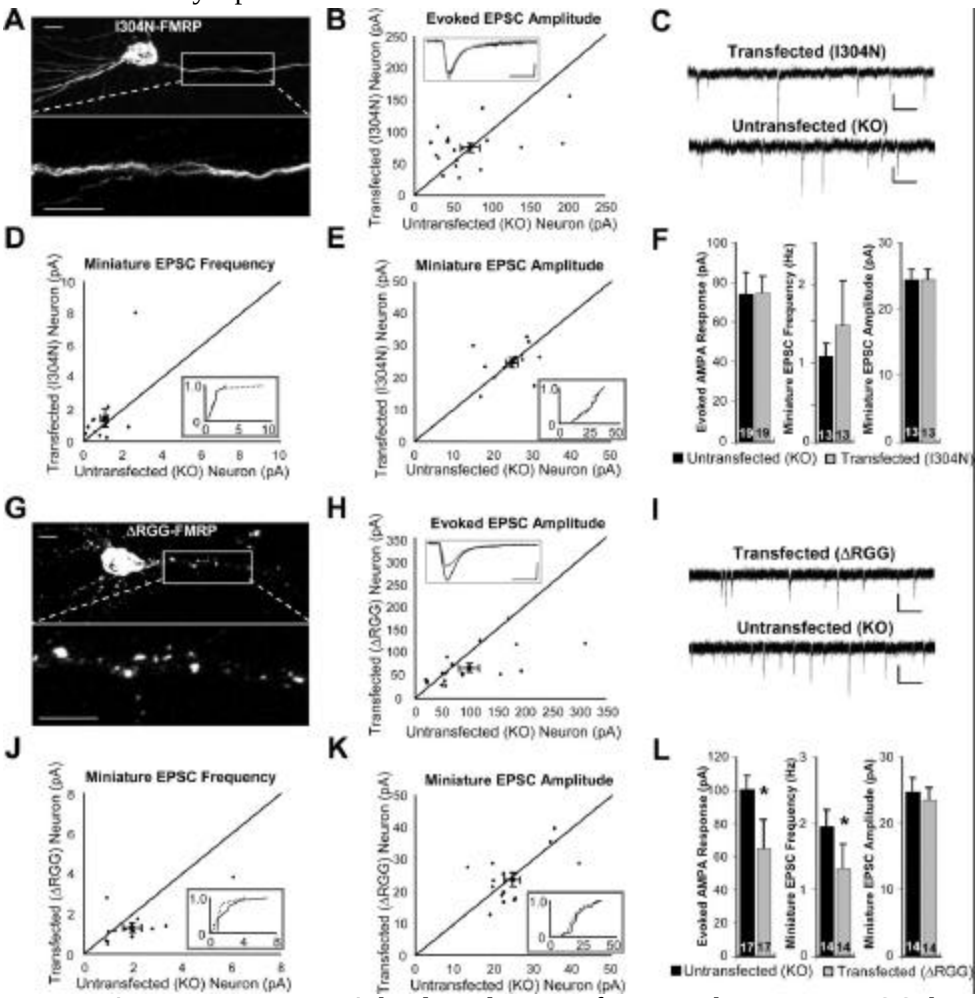

Figure 2.5. An intact KH2 RNA-binding domain of FMRP, but not an RGG box, is required to reduce synapse function. ***A***, Expression pattern of I304N-FMRP-GFP fusion protein in a CA1 pyramidal neuron in slice culture. ***B***, Dot plot of the peak amplitude of the evoked AMPAR-EPSCs from paired recordings of untransfected *Fmr1* KO versus I304N-FMRP transfected neurons. Inset, Representative evoked EPSCs from one neuron pair. ***C***, Representative traces of mEPSCs simultaneously recorded from an untransfected *Fmr1* KO and I304N-FMRP transfected neuron. ***D***, ***E***, Dot plot representation of the frequency (***D***) and amplitude (***E***) of mEPSCs in *Fmr1* KO versus neighboring I304N-FMRP transfected neurons. Inset, Cumulative probability distribution of mEPSC frequency and amplitude for both untransfected neurons (solid black line) and transfected I304N-FMRP-expressing neurons (dotted line). ***F***, Group data (mean + SEM) of ***B***, ***D***, and ***E***. ***G–L***, As in ***A–F***, except the transfected neurons express ΔRGG-FMRP-GFP. *$p <$ 0.05. Scale bars: ***A***, ***G***, 10 µm. Calibrations: ***B***, ***H***, insets, 20 pA, 20 ms; ***C***, ***I***, 10 pA, 500 ms.

Figure 2.6. Dephosphorylated FMRP reduces synapse function and number.

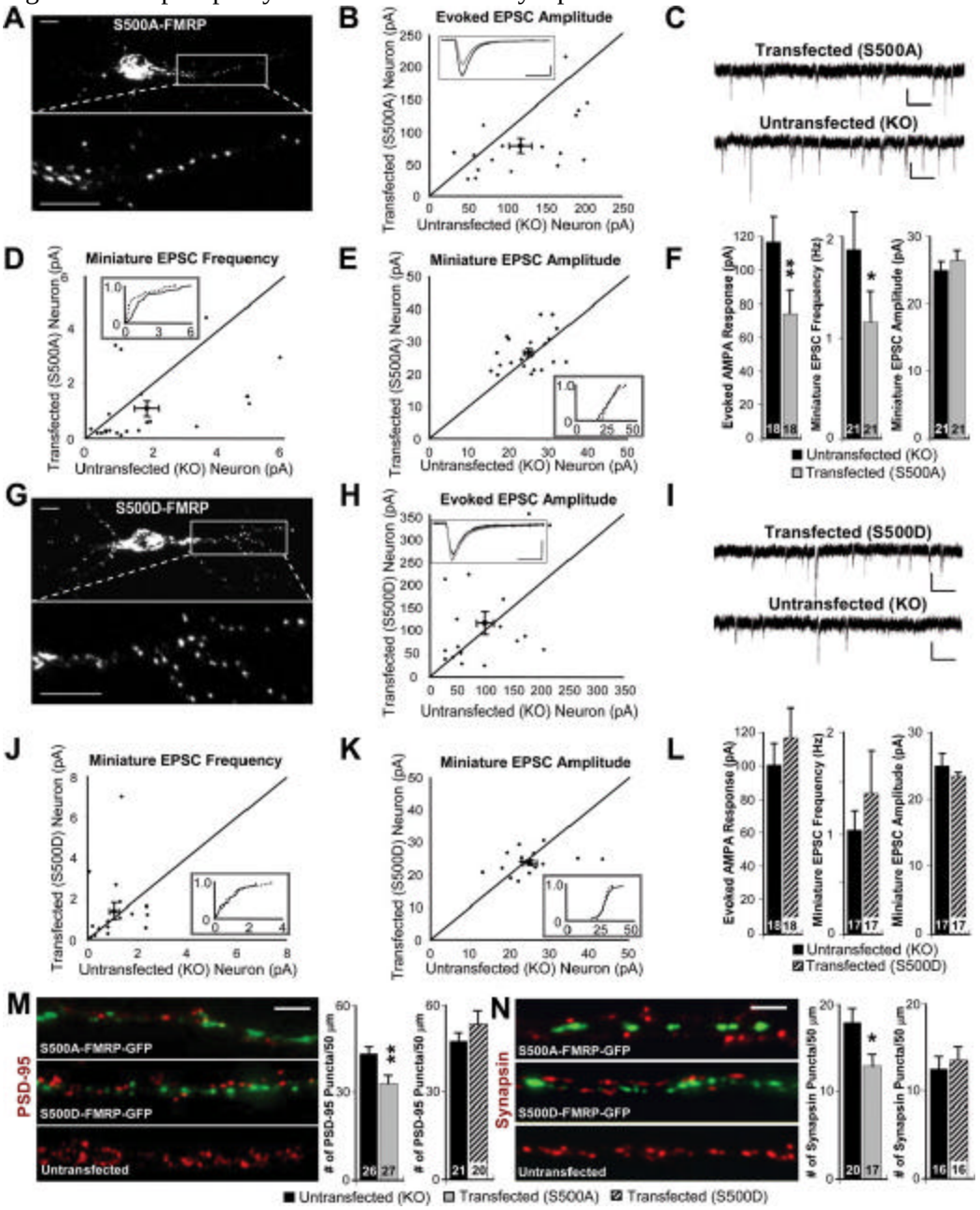

Figure 2.6. Dephosphorylated FMRP reduces synapse function and number. ***A***, Expression pattern of S500A-FMRP-GFP in CA1 pyramidal neuron in hippocampal slice cultures. ***B***, Dot plot of the peak amplitude of the evoked EPSC of paired recordings from untransfected *Fmr1* KO and neighboring S500A-FMRP transfected neuron. ***C***, Representative traces of mEPSCs simultaneously recorded from untransfected *Fmr1* KO and S500A-FMRP transfected neuron. ***D***, ***E***, Dot plot of the frequency (***D***) and amplitude (***E***) of mEPSCs from untransfected *Fmr1* KO versus neighboring S500A-FMRP-transfected neurons. Insets, Cumulative probability distribution for both untransfected neurons (solid black line) and transfected S500A-FMRP-expressing neurons (dotted line). ***F***, Group data (mean + SEM) of ***B***, ***D***, and ***E***. ***G–L***, As in ***A–F***, except the transfected neurons express S500D-FMRP-GFP. ***M***, Left, Dendrites of *Fmr1* KO dissociated hippocampal cultures transfected with either S500A-FMRP-GFP or S500D-FMRP-GFP (green) and immunofluorescence for PSD-95 (red). Right, Average number of PSD-95 puncta in neurons transfected with either S500A-FMRP-GFP or S500D-FMRP-GFP and neighboring untransfected neurons. ***N***, As in ***A***, except red is synapsin immunofluorescence. On the right is the average number of synapsin puncta. $*p < 0.05$; $**p < 0.01$. Scale bars: ***A***, ***G***, ***N***, 10 μm; ***M***, 5 μm. Calibrations: ***B***, inset, 50 pA, 20 ms; ***C***, ***I***, 20 pA, 500 ms; ***H***, inset, 25 pA, 20 ms

Figure 2.7. Expression Level of FMRP Following Transfection

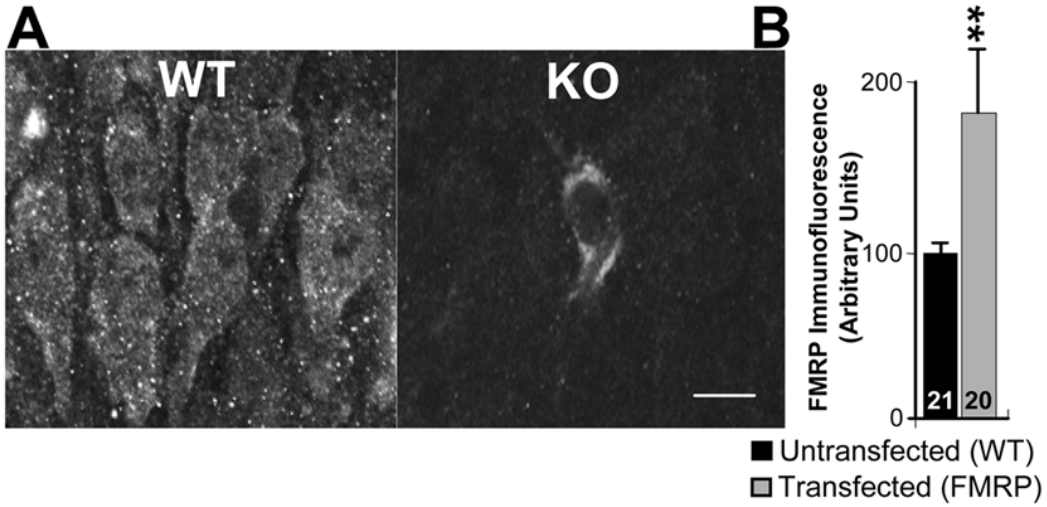

Figure 2.7. Expression Level of FMRP Following Transfection ***A***. Confocal images of FMRP expression levels in wild-type (left) and Fmr1 KO (right) hippocampal slice cultures. The Fmr1 KO slice culture was biolistically transfected with a construct expressing FMRP-GFP driven by the human FMR1 promoter. Both sets of slice cultures were fixed and immuno-labeled with 2F5 FMRP antibody and AlexaFluor568 2° antibody. Scale bar is 10 µm. ***B***. Quantification of somatic FMRP immunofluorescence from confocal images from wild-type and FMRP-transfected Fmr1 KO hippocampal slice cultures. Fluorescence in the KO untransfected neurons was considered background and was subtracted from the WT and KO transfected intensity values. Values are means + SEM. Number of cells quantified is listed on the bar graph. **$p < 0.01$.

Table 2.1: Physiological Effects of FMRP Expression on *Fmr1*-KO Neurons

Table 2.1: Physiological Effects of FMRP expression in *FMR1*-KO Neurons

	Measurement	Transfected	Untransfected	n	p-value
wtFMRP	GFP Fluorescence Level (AU)	191.4 ± 26.0	N/A	10	‡N/A
	Resting Membrane Potential (mV)	-56.41 ± 1.03	-57.41 ± 0.95	37	0.3046
	Input Resistance (MΩ)	161.08 ± 10.08	162.30 ± 9.54	37	0.9258
	Capacitance (pF)	29.67 ± 4.22	28.63 ± 4.47	21	0.8494
	NMDAR Amp. Fast Component (pA)	61.63 ± 12.84	74.40 ± 13.13	15	0.0179
	NMDAR Amp. Slow Component (pA)	31.35 ± 6.26	38.58 ± 6.23	15	0.1280
	NMDAR Decay τ^1 (ms)	34.56 ± 3.28	36.15 ± 2.87	15	0.6962
	NMDAR Decay τ^2 (ms)	280.21 ± 52.89	279.35 ± 64.65	15	0.9652
I304N-FMRP	GFP Fluorescence Level (AU)	192.6 ± 26.2	N/A	7	‡n.s.
	Resting Membrane Potential (mV)	-49.27 ± 2.18	-51.05 ± 1.87	22	0.5578
	Input Resistance (MΩ)	143.64 ± 10.82	162.05 ± 12.59	22	0.2029
ΔRGG-FMRP	GFP Fluorescence Level (AU)	301.6 ± 35.4	N/A	10	‡n.s.
	Resting Membrane Potential (mV)	-53.43 ± 1.90	-54.57 ± 0.90	21	0.5816
	Input Resistance (MΩ)	146.67 ± 11.08	172.14 ± 11.23	21	0.1432
S500A-FMRP	GFP Fluorescence Level (AU)	328.5 ± 47.2	N/A	10	‡n.s.
	Resting Membrane Potential (mV)	-53.36 ± 1.48	-55.08 ± 1.37	25	0.1252
	Input Resistance (MΩ)	164.80 ± 13.00	173.20 ± 12.28	25	0.5847
	Paired-Pulse Facilitation (S2/S1 @ 50 ms ISI)	2.11 ± 0.23	2.05 ± 0.27	18	0.6975
S500D-FMRP	GFP Fluorescence Level (AU)	345.3 ± 43.6	N/A	10	‡<0.05
	Resting Membrane Potential (mV)	-54.44 ± 1.29	-55.76 ± 0.91	25	0.2564
	Input Resistance (MΩ)	150.20 ± 14.16	162.60 ± 10.29	25	0.1381
	Paired-Pulse Facilitation (S2/S1 @ 50 ms ISI)	2.09 ± 0.27	2.02 ± 0.15	18	0.7174

AU = arbitrary units. ‡ vs. wtFMRP as measured by Tukey/Kramer Post-Hoc test.

Table 2.2: Effects of FMRP Expression on Synaptic Markers

Table 2.2: Effects of FMRP Expression on Synaptic Markers

		wtFMRP					I304N-FMRP				
		Transfected	n	Untransfected	n	p-value	Transfected	n	Untransfected	n	p-value
Surface GluR1	Puncta Intensity	1288.8 ± 57.4	20	1387.9 ± 41.98	21	0.1683	1245.8 ±167.1	16	1212.8 ± 96.1	20	0.8583
	Puncta Size	0.193 ± 0.025	20	0.208 ± 0.022	21	0.6546	0.175 ± 0.018	16	0.161 ± 0.013	20	0.5330
PSD-95	Puncta Intensity	1600.5 ± 70.1	20	1788.3 ± 87.9	24	0.1121	1738.2 ± 97.1	13	1690.3 ± 82.8	19	0.7116
	Puncta Size	0.171 ± 0.014	20	0.313 ± 0.036	24	0.0013	0.327 ± 0.039	13	0.293 ± 0.025	19	0.4514
Synapsin	Puncta Intensity	1631.2 ±252.6	20	1884.3 ± 266.8	22	0.4971	2410.5 ±189.7	13	2247.6 ± 195.6	13	0.5556
	Puncta Size	0.514 ± 0.065	20	0.547 ± 0.040	22	0.6596	0.608 ± 0.066	13	0.726 ± 0.095	13	0.3165
		S500A-FMRP					S500D-FMRP				
		Transfected	n	Untransfected	n	p-value	Transfected	n	Untransfected	n	p-value
PSD-95	Puncta Intensity	938.1 ± 50.0	27	882.2 ± 53.4	26	0.4481	852.4 ± 35.2	20	830.1 ± 38.9	21	0.6728
	Puncta Size	0.241 ± 0.032	27	0.315 ± 0.044	26	0.1731	0.311 ± 0.036	20	0.287 ± 0.043	21	0.6726
Synapsin	Puncta Intensity	1164.4± 130.8	17	1159.2 ± 113.1	20	0.9986	791.3 ± 19.6	16	788.1 ± 11.7	16	0.8907
	Puncta Size	0.533 ± 0081	17	0.568 ± 0.073	20	0.7321	0.324 ± 0.036	16	0.302 ± 0.042	16	0.6895
		Co-Cultures									
		Wild-Type	n	*Fmr1*-KO	n	p-value					
Surface GluR1	Puncta Intensity	2166.8 ±108.0	24	2030.7 ± 116.7	22	0.3991					
	Puncta Size	0.260 ± 0.025	24	0.222 ± 0.017	22	0.2254					
PSD-95	Puncta Intensity	2445.1 ±114.1	22	2395.1 ± 91.0	23	0.7321					
	Puncta Size	0.247 ± 0.017	22	0.307 ± 0.021	23	0.0323					
Synapsin	Puncta Intensity	1497.8 ± 30.2	25	1532.2 ± 28.4	24	0.4090					
	Puncta Size	0.296 ± 0.025	25	0.368 ± 0.023	24	0.0411					

CHAPTER THREE

FMRP and MEF2 Cooperatively Regulate Synapse Number

Summary

The most common form of inherited mental retardation is Fragile X Syndrome (FXS), which affects approximately 1:4000 males and 1:8000 females (Verkerk et al., 1991; O'Donnell and Warren, 2002; Turner et al., 1996). FXS is caused by loss-of-function mutations in the *Fmr1* gene, which encodes for the Fragile X mental retardation protein (FMRP) (O'Donnel and Warren, 2002). FMRP is an RNA-binding protein and has been shown to regulate translation both *in vitro* and *in vivo* via association with mRNA and polyribosomes (Laggerbauer et al., 2001; Li et al., 2001; Mazroui et al., 2002; Wang et al., 2004; Lu et al., 2004). Although there is considerable evidence suggesting that FMRP acts as a translational suppressor, FMRP is most commonly observed associated with actively translating polyribosomes, suggesting that FMRP may bi-directionally regulate the translation of its mRNA targets, possibly depending on the phosphorylation status of the protein (Feng et al., 1997; Corbin et al., 1997; Stefani et al., 2004; Ceman et al., 2003).

The most well-characterized synaptic phenotype in FXS patients and the mouse model of FXS, the *Fmr1*-knockout (*Fmr1*-KO) mouse, is an increase in the number of dendritic spines, the principle sites of excitatory synaptic connections (Hinton et al., 1991; Irwin et al., 2001; Irwin et al., 2002; Nimchinsky et al., 2001; Galvez et al., 2005; Meredith et al., 2007; Restivo et al., 2005; Hayashi et al., 2007; McKinney et al., 2005; Dolen et al., 2007). In addition, dendritic spines of FXS patients and *Fmr1*-KO mice are longer, thinner, and more tortuous, reminiscent of immature dendritic filopodia (Irwin et al., 2001; Irwin et al., 2002; McKinney et al., 2005; Meredith et al., 2007; Restivo et al., 2005). Interestingly, although the specific phenotype varies, alterations in dendritic spine number and structure are a common finding among many types of mental retardation, including FXS, Rett's Syndrome, and Down Syndrome, suggesting a common synaptic

origin in many diverse cognitive disorders (Kaufmann and Moser, 2000; Marin-Padilla, 1972; Purpura, 1975).

The increased numbers of dendritic spines observed in FXS patients and *Fmr1*-KO mice suggests that FMRP may negatively regulate synapse number. Indeed, post-synaptic expression of FMRP in *Fmr1*-KO neurons was recently demonstrated to decrease synapse number, and this synaptic loss appeared to require FMRP-dependent translational stimulation of its mRNA ligands (Pfeiffer and Huber, 2007). However, pre-synaptic expression of FMRP has been shown to increase functional connectivity between neighboring neurons (Hanson and Madison, 2007), indicative of complex regulation of synapse number by FMRP. Additional cellular factors, such as kinase/phosphatase activity, ribonucleoprotein particle (RNP) trafficking, and expression/availability of mRNA ligands of FMRP may therefore provide important points of cellular control through which to precisely regulate synapse number via FMRP; however, the mechanisms through which FMRP may regulate synapse number are unknown.

Activation of the transcription factor myocyte-enhancer factor 2 (MEF2) induces robust synapse loss in neurons in a manner similar to FMRP-dependent synapse loss (Barbosa et al., 2008; Flavell et al., 2006). Likewise, knockdown or genetic deletion of MEF2 increases synapse number (Flavell et al., 2006; Barbosa et al., 2008). MEF2 is an activity-regulated protein that is found in many cell types, but is expressed particularly strongly in muscle and neurons (Black and Olson, 1998). The MEF2 family is composed of four independent genes, MEF2A-D, which have distinct spatial and temporal expression patterns throughout development (Ikeshima et al., 1995; Lin et al., 1996; Lyons et al., 1995). In particular, MEF2A and -D display robust expression in area CA1 of the post-natal hippocampus.

Because MEF2 and FMRP both negatively regulate synapse number, and because several MEF2 transcripts are reported to be target mRNAs of FMRP (Zalfa et al., 2003; Flavell et al., 2006), I investigated a possible genetic interaction between MEF2 and FMRP. I observe that MEF2-dependent regulation of synapse number requires FMRP, as it fails to occur in *Fmr1*-KO neurons. Furthermore, FMRP expression fails to

induce synapse loss in the absence of MEF2 activity. These data strongly argue that MEF2-driven transcripts are translationally regulated by FMRP to regulate synapse elimination. These results demonstrate a novel genetic interaction and provide a mechanistic model for the increased numbers of synapses observed in FXS patients and *Fmr1*-KO mice.

Introduction

Myocyte-enhancer factor 2

The myocyte-enhancer factor 2 (MEF2) proteins, MEF2A, -B, -C, and -D, are members of the MADS-box family of transcription factors (named after MCM1, Agamous, Deficiens, and Serum response factor) (McKinsey et al., 2002). The four members of the MEF2 family are encoded by separate genes and have unique, but partially overlapping developmental and spatial expression patterns (Lyons et al., 1995; Ikeshima et al., 1995; Lin et al., 1996). In both adolescent and adult mice, MEF2A and -D are found throughout the hippocampus, while MEF2B and -C are largely restricted to the dentate gyrus. In the cerebellum, MEF2C is observed exclusively in Purkinje cells, while MEF2A and -D are found in the granule cell layer. All four isoforms are observed in the cortex of adult mice, with MEF2A having reduced levels of expression. Similar expression patterns are seen in adult human brain samples (Leifer et al., 1993). Interestingly, MEF2A, -C, and -D can be alternatively spliced to provide tissue-specific isoforms (Martin et al., 1994; Zhu et al., 2005), further complicating the distribution pattern of these proteins.

All four MEF2 proteins contain three domains: a MADS-box, a MEF2 domain, and a transcriptional activation domain. The MADS-box and MEF2 domain are highly conserved between the various isoforms, while the transcription activation domain displays less homology (McKinsey et al., 2002). The MADS-box represents the primary DNA-binding domain of the MEF2 family, associating with A/T-rich DNA sequences. The MADS-box is additionally important for dimerization in conjunction with the adjacent MEF2 domain. The MEF2 domain further regulates the affinity of DNA binding as well as many co-factor interactions. The MADS-box and MEF2 domains

appear to be the only regions of the proteins that associate with DNA, as a truncation mutant of these two domains fused to a separate transcriptional activator is sufficient to drive transcription of MEF2 target genes (Molkentin and Olson, 1996). The consensus binding site for MEF2 is 5'-CT(A/T)(A/T)AATAG-3' (Andres et al., 1995). Interestingly, in the brain, MEF2 appears to be more selective, with additional sequence constraints present in the binding site. The neuronal MEF2 consensus binding site is 5'-TGTTACT(A/T)(A/T)AAATAGA(A/T)-3' (Andres et al., 1995).

MEF2 binds to DNA as either homo- or hetero-dimers (McKinsey et al., 2002). In addition, MEF2 can act with a large number of accessory proteins which regulate MEF2 function. MEF2 itself likely acts as a co-factor for many basic helix-loop-helix (bHLH) transcription factors, such as MyoD (McKinsey et al., 2002; Black, 1998).

Many mutant forms of MEF2 have been developed to study its function and mechanism of action. The herpes simplex viral protein VP16 is a potent transcriptional activator. When fused to a truncated MEF2 mutant containing only the MADS-box and MEF2 domain, the resulting fusion protein acts as a potent, constitutively active form of MEF2 (Molkentin and Olson, 1996). On the other hand, MEF2 mutants which are capable of dimerizing and associating with co-factors, but fail to associate with DNA due to mutations in the DNA binding regions of the MADS domain, act as dominant-negative isoforms, inhibiting endogenous MEF2 activity (Molkentin and Olson, 1996). Similarly, fusion of the potent transcriptional repressor Engrailed to the C-terminal of MEF2 results in robust inhibition of MEF2-dependent transcription (Arnold et al., 2007).

The role of MEF2 in muscle development has been extensively characterized (Black, 1998). In fact, much of what is known regarding MEF2 function comes from studies in developing skeletal muscle tissue or myocytes, where it serves to activate a complex program of tissue differentiation (Potthoff and Olson, 2007). However, the MEF2 proteins also have strong expression in the developing and adult brain, and recent studies have begun to elucidate the role of MEF2 in neuronal function.

MEF2 appears to have diverse functions that differ in various cell types. For example, MEF2 promotes cell cycle progression through the transcription of *c-jun* in many non-neuronal cells (Han and Prywes, 1995), is pro-apoptotic in thymocytes (T-cell

precursors) (Blaeser et al., 2000; Woronicz et al., 1995), and it appears to play a protective, anti-apoptotic role in neurons (Mao et al., 1999; Mao and Wiedmann, 1999; Okamoto et al., 2000). Thus, tissue-specific regulation of MEF2 and its association with gene targets likely plays an important role in determining the ultimate effects of MEF2 activity.

Mechanisms of MEF2 regulation

As with many transcription factors and intracellular signaling proteins, MEF2 activity is tightly regulated by calcium-sensitive mechanisms. Interestingly, activation of either calcium-dependent kinases or calcium-dependent phosphatases serves to increase MEF2-dependent transcription, albeit through separate mechanisms.

The calcium/calmodulin-dependent protein kinase family (CaMK) is a large protein family that governs a wide array of cellular functions, both in neuronal and non-neuronal cells. Stimulation of CaMK activity increases the transcriptional activity of multiple MEF2 isoforms in several cell types (Blaeser et al., 2000; Lu et al., 2000; Passier et al., 2000; Wu et al., 2000). Interestingly, although CaMKIV directly phosphorylates MEF2D, CaMKIV may not be able to directly phosphorylate MEF2A, -B, or -C (Blaeser et al., 2000). Therefore, the mechanism of CaMK enhancement of MEF2-dependent transcription is likely indirect, through phosphorylation of other factors.

Indeed, CaMKI and CaMKIV have been shown to phosphorylate class II histone deacetylases (HDACs) (McKinsey et al., 2000). HDACs deacetylate the N-terminal of histones, condensing the chromatin and thus inhibiting transcription; this activity is opposed by histone acetyltransferases (HATs), which promote chromatin relaxation and enhance transcription (Strahl and Allis, 2000). When dephosphorylated, class II HDACs interact with the MADS-box and MEF2 domains of MEF2 and inhibit MEF2 transcriptional activity (McKinsey et al., 2001).

Phosphorylation of class II HDACs by CaMKs promotes MEF-dependent transcription through several distinct mechanisms. First, it increases the affinity of the chaperone protein 14-3-3 for the phosphorylated HDAC (McKinsey et al., 2000), which disrupts the association of HDACs with MEF2 (Grozinger and Schreiber, 2000).

Association with 14-3-3 also induces a conformational change in HDACs that reveals a nuclear export signal (NES) and conceals a nuclear localization signal (NLS), resulting the expulsion of class II HDACs from the nucleus (Grozinger and Schreiber 2000, McKinsey et al., 2001). Release of HDACs from MEF2 further allows the protein p300, a HAT, to bind to MEF2, thus promoting transcription (McKinsey et al., 2001).

MEF2 transcriptional activity is also positively regulated by the calcium-dependent serine/threonine phosphatase calcineurin. Like activation of the CaMKs, calcineurin-dependent activation of MEF2 transcriptional activity is complex.

MEF2 is phosphorylated by cyclin-dependent kinase 5 (Cdk5), which is activated in response to neurotoxins (Gong et al., 2003). Cdk5 phosphorylation of MEF2 initiates caspase-mediated cleavage of MEF2, resulting in a truncated form containing a DNA-binding domain without a transcriptional activation domain (Tang et al., 2005). This truncated form of MEF functions as a dominant negative, which inhibits transcription of MEF gene targets and induces neuronal death (Okamoto et al., 2002). Activation of calcineurin causes the dephosphorylation of MEF2 and the transcription of anti-apoptotic genes, presumably through protection against Cdk5-dependent caspase cleavage (Mao et al., 1999).

Additionally, calcineurin stimulates MEF2 activity through regulation of the NFAT (nuclear factor of activated T-cells) family of transcription factors. Several members of the NFAT family bind directly to MEF2 and stimulate MEF2-dependent transcription, in part by recruiting p300 (Blaeser et al., 2000; Youn et al., 2000). Phosphorylated NFAT is cytoplasmically localized; dephosphorylation via calcineurin induces translocation of NFAT to the nucleus, where it can associate with MEF2 (Blaeser et al., 2000).

Finally, direct dephosphorylation of MEF2 by calcineurin increases the affinity of MEF2 for its DNA binding sites (Mao et al., 1999), although it is unclear whether calcineurin activity regulates HDAC-MEF interactions (McKinsey et al., 2000).

Several additional signaling pathways have also been shown to regulate MEF2 function. Both p38 mitogen-activated protein kinase (MAPK) and extracellular signal-related protein kinase 5 (ERK5) have been shown to phosphorylate MEF2 in its

transcription activation domain (Kato et al., 1997; Yang et al., 1998), thereby enhancing its transcriptional activity, possibly even to a level that is capable of overriding HDAC-mediated transcriptional repression (McKinsey et al., 2000; Miska et al., 2001). Interestingly, ERK5 also appears capable of functioning directly as a co-factor in MEF2-dependent transcription through association with the MADS-box (Yang et al., 1998).

Protein kinase A (PKA) phosphorylates MEF2 in the MADS domain, which increases DNA binding affinity (Wang et al., 2005b). PKA-mediated phosphorylation promotes MEF2-dependent survival of granule cells in the cerebellum (Wang et al., 2005b). Cyclic AMP (cAMP), the upstream activator of PKA, is well-known to be implicated in neuronal survival, and transcription of MEF2 target genes may play a critical role in this protective effect.

In addition, the promiscuous casein kinase II (CKII) has been shown to phosphorylate MEF2C between the MADS and MEF2 domains (Molkentin and Olson, 1996). This phosphorylation, like PKA phosphorylation, increases affinity of MEF2 with its gene targets.

The PI3K? Akt pathway, which is a downstream effector of mGluR signaling, has also been demonstrated to stimulate MEF2-dependent transcription (Wiedmann et al., 2005). PI3K and Akt are also known to be activated by survival signals, such as insulin-like growth factor 1 (IGF-1). Indeed, inhibition of MEF2 transcriptional activity impaired IGF-1-mediated survival of cerebellar granule cells, indicating MEF2 target genes as critical mediators of IGF-1 signaling.

Finally, MEF2 may be regulated by the attachment of small ubiquitin-like modifier (SUMO) proteins. In particular MEF2A has been shown to be SUMOylated in cerebellar granule cells (Shalizi et al., 2006). SUMOylation of transcription factors typically represses their transcriptional activity (Zhao, 2007). Dephosphorylation of a key residue on MEF2 (Serine408) by calcineurin led to removal of SUMO from MEF2A, converting it from a transcriptional repressor to a transcriptional activator (Shalizi et al., 2006). Interestingly, regulation of MEF2A SUMOylation impacts the synaptic development of dendritic claws on the tips of granule neuron terminals in the cerebellum (see below).

Given the wide array of regulatory mechanisms governing MEF2 function, it is intriguing to consider the possibility that the relative affinity for select MEF2 target genes may also be modulated by which intracellular signal is activated. Thus, activation of one second messenger or kinase may induce the transcription of MEF2-dependent anti-apoptotic genes, while activation of a second messenger or kinase may induce the transcription of genes responsible for neuronal differentiation or maturation. Such a mechanism of action has yet to be validated, however.

MEF2-dependent regulation of synapse number and maturation

Recent evidence strongly implicates MEF2-dependent transcription as a key regulator of synapse number and synaptic differentiation and maturation. In hippocampal neurons, MEF2 has been repeatedly demonstrated to negatively regulate synapse number, both at the functional and structural level. Acute knock-down of MEF2A and -D in hippocampal dissociated cultures resulted in a significant increase in both visually identified synapses and in mEPSC frequency, with no change in the mEPSC amplitude (Flavell et al., 2006). Likewise, activation of MEF2-dependent transcription led to a significant decrease in synapse number (Flavell et al., 2006). Importantly, the increase in synaptic connections following MEF2 knockdown required NMDAR activation, L-type calcium channel function, and calcineurin activity, indicating that neuronal activity is necessary (Flavell et al., 2006).

Similar findings were observed in a mouse line in which MEF2C expression was abolished in the hippocampal dentate gyrus (Barbosa et al., 2008). Specifically, MEF2C-KO neurons displayed increased mEPSC frequency with no change in mEPSC amplitude (Barbosa et al., 2008). Furthermore, the maximum amplitude of evoked EPSCs was higher in MEF2C-KO neurons, indicative of increased synapse number (Barbosa et al., 2008). Over-activation of MEF2C with a constitutively active form reversed these observations, indicating that MEF2C activity negatively correlates with synapse number (Barbosa et al., 2008). In confirmation of this model, MEF2C expression also negatively correlated with dendritic spine number (Barbosa et al., 2008). Electron micrography of the synaptic ultrastructure revealed no MEF2-mediated changes in synapse form or

structure, suggesting that MEF2 may preferentially regulate synapse number rather than synaptic function or maturation (Barbosa et al., 2008).

However, MEF2 does appear to regulate synaptic maturation in at least one brain region. During the development of the cerebellum, dendritic tips of granule neurons undergo a characteristic differentiation from long, tapered tips to the mature dendritic claw, which consists of an overall cup-like appearance with multiple serrated surfaces (Shalizi et al., 2006). Knock-down of MEF2A resulted in an impairment of dendritic claw formation (Shalizi et al., 2006). This effect was reported to be due to transcriptional de-repression of MEF2A gene targets. A majority of MEF2A was observed to be SUMOylated (Shalizi et al., 2006), which would convert MEF2A to a transcriptional repressor (see above). Loss of MEF2A, therefore, would allow additional transcription factors (perhaps MEF2B, -C, or -D) to initiate transcription, thereby inhibiting dendritic claw formation. This view was supported by data demonstrating that expression of a mutant MEF2 construct, in which the potent transcriptional repressor Engrailed was fused to the MADS-box and MEF2 domain of MEF2, enhanced dendritic claw differentiation. Interestingly, calcineurin dephosphorylation was reported to inhibit SUMOylation, possibly providing a site for cellular regulation of MEF2 transcription in these neurons.

Finally, knockout of MEF2C in the neocortex resulted in abnormal cortical organization and neuronal distribution (Li et al., 2008). These data implicate MEF2-dependent transcription in neuron-wide morphological changes. In support of these results, MEF2D expression positively correlates with neurite length (Lam and Chawla, 2007), indicative of complex regulation of synaptic, dendritic, and neuronal structure and migration by MEF2.

Possible links between MEF2, FMRP, and autism

Mutations in the transcription factor methyl-CpG-binding protein 2 (MeCP2) result in Rett's Syndrome, a common form of mental retardation that encompasses many autistic phenotypes. Interestingly, MeCP2 has recently been demonstrated to positively regulate the expression of MEF2 (Chahrour et al., 2008). Furthermore, a recent study demonstrated that several MEF2 transcriptional targets are genetically linked with autism

(Morrow et al., 2008). Thus, there appears to be a connection between MEF2 and mental retardation and autism. Roughly 30% of FXS patients are autistic, making it a common cause of autism; perhaps FXS-related autism has biological underpinnings in altered MEF2 activity.

The phenotype of enhanced functional synapse and dendritic spine number in neurons lacking MEF2 function is strikingly similar to that observed in neurons lacking FMRP expression – both proteins negatively regulate synapse number. In addition, several MEF2-dependent transcripts are known mRNA targets for FMRP. In particular, the mRNA for *arc* is reported to be transcribed by MEF2 (Flavell et al., 2006); this mRNA is also a reported ligand for FMRP (Zalfa et al., 2003).

Based on the above data, I investigated whether FMRP and MEF2 may interact to co-regulate excitatory synapse number. I observe that activation of MEF2-dependent transcription in wild-type hippocampal neurons results in a robust loss of functional synaptic connections. Likewise, inhibition of MEF2 activity with a dominant negative form of MEF2 results in an increase in synapse number in wild-type neurons. However, neither activation nor inhibition of MEF2 transcriptional activity is capable of regulating synapse number in *Fmr1*-KO neurons, suggesting that MEF2 requires downstream FMRP-dependent translation of its transcripts to induce synapse loss. Similarly, although FMRP expression in *Fmr1*-KO neurons leads to a loss of both functional and structural synapses, in the presence of a dominant negative form of MEF2, FMRP fails to decrease synapse number in *Fmr1*-KO neurons, suggesting that FMRP requires MEF2-derived transcripts to regulate synapse number. These data demonstrate a novel genetic interaction between FMRP and MEF2 and provide a mechanistic model for the increased numbers of synapses observed in FXS patients and *Fmr1*-KO mice.

Materials and Methods

Hippocampal slice cultures, constructs, transfection, and drug treatments

Organotypic hippocampal slice cultures (OHSCs) were prepared from postnatal day 6 (P6) WT or *Fmr1*-KO mice bred from the congenic C57BL/6 mouse strain (Jackson Laboratories, Bar Harbor, ME) using previously published protocols (Stoppini

et al., 1991). Biolistic transfection and gold bullet preparation were performed with the Helios Gene Gun system (Bio-Rad, Hercules, CA) according to the manufacturer's protocols (McAllister, 2004). Slice cultures were biolistically transfected 3 days after plating and recorded 3-7 days thereafter. The equivalent age of the cultures at the time of all electrophysiology experiments was 12-16 days. MEF2 was allowed to express for 16-48 hours for all MEF2-VP16-ER^{TM} and MEF2-VP16 experiments. MEF2-Engrailed was allowed to express for 3-7 days. 4-hydroxytamoxifen (4OHT, Sigma) was prepared as a stock solution in ethanol; the final concentration of ethanol in slice culture media for all experiments was 0.1%, which is the concentration of ethanol used as a vehicle control. 4OHT was applied at a final concentration of either 1 µM or 10 µM (no difference was observed due to drug concentration and the values of these two conditions are pooled in the presented data) into the media of the slice cultures. After adding the drug to the media, a single, 50 µl aliquot of the media+drug/vehicle was dropped on top of the slices and allowed to filter through to the rest of the media. All FMRP-green fluorescent protein (GFP)-expressing and enhanced GFP (EGFP)-expressing constructs were described previously (Pfeiffer and Huber, 2007). MEF2-VP16-ER^{TM}, MEF2? DBD-VP16-ER^{TM}, and MEF2-VP16 constructs, as well as MRE-EGFP, were described previously (Flavell 2006) and/or provided by Christopher Cowan (UT Southwestern, Dallas, TX). The MEF2-Engrailed construct was provided by Eric Olsen (UT Southwestern, Dallas, TX) and was described previously (Shalizi 2006). p-mCherry was provided by Thomas Südhof (UT Southwestern, Dallas, TX).

Electrophysiology

Simultaneous whole-cell recordings were obtained from CA1 pyramidalneurons in slice cultures visualized using infrared-DIC and GFP fluorescence to identify transfected and nontransfected neurons (Pfeiffer and Huber, 2007). Recordings were made at 30°C in a submersion chamber perfused at ~3 ml/min with artificial CSF (ACSF) containing the following (in mM): 119 NaCl, 2.5 KCl, 26 NaHCO3, 1 NaH_2PO_4, 11 D-Glucose, 3 CaCl2, 2 MgCl2, 0.1 picrotoxin, 0.002 2-chloro-adenosine, 0.1% DMSO, pH 7.28, 320 mOsm and saturated with 95% O_2/5%CO_2. For all intracellular recordings, the

neuron was clamped at –60 mV through whole-cell recording pipettes (~3–7 MΩ) filled with an intracellular solution containing the following (in mM): 2.5 BAPTA, 125 Cs-Meth, 6 CsCl, 3 NaCl, 10 HEPES, 10 sucrose, 2 QX-314, 10 tetraethylammonium-Cl, 4 ATP-Mg, 0.4 GTP-Na, 14 phosphocreatine-Tris, pH 7.2, 285 mOsm. For mEPSC measurements, the ACSF was supplemented with 1 µM TTX. Synaptic responses were evoked by single bipolar electrode placed in stratum radiatum of area CA1 (along the Schaeffer collaterals) 50–200 µm from the recorded neurons with monophasic current pulses (5–40 µA, 200 µs). Capacitance, series resistance, and input resistance were measured in voltage clamp with a 400 ms, –10 mV step from a –60 mV holding potential (filtered at 30 kHz, sampled at 50 kHz). Cells were only used for analysis if the series resistance was <30 M? and was stable throughout the experiment. Input resistance ranged from 75 to 350 M? . Data were not corrected for junction potential.

Synaptic potentials were filtered at 2 kHz, acquired and digitized at 10 kHz on a personal computer using custom software (Labview; National Instruments, Austin, TX). Miniature EPSCs (mEPSCs) were detected off-line using an automatic detection program (MiniAnalysis; Synaptosoft, Decatur, GA) with a detection threshold set at a value greater than at least 2 SD of the noise values, followed by a subsequent round of visual confirmation. The detection threshold remained constant for the duration of each experiment. Significant differences between transfected and nontransfected neurons were determined using a paired *t* test.

Results

MEF2 activation induces loss of excitatory synaptic connections in wild-type neurons

MEF2 has been previously shown to reduce the number of excitatory synapses in hippocampal dissociated cultures (Flavell et al., 2006). To examine whether the mechanisms underlying MEF2-induced synapse loss are present in organotypic hippocampal slice culture (OHSC), I acutely expressed a tamoxifen-inducible, constitutively active form of MEF2 (MEF2-VP16-ER^{TM}) in OHSCs prepared from P6 *Fmr1*-KO mice. MEF2-VP16-ER^{TM} contains the complete DNA-binding region of MEF2 fused to the herpes simplex transcriptional activator VP16 to create a constitutively active

form of MEF2 (Flavell et al., 2006; Molkentin et al., 1996). MEF2-VP16-ER™ is cytoplasmically localized due to the addition of a mutated form of the ligand-binding domain of the estrogen receptor (ER™), preventing transcription from exogenous MEF2. Application of 4-hydroxytamoxifen (4OHT) induces rapid nuclear transport of MEF2-VP16-ER™, initiating MEF2-dependent transcription in a temporally restricted manner. This construct was recently thoroughly tested and found to be localized to the nucleus and transcriptionally active only upon the addition of 4OHT (Flavell et al., 2006). Neurons were biolistically co-transfected at 3 DIV with a plasmid expressing MEF2-VP16-ER™ and a second plasmid expressing GFP (pC3-EGFP) to fluorescently tag the transfected neurons. Biolistic co-transfection of multiple constructs is highly efficient, resulting in nearly 100% co-expression in transfected neurons (Wirth and Wahle, 2003) (personal observations).

24-48 hours after 4OHT application, simultaneous whole-cell patch-clamp recordings were obtained from untransfected wild-type and neighboring transfected MEF2-VP16-ER™-expressing CA1 pyramidal neurons (hereafter referred to as "neuron pairs"). AMPA receptor (AMPAR)-mediated EPSCs were evoked with paired pulses of extracellular stimulation of Schaffer collateral axons (50 ms inter-stimulus interval, ISI) and were measured in the neuron pairs held at −60 mV. I observed a ~40% reduction in the amplitude of EPSCs in neurons transfected with MEF2-VP16-ER™ (transfected 63.4 ± 4.9 pA; untransfected 107.0 ± 13.4 pA; $n = 37$, $p < 0.01$) (Fig. 3.1*D-F*). No significant difference was observed between transfected and untransfected neurons in resting membrane potential or input resistance, indicating that overall neuronal health and subthreshold membrane conductances were unaffected by transfection of MEF2-VP16-ER™. These data indicate that acute, postsynaptic activation of MEF2 reduces evoked synaptic transmission.

MEF2 activation reduces the frequency of miniature EPSCs in WT neurons

Several synaptic changes can account for the observed reduction in evoked EPSCs following MEF2 activation, including decreases in synapse number, strength of individual synapses, or presynaptic release probability. To begin to differentiate between

these possibilities, I measured the effects of MEF2 activation on spontaneous (action-potential independent) mEPSCs in neuron pairs in the presence of TTX (1 μM). mEPSC amplitude is indicative of the strength of individual functional synapses, whereas mEPSC frequency is dependent on synapse number as well as presynaptic release probability. The frequency of mEPSCs was reduced by ~40% in wtFMRP-GFP-expressing cells as compared with untransfected *Fmr1*-KO neurons (transfected 1.21 ± 0.24 Hz; untransfected 2.04 ± 0.31 Hz; $n = 39$, $p < 0.05$), whereas the amplitude of mEPSCs was unchanged (transfected 16.5 ± 0.8 pA; untransfected 17.7 ± 1.1 pA; $n = 39$, $p = 0.12$) (Fig. 3.1*A-C,F*). Therefore, postsynaptic MEF2 activation reduces synaptic transmission not by reducing the strength of individual synapses, but by either decreasing presynaptic glutamate release probability or the number of synapses.

MEF2 activation does not affect short-term plasticity

To differentiate between potential MEF2 effects on synapse number vs. pre-synaptic release probability, I measured the paired-pulse ratio of evoked EPSCs after rapid, successive stimuli in neuron pairs. Paired-pulse ratio (a ratio of the EPSC amplitude of the second pulse to that of the first pulse) is inversely proportional to presynaptic release probability and provides a relative indicator of this measure (Manabe et al., 1993). There was no effect of MEF2 activation on the paired-pulse ratio at an interstimulus interval of 50 ms (transfected 2.08 ± 0.07; untransfected 2.14 ± 0.12; $n = 34$, $p = 0.62$) (Fig. 3.1*D,F*). These results indicate that postsynaptic expression of FMRP does not affect the presynaptic release probabilities of axons providing input to that neuron. Thus, it is likely that MEF2 activation in wild-type neurons reduces functional synapse number.

MEF2 effects on synaptic function require nuclear localization and DNA binding

To confirm that the reduction in synapse number following MEF2 activation is due to 4OHT stimulation of MEF2 transcription, I performed two additional experiments. In one set of control experiments, wild-type OHSCs were co-transfected with MEF2-VP16-ER^{TM} and pc3-EGFP and treated with vehicle. In a second set of control

experiments, wild-type OHSCs were co-transfected with pC3-EGFP and MEF2?DBD-VP16-ER^{TM}, a mutant form of MEF2 that is deficient in DNA binding and therefore unable to induce transcription (Flavell et al., 2006), and treated with 4OHT. Neither of these conditions produced any effect on AMPAR-mediated EPSCs, mEPSC amplitude or frequency, paired-pulse ratio, input resistance, or resting membrane potential (Fig. 3.1*G–R*, data not shown).

MEF2 dominant negative increases functional synapse number in WT neurons

Recent data indicate that decreasing MEF2 activity can increase both functional and structural synapse number (Flavell et al., 2006; Barbosa et al., 2008). These results indicate that there exists a tonic, basal level of MEF2 activity which negatively regulates synapse number; when this basal level of MEF2 function is removed, synapse number increases. To test whether acute inhibition of MEF2 activity can regulate functional synapse number, I co-transfected wild-type OHSCs with pC3-EGFP and MEF2-Engrailed, a dominant negative form of MEF2 in which the potent transcriptional repressor Engrailed has been fused to the DNA-binding and dimerization domains of MEF2 (Shalizi et al., 2006). MEF2-Engrailed is capable of hetero-dimerizing with endogenous MEF2, thereby preventing MEF2-dependent transcription.

Expression of MEF2-Engrailed in wild-type neurons resulted in a robust increase in evoked AMPAR-mediated EPSC amplitude (transfected 186.1 ± 26.0 pA; untransfected 101.7 ± 26.4 pA; n = 10, $p < 0.05$) (Fig. 3.1*P-R*). Furthermore, MEF2-Engrailed caused a significant increase in mEPSC frequency (transfected 1.76 ± 0.28 Hz; untransfected 1.08 ± 0.14 Hz; n = 19, $p < 0.01$), with no change in the paired-pulse ratio (transfected 2.12 ± 0.22; untransfected 1.89 ± 0.14; n = 10, $p = 0.35$) (Fig. 3.1*M,N,R*). Interestingly, mEPSC amplitude was also mildly increased by MEF2-Engrailed expression (transfected 15.6 ± 1.0 pA; untransfected 12.9 ± 0.7 pA; n = 19, $p < 0.05$) (Fig. 3.2*M,O,R*). These data indicate that acute inhibition of MEF2 activity is sufficient to increase functional synapse number.

Neither MEF2 activation nor MEF2 inhibition alters synapse number in Fmr1-*KO neurons*

To examine whether MEF2-dependent changes in synapse number are present in *Fmr1*-KO neurons, I repeated the above experiments in OHSCs prepared from *Fmr1*-KO mice. Surprisingly, expression of MEF2-VP16-ER^{TM} and subsequent treatment with 4OHT had no effect on any measure of synaptic function in *Fmr1*-KO neurons (evoked AMPAR-mediated amplitude: transfected 80.0 ± 7.8 pA, untransfected 89.7 ± 7.4 pA, n = 41, p = 0.17; mEPSC frequency: transfected 1.19 ± 0.22 Hz, untransfected 1.20 ± 0.23 Hz, n = 20, p = 0.97; mEPSC amplitude: transfected 21.6 ± 0.9 pA, untransfected 22.9 ± 0.1.3 pA, n = 20, p = 0.43; paired-pulse ratio: transfected 1.98 ± 0.10, untransfected 1.97 ± 0.09, n = 40, p = 0.90) (Fig 3.2*A-F*). Similarly, expression of MEF2-Engrailed also produced no changes in synaptic function (evoked AMPAR-mediated amplitude: transfected 89.2 ± 9.2 pA, untransfected 102.1 ± 14.9 pA, n = 14, p = 0.30; mEPSC frequency: transfected 1.59 ± 0.18 Hz, untransfected 1.74 ± 0.18 Hz, n = 19, p = 0.50; mEPSC amplitude: transfected 15.8 ± 1.1 pA, untransfected 15.4 ± 0.8 pA, n = 19, p = 0.77; paired-pulse ratio: transfected 2.32 ± 0.19, untransfected 2.13 ± 0.11, n = 14, p = 0.35) (Fig 3.2*M-R*). These data strongly suggest that MEF2-depedent regulation of synapse number requires FMRP activity.

A non-inducible, constitutively active form of MEF2 induces synapse loss in WT neurons, but not Fmr1-*KO neurons*

In the absence of a positive control for 4OHT activity, it could be argued that MEF2-VP16-ER^{TM} fails to regulate synapse number in *Fmr1*-KO neurons simply because the drug was non-functional in those slices and MEF2-dependent transcription was not activated. To overcome this potential critique, I utilized MEF2-VP16 (without ER^{TM}), which is a constitutively active form of MEF2 that is permanently localized to the nucleus, thus eliminating precise temporal control over MEF2 activation, but also negating the need for 4OHT application. Furthermore, I utilized an additional reporter construct in which EGFP expression is driven by the MEF2-responsive element (MRE). MRE-EGFP produces intense EGFP expression only when MEF2 is activated.

To confirm that the MRE-EGFP construct is regulated exclusively by MEF2, I co-transfected MRE-GFP with MEF2-VP16-ER^{TM}, along with p-mCherry as a reporter of transfection into wild-type OHSCs. In the absence of 4OHT, EGFP expression was minimal, with only a small handful of mCherry-positive neurons have any detectable EGFP (Fig 3.4*A*). This minimal EGFP expression was likely due to the activity of endogenous MEF2. However, following treatment with 4OHT, EGFP was rapidly (< 24 hours) and robustly expressed in greater than 80% of the transfected neurons (Fig 3.4*A*). 4OHT induction of EGFP expression was abolished by expression of the DNA binding mutant MEF2DBD-VP16-ER^{TM} (data not shown). Thus, MRE-EGFP is a reliable marker of MEF2 activity.

I co-transfected wild-type and *Fmr1*-KO OHSCs with MEF2-VP16 and MRE-EGFP and repeated the above experiments to confirm whether MEF2-induced synapse loss is absent in *Fmr1*-KO neurons. Co-expression of MRE-EGFP and MEF2-VP16 produced robust EGFP expression in both WT and *Fmr1*-KO neurons, indicating that MEF2-dependent transcription is functional in the absence of FMRP.

As with 4OHT activation of MEF2-VP16-ER^{TM}, expression of MEF2-VP16 in wild-type neurons resulted in a significant decrease in functional synapse number (Fig 3.5*A-F*, figure and data still in preparation). However, MEF2-VP16 expression in *Fmr1*-KO neurons once again failed to alter any aspect of synaptic function (Fig 3.5*G-L*, figure and data still in preparation). These data argue convincingly that FMRP is required for MEF2-regulated synapse loss.

Acute, postnatal expression of FMRP in Fmr1*-KO neurons rescues the ability of MEF2 to regulate synapse number*

The inability of MEF2 to affect synapse number in *Fmr1*-KO neurons may be due to a loss of immediate FMRP function or it may be due to developmental changes in neuronal or transcriptional function resulting from loss of FMRP over the lifetime of the neuron. To differentiate between these two alternatives, I co-expressed FMRP-GFP-hpr (an FMRP-GFP fusion protein driven by the endogenous human *Fmr1* promoter), MEF2-VP16, and MRE-EGFP in *Fmr1*-KO neurons. GFP fluorescence for both FMRP-GFP

and MRE-driven EGFP was easily differentiated by the fact that MRE-driven GFP was diffusely expressed throughout the entire nucleus, soma, and dendritic arbors, while FMRP-GFP was tightly localized to discrete puncta throughout the dendrites. Thus, co-expression of FMRP-GFP and MRE-driven EGFP resulted in a GFP-filled neuron speckled with intense FMRP-GFP puncta.

Acute, postnatal expression of FMRP rescued the ability of MEF2-VP16 to decrease synapse number (evoked AMPAR-mediated amplitude: transfected ± pA, untransfected ± pA, n = , p = 0.; mEPSC frequency: transfected ± Hz, untransfected ± Hz, n = , p < 0.; mEPSC amplitude: transfected ± pA, untransfected ± pA, n = , p = 0.; paired-pulse ratio: transfected ± , untransfected ± , n = , p = 0.) (Fig 3.3*G-L*, figure and data still in preparation). Thus, the failure of MEF2 to regulate synapse number in *Fmr1*-KO neurons is not due to developmental impairments, but rather to an immediate loss of FMRP function.

FMRP-dependent synapse loss is abolished by co-expression of a dominant negative form of MEF2

I next sought to determine if MEF2 activity is required for FMRP-dependent synapse loss. Previous work (described in Chapter 2) demonstrates that acute FMRP expression in *Fmr1*-KO neurons results in functional and structural loss of synapses (Pfeiffer and Huber, 2007). I confirmed that transfection of FMRP-GFP-hpr induced synapse loss in *Fmr1*-KO neurons (evoked AMPAR-mediated amplitude: transfected 83.4 ± 7.6 pA, untransfected 107.5 ± 12.7 pA, n = 21, p = 0.08; mEPSC frequency: transfected 1.57 ± 0.24 Hz, untransfected 1.98 ± 0.33 Hz, n = 19, p < 0.05; mEPSC amplitude: transfected 14.5 ± 1.1 pA, untransfected 14.8 ± 1.2 pA, n = 19, p = 0.86; paired-pulse ratio: transfected 2.13 ± 0.22, untransfected 2.06 ± 0.13, n = 21, p = 0.77) (Fig 3.3*A-F*). Importantly, the effect induced by FMRP-GFP alone is much less than the effect of co-expression of FMRP-GFP with MEF2-VP16 (Fig 3.3*G-L*, in preparation), consistent with total MEF2 levels being inversely proportional to synapse number.

Interestingly, when FMRP-GFP-hpr was co-transfected into *Fmr1*-KO neurons alongside MEF2-Engrailed, it failed to induce synapse loss. (evoked AMPAR-mediated

amplitude: transfected 130.8 ± 17.3 pA, untransfected 114.7 ± 14.1 pA, n = 24, p = 0.37; mEPSC frequency: transfected 2.70 ± 0.44 Hz, untransfected 1.68 ± 0.30 Hz, n = 19, p < 0.05; mEPSC amplitude: transfected 15.9 ± 0.9 pA, untransfected 14.5 ± 0.9 pA, n = 19, p < 0.05; paired-pulse ratio: transfected 1.86 ± 0.07, untransfected 1.94 ± 0.10, n = 21, p = 0.38) (Fig 3.3*M-R*) In fact, there is a significant increase in the mEPSC frequency and amplitude, reminiscent of the increase observed when MEF2-Engrailed is expressed in wild-type neurons. FMRP-GFP localization was not affected by co-expression with MEF2-Engrailed (personal observations, data not shown), indicating that FMRP association with RNA granules and/or dendritic polyribosomes was not altered following MEF2 inhibition. These data strongly suggest that both FMRP and MEF2 act in the same pathway to co-regulate synapse number.

MEF2-dependent transcription is functional in Fmr1*-KO neurons*

It is possible that MEF2 fails to regulate synapse number in *Fmr1*-KO neurons simply because the transcriptional activity of MEF2 is compromised in the absence of FMRP. To test this possibility, Julia Wilkerson prepared dissociated neuronal cultures from wild-type or *Fmr1*-KO mice and co-transfected them with MEF2-VP16-ER^{TM}, MRE-EGFP (as a marker for MEF2 activity), and p-mCherry (as a marker for transfection). 8 hours post-transfection, neurons were treated with 4OHT or vehicle and EGFP-positive (EGFP^{+}) neurons were quantified 16-24 later. The percentage of mCherry-positive (mCherry^{+}) neurons co-expressing EGFP prior to 4OHT treatment was minimal in both wild-type and *Fmr1*-KO neurons (~20%). EGFP expression in the absence of 4OHT was very dim and just above our detection threshold of 2 times the background fluorescence (personal observations, data not shown). Induction of MEF2-VP16-ER^{TM} activity with 4OHT led to extremely robust EGFP expression in virtually all mCherry-positive neurons of both genotypes (~80%) (Fig 3.4*A*). The failure of 4OHT application to elicit EGFP expression in 100% of mCherry^{+} neurons is likely due to inherent imperfection of co-transfection in dissociated cultures rather than a failure of 4OHT to induce MEF2-dependent transcription of MRE-driven EGFP. The ratio of EGFP^{+}/mCherry^{+} neurons was significantly increased following 4OHT treatment for both

wild-type and *Fmr1*-KO neurons. Importantly, the ratio of $EGFP^+/mCherry^+$ cells following 4OHT induction was not different between the two genotypes, indicating that loss of FMRP does not affect MEF2-dependent transcription. Furthermore, quantification of the intensity of EGFP expression in $EGFP^+$ neurons revealed that *Fmr1*-KO neurons had elevated expression of GFP following 4OHT treatment (Fig 3.3*B*). Thus, these data suggest that MEF2-dependent transcription is functional and may even be slightly enhanced in the absence of FMRP.

To more directly test whether MEF2-dependent transcription is functional in *Fmr1*-KO neurons, I examined whether endogenous MEF2 is capable of inducing the transcription of a well-defined MEF2 target gene, *Nur-77* (Flavell et al., 2006; Shalizi et al., 2006). Both wild-type and *Fmr1*-KO OHSCs were grown to equivalent age 12 days. The media was then replaced with equi-osmotic media containing 55 mM KCl to induce prolonged neuronal depolarization. This protocol is commonly used to induce robust endogenous MEF2 activation (Flavell et al., 2006). Slices were harvested at 0hr, 0.5 hr, 1 hr, 3 hr, and 6 hr timepoints and probed for *Nur-77* mRNA levels with RT-PCR. Makoto Taniguchi isolated the mRNA and performed the RT-PCR experiments. Although there is a subtle, but significant decrease in the levels of *Nur-77* mRNA following neuron depolarization in *Fmr1*-KO slices, it is clear that *Nur-77* transcription is strongly induced in the absence of FMRP (Fig 3.3*C*, in preparation). Furthermore, both the onset and offset of *Nur-77* mRNA expression is similar between wild-type and *Fmr1*-KO slices, suggesting that the regulatory mechanisms underlying MEF2-dependent transcription are intact in *Fmr1*-KO mice. Combined, these data argue that MEF2 transcriptional activity is present and largely normal in the absence of FMRP.

Discussion

MEF2 fails to regulate synapse number in Fmr1*-KO neurons*

In accordance with previous studies (Flavell et al., 2006; Barbosa et al., 2008), I have demonstrated that activation of MEF2-dependent transcription negatively regulates the number of functional synapses in wild-type neurons. This synapse loss was dependent upon both nuclear localization and DNA binding, as it was blocked by

cytoplasmic restriction of MEF2 or by mutations in MEF2 that impair DNA binding. Furthermore, inhibition of endogenous MEF2 with a dominant negative form increased functional synapse number, indicating that basal levels of endogenous MEF2 actively induce synapse loss.

Two recent studies have linked MEF2 with autism and mental retardation (Charuour et al., 2008; Morrow et al., 2008), suggesting that precise control of either MEF2 function or the activity of MEF2 transcripts may be important for proper neuronal development or function. Interestingly, MEF2 fails to alter synapse number in *Fmr1*-KO mice, providing additional evidence of MEF2 disregulation in a mouse model of mental retardation. Neither a constitutively active form nor a dominant negative form of MEF2 produce any changes in synapse number or function in neurons lacking FMRP expression, suggesting that neither exogenous nor endogenous MEF2 is capable of regulating synapse number in the absence of FMRP.

Acute postnatal expression of FMRP in *Fmr1*-KO neurons rescues the ability of MEF2 to regulate synapse number. Thus, the inability of MEF2 to alter synapse number in *Fmr1*-KO neurons is not due to altered developmental programs, but rather due to an immediate lack of FMRP function. Importantly, MEF2-driven transcription appears largely normal in *Fmr1*-KO neurons, indicating that the failure of MEF2 to regulate synapse number in the absence of FMRP is not due to impairment in MEF2-driven transcription. These data provide a compelling argument that MEF2-dependent synapse loss requires FMRP function.

FMRP fails to regulate synapse number in the absence of MEF2 transcription

Alterations in the number and morphology of dendritic spines have been observed in FXS patients and *Fmr1*-KO mice, both *in vivo* and in cultured neurons (Braun and Segal, 2000; Irwin et al., 2001; Nimchinsky et al., 2001; Bagni and Greenough, 2005; Antar et al., 2006; Grossman et al., 2006a,b, Pfeiffer and Huber 2007, Dolen 2007). Recent work has demonstrated that acute postsynaptic expression of FMRP in *Fmr1*-KO neurons decreases the number of functional and structural synapses (Pfeiffer

and Huber, 2007). However, the mechanism of FMRP-mediated synapse elimination is unclear.

In this report, I observe that expression of a dominant-negative form of MEF2, MEF2-Engrailed, abolishes the ability of FMRP to decrease synapse number. FMRP displays a punctate expression pattern throughout the dendritic arbors (Pfeiffer and Huber 2007; Antar et al., 2004) and expression of MEF2-Engrailed did not affect the localization of exogenous FMRP (personal observations, data not shown), indicating that MEF2-Engrailed did not affect FMRP interactions with RNA granules or dendritically localized polyribosomes. However, I can not rule out the possibility that MEF2-Engrailed expression disrupts specific molecular interactions of FMRP.

Possible mechanisms of MEF2-FMRP cooperative regulation of synapse number

The canonical function of MEF2 is transcriptional activation, while the canonical function of FMRP lies in translational regulation of mRNA targets. It is possible that FMRP is a required co-factor for MEF2-dependent transcription, such that in *Fmr1*-KO mice, MEF2 is unable to properly initiate transcription of its gene targets. Data demonstrating relatively normal MEF2-mediated transcription in *Fmr1*-KO mice suggests that this is not the case, however, it is possible that FMRP may directly mediate the transcription of select gene targets that have not yet been identified. Alternatively, MEF2 may play a direct role in FMRP-mediated translational regulation such that in the presence of MEF2, translation of FMRP target mRNAs is altered. Again, this seems unlikely to be the case as MEF2-VP16-ER^{TM} only induces synapses when it is trafficked to the nucleus, while FMRP is nearly exclusively cytoplasmically localized (Feng et al., 1997). This also largely rules out the possibility that FMRP and MEF2 interact directly with synaptic proteins to decrease synapse number.

The most likely mechanism through which MEF2 and FMRP act in concert to co-regulate synapse number is one in which one or more MEF2-driven transcripts which code for proteins necessary for synapse loss are translationally regulated by FMRP (Fig 3.6). Increased MEF2 activity (such as following MEF2-VP16 expression) results in increased levels of MEF2-driven transcripts, which are translationally regulated by

FMRP to induce increased synapse loss. In the absence of MEF2 activity (such as following MEF2-Engrailed expression), MEF2-driven transcripts are absent, resulting in an observed increase in synapse number. In the absence of FMRP, MEF2-driven transcripts are either unable to be translated or are translated inappropriately, resulting in the absence or impaired localization/function of the proteins necessary for synapse elimination. Therefore, without FMRP, increasing or decreasing MEF2 activity does not result in any changes in synapse number.

One piece of data not consistent with the above model, however, is the increase in mEPSC frequency and amplitude following co-expression of MEF2-Engrailed and FMRP-GFP in *Fmr1*-KO mice, similar to what was seen with MEF2-Engrailed expression alone in wild-type neurons. On the surface, this seems to be a rescue of the wild-type phenotype of increased synapse number following MEF2 inhibition. However, the above model suggests that in *Fmr1*-KO neurons, MEF2 transcripts are being produced at basal levels, but they are not being properly translated due to lack of FMRP. Thus, basal synapse number in *Fmr1*-KO neurons should be at a level comparable to synapse number in wild-type neurons following MEF2 inhibition. Indeed, MEF2-Engrailed expression in *Fmr1*-KO neurons fails to alter synapse number, suggesting that synapse number might be at or near a maximum level. If MEF2-Engrailed and FMRP are co-expressed in *Fmr1*-KO neurons, MEF2 transcripts should decrease while FMRP expression increases. The above model would predict no change in synapse number or function in *Fmr1*-KO neurons because the MEF2-dependent transcripts that were present prior to MEF2-Engrailed expression were not being translated (due to the absence of FMRP), so elimination of those transcripts (due to MEF2-Engrailed) should not lead to any changes in protein expression or function, and therefore should not alter synapse number. However, we observe a significant increase in mEPSC frequency and amplitude following co-expression of MEF2-Engrailed and FMRP. Interestingly, evoked AMPAR-mediated EPSC amplitude is unchanged, whereas it is strongly increased in wild-type neurons expressing MEF2-Engrailed. Thus, the phenotype is not completely identical between wild-type neurons expressing MEF2-Engrailed and *Fmr1*-KO neurons co-expressing MEF2-Engrailed and FMRP.

In Chapter 4, I report that FMRP expression in very young *Fmr1*-KO neurons (equivalent day p6-7) results in an increase in synaptic function. One potential explanation for this may be that the transcripts available for FMRP-dependent translational regulation are altered in young vs. older neurons. MEF2 expression in the hippocampus begins around p7 and increases up to p21, a timecourse that mirrors a period of intense synapse elimination in the brain (Flavell et al., 2006). Thus, MEF2 expression may account for a developmental shift in the pool of mRNA targets available for FMRP. MEF2-Engrailed expression might reduce the availability of MEF2-dependent "synapse elimination" mRNAs, providing FMRP unabated access to the "synapse strengthening" mRNAs that may still be produced by other transcription factors. This model of bi-directional regulation of synaptic strength by FMRP is discussed further in Chapters 4 and 5.

Inhibition of MEF2 activity increases synaptic strength as well as synapse number

I observe that, in addition to increased numbers of synapses, inhibition of MEF2 activity with MEF2-Engrailed results in post-synaptic strengthening of synaptic connections, as the mEPSC amplitude is increased following MEF2-Engrailed expression. The finding of increased mEPSC amplitude following MEF2-Engrailed expression further raises the intriguing notion that MEF2 may regulate more than just synapse number. Indeed, MEF2 has been demonstrated to affect many aspects of neuronal function, from survival to migration to dendritic differentiation (Mao et al., 1999; Okamoto et al., 2000; Flavell et al., 2006; Shalizi et al., 2006; Barbosa et al., 2008; Li et al., 2008). Thus, it is possible that MEFs may negatively regulate the maturation or strength of excitatory synaptic connections. Loss of MEF2 function, therefore, increases rate of maturation or synaptic strength, presumably through increased AMPAR expression at the surface of the postsynapse. Surprisingly, increased activity of MEF2 did not alter mEPSC amplitude, suggesting that basal levels of endogenous MEF2 are sufficient to saturate this particular downstream effect. As with MEF2-dependent regulation of synapse number, the ability of MEF2 inhibition to increase synaptic

strength also seems to be regulated by FMRP, as mEPSC amplitude is unaffected by MEF2-Engrailed expression in *Fmr1*-KO neurons.

MEF2 may differentially regulate transcription of its gene targets

Thus, it is possible that the observed increase in mEPSC frequency in both wild-type neurons expressing MEF2-Engrailed and in *Fmr1*-KO neurons co-expressing MEF2-Engrailed and FMRP results from an increased detection threshold, as synapses with mEPSC amplitudes too small to be detected were strengthened to the point of detection. This may partially account for the unexpected increase in mEPSC frequency in *Fmr1*-KO neurons following co-expression of FMRP and MEF2-Engrailed.

Although MEF2 is canonically thought of as a transcriptional activator, it is known that MEF2 can act as both a transcriptional activator and a transcriptional repressor depending on its association with co-factors or its phosphorylation status (Gong et al., 2003; Tang et al., 2005; Li et al., 2001; Okamoto et al., 2002; Mao et al., 1999; McKinsey et al., 2002). It is intriguing, therefore, to consider that MEF2 may differentially regulate the transcription of multiple targets, inhibiting the transcription of some while stimulating the transcription of others.

In this model, activation of MEF2 may increase the transcription of mRNAs necessary for synapse elimination, while simultaneously inhibiting the transcription of mRNAs necessary for synapse strengthening (possibly by increasing the production of a second transcriptional repressor). Thus, decreased MEF2 activity following MEF2-Engrailed expression, would result in decreased "synapse loss" mRNAs and increased "synapse strengthening" mRNAs, leading to a larger number of stronger synaptic connections. This model requires extensive testing to confirm and I postulate it only to spur future experimentation.

Arc mRNA as a possible link between MEF2 and FMRP

Several MEF2-dependent transcripts are known mRNA targets for FMRP. In particular, the mRNA for *Arc* is reported to be transcribed by MEF2 (Flavell et al., 2006) and translationally regulated by FMRP (Zalfa et al., 2003). The role that activity-

regulated cytoskeletal protein (Arc, also known as Arg3.1) plays in synaptic function is still largely unclear, although recent evidence suggests that it is critical for AMPAR internalization during LTD (Waung et al., 2008). Prolonged application of LTD-inducing stimuli has been reported to induce synapse loss (Shinoda et al., 2005). It is therefore conceivable that Arc-mediated AMPAR internalization is a necessary initial step in synapse elimination. In the absence of MEF2 activity, *Arc* (as well as other synapse elimination mRNAs) is not transcribed and synapse elimination fails to occur. Recent studies on FMRP-dependent synapse loss strongly implicate that FMRP stimulation of translation is necessary to eliminate synapses, as a mutant form of FMRP that preferentially associates with actively translating polyribosomes induces synapse loss, while a form that associated with stalled polyribosomes does not (Pfeiffer and Huber, 2007). Therefore, in the absence of FMRP, *Arc* (and other synapse elimination mRNAs) may not properly translated, leading to an increased number of synapses. Thus, *Arc* mRNA may provide a molecular link between MEF2-dependent transcription and FMRP-mediated translational regulation. Future experiments determining a possible connection between these three proteins will likely prove insightful.

Implications for Fragile X Syndrome

The findings of a phenotypic interaction between MEF2 and FMRP suggest several implications for FXS. MEF2 is known to regulate many important processes in both neuronal and non-neuronal cells. In particular, MEF2 has been found to be a key regulator of many developmental programs in a wide array of cell types, including skeletal and cardiac muscle, neural crest cells, endothelial cells, immune cells, and neurons (Potthoff and Olson, 2007). It is doubtful that FMRP may regulate the translation of all MEF2-dependent transcripts; however, the possibility emerges that the translation of some MEF2 gene targets may be altered in FXS patients and *Fmr1*-KO mice, resulting in altered or impaired development of these tissue types. Understandably, a majority of research on FXS has been focused on the brain. However, it is possible that elucidating the role that FMRP plays in other cell types will shed light on its neuronal function.

Recently, a homolog of FMRP, Fragile X Related Protein 1 (FXR1), was demonstrated to be critical for cardiac and skeletal muscle development (Mientjes et al., 2004). FMRP has two homologs, FXR1 and FXR2, which likely function similarly to FMRP, as they have similar RNA-binding motifs (see below) and are colocalized with FMRP (De Diego Otero et al., 2002; Bakker et al., 2000; Kanai et al., 2004). MEF2 is a critical regulator of both cardiac and skeletal muscle development (Potthoff and Olson, 2004). This finding suggests that MEF2-derived transcripts may be translationally regulated by the FMRP family of proteins and implies a conserved mechanism for transcriptional and translational regulation in multiple cell types.

These data present a compelling link between MEF2-dependent transcription and FMRP-regulated translation and strongly suggest that additional MEF2-mediated processes may be altered in *Fmr1*-KO mice. The most well-characterized phenotype of MEF2 activity in neurons is an anti-apoptotic neuro-protective effect (McKinsey et al., 2002). In addition, a recent study implicates MEF2 function in regulation of dendritic claw formation in cerebellar granule cells (Shalizi et al., 2006). It will be interesting to see if these phenotypes are altered in *Fmr1*-KO mice or FXS patients.

Figure 3.1. Acute postsynaptic MEF2 activity negatively regulates functional synapse number in wild-type neurons.

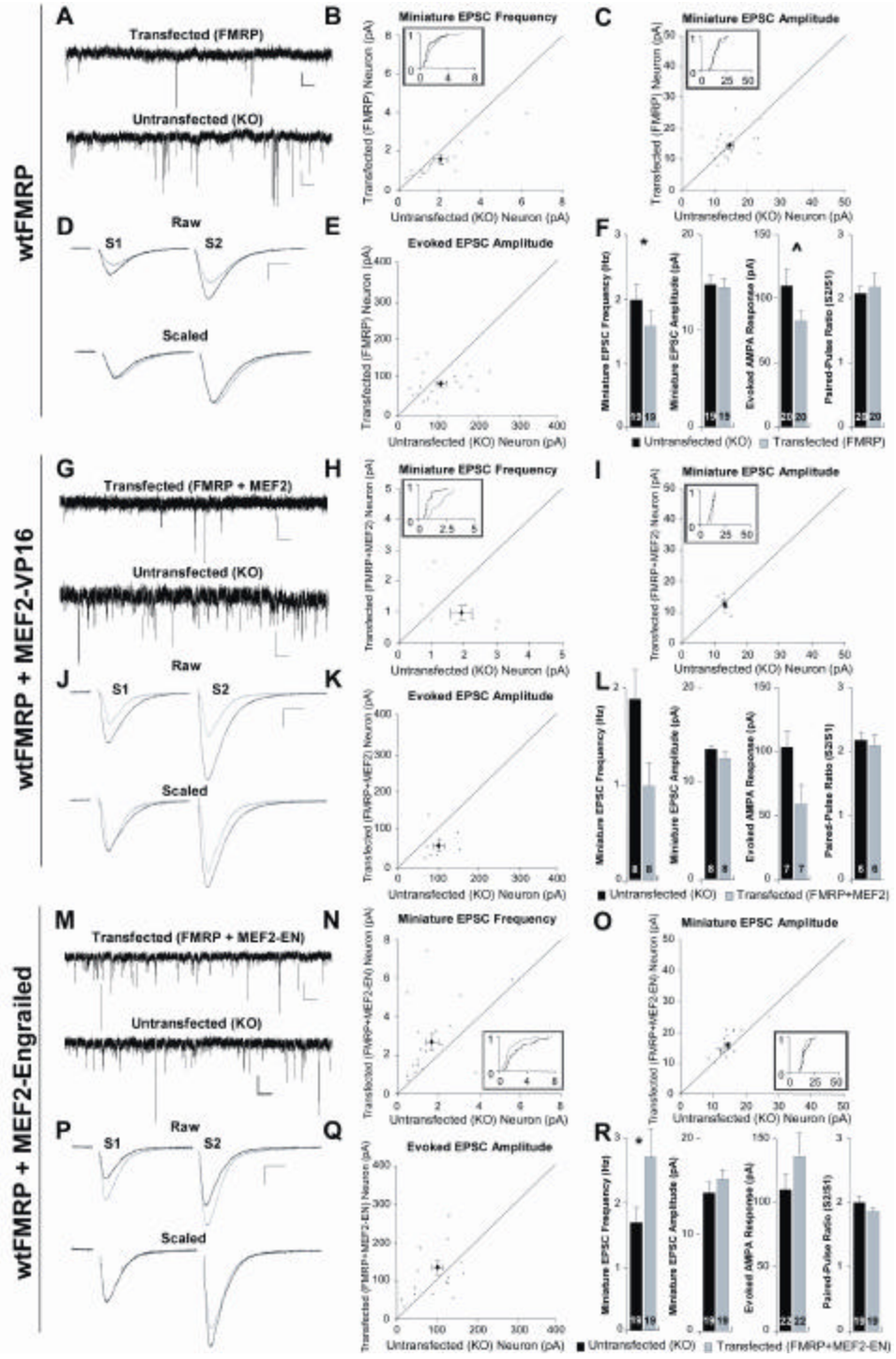

Figure 3.1. Acute postsynaptic MEF2 activity negatively regulates functional synapse number in wild-type neurons. ***A-F***, Organotypic hippocampal slice cultures from p6 wild-type mice were biolistically transfected with MEF2-VP16-ER^{TM} and treated with 4-hydroxytamoxifen to induce MEF2-VP16-ER^{TM} activation. ***A***, Representative traces of mEPSCs simultaneously recorded from an untransfected wild-type neuron and a neighboring MEF2-VP16-ER^{TM} transfected neuron. Calibration: 10 pA, 500 ms. ***B***, ***C***, Dot plot representation of the frequency (***B***) and amplitude (***C***) of mEPSCs in paired recordings. In this and all figures, the diagonal line represents the values where the EPSC amplitudes from transfected and untransfected cells are equal. The large diamond represents mean ± SEM. Inset, Cumulative probability distributions for both untransfected neurons (solid black line) and transfected, MEF2-expressing neurons (dotted line). Each point on the curve represents the average mEPSC frequency and amplitude from an individual neuron. The *x*-axis is the mEPSC frequency (***B***) or amplitude (***C***). The *y*-axis is the cumulative probability. ***D***, Average of 25 consecutive traces from a representative experiment simultaneously recorded from an untransfected wild-type neurons and a neighboring MEF2-VP16-ER^{TM} transfected neuron. Calibration: 50 pA, 10 ms. Stimulation artifact has been digitally removed for clarity. ***E***, Dot plot of the peak amplitude of the evoked AMPAR-mediated EPSCs of paired recordings. ***F***, Average mEPSC frequency, mEPSC amplitude, AMPAR-mediated EPSC amplitude, and paired-pulse ratio (second response amplitude/first response amplitude) from untransfected wild-type and MEF2-VP16-ER^{TM} transfected cells. ***G-L***, as **(*A-F*)**, except cells were treated with vehicle (0.1% ethanol) instead of tamoxifen. ***M-R***, as **(*A-F*)**, except cells were transfected with a dominant-negative form of MEF2, MEF2-Engrailed. In this and all figures, averages are plotted + SEM and *n* is plotted on each bar. $*p < 0.05$.

Figure 3.2. Acute postsynaptic MEF2 activity fails to alter functional synapse number in *Fmr1*-KO neurons.

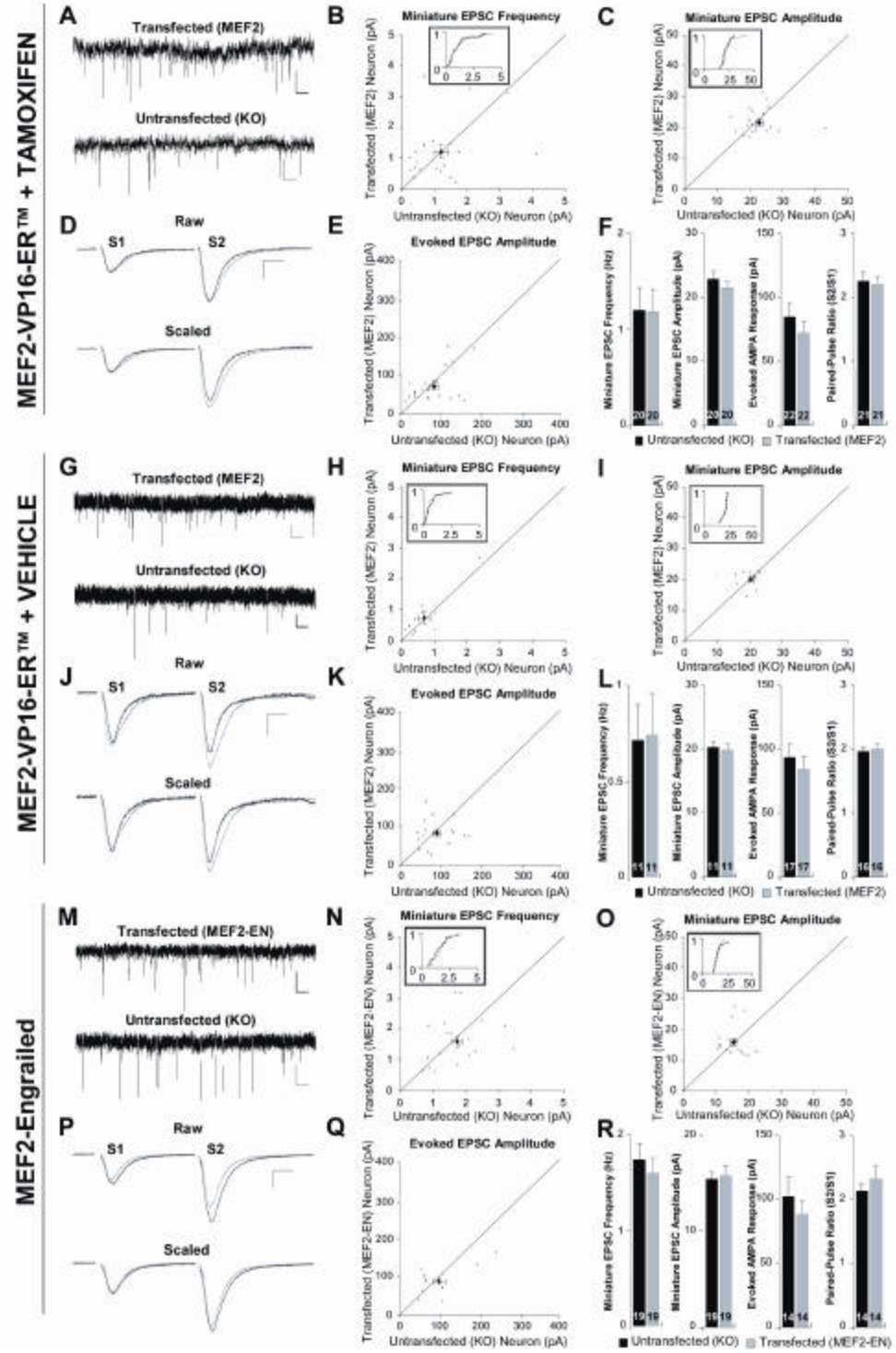

Figure 3.2. Acute postsynaptic MEF2 activity fails to alter functional synapse number in *Fmr1*-KO neurons. ***A-F***, Organotypic hippocampal slice cultures from p6 *Fmr1*-KO mice were biolistically transfected with MEF2-VP16-ER^{TM} and treated with 4-hydroxytamoxifen to induce MEF2-VP16-ER^{TM} activation. ***A***, Representative traces of mEPSCs simultaneously recorded from an untransfected KO neuron and a neighboring MEF2-VP16-ER^{TM} transfected neuron. Calibration: 10 pA, 500 ms. ***B***, ***C***, Dot plot representation of the frequency (***B***) and amplitude (***C***) of mEPSCs in paired recordings. The large diamond represents mean ± SEM. Inset, Cumulative probability distributions for both untransfected neurons (solid black line) and transfected, MEF2-expressing neurons (dotted line). Each point on the curve represents the average mEPSC frequency and amplitude from an individual neuron. The *x*-axis is the mEPSC frequency (***B***) or amplitude (***C***). The *y*-axis is the cumulative probability. ***D***, Average of 25 consecutive traces from a representative experiment simultaneously recorded from an untransfected *Fmr1*-KO neurons and a neighboring MEF2-VP16-ER^{TM} transfected neuron. Calibration: 50 pA, 10 ms. Stimulation artifact has been digitally removed for clarity. ***E***, Dot plot of the peak amplitude of the evoked AMPAR-mediated EPSCs of paired recordings. ***F***, Average mEPSC frequency, mEPSC amplitude, AMPAR-mediated EPSC amplitude, and paired-pulse ratio (second response amplitude/first response amplitude) from untransfected *Fmr1*-KO and MEF2-VP16-ER^{TM} transfected cells. ***G-L***, as **(*A-F*)**, except cells were treated with vehicle (0.1% ethanol) instead of tamoxifen. ***M-R***, as **(*A-F*)**, except cells were transfected with a dominant-negative form of MEF2, MEF2-Engrailed.

Figure 3.3. Phenotypic interactions between FMRP and MEF2 in functional synapse number regulation.

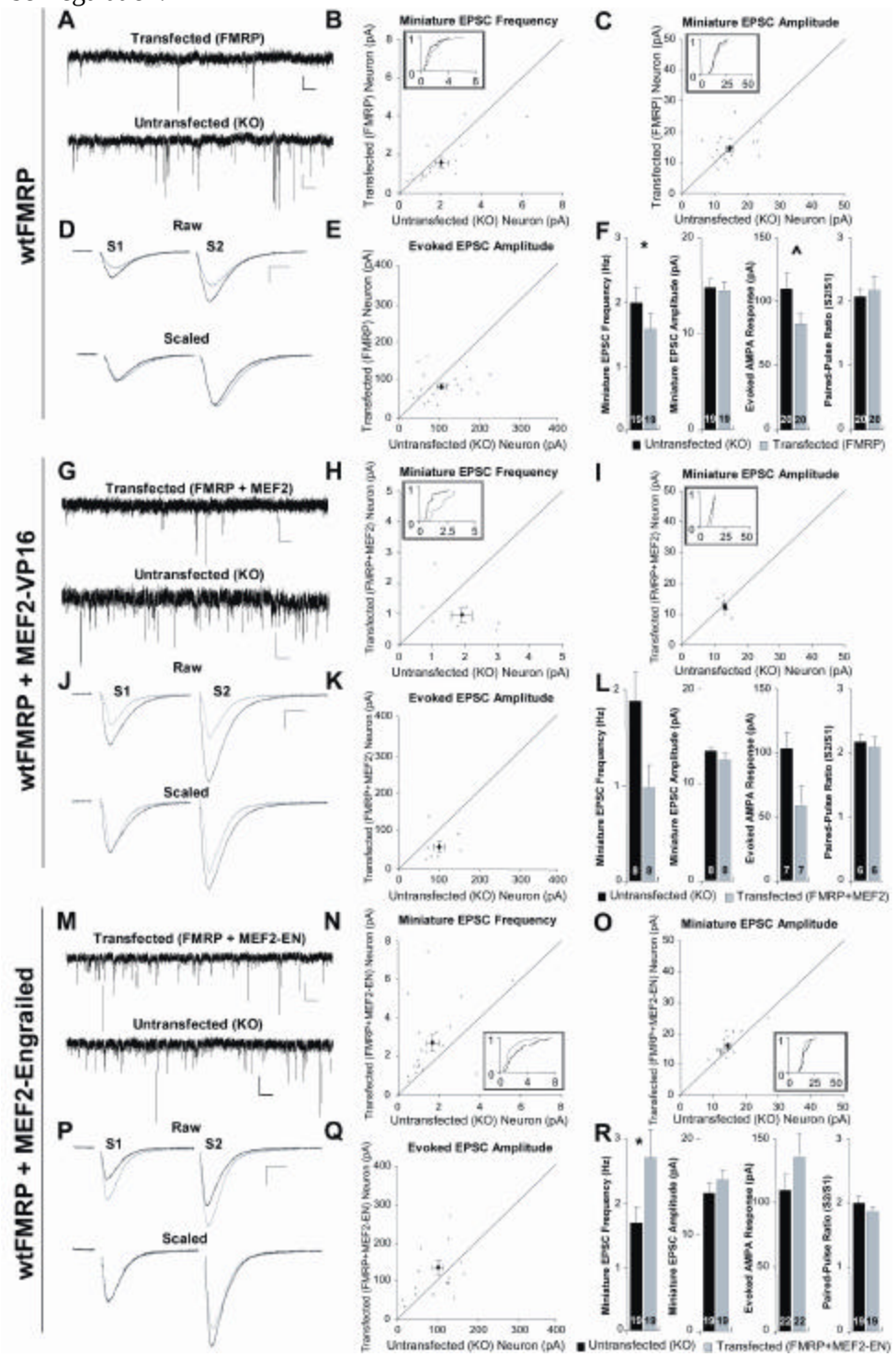

Figure 3.3. Phenotypic interactions between FMRP and MEF2 in functional synapse number regulation. ***A-F***, Organotypic hippocampal slice cultures from p6 *Fmr1*-KO mice were biolistically transfected with wtFMRP-GFP-hpr. ***A***, Representative traces of mEPSCs simultaneously recorded from an untransfected KO neuron and a neighboring FMRP transfected neuron. Calibration: 10 pA, 500 ms. ***B***, ***C***, Dot plot representation of the frequency (***B***) and amplitude (***C***) of mEPSCs in paired recordings. The large diamond represents mean ± SEM. Inset, Cumulative probability distributions for both untransfected neurons (solid black line) and transfected, FMRP-expressing neurons (dotted line). Each point on the curve represents the average mEPSC frequency and amplitude from an individual neuron. The *x*-axis is the mEPSC frequency (***B***) or amplitude (***C***). The *y*-axis is the cumulative probability. ***D***, Average of 25 consecutive traces from a representative experiment simultaneously recorded from an untransfected *Fmr1*-KO neurons and a neighboring FMRP transfected neuron. Calibration: 50 pA, 10 ms. Stimulation artifact has been digitally removed for clarity. ***E***, Dot plot of the peak amplitude of the evoked AMPAR-mediated EPSCs of paired recordings. ***F***, Average mEPSC frequency, mEPSC amplitude, AMPAR-mediated EPSC amplitude, and paired-pulse ratio (second response amplitude/first response amplitude) from untransfected *Fmr1*-KO and FMRP transfected cells. ***G-L***, as **(*A-F*)**, except cells were co-transfected with wtFMRP-GFP-hpr and MEF2-VP16. ***M-R***, as **(*A-F*)**, except cells were co-transfected with wtFMRP-GFP-hpr and a dominant-negative form of MEF2, MEF2-Engrailed. $*p < 0.05$.

Figure 3.4. MRE-EGFP expression in WT and *Fmr1*-KO neurons following activation of MEF2-VP16-ER^{TM} with 4-hydroxytamoxifen.

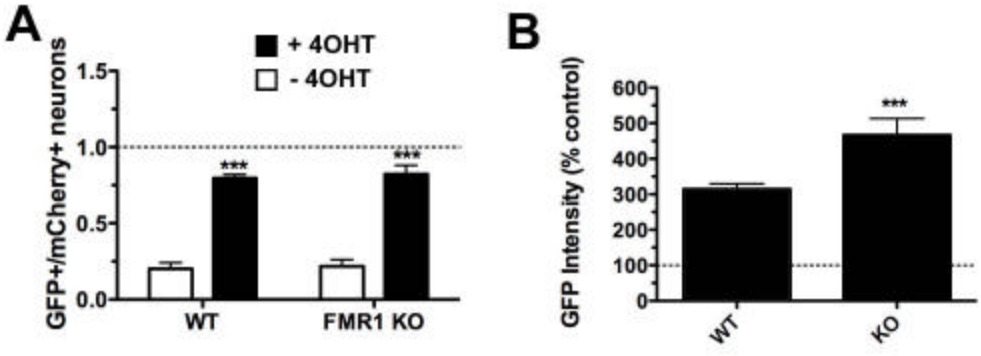

Figure 3.4. MRE-EGFP expression in WT and *Fmr1*-KO neurons following activation of MEF2-VP16-ER^{TM} with 4-hydroxytamoxifen. ***A***, Dissociated cultures prepared from p0 wild-type or *Fmr1*-KO mice were simultaneously co-transfected with three constructs: p-mCherry, MRE-EGFP, and MEF2-VP16-ER^{TM}. Sister cultures were treated with either 4OHT or vehicle and ratio of GFP^{+} to mCherry^{+} neurons was determined. ***B***, EGFP expression in GFP^{+} neurons was quantified for both wild-type and *Fmr1*-KO neurons.

Figure 3.5. Constitutively active MEF2 induces synapse loss in WT, but not *Fmr1*-KO neurons.

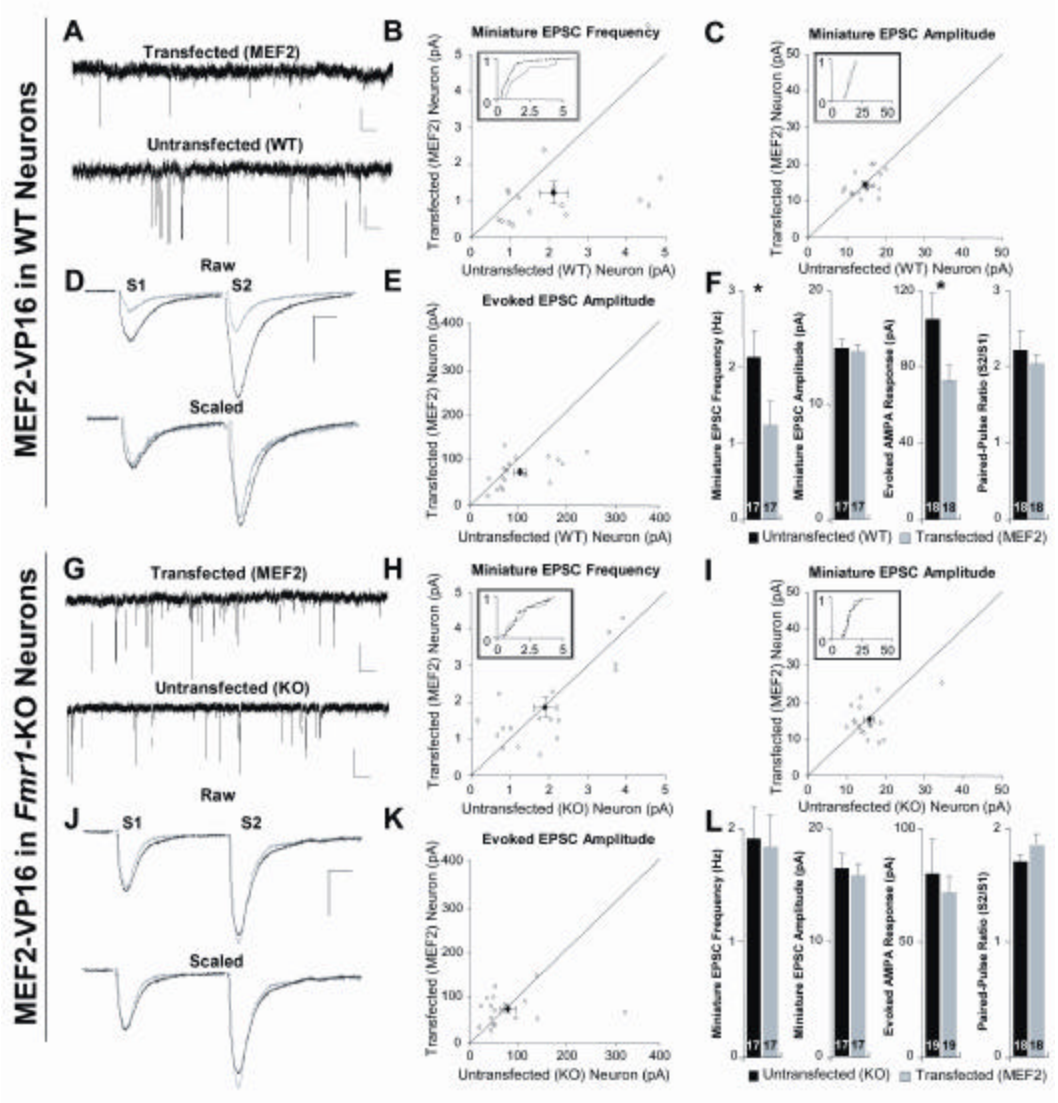

Figure 3.5. Constitutively active MEF2 induces synapse loss in WT, but not *Fmr1*-KO neurons. ***A-F***, Organotypic hippocampal slice cultures from p6 WT mice were biolistically transfected with MEF2-VP16. ***A***, Representative traces of mEPSCs simultaneously recorded from an untransfected WT neuron and a neighboring MEF2-VP16 transfected neuron. Calibration: 10 pA, 500 ms. ***B***, ***C***, Dot plot representation of the frequency (***B***) and amplitude (***C***) of mEPSCs in paired recordings. The large diamond represents mean ± SEM. Inset, Cumulative probability distributions for both untransfected neurons (solid black line) and transfected, MEF2-VP16-expressing neurons (dotted line). Each point on the curve represents the average mEPSC frequency and amplitude from an individual neuron. The *x*-axis is the mEPSC frequency (***B***) or amplitude (***C***). The *y*-axis is the cumulative probability. ***D***, Average of 25 consecutive traces from a representative experiment simultaneously recorded from an untransfected WT neurons and a neighboring MEF2-VP16 transfected neuron. Calibration: 50 pA, 10 ms. Stimulation artifact has been digitally removed for clarity. ***E***, Dot plot of the peak amplitude of the evoked AMPAR-mediated EPSCs of paired recordings. ***F***, Average mEPSC frequency, mEPSC amplitude, AMPAR-mediated EPSC amplitude, and paired-pulse ratio (second response amplitude/first response amplitude) from untransfected WT and MEF2-VP16 transfected cells. ***G-L***, as **(*A-F*)**, except slice cultures were prepared from p6 *Fmr1*-KO mice.

Figure 3.6. Model of MEF2 and FMRP interaction in control of translation.

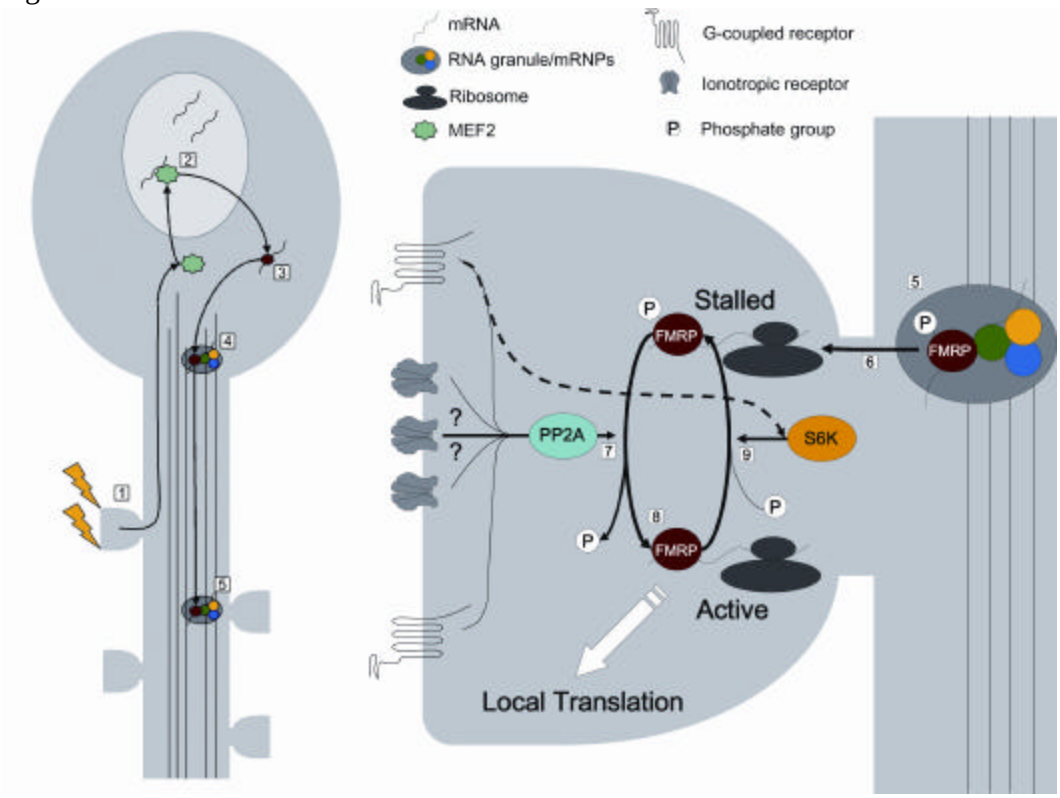

Figure 3.6. Model of MEF2 and FMRP interaction in control of translation. ***1***, Synaptic stimulation results in intracellular signaling cascades, likely through calcium-dependent proteins such as calcineurin. ***2***, Synaptic activity leads to the activation of MEF2 (which is normally localized in the nucleus – the picture shows it in the cytoplasm for clarity). ***3***, Activation of MEF2 results in the transcription of several mRNAs. ***4***, These RNAs are bound by FMRP and associated with RNPs. ***5***, FMRP-mRNA complexes are transported along dendrites via RNPs. FMRP remains bound to mRNA in RNPs at or near dendritic spines. The mRNA targets of FMRP are held translationally dormant. FMRP is likely maintained in a phosphorylated state by persistent activity of CKII and S6K. ***6***, Cellular signals promote the movement of FMRP-bound mRNAs to polyribosomes at or near dendritic spines. Phosphorylated FMRP associates with mRNA-polyribosome complexes and holds them in a translationally arrested state. ***7***, Cellular signals, presumably from group I mGluRs, rapidly activate PP2A, which dephosphorylates FMRP. ***8***, Dephosphorylated FMRP allows or stimulates the translation of its bound mRNA targets, leading to a rapid burst of local, dendritic translation, which results in the elimination of synapses. ***9***, Activation of group I mGluRs lead to the slower activation of S6K, which re-phosphorylates FMRP and ends the period of local translation.

CHAPTER FOUR

Investigations into the Mechanisms of FMRP-Dependent Synapse Loss

Introduction

To briefly summarize the findings reported in Chapters 2 and 3, I observe that acute postsynaptic expression of FMRP in *Fmr1* knock-out (KO) neurons results in a decrease in the number of functional and structural excitatory synapses without an effect on their synaptic strength or maturational state. Similarly, wild-type (WT) neurons have fewer synapses than neighboring *Fmr1*-KO neurons. Furthermore, the transcription factor MEF2, which negatively regulates synapse number in WT neurons, fails to affect synapse number in *Fmr1*-KO mice, indicating a mechanistic link between these two proteins. These data suggest that FMRP is important for the natural process of MEF2-dependent synapse elimination, such that in the absence of FMRP (as in Fragile X syndrome), an increased number of synaptic connections are observed. Finally, experiments with FMRP constructs containing single-site mutations indicate that translation mRNA targets of FMRP are important for FMRP-dependent synapse elimination. These results are consistent with the phenotype of increased numbers of dendritic spines observed in FXS patients and *Fmr1*-KO mice (Hinton et al., 1991; Irwin et al., 2001; McKinney et al., 2005; Irwin et al., 2002; Antar et al., 2007; Meredith et al., 2007; Dolen et al., 2007).

Several questions remain unanswered regarding FMRP-dependent synapse loss. What specific changes does FMRP mediate to initiate synapse elimination? Data from the I304N-FMRP, S500A-FMRP, and S500D-FMRP mutants suggests that FMRP-dependent translation is necessary for synapse loss, indicating that changes in the protein complement of the synapse are likely to be critical for synapse elimination. These data further demonstrate that identification of the mRNA targets of FMRP may provide additional insight into the mechanisms through which FMRP induces synapse loss. Furthermore, data from the ?RGG-FMRP mutant indicates that FMRP association with G-quartet-containing mRNAs, which were canonically believed to be the primary mRNA

targets of FMRP, are not important for FMRP-dependent synapse loss, narrowing the pool of potentially target mRNAs necessary for synapse loss.

What upstream affectors of FMRP function play a role in synapse loss following FMRP expression? Work on the S500A-FMRP and S500D-FMRP mutants strongly implicates FMRP phosphorylation as a critical step in FMRP-mediated synapse loss. As S500A-FMRP initiated robust synapse loss, while S500D-FMRP failed to affect synapse number or function, it seems likely that inhibition of an FMRP kinase or activation of an FMRP phosphatase is a necessary event for FMRP-dependent synapse elimination.

Finally, the observation that MEF2 and FMRP act cooperatively to negatively regulate synapse number suggests additional means of cellular control of synapse loss. FMRP expression is critical for MEF2-induced synapse loss, and MEF2 transcriptional activity is required for FMRP-dependent synapse loss. Therefore, cellular signals that impair or activate MEF2 may also play a key role in the regulation of synapse number by FMRP. MEF2 is known to be regulated by many post-translational modifications and through association with co-factors and accessory proteins. In particular, MEF2 is regulated by the calcium/calmodulin-mediated kinase (CaMK) family and by the serine/threonine phosphatase calcineurin (McKinsey et al., 2002). Indeed, MEF2-mediated synapse loss is blocked by inhibitors of calcium entry into the post-synapse (Flavell 2006). Thus, blockade of calcium entry or downstream effectors of calcium signaling may similarly impair FMRP-dependent synapse loss.

The biological mechanisms underlying FMRP-dependent synapse loss are likely to be complex. Precise control of mRNA expression, kinase and phosphatase activity, cytoskeletal regulation, and expression and localization of pre- and post-synaptic proteins are just a few of the regulatory mechanisms likely to play a key role in FMRP-dependent synapse loss. The largely preliminary work described in this Chapter is aimed at uncovering the molecular pathways through which FMRP regulates synapse number.

Materials and Methods

Hippocampal slice cultures and FMRP transfection

Organotypic hippocampal slice cultures were prepared from postnatalday 6 (P6) WT or *Fmr1*-KO mice bred from the congenic C57BL/6 mouse strain (Jackson Laboratories, Bar Harbor, ME) using previously published protocols (Stoppini et al., 1991). Biolistic transfection and gold bullet preparation were performed with the Helios Gene Gun system (Bio-Rad, Hercules, CA) according to the manufacturer's protocols (McAllister, 2004). All FMRP-green fluorescent protein (GFP) constructs were obtained from Dr. Jennifer Darnell at Rockefeller University and are driven by the human *FMR1* promoter. Construction of the GFP-tagged FMRP (wtFMRP-GFP) as well as I304N FMRP and arginine/glycine-rich box (RGG) deletion (ΔRGG) FMRP have been described previously (Darnell et al., 2005b). The S500A and S500D mutations were introduced into wtFMRP-GFP by QuikChange site-directed mutagenesis (Stratagene, La Jolla, CA) of the *Kpn*I-fragment, which was subcloned into pBluescript for mutagenesis and then replaced in the WT construct.

Dissociated culture and immunocytochemistry

Dissociated CA3–CA1 hippocampal cultures (dentate gyrus was cutoff) were prepared from P0–P1 WT and *Fmr1*-KO mice using modified, previously published protocols (Brewer et al., 1993). Neurons were plated at a density of 250 neurons/mm^2 on poly-D-lysine/laminin or matrigel coated coverslips. At 7 days *in vitro* (DIV), cultures were transfected with either calcium phosphate or Lipofectamine 2000 (Invitrogen, Eugene, OR). At 12 DIV, cells were fixed in 4% paraformaldehyde (PFA)/4% sucrose for 15 min at 37°C, blocked in PBS/10% goat serum and labeled with 1° antibody against the extracellular N terminus of glutamate receptor 1 (GluR1; 1:50; Calbiochem, La Jolla, CA). For the postsynaptic marker 95 kDa postsynaptic density protein (PSD-95) and synapsin, neurons were permeabilized with 0.2% Triton-X for 1 h before treatment with 1° antibodies to PSD-95 (1:800; Affinity Bioreagents, Golden, CO), synapsin (1:1,000; provided by Dr. Thomas Sudhof, University of Texas Southwestern Medical Center), or 2F5 monoclonal FMRP antibody (1:400) (Gabel et al., 2004) (provided by Dr. Justin

Fallon, Brown University, Providence, RI, and Dr. Jennifer Darnell, Rockefeller University, New York, NY) for 1 h and AlexaFluor-conjugated 2° antibodies (1:300, 1 h; Invitrogen). Hippocampal slice cultures were fixed in 4% PFA (4°C, overnight) permeabilized with 0.7% Triton-X (4°C, overnight). The slices were treated with 2F5 FMRP antibody (1:400) and AlexaFluor 2° antibody (1:300 both overnight at 4°C).

Fluorescence was detected using a Nikon (Tokyo, Japan) TE2000 inverted microscope equipped with a cooled CCD camera (dissociated neuron culture) or a Zeiss (Oberkochen, Germany) LSM 510 Meta confocal microscope (slice sections). Images were analyzed and quantitated using MetaMorph software (Universal Imaging, Downingtown, PA). Healthy neurons are first identified by their smooth soma and multiple processes under differential interference contrast (DIC) microscopy. For synaptic staining, immunoreactive puncta are defined as discrete points along a dendrite (within 50 μm from the soma) with fluorescence intensity at least twice the background staining of a region adjacent to the dendrite. Significant differences between *Fmr1*-KO neurons and WT or FMRP-transfected neurons were determined with an unpaired *t* test. For all group data, averages +SEM are plotted and *n* (number of cells) is on each bar (*$p < 0.05$; **$p < 0.01$; ***$p < 0.001$).

Electrophysiology

Simultaneous whole-cell recordings were obtained from CA1 pyramidal neurons in slice cultures visualized using infrared-DIC and GFP fluorescence to identify transfected and nontransfected neurons (Gibson et al., 2006). Recordings were made at 30°C in a submersion chamber perfused at 3 ml/min with artificial CSF (ACSF) containing the following (in mM): 119 NaCl, 2.5 KCl, 26 NaHCO3, 1 NaH_2PO_4, 11 D-Glucose, 3 CaCl2, 2 MgCl2, 0.1 picrotoxin, 0.002 2-chloro-adenosine, 0.1% DMSO, pH 7.28, 320 mOsm and saturated with 95% O_2/5%CO_2. For all intracellular recordings, the neuron was clamped at –60 mV through whole-cell recording pipettes (~3–7 MΩ) filled with an intracellular solution containing the following (in mM): 2.5 BAPTA, 125 Cs-Meth, 6 CsCl, 3 NaCl, 10 HEPES, 10 sucrose, 2 QX-314, 10 tetraethylammonium-Cl, 4 ATP-Mg, 0.4 GTP-Na, 14 phosphocreatine-Tris, pH 7.2, 285 mOsm. For isolated NMDA

receptor (NMDAR) measurements, the ASCF was supplemented with 20 µM DNQX and 20 µM glycine and the neuron was clamped at +50 mV. For mEPSC measurements, the ACSF was supplemented with 1 µM TTX. Synaptic responses were evoked by single bipolar electrode placed in stratum radiatum of area CA1 (along the Schaeffer collaterals) 50–200 µm from the recorded neurons with monophasic current pulses (5–40 µA, 200 µs). For minimal stimulation experiments, a glass theta-tube electrode was filled with ACSF and positioned in the stratum radiatum along the Schaeffer collaterals ~20–50 µm from the recorded neurons. Once a synaptic response was obtained, the stimulation intensity was gradually decreased until synaptic failures and synaptic successes could be clearly distinguished in both neurons (typically 0.5–5 µA). Capacitance, series resistance, and input resistance were measured in voltage clamp with a 400 ms, –10 mV step from a –60 mV holding potential (filtered at 30 kHz, sampled at 50 kHz). The capacitance was calculated by first obtaining the decay time constant of a current transient induced by a voltage step (the faster time constant of a double-exponential decay fitted to the first 20 ms) and then dividing this by the series resistance. Cells were only used for analysis if the series resistance was <30 M? and was stable throughout the experiment. Input resistance ranged from 75 to 350 M? . Data were not corrected for junction potential.

Synaptic potentials were filtered at 2 kHz, acquired and digitized at 10 kHz on a personal computer using custom software (Labview; National Instruments, Austin, TX). Time constants (t) of the decay of isolated NMDAR EPSCs were determined by fitting the decay of the maximum amplitude of NMDAR EPSC with a double exponential in LabView using the Levenberg-Marquardt algorithm to determine the least-squares set of coefficients that best fit the set of input data points (*X*,*Y*) as expressed by a nonlinear function $y = f(x,a)$, where a is the set of coefficients. Miniature EPSCs (mEPSCs) were detected off-line using an automatic detection program (MiniAnalysis; Synaptosoft, Decatur, GA) with a detection threshold set at a value greater than at least 2 SD of the noise values, followed by a subsequent round of visual confirmation. The detection threshold remained constant for the duration of each experiment. Failures and successes were defined as responses with amplitudes less than or >10 pA, respectively, followed by a subsequent round of visual confirmation for each qualification without knowledge of

the transfection state of the neuron. The percentage of silent synapses calculated as 1 – ln(failure rate at –60 mV)/ln(failure rate at +50), as described previously (Liao et al., 1995). Significant differences between transfected and nontransfected neurons were determined using a paired *t* test.

Results and Discussion

FMRP is less effective in a different background genetic strain

Distinct genetic strains of mice have inherent differences in the expression and function of many genes (Silva et al., 1997; Gerlai et al., 1996). There are at least two distinct genetic strains of mice which lack FMRP expression: C57/Bl6 and FVB (Yan et al., 2005; Dobkin et al., 2000). Although both strains appear to share many core phenotypes following genetic deletion of *Fmr1*, the extent of these phenotypes may differ depending on the background genetic strain. For instance, the FVB *Fmr1*-KO strain appears to be more susceptible to audiogenic seizures than the C57/Bl6 *Fmr1*-KO strain, even though both strains show heightened sensitivity to audiogenic seizures as compared to WT littermates (Yan et al., 2005). Furthermore, while both *Fmr1*-KO strains are impaired in cognitive memory tasks such as a water maze, the FVB strain displays pronounced impairments, while the C57/Bl6 strain shows only mild deficiencies (Dobkin et al., 2000). Thus, it is of interest to determine whether FMRP expression can induce synapse loss in both strains as differences in the effectiveness of FMRP in certain strains may provide insight in the mechanism of FMRP function.

Earlier work described in Chapter 2 examining the effect of FMRP-dependent synapse loss (Pfeiffer and Huber, 2007) had been performed using *Fmr1*-KO mice of the C57/Bl6 background strain. The literature suggests that the FVB *Fmr1*-KO genetic strain may display the "stronger" behavioral phenotype, although it should be noted that only a handful of studies have directly examined differences between FVB *Fmr1*-KO mice and C57/Bl6 *Fmr1*-KO mice. Interestingly, comparisons across multiple studies suggest that the C57/Bl6 *Fmr1*-KO mouse may display a stronger dendritic spine phenotype than FVB *Fmr1*-KO mice do (Irwin et al., 2002; Nimchinsky et al., 2001; Galvez et al., 2005; McKinney et al., 2005; Restivo et al., 2005; Dolen et al., 2007; Hayashi et al., 2007).

Thus, I hypothesized that if FVB mice display a weaker spine phenotype following FMRP loss, they might also display an weaker phenotype in response to acute FMRP expression. To test this hypothesis, I biolistically transfected organotypic hippocampal slice cultures (OHSCs) prepared from FVB *Fmr1*-KO mice with a construct expressing wild-type FMRP at near-endogenous levels (Pfeiffer and Huber, 2007).

Three to seven days post-transfection, I obtained simultaneous whole-cell patch-clamp recordings from untransfected *Fmr1*-KO and neighboring transfected FMRP-expressing CA1 pyramidal neurons (hereafter referred to as "neuron pairs"). AMPA receptor (AMPAR)-mediated EPSCs were evoked with extracellular stimulation of Schaffer collateral axons and were measured in the neuron pairs held at –60 mV. I observed a trend toward decreased amplitude of evoked AMPAR EPSCs, although the effect failed to reach statistical significance (Fig 4.1*C,D*, Table 4.1).

The effects of FMRP on evoked AMPAR EPSC amplitude in the C57/Bl6 *Fmr1*-KO strain often appeared subtle and somewhat inconsistent (personal observations), likely due to inherent variability in multiple aspects of the experimental paradigm. In C57/Bl6 *Fmr1*-KO slice cultures, FMRP expression resulted in a more consistent effect on the frequency of action-potential independent spontaneous EPSCs (mEPSC) than it did on extracellularly evoked EPSCs. Therefore, to further examine whether FMRP may negatively regulate synapse number in the FVB *Fmr1*-KO background, I recorded mEPSCs of neuron pairs in the presence of TTX (1 μM). As with the experiments performed in C57/Bl6 slice cultures, I observe no effect of FMRP expression on mEPSC amplitude (Fig 4.1*B,D*, Table 4.1). However, with a small number of experiments, there is again a trend toward decreased frequency of mEPSC (Fig 4.1*A,D*, Table 4.1). A single outlier skews the average of the data; removal of this experiment results in a p-value of 0.09.

Thus, preliminary data suggests that FMRP is capable of reducing functional synapse number in the FVB *Fmr1*-KO background. However, this synaptic loss does not appear to be as robust in the FVB *Fmr1*-KO genetic strain as it is in the C57/Bl6 *Fmr1*-KO background. These experiments were ended prematurely, but I am confident that with increased numbers of experiments, a significant reduction in functional synapse

number would be observed. Considering that the FVB *Fmr1*-KO mouse is reported to have exaggerated behavioral phenotypes as compared to the C57/Bl6 *Fmr1*-KO mouse, it is somewhat surprising that FMRP expression failed to induce as robust of an effect on synapse number in the FVB background as in the C57/Bl6 background. Perhaps the behavioral phenotypes that are enhanced in the FVB strain (Dobkin et al., 2000; Yan et al., 2005) are co-regulated by different factors than the synapse number phenotype investigated in these assays. Alternatively, loss of FMRP in the FVB background may impose a greater strain on the neurons than in C57/Bl6 mice, leading to compensatory changes that mask or partially occlude FMRP-dependent synapse loss.

Comparions of multiple studies in the FXS literature indicate that, in opposition to the enhanced behavioral phenotypes observed in the FVB *Fmr1*-KO mouse, the phenotype of increased spine number may be less robost in the FVB strain than in the C57/Bl6 strain. These data suggest that the FVB mice may therefore be less susceptible to FMRP-mediated synapse elimination, which is what my data demonstrate. Due to the lack of a robust effect in the FBV strain, all additional experiments described throughout this manuscript were performed in C57/Bl6 mice.

siRNA-mediated knock-down of FMRP decreases synaptic function

FXS patients and *Fmr1*-KO mice display increased numbers of dendritic spines (Irwin et al., 2001, Mckinney et al., 2005; Irwin et al., 2002; Antar et al., 2007; Meredith et al., 2007; Dolen et al., 2007). In addition, post-synaptic expression of FMRP decreases excitatory synaptic connection in *Fmr1*-KO neurons (Pfeiffer and Huber, 2007). Furthermore, side-by-side comparisons of wild-type and *Fmr1*-KO neurons revealed a significant increase in synapse number in the absence of FMRP (Pfeiffer and Huber, 2007). These data strongly suggest that FMRP negatively regulates synapse number and further indicate that acute loss of FMRP expression or function may lead to an increase in functional synapse number.

Small interfering RNA (siRNA) is a class of short, 18-25 nucleotide-long RNA. siRNAs interact with specific mRNA targets through complimentary base-pair association, and this interaction has been shown to regulate the expression and/or

translational efficacy of the mRNA ligand (Bartel et al., 2004). Perfect complementarity between a siRNA and a mRNA target results in the activation of the RNA interference (RNAi)-induced signaling complex (RISC) and degradation of the mRNA target. The use of siRNA-mediated degradation of specific mRNAs has become a common experimental method in molecular biology, allowing for precise, acute knock-down in the expression of a target protein. Unfortunately, off-target effects, likely induced by either non-specific association of the siRNA with a second non-target mRNA or simply through activation of the RISC machinery itself, are a common occurrence in experiments utilizing siRNA. Therefore, standard practice for siRNA-mediated knock-down entails the use of two unique siRNAs which target distinct regions of the target mRNA, as well as the use of an RNAi-resistance form of the target mRNA, which is used to rescue the siRNA-mediated effect.

To test whether acute loss of FMRP might increase synapse number, I utilized siRNA-mediated knockdown of FMRP in wild-type neurons. Two siRNA constructs were used, each targeting a separate region of the endogenous mouse FMRP. These constructs were expressed in C2C12 murine myoblasts, and were shown to effectively decrease expression FMRP to 10% of endogenous levels (Fig 4.2*I*). Each siRNA construct was separately biolistically transfected into wild-type organotypic hippocampal slice cultures, along with a GFP-expressing construct to allow identification of the transfected neurons. Three to five days post-transfection, I obtained simultaneous whole-cell patch-clamp recordings from untransfected *Fmr1*-KO and neighboring transfected FMRP-expressing CA1 pyramidal neurons (hereafter referred to as "neuron pairs"). AMPAR-mediated EPSCs were evoked with extracellular stimulation of Schaffer collateral axons (using a pair of pulses at a 50 ms inter-stimulus interval) and were measured in the neuron pairs held at –60 mV. TTX was then applied to the neurons and mEPSCs were recorded.

Surprisingly, expression of either siRNA construct induced a trend toward decreased AMPAR-mediated EPSCs and mEPSC frequency, rather than the increase in synaptic function that I anticipated (Table 4.1). Despite reports in the literature demonstrating the use of biolistic transfection with siRNA (Eto et al., 2002), I was

concerned that the siRNA constructs may be degraded prior to transfection. In addition, while I could identify transfected neurons with the co-transfected GFP-expressing construct, I could not confirm how long the siRNA remained functional in the neuron before it was degraded. To overcome these concerns, I constructed a plasmid which bicistronically expressed both GFP and a short 56-bp palindromic stretch of RNA (pSuper-anti-FMRP). This short RNA was designed to fold into a hairpin structure that could be recognized by the RISC complex, where it would be processed into a fully-functional siRNA. I prepared two such constructs, each of which expressed a siRNA that was identical in sequence to those used in the above experiments, biolistically transfected them into wild-type slice cultures, and repeated the above electrophysiological recordings five to ten days post-transfection.

Interestingly, transfection of either pSuper-anti-FMRP construct also resulted in a trend toward decreased AMPAR-mediated EPSCs and mEPSC frequency (Table 4.1). When the data for all four conditions (both siRNAs and both plasmid-expressed siRNAs) are combined, there is a clear and significant reduction in evoked AMPAR-mediated responses and mEPSC frequency, with no effect on paired-pulse facilitation or mEPSC amplitude (Fig 4.2*A-D*, Table 4.1), consistent with a reduction in synapse number.

The findings of reduced synapse number following expression of siRNAs targeting FMRP mRNA is perplexing. If FMRP negatively regulates synapse number, why doesn't acute loss of FMRP lead to an increase in the number of functional synapses? It is important to note that although we confirmed that expression of the siRNA constructs in C2C12 myoblasts lead to robust loss of FMRP protein, it is unknown whether expression of these constructs in neurons results in a similar loss of FMRP expression. Hippocampal pyramidal neurons have large, extensive dendritic arbors and *fmr1* mRNA has been shown to be dendritically localized. Thus, it may be difficult for a siRNA to reach a dendritic location. In addition, dendritically localized mRNAs, which are thought to be largely sequestered in RNPs or RNA granules, may be protected from siRNA-mediated degradation. Although some of the RISC machinery has been demonstrated to exist in dendrites, it is unknown if siRNA-mediated mRNA degradation occurs in dendrites. Furthermore, although FMRP appears to be susceptible

to activity-dependent degradation (Hou et al., 2008), it is unknown what the half-life of dendritically localized FMRP may be. Thus, it is unclear if expression of siRNAs targeting *fmr1* mRNA result in actual loss of FMRP in neurons. Immunological staining of FMRP in neurons following siRNA expression would be useful to determine the duration and extent, if any, of siRNA-mediated knock-down of FMRP.

However, even if the siRNA constructs failed to alter FMRP expression levels, it is still curious that there was a reduction in the number of synapses. The most likely explanation for the decrease in synapse number following siRNA expression comes from a recent study demonstrating that expression of siRNA constructs is sufficient to induce synapse loss through off-target, non-specific effects (Alvarez et al., 2006). Importantly, this study reported that non-specific synapse loss due to off-target siRNA-mediated effects was accompanied by an increase in input resistance. Following expression of FMRP-targeting siRNAs, I observe a significant increase in the input resistance of transfected neurons compared to neighboring, untransfected neurons (Table 4.1). Thus, it seems likely that the synapse loss that I observe following expression of siRNAs or the pSuper-anti-FMRP plasmids results from non-specific effects due to activation of the RNAi machinery.

It is therefore unclear from these studies alone whether loss of FMRP results in changes in synapse number.

CRE-mediated genetic deletion of FMRP fails to alter synapse number

As an alternate means of acutely decreasing FMRP expression, I utilized Cre-mediated recombination to knock-out the *Fmr1* gene. Cre recombinase is a protein which recognizes specific sequences of DNA known as *LoxP* sites and catalyzes their recombination, effectively removing stretches of DNA between nearby *LoxP* sites. Recently, a genetically engineered mouse was produced in which the promoter and first exon of the *Fmr1* gene was flanked by *LoxP* sites (Floxed-*Fmr1*) (Mientjes et al., 2005). Expression of Cre recombinase in cells of this mouse results in rapid genetic deletion of *Fmr1*.

To examine the effects of Cre-mediated FMRP deletion on synaptic function, I prepared organotypic hippocampal slice cultures from Floxed-*Fmr1* mice and biolistically transfected them with a plasmid expressing Cre-recombinase fused to GFP. As a control for Cre expression, identical experiments were performed in wild-type cultures. To confirm that FMRP expression was effectively reduced following Cre expression, I attempted to perform immunocytochemistry (IC) on several slice cultures following transfection and probed the cultures using an antibody against FMRP (2F5). However, I was unable to detect differences in FMRP expression following Cre transfection in Floxed-*Fmr1* neurons (data not shown). It should be noted that the IC protocol that was used was not the most efficient. Our lab has recently developed a much more sensitive IC assay which should be used to more accurately determine FMRP protein levels following Cre-mediated recombination.

Three to seven days post-transfection, I obtained paired recordings from transfected, Cre-expressing (*Fmr1*-excised) neurons, and neighboring untransfected neurons. AMPAR-mediated EPSCs were evoked with extracellular stimulation of Schaffer collateral axons (using a pair of pulses at a 50 ms inter-stimulus interval) and were measured in the neuron pairs held at –60 mV. TTX was then applied to the neurons and mEPSCs were recorded.

Very few experiments were performed in these cultures, owing primarily to my personal doubts as to the efficacy of the Cre-mediated knock-down. Preliminary data suggests that Cre expression seemed to reduce both evoked AMPAR-mediated responses as well as mEPSC frequency in both WT and Floxed-*Fmr1* slices (Fig 4.2*E-H*, Table 4.1). However, I am reluctant to draw any conclusions from these data due to the fact that the number of experiments is small and the certainty of FMRP knock-down is low.

Unfortunately, therefore, I was unable to determine what effect acute reductions in FMRP function may have on synapse number.

Paired recordings in mosaic mice reveal alterations in miniature event frequency

As described in Chapter 2, the mathematical variance and SD of evoked AMPAR-mediated responses and mEPSC frequency were greater between neurons on different slices than between neurons within the same slice, thus precluding detection of differences between WT and *Fmr1*-KO slices. In fact, when we were able to make side-by-side comparisons of WT and *Fmr1*-KO neurons in dissociated culture, we were able to observe significant differences in synapse number between the two genotypes. I therefore sought to establish an experimental paradigm that would allow me to electrophysiologically detect differences in synapse number between WT and *Fmr1*-KO neurons in slices.

To accomplish this goal, I utilized *Fmr1*-Mosaic mice, in which roughly half of the neurons are wild-type for FMRP expression and half are *Fmr1*-KO due to X-inactivation. In females, X-inactivation results in the selective repression of genes from one X chromosome. The specific mechanisms through which X-inactivation occurs are incompletely defined, and the decision of which X chromosome is chosen for inactivation appears to be largely due to chance. Thus, in females heterozygous for *Fmr1*, roughly half of their neurons express normal levels of FMRP (the *Fmr1*-null X chromosome is inactivated), while FMRP expression is absent in the other half (the *Fmr1*-wild type X chromosome is inactivated). Recently, a mouse line was created which harbors a gene encoding for *GFP* on the X chromosome. Crossing this X-linked *GFP* mouse line with the *Fmr1*-KO line produces the *Fmr1*-Mosaic line, in which GFP expression correlates with FMRP expression, while the absence of GFP correlates with FMRP deletion. Female mice of the F1 generation, which are heterozygous for both *GFP* and *Fmr1*, were used for the following experiments.

To confirm that GFP expression correlated to FMRP expression Kris Loerwald and Jay Gibson performed IC on acute hippocampal and cortical slices from *Fmr1*-Mosaic animals, probing for both GFP and FMRP. The protocol was more effective than the one used to determine Cre-mediated FMRP knock-down, and it was clear that GFP-positive neurons were consistently FMRP-positive, and GFP-negative neurons were

consistently FMRP-negative. Thus, this mouse line was an attractive model in which to examine electrophysiological differences between WT and *Fmr1*-KO neurons.

I prepared organotypic hippocampal slice cultures from *Fmr1*-Mosaic mice and obtained paired whole-cell recordings from a GFP-positive and a GFP-negative neuron. AMPAR-mediated EPSCs were evoked with extracellular stimulation of Schaffer collateral axons (using a pair of pulses at a 50 ms inter-stimulus interval) and were measured in the neuron pairs held at –60 mV. TTX was then applied to the neurons and mEPSCs were recorded.

I observed a trend toward decreased mEPSC frequency in the GFP-expressing neurons, with no effect on evoked AMPAR-mediated responses (Fig 4.3*A*). The number of experiments was too small, however, to draw many conclusions from the data. When I combine these data with data obtained by Darya Fakhretdinova in similar experiments, there is a significant reduction in mEPSC frequency, with no effect on mEPSC amplitude (data not shown). Thus, in *Fmr1*-Mosaic cultures, post-synaptic expression of FMRP appears to negatively regulate mEPSC frequency. More work remains to be done to determine if this decrease in mEPSC frequency is due to a decrease in synapse number. Namely, more evoked AMPAR-mediated responses need to be obtained and paired-pulse facilitation needs to be measured to determine if changes in pre-synaptic release probability can account for the observed decrease in mEPSC frequency.

The *Fmr1*-Mosaic mouse line may prove to be a particularly useful tool for continued investigations into FMRP function. Biolistic transfection, although sufficient for many of the studies described in this manuscript, leaves much to be desired in terms of an experimental paradigm. First, despite taking great pains to avoid overexpression of the gene of interest, such as using the human *FMR1* promoter to drive FMRP expression, the levels of protein production from an exogenous gene will never exactly match the levels of production from the endogenous gene. In addition, acute expression of a protein may result in rapid cellular changes which are quickly negated or exacerbated by compensatory or homeostatic mechanisms, leading to incorrect assumptions regarding the protein's function. Furthermore, biolistic transfection requires that neurons be grown in culture, producing changes in neuronal behavior and introducing additional variables.

Finally, biolistic transfection affects, at best, only a few dozen of the several thousand neurons in the culture, making extended studies tedious and inefficient. The use of *Fmr1*-mosaic mice accounts for all of these concerns while potentially maintaining the original phenotype of reduced synapses in FMRP-expressing neurons as compared to *Fmr1*-KO neurons.

The finding of increased mEPSC frequency, and presumably increased synapse number, in *Fmr1*-KO neurons of *Fmr1*-Mosaic slices is somewhat at odds with a recent study that examined local connectivity between CA3 neurons in *Fmr1*-Mosaic slices (Hanson 2007). Consistent with our findings that mEPSC amplitude is unaffected by FMRP expression, Hanson and Madison report no change in the amplitude of EPSCs of synaptically connected CA3 neurons. However, they report that pre-synaptic loss of FMRP significantly decreases functional connectivity between CA3 neurons, whereas post-synaptic expression of FMRP has no effect on connectivity. Post-synaptic FMRP-induced synapse loss may occur throughout the dendrite, encompassing synaptic inputs from both nearby and distant neuronal partners. Hanson and Madison, on the other hand, exclusively examine synapses between neighboring neurons. Thus, FMRP may have distinct effects on local synapses between nearby neurons from those that it has on synapses that connect neurons from distant brain regions. This affect may be more pronounced if local connections occur exclusively in a particular region of the dendritic arbor which may be less responsive to FMRP-induced synapse loss. Alternatively, loss of FMRP may result in a global, wide-spread increase in synapses, which is partially countered by pre-synaptic homeostatic mechanisms on a local level. Additional experiments are necessary to determine the precise synaptic changes that occur following FMRP loss.

Paired recordings of CA3 neurons in WT and Fmr1-*KO neurons reveals altered connectivity*

Experiments elucidating the mechanisms of FMRP function are made more difficult by the fact that nearly every phenotype caused by expression (in my own experiments) or loss of FMRP (work from other labs on the *Fmr1*-KO mouse) is subtle.

For example, my work shows a clear reduction in synapse number following increased FMRP expression. This is reflected, in part, by a reduction in mEPSC frequency. However, a direct comparison of mEPSC frequency between neurons of wild-type OHSCs and neurons of *Fmr1*-KO OHSCs fails to display a significant difference. I believe that this is due to the inherent variability imposed by culturing conditions, which results in a significantly greater statistical variance between neurons on different slices than between neurons within the same slice. In fact, the statistical variance between slices is roughly 40%, while the FMRP-induced decrease in synapse number is roughly 20-30%. Thus, I believe that there exists a difference in synapse number between neurons of wild-type and *Fmr1*-KO OHSCs, but this difference is masked by the inherent variability imposed by the cultures. In support of this hypothesis, when I culture wild-type and *Fmr1*-KO neurons in the same dish, I minimize culture variability and observe a significant decrease in synapse number in FMRP expressing neurons. Furthermore, recordings in *Fmr1*-Mosaic slices also revealed a significant different in mEPSC frequency when neuron pairs are able to recorded from within the same slice.

I sought to establish an electrophysiological paradigm that would allow detection of synaptic differences between wild-type and *Fmr1*-KO slice cultures. To this end, I looked to paired recordings of CA3 pyramidal neurons. CA3 neurons are known to have a high rate of synaptic connection with each other. I hypothesized that if FMRP negatively regulates synapse number, then perhaps the connection rate between CA3 neurons would be decreased in wild-type compared to *Fmr1*-KO neurons.

I prepared OHSCs from p6 wild-type or *Fmr1*-KO littermates and obtained whole cell recordings from a pair of neighboring CA3 pyramidal neurons. One of the neuron pair (Cell 1) was held in current clamp and stimulated to fire an action potential with a depolarizing injection of current. The other (Cell 2) was held in voltage clamp and responses were measured. Then, the experiment was reversed such that Cell 1 was held in voltage clamp and Cell 2 was held in current clamp and stimulated to fire action potentials. In each experimental set-up, a train of 30 action potential-inducing depolarizations was delivered. EPSCs in the post-synaptic neuron were then identified and measured.

This work is very preliminary, but indications are that connectivity between CA3 neurons is reduced in *Fmr1*-KO OHSCs as compared to wild-type OHSCs (data not shown). This is similar to a finding reported by Hanson and Madison (2007) that was released after these studies had been performed (see above for a discussion of these findings). Importantly, when a connection existed, the size of the response was not affected by the expression of FMRP. This is consistent with a lack of change in mEPSC amplitude following FMRP expression.

An important follow-up experiment would be to examine the failure rates of connected pairs. If post-synaptic FMRP expression negatively regulates synapse number, it would be expected that locally connected wild-type neuron pairs should have increased failure rates as compared to locally connected *Fmr1*-KO neuron pairs. This analysis was not performed on the littermate-controlled experiments described above. However, such analysis was made of data from earlier paired recordings obtained from non-littermate wild-type and *Fmr1*-KO OHSCs. These experiments provided roughly similar findings of decreased connectivity between *Fmr1*-KO CA3 neurons as compared to wild-type CA3 neurons. However, when a connection existed, the rate of failures was significantly increased for wild-type neuron pairs (data not shown), consistent with the findings of reduced synapse number following FMRP expression. It is important note that not every experiment was analyzed in this manner due to the time-consuming nature of quantifying every response as a failure or success. However, this assay may be worth exploring in greater depth in future experiments.

Effects of FMRP expression in WT neurons

The fact that FMRP expression induces synapse loss when expressed in *Fmr1*-KO neurons raises an interesting question: Does FMRP have a dose-dependent effect on synapse number? In other words, does the level of FMRP expression inversely correlate with the number of functional synapses? To address this question, it would be ideal to compare the relative synaptic differences between transfected vs. untransfected neurons while simultaneously quantifying the levels of FMRP-GFP expression for every experiment; unfortunately, I did not do this. However, the question can still be answered

by overexpressing FMRP in wild-type neurons. If FMRP has a dose-dependent effect on synapse number, then overexpression of FMRP in WT neurons should induce synapse reduction roughly as well as expression of FMRP in *Fmr1*-KO neurons does. However, if FMRP acts as a gate to merely allow synapse regulation to occur, then once a critical level is reached, additional FMRP may have no further effect on synapse number. Current evidence suggests that many neuronal functions that are governed by FMRP display a dose-dependent effect of FMRP expression levels. Specifically, investigation of a mouse line which overexpresses FMRP (*Fmr1*-YAC) demonstrates several phenotypes opposite of the *Fmr1*-KO, indicating that FMRP works along a continuum to regulate neuronal function.

To test the question of whether overexpression of FMRP in WT neurons might induce synapse loss, I prepared organotypic hippocampal slice cultures from WT mice and rats and biolistically transfected them with a construct expressing wild-type FMRP. Three to seven days post-transfection, I obtained paired recordings from transfected, FMRP-overexpressing neurons, and neighboring untransfected WT neurons. AMPAR-mediated EPSCs were evoked with extracellular stimulation of Schaffer collateral axons (using a pair of pulses at a 50 ms inter-stimulus interval) and were measured in the neuron pairs held at –60 mV. TTX was then applied to the neurons and mEPSCs were recorded.

Preliminary data suggests that FMRP does, in fact, reduce synaptic function in wild-type neurons (Fig 4.4*A-D*, Table 4.1). Interestingly, FMRP overexpression in wild-type neurons appears to reduce synaptic function through postsynaptic mechanisms, as the mEPSC amplitude is reduced, while the mEPSC frequency is unchanged.

I304N-FMRP and S500D-FMRP do not act as dominant negative forms

Two mutant forms of FMRP, I304N-FMRP and S500D-FMRP, fail to induce synapse loss in *Fmr1*-KO neurons. It is possible that these point mutants merely fail to induce synapse loss because they are incapable of functioning as wild-type FMRP does. However, both of these isoforms continue to associate with mRNA – I304N-FMRP continues to associate with mRNA through the RGG both, while the S500D mutation has

no reported effect on RNA binding (Ceman et al., 2003) – and thus may act to sequester necessary mRNA targets away from endogenous FMRP, thereby acting as dominant negatives. Additionally, I304N-FMRP displays a diffuse expression pattern, clearly distinct from the punctate pattern of wild-type FMRP expression. If I304N-FMRP is able to associate with a binding partner that is necessary for endogenous FMRP function, it may act as a dominant negative by pulling the co-factor away from the synapse, preventing it from interacting with endogenous FMRP.

To test whether these two point mutations confer dominant negative status upon FMRP, I biolistically transfected them into wild-type organotypic hippocampal cultures. Three to seven days post-transfection, I obtained paired recordings from transfected, mutant-FMRP-expressing neurons, and neighboring untransfected WT neurons. AMPAR-mediated EPSCs were evoked with extracellular stimulation of Schaffer collateral axons (using a pair of pulses at a 50 ms inter-stimulus interval) and were measured in the neuron pairs held at –60 mV. TTX was then applied to the neurons and mEPSCs were recorded.

Preliminary data suggests that neither of these constructs induces any change in synaptic function when expressed on a wild-type background (Fig 4.4*E-L*, Table 4.1). Thus, they do not appear to act as a dominant negative form of FMRP. Rather, they appear to be merely loss-of-function forms, at least for this assay. This is particularly interesting in the case of I304N-FMRP, as this mutant form was first discovered in a patient with particularly severe FMRP. Thus, it was thought that I304N-FMRP may represent a toxic gain-of-function mutation. These data indicate that, at least in this assay, I304N-FMRP does not display any phenotype when expressed in wild-type or *Fmr1*-KO neurons. Thus, it seems likely that the severity of FXS in the patient harboring the I304N mutation stems from additional genetic factors and not from the mutation itself.

Further insight comes from the fact that S500D-FMRP fails to elicit changes in synapse number in wild-type neurons. This phosphorylation mutant has been reported to be associated with stalled polyribosomes, presumably leading to the translational suppression of its target mRNAs. I originally hypothesized that expression of S500D-

FMRP in wild-type neurons may act as a mRNA sink, sequestering the targets of endogenous FMRP. The fact that neurons expressing endogenous FMRP have reduced numbers of synapses as compared to *Fmr1*-KO neurons (see above and Chapter 2) indicates that endogenous FMRP acts to decrease synapse number, presumably through translational regulation of its mRNA ligands. Thus, by sequestering the mRNA targets of endogenous FMRP with S500D-FMRP, I anticipated seeing an increase in the number of synapses, essentially producing an *Fmr1*-KO-like phenotype. The fact that I observed no change following S500D-FMRP expression indicates that endogenous FMRP may effectively out-compete with S500D-FMRP for access to mRNA targets or other resources necessary for synapse elimination.

Role of synaptic activity, NMDA receptors, and CaMKII in FMRP-dependent synapse loss.

Many forms of long-term synaptic change are induced by activity-dependent stimulation of NMDARs. NMDARs are canonically believed to function as coincidence detectors, becoming active only when the presynapse releases neurotransmitter and the post-synapse is sufficiently depolarized by AMPAR-mediated current. In particular, calcium influx through NMDARs is critically important for many NMDAR-mediated effects. Importantly MEF2-mediated transcription is sensitive to calcium influx through NMDARs, suggesting that MEF2-dependent synapse loss may be sensitive to NMDAR function (Flavell 2006). Recently, NMDARs were shown to interact with PP2A, the protein phosphatase responsible for dephosphorylating FMRP (Chan et al., 2001), further linking NMDAR function with MEF2/FMRP-mediated synapse elimination. In addition, MEF2 function is sensitive to calcium influx through L-type calcium channels, which are activated in response to post-synaptic depolarization (Flavell et al., 2006). These data indicate that calcium influx due to synaptic activity may regulate FMRP-dependent synapse loss.

I therefore considered whether FMRP-dependent synapse loss requires synaptic activity, hypothesizing that synaptic activity may be necessary to stimulate MEF2-dependent transcription, to activate FMRP-mediated translation, or to initiate additional

signaling cascades necessary for synapse elimination. To test this hypothesis, I prepared OHSCs from *Fmr1*-KO mice and biolistically transfected them with FMRP. Immediately prior to transfection, the Na-channel blocker TTX (1 µM) was added to the media to abolish action potential-driven synaptic transmission. TTX was maintained in the media throughout the experiment until the slices were placed in the recording chamber three to seven days post-transfection, at which point I obtained paired recordings from transfected, FMRP-expressing neurons, and neighboring untransfected *Fmr1*-KO neurons. AMPAR-mediated EPSCs were evoked with extracellular stimulation of Schaffer collateral axons (using a pair of pulses at a 50 ms inter-stimulus interval) and were measured in the neuron pairs held at –60 mV. TTX was then applied to the neurons and mEPSCs were recorded.

Preliminary data suggests that application of TTX does not block the synapse loss induced by FMRP expression. In fact, it seems to enhance the effect, although caution should be used when interpreting these data because of the low number of experiments (Fig 4.5*A-D*, Table 4.1). In addition to a trend toward reduced AMPAR-mediated EPSCs and mEPSC frequency, there is also a significant reduction in mEPSC amplitude and a trend toward increased input resistance.

Although NMDARs can are thought to be primarily important in action potential-dependent phenomena, there is evidence that they can be activated by spontaneous, action potential-independent neurotransmitter release (Sutton et al., 2007; Sutton et al., 2006; Sutton et al., 2004). In fact, NMDAR activation via miniature events has been shown to regulate post-synaptic protein expression and be important for regulating the strength of the post-synapse (Sutton et al., 2007; Sutton et al., 2006; Sutton et al., 2004). Thus, it is possible that even in the presence of TTX, NMDAR activation may play a role in FMRP-dependent synapse loss.

To examine whether NMDAR activation was required for FMRP-mediated synapse loss, I repeated the above experiments except I added the NMDAR antagonist AP5 (100 µM) to the media instead of TTX. Again, the data are too preliminary to draw any solid conclusions from, but it appears as though AP5 treatment blocks the ability of FMRP to eliminate synapses (Fig 4.5*E-H*, Table 4.1). Interestingly, FMRP expression in

AP5-treated slices resulted in a trend toward an increased paired-pulse ratio and a very significant decrease in input resistance. The mechanisms underlying these specific changes are unknown.

There are a number of calcium responsive proteins in the post-synapse that are capable of regulating synaptic function, but calcium/calmodulin-mediated protein kinase II (CaMKII) is perhaps the most well-studied. CaMKII is reported to participate in a diverse range of functions in neurons, from synaptic plasticity and memory to microtubule regulation and neurite outgrowth (Yamaouchi et al., 2005).

To investigate whether CaMKII signaling is important for FMRP-mediated synapse loss, I repeated the above experiments except I added the CaMKII antagonist KN-93 (20 µM) to the media instead of TTX. As a control for off-target effects of KN-93, I performed an additional set of experiments with a non-functional analog of KN-93, KN-92 (20 µM). These data are far too preliminary to draw any conclusions from (Table 4.1).

mGluR activity is not required for FMRP-dependent synapse loss

There is considerable evidence in the literature indicating a link between mGluR activity and FMRP function. As described in detail in Chapter 1, mGluR-LTD in both the hippocampus and the cerebellum is enhanced in *Fmr1*-KO mice (Huber et al., 2002; Hou et al., 2006; Koekkoek et al., 2005). In addition, mGluR-LTD in *Fmr1*-KO mice is no longer blocked by acute administration of protein synthesis inhibitors (Nosyreva et al., 2005; Hou et al., 2006). mGluR-induced epileptiform bursts are also enhanced in *Fmr1*-KO mice (Chuang et al., 2005). LTP in cortex and amygdala, which is dependent upon mGluR activity, is absent or significantly impaired in *Fmr1*-KO mice (Li et al., 2002; Zhao et al., 2005; Larson et al., 2005; Desai et al., 2006; Wilson et al., 2007; Meredith et al., 2007). mGluR-mediated protein synthesis is absent in *Fmr1*-KO mice and many proteins that are synthesized in response to mGluR activation have elevated expression levels in the absence of FMRP (Ronesi et al., 2008; Lu et al., 2004; Hou et al., 2006; Zalfa et al., 2007). Finally, FMRP expression, dendritic localization, and phosphorylation status are regulated by mGluR activity (Narayanan et al., 2007;

Narayanan et al., 2008; Todd et al., 2000; Hou et al., 2006; Wieler et al., 1997; Antar et al., 2004; Wang et al., 2007; Ferrari et al., 2007). These data formed the basis for the "mGluR theory of FXS," which hypothesizes that many phenotypes of FXS result from enhanced and unregulated mGluR activity (Bear et al., 2004).

Given the above links between mGluR and FMRP function, I hypothesized that activation of the group I mGluRs (mGluR1 and mGluR5) would be required for FMRP-dependent synapse loss, likely as an upstream signaling mechanism to initiate FMRP-mediated translation. Thus, in the absence of group I mGluR function, I postulated that FMRP expression would have no effect on synapse number. Indeed, several recent studies have demonstrated that total or partial impairment of group I mGluR activity reverses several phenotypes of FMRP loss (Dolen et al., 2007; Chuang et al., 2005; Yan et al., 2005; McBride et al., 2005; Tucker et al., 2006), suggesting that re-expression of FMRP in these rescue models may not produce any effect.

To directly test whether group I mGluR function is required for FMRP-dependent synapse loss, I prepared OHSCs from *Fmr1*-KO mice and biolistically transfected them with FMRP. Immediately prior to transfection, the group I mGluR antagonist LY341495 (20 µM) was added to the media to abolish all group I mGluR activity. LY341495 was maintained in the media throughout the experiment until the slices were placed in the recording chamber three to seven days post-transfection, at which point I obtained paired recordings from transfected, FMRP-expressing neurons, and neighboring untransfected *Fmr1*-KO neurons. AMPAR-mediated EPSCs were evoked with extracellular stimulation of Schaffer collateral axons (using a pair of pulses at a 50 ms inter-stimulus interval) and were measured in the neuron pairs held at –60 mV. TTX was then applied to the neurons and mEPSCs were recorded.

Interestingly, like treatment with TTX (see above), application of LY341495 appeared to enhance the ability of FMRP to eliminate synaptic connections (Fig 4.6*A-D*, Table 4.1), suggesting that mGluR activity may antagonize FMRP function and/or increase synapse number. Once again, caution must be used in interpreting these data, as only a small number of experiments were performed.

To further examine the effects of group I mGluR function on FMRP-mediated synapse loss, I over-expressed FMRP in OHSCs which lack expression of mGluR5 (mGluR5-KO) and repeated the above experimental protocol. Again, as with pharmacological blockade of mGluRs, I observe an enhancement of synapse loss following FMRP expression in OHSCs made from mGluR5-KO mice as compared with those made from wild-type littermates (Fig 4.6*E-H*, Table 4.1).

These data are particularly surprising and perplexing considering the evidence in the field linking mGluR activity and FMRP function. One possible explanation for these data comes from work describing the signaling cascades connecting group I mGluRs and FMRP. Dephosphorylated FMRP, but not phosphorylated FMRP, induces synapse loss, suggesting that regulation of the phosphorylation status of FMRP may determine its effects on synapse number. mGluR stimulation leads to the rapid (<1 minute) dephosphorylation of FMRP, followed shortly thereafter (5-10 minutes) by hyperphosphorylation of FMRP (Narayanan et al., 2007), providing a narrow temporal window during which FMRP-dependent translation may occur. The reported kinase for FMRP is S6K (Narayanan et al., 2008), while the phosphatase responsible for dephosphorylating FMRP is protein phosphatase 2A (PP2A) (Narayanan et al., 2007). Interestingly, PP2A and S6K are both activated by mGluR stimulation on a time scale consistent with FMRP phosphorylational regulation: PP2A is activated within seconds of mGluR stimulation, while S6K is not activated until approximately 10 minutes later. Thus, mGluR activation may be required not only for activity-dependent dephosphorylation of FMRP, but it may also be necessary for maintaining FMRP in a phosphorylated state under basal conditions. In the absence of mGluR activity, therefore, FMRP may become dephosphorylated through additional pathways which are not capable of efficiently re-phosphorylating it, leading to an increase in the relative amounts of dephosphorylated vs. phosphorylated FMRP. If this model is correct, one would expect mGluR5-KO mice to have reduced basal phosphorylation of their endogenous FMRP and, thus, may be expected to have fewer synaptic connections than their wild-type littermates. To my knowledge, this has not been examined in mGluR5-KO mice.

Okadaic acid, an inhibitor of PP2A, blocks FMRP-dependent synapse loss

It is likely that FMRP bi-directionally regulates the translation of its mRNA targets. Recent evidence suggests that the phosphorylation status of FMRP may act as a molecular switch to regulate the translation of FMRP-bound mRNAs. As described previously, FMRP contains a phosphorylation domain which is largely governed by a key serine at residue 500 (S500) (Ceman et al., 2003). When this serine is converted to an aspartic acid to mimic the phosphorylated state, FMRP is observed to associate with stalled polyribosomes, while an alanine substitution at this site, mimicking the dephosphorylated state and inhibiting phosphorylation throughout the domain, causes FMRP to associate more strongly with actively translating ribosomes (Ceman et al., 2003). Thus, phosphorylation of FMRP may lead to the translational suppression of its target mRNAs, while dephosphorylation would allow their translation.

As described above, the phosphatase responsible for dephosphorylating FMRP is PP2A, which is rapidly activated in response to mGluR activity (Narayanan et al., 2007). Earlier work with phosphorylation mutants of FMRP demonstrates that S500A-FMRP induces synapse loss to a similar level as wild-type FMRP, while S500D-FMRP fails to affect synapse number. These data strongly argue that dephosphorylation of FMRP is a necessary step for FMRP-induced synapse loss. Therefore, I hypothesized that inhibition of PP2A would result in hyperphosphorylation of FMRP, preventing FMRP from initiating synapse loss.

To test this hypothesis, I prepared OHSCs from *Fmr1*-KO mice and biolistically transfected them with FMRP. Immediately prior to transfection, the PP2A inhibitor okadaic acid (0.5 nM) was added to the media to abolish PP2A activity. Okadaic acid was maintained in the media throughout the experiment until the slices were placed in the recording chamber three to seven days post-transfection, at which point I obtained paired recordings from transfected, FMRP-expressing neurons, and neighboring untransfected *Fmr1*-KO neurons. AMPAR-mediated EPSCs were evoked with extracellular stimulation of Schaffer collateral axons (using a pair of pulses at a 50 ms inter-stimulus interval) and were measured in the neuron pairs held at –60 mV. TTX was then applied to the neurons and mEPSCs were recorded.

Cultures treated with vehicle control (0.1% DMSO) displayed reduced functional synapses following FMRP expression (Table 4.1). Cultures treated with okadaic acid also displayed a reduction in mEPSC frequency (Fig 4.7*A-B,D*, Table 4.1), indicating that okadaic acid may not completely block the effects of FMRP on synapse number. However, okadaic acid did prevent FMRP from reducing the amplitude of AMPAR-mediated EPSCs (Fig 4.7*C,D*, Table 4.1). Thus, it appeared as though okadaic acid may partially block the effects of FMRP on synapse number.

To test whether this blockade was directly through regulation of FMRP phosphorylation, I utilized the S500A-FMRP phosphorylation mutant. This mutant induces synapse loss to a similar extent as wild-type FMRP (as described in Chapter 2) and should be insensitive to changes in PP2A activity. I repeated the above experiments, transfecting the cultures with S500A-FMRP rather than wild-type FMRP.

Unfortunately, S500A-FMRP failed to alter synapse number, either in okadaic acid-treated or in vehicle-treated cultures (Fig 4.7*E-H*, Table 4.1). The inability of S500A-FMRP to regulate synapse number in this experiment is concerning, as it calls into question the findings reported in Chapter 2. I am at a loss to explain these findings. The number of experiments is reasonably high, yet there does not appear to be even a trend toward reduced synaptic function following S500A-FMRP expression. The dendritic localization of S500A-FMRP appeared normal (personal observations), and the overall health of the neurons (as measured by resting membrane potential and input resistance) was within normal ranges (data not shown). The only discrepancy I observe is that the frequency of mEPSCs, regardless of transfection status or drug treatment, was particularly low for nearly all cells in this set of experiments (including the experiments using wild-type FMRP) as compared with previous and more recent experiments. Previous data demonstrate that inhibition of activity can exacerbate FMRP-mediated effects on synapse loss. Thus, it stands to reason that increased activity may impair FMRP-dependent synapse loss. Heightened synaptic activity often leads to a homeostatic reduction in synapse number, which is reflected as reduced mEPSC frequency. Thus, perhaps conditions isolated to this set of experiments (media formulations, for example) may have led to increased synaptic activity. This is an unsatisfactory explanation,

however. Unfortunately, therefore, I am unable to draw any solid conclusions based upon this data. I personally believe these experiments are worth addressing at some point in the future.

Requirement of RNAi machinery for FMRP-mediated synapse loss

It is unknown exactly how FMRP may regulate translation, but one proposed mechanism for FMRP-dependent translational inhibition is through association with microRNAs (miRNAs), which are short, 20-25 nucleotide, noncoding RNAs. miRNAs are thought to suppress translation through association with the Argonaut proteins, members of the RNA-induced silencing complex (RISC), which in turn guide miRNAs to mRNA targets containing complementary sequences (Bartel et al., 2004). Near-perfect complementarity results in the RISC-dependent degradation of the targeted mRNA, while imperfect complementarity leads to inhibition of translation through an as-of-yet indeterminate mechanism (Bartel et al., 2004). One member of the Argonaut family, Argonaut 2 (AGO2), has been shown to interact with the *Drosophila* homolog of FMRP, dFmr1 (Caudy et al., 2002; Jin et al., 2004; Ishizuka et al., 2002). In addition, mammalian FMRP associates with eIF2C2, a mammalian Argonaut protein, although this interaction was not shown to be direct (Jin et al., 2004). Importantly, down-regulation of another *Drosophila* Argonaut protein, AGO1, suppressed some of the phenotypes associated with dFmr1 overexpression, implicating the Argonaut proteins as necessary components of dFmr1 function (Jin et al., 2004). It is therefore intriguing to consider the possibility that FMRP may regulate translation of its mRNA ligands via interactions with components of the RISC complex.

To examine whether association with the RISC complex or miRNAs is necessary for FMRP-dependent synapse elimination, I obtained a pharmacological inhibitor of miRNA production (RNAi-I) from Dr. Peng Jin at Emory University. Termed RNAi-I, this drug blocks the production of miRNAs, presumably through interactions with the RISC complex protein Dicer. I prepared OHSCs from *Fmr1*-KO mice and biolistically transfected them with FMRP. Immediately prior to transfection, RNAi-I (100 µM) was added to the media. RNAi-I was maintained in the media throughout the experiment

until the slices were placed in the recording chamber three to seven days post-transfection, at which point I obtained paired recordings from transfected, FMRP-expressing neurons, and neighboring untransfected *Fmr1*-KO neurons. AMPAR-mediated EPSCs were evoked with extracellular stimulation of Schaffer collateral axons (using a pair of pulses at a 50 ms inter-stimulus interval) and were measured in the neuron pairs held at –60 mV. TTX was then applied to the neurons and mEPSCs were recorded.

I performed only a very limited number of experiments with RNAi-I; however, preliminary data suggests that this drug successfully blocks the ability of FMRP to induce synapse loss (Fig 4.8*A-D*, Table 4.1). The removal of synapses following FMRP expression appears to require FMRP-mediated stimulation of translation. These data implicate association with miRNA as a critical mediator of this translation. Interactions with miRNA may help target FMRP to appropriate mRNA ligands or may facilitate trafficking of FMRP-mRNA complexes to polyribosomes. This is a particularly interesting finding that warrants further investigation, especially with regard to the observed phenotypic interaction between FMRP and MEF2, as reported in Chapter 3. A potential link between FMRP, MEF2, and miRNA production will be discussed further in Chapter 5.

FMRP's effects on synapse number are developmentally regulated

There are at least three distinct ways in which FMRP may negatively regulate the number of functional synaptic connections – through inhibition of synaptogenesis, impairment of proper synapse maturation, or enhancement of synapse elimination (described in detail in Chapter 5). The fact that postsynaptic expression of FMRP in *Fmr1*-KO neurons fails to alter the AMPA/NMDA ratio, the number of silent synapses, or the decay rate of NMDAR-mediated EPSCs strongly suggests that FMRP does not affect synapse maturation in this assay. Therefore, it stands to reason that FMRP decreases synapse number by enhancing synapse pruning or by impairing the formation of new synaptic connections.

During development, the brain undergoes a period of massive synaptogenesis, followed by a period of synaptic pruning. In the adult stage, it is believed that both synaptogenesis and synaptic pruning continue to occur, although their relative activities are roughly equalized such that total synapse number is maintained. The initial period of synaptic pruning is thought to begin shortly after the first postnatal week (Sorra and Harris, 2000); prior to this time, synapse number largely increases due to an enhancement in synaptogenesis. Thus, temporal expression of FMRP during periods of increased synaptogenesis or synapse pruning may provide inside insight into whether it is eliminating synapses or inhibiting the formation of new connections. In all previous experiments, cultures were the equivalent age of p12-16 mice, a period when both synaptogenesis and synapse elimination are on-going at roughly even levels (De Simoni et al., 2003).

I hypothesized that FMRP-induced synapse loss is due to activation of synapse pruning mechanisms and would therefore be less efficient at developmental timepoints when these mechanisms are less effective. To test this hypothesis, I prepared OHSCs from very young (p2) *Fmr1*-KO mice and biolistically transfected them with FMRP. I transfected the cultures two days thereafter and performed electrophysiological recordings 2-3 days post-transfection. Thus, the cultures were the equivalent age of p6-7 mice, a period where synaptogenesis outweighs synapse pruning (De Simoni et al., 2003). I obtained paired recordings from transfected, FMRP-expressing neurons, and neighboring untransfected *Fmr1*-KO neurons. AMPAR-mediated EPSCs were evoked with extracellular stimulation of Schaffer collateral axons (using a pair of pulses at a 50 ms inter-stimulus interval) and were measured in the neuron pairs held at –60 mV. TTX was then applied to the neurons and mEPSCs were recorded.

Surprisingly, I observe that FMRP expression results in an increase in synaptic function in young neurons (Fig 4.9*A-D*, Table 4.1). Specifically, evoked AMPAR-mediated EPSC amplitude is increased and there is a trend toward an increase in mEPSC frequency. Interestingly, the paired-pulse ratio is decreased, indicative of an increase in pre-synaptic release probability.

Previous experiments in older (equivalent p12-16) cultures had relied on 3-7 days of FMRP expression to induce changes in synapse number. Thus, I was concerned that only 2-3 days may not be sufficient time to see FMRP-dependent changes in synapse number. Therefore, I repeated the above experimental time course on *Fmr1*-KO OHSCs prepared from p6 mice. Short-term expression of FMRP failed to elicit changes in evoked AMPAR-mediated EPSCs (mEPSCs were not examined) (Fig 4.9*E-H*, Table 4.1).

These data are difficult to interpret. I expected that if FMRP impaired synaptogenesis, that expressing it in young cultures, where synaptogenesis outweighs synapse elimination, would result in an enhanced effect on synapse number. Alternatively, if FMRP plays a role in synapse pruning, I anticipated that expression at a timepoint when the synapse elimination machinery is less active would lead to a reduced effect. Unfortunately, I observe neither expected result. Instead, FMRP appears to have opposite effects in young vs. older cultures. These data suggest that FMRP may bi-directionally regulate synapse number and/or function depending on the developmental state of the neuron. This result is discussed in depth in Chapter 5.

Strangely, FMRP fails to induce any changes after only 2-3 days of expression in older cultures; however, such limited expression is sufficient to increase synaptic function in younger cultures. This may be due to the bi-directional effect of FMRP. Perhaps FMRP-dependent synapse loss in older neurons occurs at a slower timescale than the FMRP-dependent increase in synaptic function in young neurons. More experiments are necessary to both confirm this preliminary finding and to elucidate the possible mechanisms underlying this synaptic enhancement.

Figure 4.1

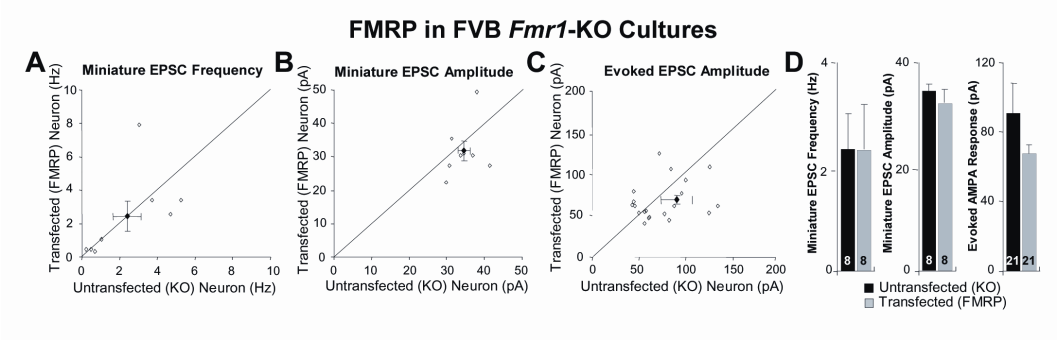

Figure 4.1. FMRP-mediated synapse loss is less robust in the FVB genetic background. ***A***-***D***, Organotypic hippocampal slice cultures from p6 FVB *Fmr1*-KO mice were biolistically transfected with wtFMRP-GFP-hpr. ***A***, ***B***, Dot plot representation of the frequency (***A***) and amplitude (***B***) of mEPSCs in paired recordings. The large diamond represents mean ± SEM. ***C***, Dot plot of the peak amplitude of the evoked AMPAR-mediated EPSCs of paired recordings. ***D***, Average mEPSC frequency, mEPSC amplitude, and AMPAR-mediated EPSC amplitude from untransfected *Fmr1*-KO and FMRP transfected cells.

Figure 4.2. Effects of FMRP knock-down or deletion on functional synapse number.

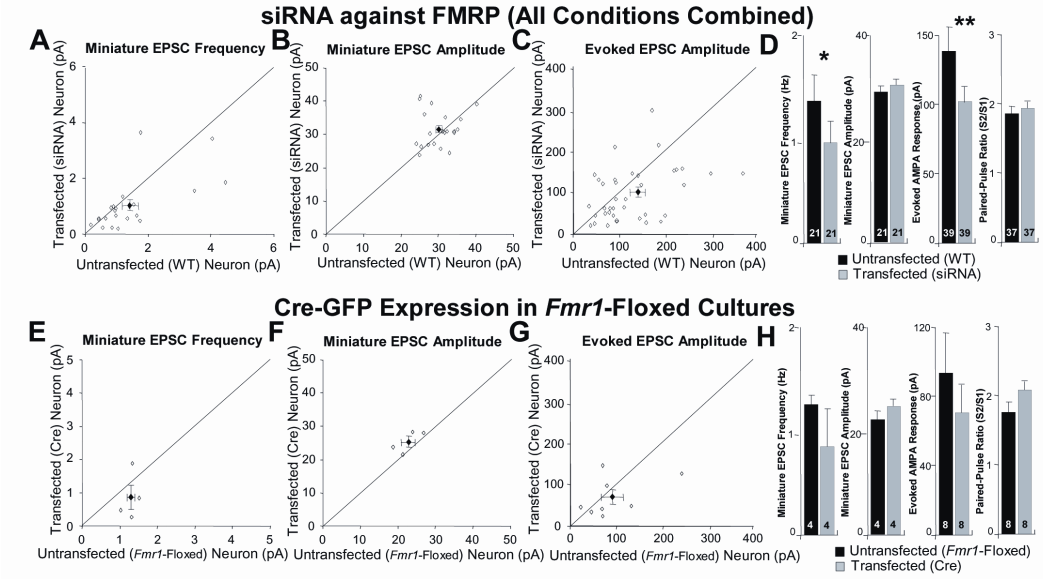

Figure 4.2. Effects of FMRP knock-down or deletion on functional synapse number. ***A-D***, Organotypic hippocampal slice cultures from p6 wild-type mice were biolistically transfected with either siRNA or plasmids expressing siRNA targeted against FMRP. Reported data is cumulative from two distinct siRNAs and plasmid-produced siRNAs. ***A***, ***B***, Dot plot representation of the frequency (***A***) and amplitude (***B***) of mEPSCs in paired recordings. The large diamond represents mean ± SEM. ***C***, Dot plot of the peak amplitude of the evoked AMPAR-mediated EPSCs of paired recordings. ***D***, Average mEPSC frequency, mEPSC amplitude, AMPAR-mediated EPSC amplitude, and paired-pulse ratio (second response amplitude/first response amplitude) from untransfected and transfected cells. ***E-H***, as **(*A-D*)**, except slice cultures were prepared from *Fmr1*-Floxed mice and cells were transfected with Cre-GFP. $*p < 0.05$.

Figure 4.3. Effects of FMRP on synapse number in *Fmr1*-Mosaic mice and local connections between CA3 pyramidal neurons.

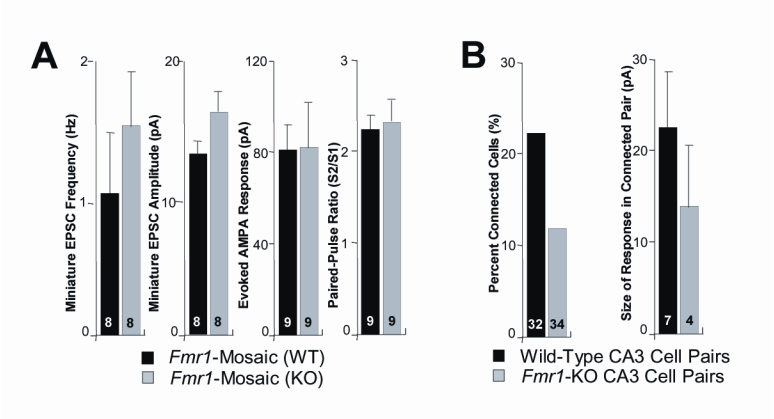

Figure 4.3. Effects of FMRP on synapse number in *Fmr1*-Mosaic mice and local connections between CA3 pyramidal neurons. ***A***, Organotypic hippocampal slice cultures from p6 *Fmr1*-Mosaic mice were prepared and paired recordings were obtained from GFP-positive (WT) and GFP-negative (KO) cells. Average mEPSC frequency, mEPSC amplitude, AMPAR-mediated EPSC amplitude, and paired-pulse ratio (second response amplitude/first response amplitude) from GFP-positive (WT) and GFP-negative (KO) cells. ***B***, Percent connected cell pairs and average amplitude of connected cell pairs in CA3 neurons in organotypic hippocampal slice cultures prepared from p6 wild-type and *Fmr1*-KO littermates.

Figure 4.4. Effects of FMRP overexpression or mutant FMRP expression in wild-type neurons.

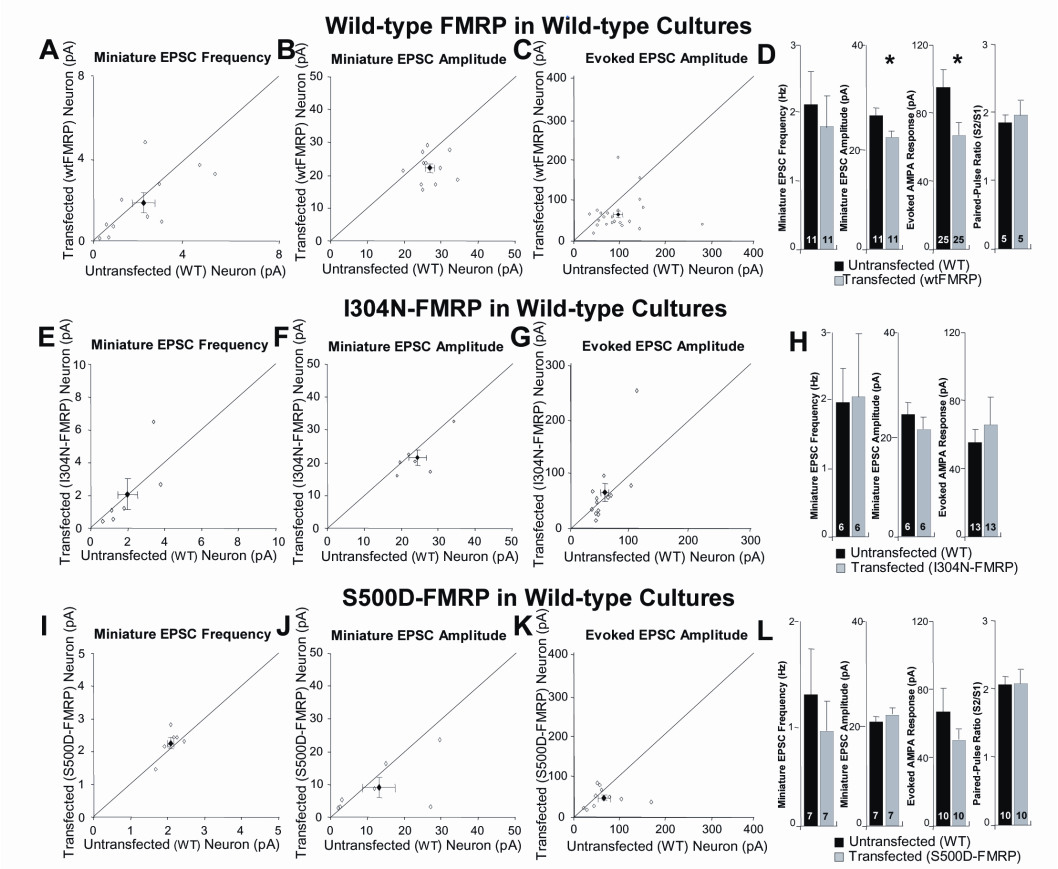

Figure 4.4. Effects of FMRP overexpression or mutant FMRP expression in wild-type neurons. ***A-D***, Organotypic hippocampal slice cultures from p6 wild-type mice were biolistically transfected with wtFMRP-GFP-hpr. ***A***, ***B***, Dot plot representation of the frequency (***A***) and amplitude (***B***) of mEPSCs in paired recordings. The large diamond represents mean ± SEM. ***C***, Dot plot of the peak amplitude of the evoked AMPAR-mediated EPSCs of paired recordings. ***D***, Average mEPSC frequency, mEPSC amplitude, AMPAR-mediated EPSC amplitude, and paired-pulse ratio (second response amplitude/first response amplitude) from untransfected and transfected cells. ***E-H***, as **(*A-D*)**, except slice cultures were transfected with I304N-FMRP-GFP-hpr. ***I-L***, as **(*A-D*)**, except slice cultures were transfected with S500D-FMRP-GFP-hpr. $*p < 0.05$.

Figure 4.5. Effects of activity inhibition or NMDAR inhibition on FMRP-mediated synapse loss.

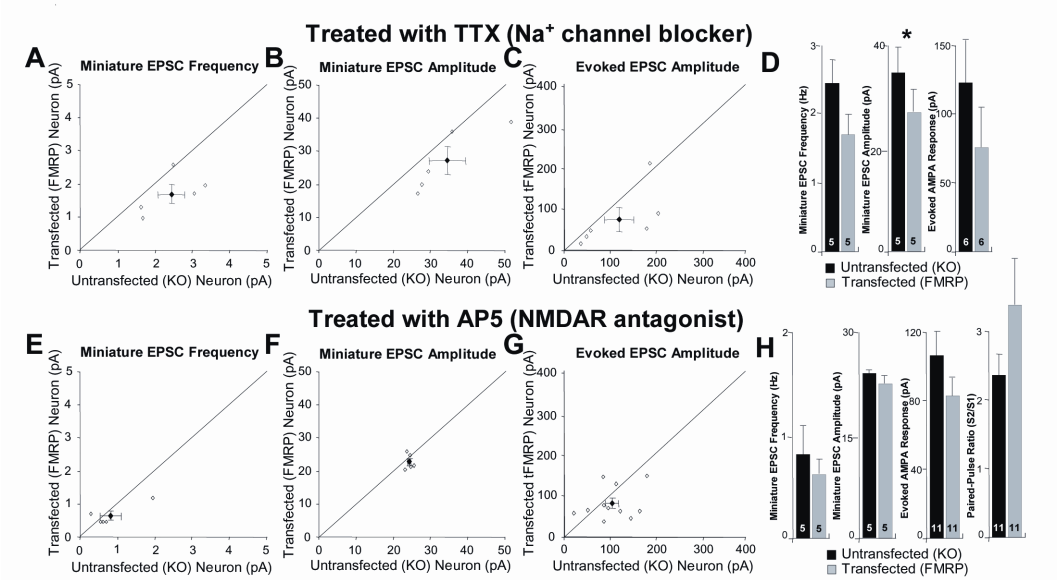

Figure 4.5. Effects of activity inhibition or NMDAR inhibition on FMRP-mediated synapse loss. ***A-D***, Organotypic hippocampal slice cultures from p6 *Fmr1*-KO mice were biolistically transfected with wtFMRP-GFP-hpr and continuously treated with 1 µM tetrodotoxin (TTX). ***A***, ***B***, Dot plot representation of the frequency (***A***) and amplitude (***B***) of mEPSCs in paired recordings. The large diamond represents mean ± SEM. ***C***, Dot plot of the peak amplitude of the evoked AMPAR-mediated EPSCs of paired recordings. ***D***, Average mEPSC frequency, mEPSC amplitude, AMPAR-mediated EPSC amplitude, and paired-pulse ratio (second response amplitude/first response amplitude) from untransfected and transfected cells. ***E-H***, as **(*A-D*)**, except slice cultures were treated with 100 µM AP5. *$p < 0.05$.

Figure 4.6. Effects of group I mGluR inhibition on FMRP-mediated synapse loss.

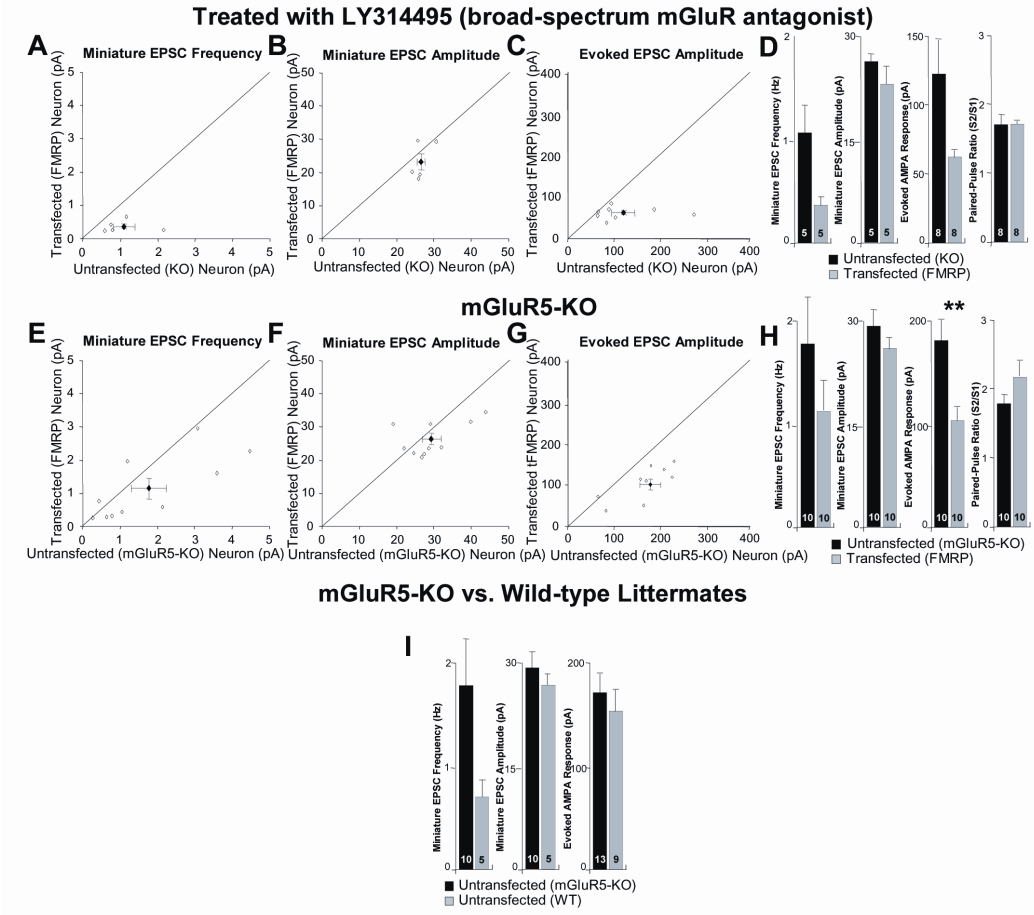

Figure 4.6. Effects of group I mGluR inhibition on FMRP-mediated synapse loss. ***A*-*D***, Organotypic hippocampal slice cultures from p6 *Fmr1*-KO mice were biolistically transfected with wtFMRP-GFP-hpr and continuously treated with 20 µM LY341495. ***A***, ***B***, Dot plot representation of the frequency (***A***) and amplitude (***B***) of mEPSCs in paired recordings. The large diamond represents mean ± SEM. ***C***, Dot plot of the peak amplitude of the evoked AMPAR-mediated EPSCs of paired recordings. ***D***, Average mEPSC frequency, mEPSC amplitude, AMPAR-mediated EPSC amplitude, and paired-pulse ratio (second response amplitude/first response amplitude) from untransfected and transfected cells. ***E*-*H***, as **(*A*-*D*)**, except slice cultures were prepared from mGluR5-KO mice and were not treated with LY341495. ***I***, Average mEPSC frequency, mEPSC amplitude, and AMPAR-mediated EPSC amplitude from untransfected from slice cultures prepared from wild-type and mGluR5-KO littermates. $^{**}p < 0.01$.

Figure 4.7. Effects of protein phosphatase 2A (PP2A) inhibition on FMRP-mediated synapse loss.

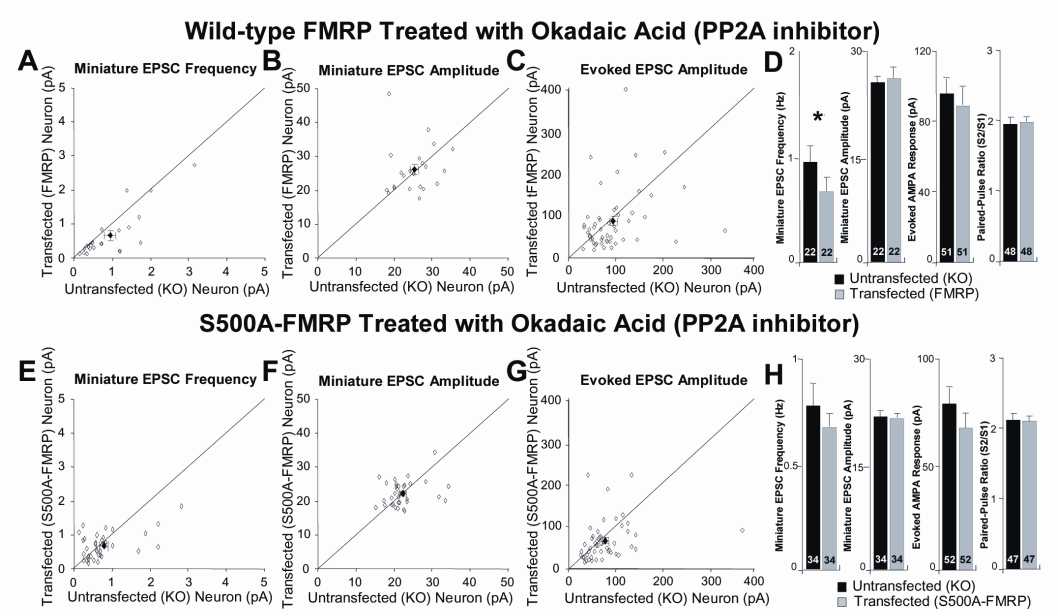

Figure 4.7. Effects of protein phosphatase 2A (PP2A) inhibition on FMRP-mediated synapse loss. ***A-D***, Organotypic hippocampal slice cultures from p6 *Fmr1*-KO mice were biolistically transfected with wtFMRP-GFP-hpr and continuously treated with 0.5 nM okadaic acid. ***A***, ***B***, Dot plot representation of the frequency (***A***) and amplitude (***B***) of mEPSCs in paired recordings. The large diamond represents mean ± SEM. ***C***, Dot plot of the peak amplitude of the evoked AMPAR-mediated EPSCs of paired recordings. ***D***, Average mEPSC frequency, mEPSC amplitude, AMPAR-mediated EPSC amplitude, and paired-pulse ratio (second response amplitude/first response amplitude) from untransfected and transfected cells. ***E-H***, as **(*A-D*)**, except slice cultures were transfected with S500A-FMRP-GFP-hpr.

Figure 4.8. Effects of miRNA production on FMRP-mediated synapse loss.

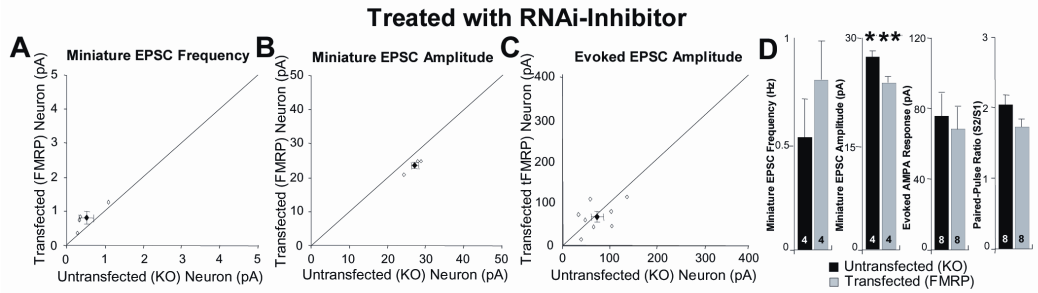

Figure 4.8. Effects of miRNA production on FMRP-mediated synapse loss. ***A-D***, Organotypic hippocampal slice cultures from p6 *Fmr1*-KO mice were biolistically transfected with wtFMRP-GFP-hpr and continuously treated with 100 µM RNAi-I. ***A***, ***B***, Dot plot representation of the frequency (***A***) and amplitude (***B***) of mEPSCs in paired recordings. The large diamond represents mean ± SEM. ***C***, Dot plot of the peak amplitude of the evoked AMPAR-mediated EPSCs of paired recordings. ***D***, Average mEPSC frequency, mEPSC amplitude, AMPAR-mediated EPSC amplitude, and paired-pulse ratio (second response amplitude/first response amplitude) from untransfected and transfected cells.

Figure 4.9. Developmental effects of FMRP expression on synaptic function.

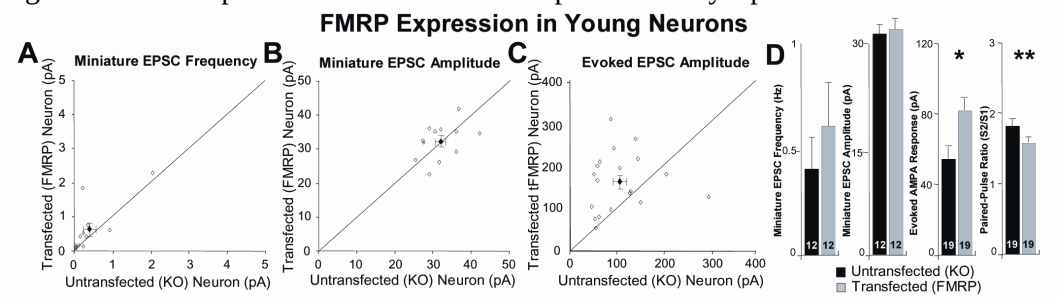

Figure 4.9. Developmental effects of FMRP expression on synaptic function. ***A-D***, Organotypic hippocampal slice cultures from p2 *Fmr1*-KO mice were biolistically transfected with wtFMRP-GFP-hpr. ***A***, ***B***, Dot plot representation of the frequency (***A***) and amplitude (***B***) of mEPSCs in paired recordings. The large diamond represents mean ± SEM. ***C***, Dot plot of the peak amplitude of the evoked AMPAR-mediated EPSCs of paired recordings. ***D***, Average mEPSC frequency, mEPSC amplitude, AMPAR-mediated EPSC amplitude, and paired-pulse ratio (second response amplitude/first response amplitude) from untransfected and transfected cells.

Table 4.1: Investigations into the Mechanisms of FMRP-Dependent Synapse Loss

Condition	Measurement	Transfected	Untransfected	n	p-value
FVB Fmr1-KO mice					
	mEPSC frequency (Hz)	2.42 ± 0.91	2.43 ± 0.72	8	0.9886
	mEPSC amplitude (pA)	31.9 ± 2.9	34.2 ± 1.4	8	0.4183
	Evoked AMPAR-mediated EPSC (pA)	68.1 ± 5.1	91.8 ± 17.0	21	0.1521
	Paired-pulse ratio (S2/S1)	n.d.	n.d.	0	n.d.
	Resting Membrane Potential (mV)	-53.8 ± 1.0	-54.6 ± 1.1	21	0.4316
	Input Resistance (M?)	168.8 ± 10.7	165.5 ± 8.8	21	0.8287
FMRP si-RNA-mediated knock-down					
siRNA 1 in WT neurons	mEPSC frequency (Hz)	0.96 ± 0.18	1.49 ± 0.50	7	0.1980
	mEPSC amplitude (pA)	30.4 ± 1.6	29.5 ± 1.5	7	0.6575
	Evoked AMPAR-mediated EPSC (pA)	94.6 ± 20.1	113.3 ± 19.2	12	0.2753
	Paired-pulse ratio (S2/S1)	2.03 ± 0.19	1.84 ± 0.18	12	0.0709
	Resting Membrane Potential (mV)	-50.9 ± 1.25	-54.5 ± 1.7	12	0.1565
	Input Resistance (M?)	171.7 ± 11.2	153.8 ± 12.7	12	0.1829
siRNA 2 in WT neurons	mEPSC frequency (Hz)	n.d.	n.d.	0	n.d.
	mEPSC amplitude (pA)	n.d.	n.d.	0	n.d.
	Evoked AMPAR-mediated EPSC (pA)	91.6 ± 18.9	118.1 ± 19.3	8	0.0973
	Paired-pulse ratio (S2/S1)	1.76 ± 0.23	1.66 ± 0.15	7	0.6315
	Resting Membrane Potential (mV)	-56.8 ± 2.5	-52.5 ± 1.5	8	0.2094
	Input Resistance (M?)	179.4 ± 32.0	167.5 ± 6.5	8	0.6813
pSuper-mediated siRNA 1 in WT neurons	mEPSC frequency (Hz)	1.67 ± 0.50	1.89 ± 0.50	7	0.6285
	mEPSC amplitude (pA)	29.0 ± 1.8	32.1 ± 1.6	7	**0.0266**
	Evoked AMPAR-mediated EPSC (pA)	129.4 ± 28.3	182.0 ± 37.2	8	0.2457
	Paired-pulse ratio (S2/S1)	2.22 ± 0.27	2.01 ± 0.26	8	0.2991
	Resting Membrane Potential (mV)	-54.4 ± 2.3	-57.4 ± 1.0	8	0.1419
	Input Resistance (M?)	158.1 ± 10.8	128.8 ± 14.3	8	**0.0012**
pSuper-mediated siRNA 2 in WT neurons	mEPSC frequency (Hz)	0.41 ± 0.07	0.94 ± 0.23	7	0.0654
	mEPSC amplitude (pA)	34.1 ± 2.3	27.8 ± 1.6	7	0.0668
	Evoked AMPAR-mediated EPSC (pA)	100.8 ± 25.7	158.1 ± 48.0	11	0.1262
	Paired-pulse ratio (S2/S1)	1.65 ± 0.10	1.76 ± 0.09	10	0.4713
	Resting Membrane Potential (mV)	-52.3 ± 1.6	-53.9 ± 2.2	11	0.5849
	Input Resistance (M?)	180.0 ± 23.6	132.3 ± 8.7	11	0.1069
All siRNA combined in WT neurons	mEPSC frequency (Hz)	1.01 ± 0.21	1.43 ± 0.25	21	**0.0440**
	mEPSC amplitude (pA)	31.1 ± 1.2	29.8 ± 0.9	21	0.3460
	Evoked AMPAR-mediated EPSC (pA)	102.9 ± 11.2	141.0 ± 17.0	39	**0.0089**
	Paired-pulse ratio (S2/S1)	1.92 ± 0.10	1.83 ± 0.09	37	0.2094
	Resting Membrane Potential (mV)	-53.2 ± 0.9	-54.5 ± 0.9	39	0.3391
	Input Resistance (M?)	172.8 ± 9.9	145.4 ± 5.9	39	**0.0103**

Table 4.1: Investigations into the Mechanisms of FMRP-Dependent Synapse Loss (cont.)

Condition	Measurement	Transfected	Untransfected	n	p-value
Cre-GFP mediated knockdown of FMRP					
Cre-GFP in Fmr1-Floxed neurons	mEPSC amplitude (pA)	25.4 ± 1.6	22.3 ± 1.8	4	0.1171
	Evoked AMPAR-mediated EPSC (pA)	70.8 ± 16.2	92.8 ± 24.5	8	0.3511
	Paired-pulse ratio (S2/S1)	2.04 ± 0.16	1.72 ± 0.15	8	0.2053
	Resting Membrane Potential (mV)	-62.3 ± 1.9	-56.3 ± 3.7	8	0.1743
	Input Resistance (M?)	143.1 ± 19.1	111.3 ± 5.4	8	0.1156
	mEPSC frequency (Hz)	0.74 ± 0.08	0.98 ± 0.16	4	0.1831
Cre-GFP in WT neurons	mEPSC amplitude (pA)	24.0 ± 1.3	27.5 ± 1.2	4	0.1632
	Evoked AMPAR-mediated EPSC (pA)	102.6 ± 16.3	176.7 ± 37.8	4	0.0751
	Paired-pulse ratio (S2/S1)	1.82 ± 0.09	1.85 ± 0.10	4	0.7450
	Resting Membrane Potential (mV)	-64.6 ± 2.7	-67.4 ± 3.1	5	0.3766
	Input Resistance (M?)	138.0 ± 17.4	120.0 ± 7.1	5	0.1813
FMRP expression in WT rat neurons					
Wild-Type FMRP in rat neurons	mEPSC frequency (Hz)	n.d.	n.d.	0	n.d.
	mEPSC amplitude (pA)	n.d.	n.d.	0	n.d.
	Evoked AMPAR-mediated EPSC (pA)	69.5 ± 9.2	78.4 ± 10.3	14	0.3465
	Paired-pulse ratio (S2/S1)	n.d.	n.d.	0	n.d.
	Resting Membrane Potential (mV)	-55.7 ± 1.0	-51.9 ± 1.2	20	**0.0127**
	Input Resistance (M?)	185.0 ± 16.3	207.0 ± 17.3	20	0.2866
wtFMRP in WT mouse neurons	mEPSC frequency (Hz)	1.82 ± 0.47	2.15 ± 0.50	11	0.4079
	mEPSC amplitude (pA)	22.2 ± 1.4	26.7 ± 1.2	22	**0.0277**
	Evoked AMPAR-mediated EPSC (pA)	66.6 ± 8.03	95.0 ± 10.1	25	**0.0280**
	Paired-pulse ratio (S2/S1)	1.96 ± 0.20	1.83 ± 0.11	5	0.2262
	Resting Membrane Potential (mV)	-54.7 ± 1.1	-56.0 ± 1.2	26	0.2790
	Input Resistance (M?)	153.0 ± 14.1	172.7 ± 12.8	26	0.1153
I304N-FMRP in WT mouse neurons	mEPSC frequency (Hz)	2.07 ± 0.93	1.97 ± 0.53	6	0.8818
	mEPSC amplitude (pA)	21.5 ± 2.4	24.3 ± 2.4	6	0.1470
	Evoked AMPAR-mediated EPSC (pA)	65.7 ± 16.8	56.0 ± 6.7	13	0.4506
	Paired-pulse ratio (S2/S1)	n.d.	n.d.	0	n.d.
	Resting Membrane Potential (mV)	-54.6 ± 1.3	-53.8 ± 1.5	13	0.7142
	Input Resistance (M?)	141.9 ± 9.2	135.8 ± 7.0	13	0.6511
S500D-FMRP in WT mouse neurons	mEPSC frequency (Hz)	0.92 ± 0.30	1.30 ± 0.44	7	0.3240
	mEPSC amplitude (pA)	22.4 ± 1.6	20.9 ± 0.9	7	0.2645
	Evoked AMPAR-mediated EPSC (pA)	49.9 ± 7.2	67.2 ± 13.9	10	0.2891
	Paired-pulse ratio (S2/S1)	2.05 ± 0.20	2.05 ± 0.11	10	0.9943
	Resting Membrane Potential (mV)	-59.2 ± 1.5	-60.4 ± 1.2	13	0.4229
	Input Resistance (M?)	133.5 ± 14.2	113.8 ± 9.3	13	0.2285

Table 4.1: Investigations into the Mechanisms of FMRP-Dependent Synapse Loss (cont.)

Condition	Measurement	Transfected	Untransfected	n	p-value
wtFMRP in *Fmr1*-KO neurons					
Treated with TTX	mEPSC frequency (Hz)	1.69 ± 0.28	2.44 ± 0.35	5	0.0577
	mEPSC amplitude (pA)	27.1 ± 4.3	34.6 ± 4.9	5	**0.0329**
	Evoked AMPAR-mediated EPSC (pA)	76.2 ± 28.7	121.6 ± 32.7	6	0.1345
	Paired-pulse ratio (S2/S1)	n.d.	n.d.	0	n.d.
	Resting Membrane Potential (mV)	-60.0 ± 1.5	-61.5 ± 1.8	6	0.2956
	Input Resistance (M?)	243.3 ± 19.3	188.3 ± 22.1	6	0.0797
Treated with AP5	mEPSC frequency (Hz)	0.64 ± 0.14	0.82 ± 0.29	5	0.3937
	mEPSC amplitude (pA)	22.5 ± 1.1	24.0 ± 0.4	5	0.2939
	Evoked AMPAR-mediated EPSC (pA)	82.7 ± 11.8	106.0 ± 14.4	11	0.1717
	Paired-pulse ratio (S2/S1)	3.38 ± 0.67	2.34 ± 0.31	11	0.0634
	Resting Membrane Potential (mV)	-58.3 ± 2.1	59.7 ± 1.2	11	0.5303
	Input Resistance (M?)	159.1 ± 13.4	206.4 ± 17.3	11	**0.0005**
Treated with KN-93	mEPSC frequency (Hz)	1.34	1.97	1	N/A
	mEPSC amplitude (pA)	31.4	29.4	1	N/A
	Evoked AMPAR-mediated EPSC (pA)	130.9 ± 24.8	113.9 ± 52.1	4	0.8199
	Paired-pulse ratio (S2/S1)	n.d.	n.d.	0	n.d.
	Resting Membrane Potential (mV)	-51.5 ± 0.3	-53.5 ± 2.4	4	0.4153
	Input Resistance (M?)	225 ± 42.1	232.5 ± 11.8	4	0.8297
Treated with KN-92	mEPSC frequency (Hz)	0.56 ± 0.21	0.78 ± 0.26	4	0.1553
	mEPSC amplitude (pA)	26.6 ± 3.25	22.13 ± 1.29	4	0.3082
	Evoked AMPAR-mediated EPSC (pA)	95.4 ± 17.1	90.9 ± 21.2	5	0.8215
	Paired-pulse ratio (S2/S1)	n.d.	n.d.	0	n.d.
	Resting Membrane Potential (mV)	-53.0 ± 1.3	-54.0 ± 1.2	5	0.6864
	Input Resistance (M?)	276.0 ± 51.0	198 ± 47.6	5	0.3044
wtFMRP in *Fmr1*-KO neurons					
Treated with LY341495	mEPSC frequency (Hz)	0.37 ± 0.08	1.08 ± 0.28	5	0.0795
	mEPSC amplitude (pA)	23.3 ± 2.5	26.4 ± 1.1	5	0.2019
	Evoked AMPAR-mediated EPSC (pA)	62.5 ± 4.9	121.4 ± 26.4	8	0.0628
	Paired-pulse ratio (S2/S1)	1.71 ± 0.05	1.71 ± 0.14	8	0.9935
	Resting Membrane Potential (mV)	-61.3 ± 2.2	-62.4 ± 1.9	8	0.7633
	Input Resistance (M?)	114.4 ± 8.6	109.4 ± 9.7	8	0.4248
wtFMRP in mGluR5-KO neurons	mEPSC frequency (Hz)	1.13 ± 0.31	1.77 ± 0.46	10	0.0681
	mEPSC amplitude (pA)	26.2 ± 1.6	29.4 ± 2.4	10	0.1582
	Evoked AMPAR-mediated EPSC (pA)	102.4 ± 13.3	178.6 ± 22.1	10	**0.0053**
	Paired-pulse ratio (S2/S1)	2.15 ± 0.23	1.77 ± 0.11	10	0.1267
	Resting Membrane Potential (mV)	-57.0 ± 1.2	-55.3 ± 1.7	11	0.4181
	Input Resistance (M?)	205.9 ± 26.3	185.9 ± 15.8	11	0.5040

Table 4.1: Investigations into the Mechanisms of FMRP-Dependent Synapse Loss (cont.)

Condition	Measurement	Transfected	Untransfected	n	p-value
Okadaic Acid					
Wild-Type FMRP treated with Okadaic Acid	mEPSC frequency (Hz)	0.67 ± 0.15	0.95 ± 0.16	22	**0.0046**
	mEPSC amplitude (pA)	25.9 ± 1.5	25.1 ± 1.1	22	0.6519
	Evoked AMPAR-mediated EPSC (pA)	88.8 ± 10.3	95.9 ± 8.5	51	0.5351
	Paired-pulse ratio (S2/S1)	1.97 ± 0.08	1.96 ± 0.07	48	0.9183
	Resting Membrane Potential (mV)	-60.8 ± .7	-59.6 ± 0.9	54	0.1583
	Input Resistance (M?)	124.5 ± 6.2	128.9 ± 4.8	54	0.4100
Wild-Type FMRP treated with Vehicle	mEPSC frequency (Hz)	0.94 ± 0.18	1.26 ± 0.21	17	0.0831
	mEPSC amplitude (pA)	25.0 ± 1.4	24.7 ± 1.0	17	0.8186
	Evoked AMPAR-mediated EPSC (pA)	87.0 ± 13.2	121.2 ± 14.2	26	**0.0274**
	Paired-pulse ratio (S2/S1)	2.10 ± 0.17	2.01 ± 0.14	24	0.6113
	Resting Membrane Potential (mV)	-59.7 ± 1.1	-58.9 ± 1.3	27	0.6136
	Input Resistance (M?)	125.6 ± 9.7	131.7 ± 8.0	27	0.4859
S500A-FMRP treated with Okadaic Acid	mEPSC frequency (Hz)	0.69 ± 0.07	0.79 ± 0.11	34	0.2987
	mEPSC amplitude (pA)	22.1 ± 0.63	22.2 ± 0.78	34	0.8585
	Evoked AMPAR-mediated EPSC (pA)	67.7 ± 6.6	78.9 ± 7.4	52	0.1864
	Paired-pulse ratio (S2/S1)	2.09 ± 0.07	2.10 ± 0.08	47	0.8906
	Resting Membrane Potential (mV)	-59.7 ± 0.6	-60.2 ± 0.6	55	0.5026
	Input Resistance (M?)	123.1 ± 6.3	125.9 ± 5.1	55	0.6458
S500A-FMRP treated with Vehicle	mEPSC frequency (Hz)	1.10 ± 0.43	0.88 ± 0.18	17	0.6213
	mEPSC amplitude (pA)	22.8 ± 1.2	21.8 ± 0.7	17	0.4260
	Evoked AMPAR-mediated EPSC (pA)	69.7 ± 9.7	79.4 ± 10.3	19	0.5113
	Paired-pulse ratio (S2/S1)	2.08 ± 0.11	1.90 ± 0.07	19	0.2129
	Resting Membrane Potential (mV)	-57.4 ± 0.9	-58.4 ± 1.1	25	0.4058
	Input Resistance (M?)	142.6 ± 17.0	146.8 ± 13.1	25	0.7680
RNAi-Inhibitor					
RNAi-Inhibitor	mEPSC frequency (Hz)	0.80 ± 0.18	0.53 ± 0.19	4	0.0580
	mEPSC amplitude (pA)	23.4 ± 0.9	27.1 ± 1.0	4	**0.0003**
	Evoked AMPAR-mediated EPSC (pA)	68.0 ± 12.0	74.4 ± 13.4	8	0.6400
	Paired-pulse ratio (S2/S1)	1.73 ± 0.11	2.05 ± 0.12	8	0.0784
	Resting Membrane Potential (mV)	-60.1 ± 2.4	-57.1 ± 2.5	8	0.3744
	Input Resistance (M?)	193.8 ± 34.2	201.2 ± 18.7	8	0.8435
Vehicle	mEPSC frequency (Hz)	0.58 ± 0.27	0.87 ± 0.33	4	0.5529
	mEPSC amplitude (pA)	21.8 ± 0.6	23.3 ± 1.4	4	0.3479
	Evoked AMPAR-mediated EPSC (pA)	71.6 ± 11.8	100.6 ± 18.2	6	0.2481
	Paired-pulse ratio (S2/S1)	1.73 ± 0.11	1.92 ± 0.26	6	0.3862
	Resting Membrane Potential (mV)	-58.0 ± 1.9	-61.3 ± 1.4	6	0.1527
	Input Resistance (M?)	146.7 ± 20.4	157.5 ± 14.9	6	0.7710

Table 4.1: Investigations into the Mechanisms of FMRP-Dependent Synapse Loss (cont.)

Condition	Measurement	Transfected	Untransfected	n	p-value
Young Cultures					
p6-7 two-day expression	mEPSC frequency (Hz)	0.61 ± 0.20	0.40 ± 0.17	12	0.1497
	mEPSC amplitude (pA)	32.4 ± 1.5	31.9 ± 1.4	12	0.7552
	Evoked AMPAR-mediated EPSC (pA)	81.3 ± 7.9	53.7 ± 7.4	19	**0.0152**
	Paired-pulse ratio (S2/S1)	1.55 ± 0.10	1.83 ± 0.10	19	**0.0047**
	Resting Membrane Potential (mV)	-55.1 ± 1.2	-53.7 ± 1.4	20	0.4634
	Input Resistance (M?)	343.0 ± 32.2	429.8 ± 40.5	20	0.0926
p12-13 two-day expression	mEPSC frequency (Hz)	0.88	0.17	1	N/A
	mEPSC amplitude (pA)	22.7	28.3	1	N/A
	Evoked AMPAR-mediated EPSC (pA)	100.8 ± 18.9	96.9 ± 17.5	14	0.8880
	Paired-pulse ratio (S2/S1)	2.43 ± 0.38	2.39 ± 0.32	13	0.9480
	Resting Membrane Potential (mV)	-49.6 ± 2.2	-48.4 ± 1.8	14	0.5255
	Input Resistance (M?)	329.6 ± 47.0	337.1 ± 46.2	14	0.8551

CHAPTER FIVE

Discussion and Implications

The data presented in this manuscript describe the effects of FMRP expression on synapse number and further detail mechanisms through which FMRP may regulate the number and function of synaptic connections. I observe that acute, postnatal expression of FMRP at near-endogenous levels in *Fmr1*-KO neurons results in a significant reduction in synapse number at both the functional and structural levels. Furthermore, I observe that endogenous FMRP expression also decreases synapse number in side-by-side comparisons of wild-type and *Fmr1*-KO neurons. I demonstrate that FMRP-mediated synapse loss requires a functional KH2 domain as well as dephosphorylation of FMRP, strongly implicating FMRP-dependent stimulation of translation as a critical step in synapse loss following FMRP expression. These data are supported by considerable work in the field of FXS demonstrating increased numbers of dendritic spines, the primary sites of excitatory synaptic contact, in the absence of FMRP expression.

I further report a unique genetic interaction between FMRP and the transcription factor MEF2. Activation of MEF2 in wild-type neurons induces robust synapse loss, while inhibition of MEF2 results in an increase in synapse number. However, neither increased nor decreased MEF2 function had any effect in *Fmr1*-KO neurons, implicating FMRP as a necessary mediator of MEF2 activity. Furthermore, inhibition of MEF2 activity prevented FMRP expression from inducing synapse loss in *Fmr1*-KO neurons, suggesting that these two proteins act in the same pathway to coordinately regulate synapse number.

These data provide insight into FMRP function and into neuronal changes that may underlie many of the behavioral and neurological phenotypes of FXS.

FMRP Regulation of Synapse Number: Synaptogenesis or Synapse Elimination?

Overall Cytoarchitecture is Unaffected by FMRP Expression

The phenotype of reduced synapse number following FMRP expression reported in Chapter 2 is observed in neurons that are the equivalent age of roughly two weeks post-natal. At this age, the gross cytoarchitecture of the hippocampus is largely established. It is unlikely, therefore, that FMRP expression reduces synapse number by inducing large-scale restructuring of the brain. This view is supported by studies reporting no global changes in the brain structure of FXS patients (Hessl et al., 2004). Furthermore, I observe no widespread alterations in the size, shape, or direction of the dendritic tree of FMRP-expressing neurons as compared with neighboring untransfected *Fmr1*-KO neurons or neurons transfected with GFP or mCherry (personal observations). This is supported by the fact that the capacitance, a gross measure of cell size, of *Fmr1*-KO neurons is unaltered by FMRP expression (Chapter 2). It is possible that FMRP expression may cause more subtle changes in dendritic morphology – in secondary or tertiary branching, length of dendrites, or pattern of growth – but only more in-depth studies will be able to adequately address this issue.

There are, then, at least three distinct ways in which FMRP may negatively regulate the number of functional synaptic connections: through inhibition of synaptogenesis, impairment of proper synapse maturation, or enhancement of synapse elimination. Although these three processes have been well-studied, the specific mechanisms underlying the growth of new synaptic connections, their development and maturation, and their elimination remain incompletely defined.

Does FMRP Reduce Synapse Number Through Inhibition of Synaptogenesis or Enhancement of Synaptic Pruning?

The data presented in Chapter 2 reveal insights into how FMRP may function to regulate synapse number. First, it is known that synaptic activity can induce homeostatic changes in neuronal and synaptic function. Such changes are often reflected as differential expression of voltage-gated channels or in growth or retraction of neuronal processes, and can be observed as changes in the resting membrane potential, input

resistance, or capacitance of the neuron. FMRP expression does not affect these three basic measures of neuronal function, suggesting that the observed synapse loss following FMRP expression is not due to a homeostatic, compensatory effect caused by alterations in global neuronal properties of firing and excitability. Rather, this appears to be a direct effect of FMRP on synapse number, although I cannot directly rule out the possibility that FMRP takes part in a homeostatic process of synapse regulation. Second, although synapse number is reduced, the qualities of the remaining synaptic connections are unchanged. mEPSC amplitude and PPF are unaltered following expression of FMRP in *Fmr1*-KO neurons, indicating that neither pre-synaptic release probability nor post-synaptic AMPAR expression are changed. Thus, FMRP appears not to affect pre- or post-synaptic function, merely synapse number. Of particular interest is the fact that FMRP does not alter the ratio of AMPAR-/NMDAR-mediated EPSCs, the number of silent synapses, or the decay rate of NMDAR-mediated EPSCs. As described above, these are all well-defined measurements of synaptic and neuronal maturation. Thus, the fact that they are not changed following FMRP expression strongly argues that FMRP does not alter synapse maturation. FMRP may therefore reduce synapse number through one of two gross mechanisms: it may inhibit the formation of new synaptic connections or it may enhance the elimination of existing synaptic connections.

Morphological evidence from FXS patients and *Fmr1*-KO mice indicate not only an increase in spine number, but also a shift toward long, thin filopodia-like spines, a phenotype indicative of immature spines. It is unclear whether the increased numbers of filopodia-like spines observed in FXS patients and *Fmr1*-KO mice represent functional synapses, although my data suggest that they might. Recent studies on filopodial growth and synaptic connections indicate that synaptogenesis of excitatory synapses seems to follow a consistent pattern of events. First, a dendritic filopodia emerges from a dendritic shaft and scans the local environment, presumably searching for a pre-synaptic partner, possibly by growing toward higher concentration gradients of neurotransmitter (Nägerl et al., 2007). Newly formed filopodia preferentially attach to synaptic terminals with pre-existing synaptic connections to other spines (Knott et al., 2006; Nägerl et al., 2007). Synaptic structures necessary for neurotransmission are not observed on connections

between newly formed connections (a few hours old) (Nägerl et al., 2007). However, such synaptic structures are observed on connections that are 15+ hours old, further confirming that nascent synapses require only a short time window to fully establish a functional connection (Knott et al., 2006; Nägerl et al., 2007). Once an axon partner is found, a primitive synaptic connection is formed (Cline, 2001). As the synapse matures, the filopodia retracts, becoming a short, stubby spine (Cline, 2001). Thus, the increased number of filopodial-like spines in the absence of FMRP expression may be due to increased synaptogenesis coupled with a lack of proper morphological maturation. If this is the case, it would indicate that maturation of morphological structure of the spine is independent of maturation of the function of the synapse, as my data strongly suggests that functional synapse maturation is unaffected by FMRP expression.

Synapse elimination may also cause an increase in long, thin dendritic spines. As mentioned previously, repeated induction of mGluR-LTD can induce synapse loss (Shinoda et al., 2005). Furthermore, activation of group I mGluRs results in the elongation of dendritic spines (Vanderklish et al., 2002), suggesting that in response to mGluR activity, spine elongation may precede synapse elimination. Thus, in the absence of FMRP, enhanced mGluR activity (Bear et al., 2004) may induce the elongation of spines and may biochemically "tag" them for elimination. However, if FMRP is necessary to complete synapse elimination, these synapses may fail to be pruned in the absence of FMRP, leading to the increased numbers of long, thin spines observed in FXS patients and *Fmr1*-KO mice. Thus, the phenotype of tortuous, filopodial-like spines may be due to either enhanced rates of synaptogenesis (coupled with impairments in spine maturation) or due to impaired synapse elimination. The morphological data alone is insufficient to tease these two possibilities apart.

If FMRP expression inhibits synaptogenesis, it might be expected that FMRP would have no effect on synaptic development or maintenance beyond the initial formation of the connection, and thus, FMRP expression would not affect those synaptic connections which have already been formed. This fits well with the observed data demonstrating that synaptic function is unaffected by FMRP expression. However, additional data does not fully agree with this model. Current evidence indicates that

synapse formation is a rapid process, and can occur in as little as one to two hours after initial filopodial contact. Synapse formation is followed by the slower process of synaptic maturation, which entails recruitment of AMPARs to "silent synapses" and an increase in efficacy of the pre-synaptic terminal. In the experiments described throughout a majority of this manuscript, exogenous FMRP is expressed in *Fmr1*-KO neurons for 3-7 days. Thus, if FMRP inhibits synaptogenesis, the untransfected neuron essentially has an additional 3-7 days to form new synaptic connections. Therefore, one might anticipate that these newly formed synapses would exist in a range of developmental states in the untransfected neuron (some fully mature, some newly formed and immature), while synapses in the transfected, FMRP-expressing neuron would all be in a fully maturational state (as they would have had 3-7 days to complete the maturation process). This may be reflected in various qualities of synaptic function, such as paired-pulse ratio, silent synapse number, mEPSC amplitude, and NMDAR-mediated EPSC decay. The fact that changes in these qualities are not observed suggests that FMRP may not act to impair synaptogenesis.

The alternative explanation – that FMRP enhances synapse pruning – is also not entirely consistent with the data. Spines appear to be highly motile, even after establishing a functional synaptic connection. It has been postulated that this movement is a constant interplay between factors attempting to eliminate the synapse and factors attempting to maintain and strengthen the synapse. Thus, tipping this balance only slightly may be sufficient to cause the elimination of an existing synaptic connection. If FMRP mediates synapse elimination, it is possible that specific synapses might be targeted for synapse elimination – for instance, synapses which receive minimal pre-synaptic input or synapses which already have only a small post-synaptic component. In fact, there is evidence that repeated application of LTD induces synapse loss, suggesting that weakened post-synaptic status predisposes a synapse for elimination (Shinoda et al., 2005). If FMRP selectively removes a specific class of synapses, one would anticipate a shift in the qualities of the remaining synapses. For example, if FMRP selectively eliminated synapses with weak pre-synaptic inputs, one would expect the remaining synapses to have stronger pre-synaptic inputs and thus display an altered paired-pulse

ratio. Similarly, if the synapses that FMRP eliminates were those with already reduced AMPAR expression, then once those synapses were eliminated, the remaining synapses would have a relatively larger average mEPSC amplitude. However, there does not appear to be any detectable functional pre- or post-synaptic differences between the synapses on FMRP-expressing neurons as compared to those on *Fmr1*-KO neurons (as measured by mEPSC amplitude, paired-pulse ratio, AMPAR/NMDAR ratio, silent synapse number, or NMDAR-mediated EPSC decay). Thus, if FMRP induces the elimination of existing synapses, it seems do so randomly – there does not appear to be a particular group of synapses that are preferentially targeted for elimination by FMRP.

The observed morphological and functional data fit slightly better with a model in which FMRP expression causes the elimination of existing synapses, but the alternative hypothesis is nearly equally viable. Thus, it is difficult to say with certainty whether synapse loss due to FMRP expression occurs through increased synapse elimination or through impaired synaptogenesis. It is possible, of course, that FMRP performs both actions – inhibiting synaptogenesis while simultaneously increasing synapse elimination. To adequately determine which mechanism may account for synapse loss, it will be necessary to perform long-term live imaging of neurons to identify whether existing spines are retracted or whether the rate of spineogenesis is decreased following FMRP expression.

Phosphorylation and localization of FMRP may suggest mechanisms of synapse loss

Data obtained using phosphorylation mutant forms of FMRP indicate that FMRP-dependent synapse loss relies upon FMRP-induced translation of an RNA target. The fact that S500D, which is believed to inhibit the translation of its RNA ligands, does not affect synapse number indicates that some mRNA or mRNAs need to be translated to decrease synapse number. Does this fact provide insight regarding the mechanism of FMRP-dependent synapse loss? It is well known that many proteins are required for synaptogenesis, so perhaps the proteins produced by FMRP expression impair the function of synaptogenesis-promoting proteins. Alternatively, if FMRP enhances synapse pruning, the newly synthesized proteins may be necessary to initiate the process

of synapse removal. Interestingly, inhibition of protein synthesis was recently demonstrated to induce the retraction and elimination of NMJ synapses *in vivo* (McCann et al., 2007). This was postulated to indicate that translational inhibition decreased the levels of a critical factor necessary for synaptic maintenance. Given the fact that FMRP-mediated translation (as opposed to inhibition of translation) is required for synapse loss makes it less likely that FMRP removes synapses by simply inhibiting their maintenance. Instead, it appears as though synapse loss (whether through increased elimination or impaired synaptogenesis) is an active process initiated by newly synthesized proteins.

Does FMRP's expression pattern tell us anything about the mechanism of FMRP-mediated synapse loss? FMRP is believed to play an important role in the regulation of local, dendritic translation. A key assumption in the field is that dendritically synthesized proteins are limited in their spatial diffusion, restricting the effects of dendritic translation to a localized set of synaptic connections. Presumably, therefore, FMRP-dependent translation likely occurs near the site where the newly synthesized proteins function to regulate synapse number. FMRP is found in punctate, granule-like structures that are dispersed throughout the dendrite (Antar et al., 2004; Pfeiffer and Huber, 2007). Regardless of whether FMRP inhibits synaptogenesis or enhances synapse pruning, fewer synapses should be observed near an FMRP-containing granule than elsewhere on the dendrite. Thus, time-lapse imaging of dendritic spines on live neurons following FMRP transfection may allow one to differentiate between the protein's effects on synapse elimination vs. synaptogenesis. If FMRP mediates synapse elimination, a retraction of spines should be observed near FMRP puncta, but not in areas distant from FMRP expression. Alternatively, if FMRP inhibits synaptogenesis, regions near FMRP puncta should experience either reduced outgrowth of filopodia or reductions in contact with axons of neighboring neurons.

Altered local vs. global synaptic function

The finding of reduced local connectivity in hippocampal area CA3 following pre-synaptic loss of FMRP, with no effect of postsynaptic deletion of FMRP (Hanson and Madison, 2007), is at odds with the data presented in Chapter 2 of this manuscript,

namely that post-synaptic expression of FMRP is observed to negatively regulate the number of synapses at both a structural and functional level. Thus, Hanson and Madison observe that loss of pre-synaptic FMRP results in decreased synapses, while the data in Chapter 2 demonstrate that loss of post-synaptic FMRP results in increased synapses. The synapse loss described in Chapter 2 following FMRP expression occurs throughout the dendrite, encompassing synaptic inputs from both nearby and distant neuronal partners. Hanson and Madison, on the other hand, exclusively examine synapses between neighboring neurons. Thus, FMRP may have distinct effects on local synapses between nearby neurons from those that it has on synapses that connect neurons from distant brain regions. Alternatively, loss of FMRP may result in a global, wide-spread increase in synapses, which is partially countered by homeostatic mechanisms on a local level. Additional experiments are necessary to determine the precise synaptic changes that occur following FMRP loss, but an overwhelming majority of the literature in the field suggests that FMRP negatively regulates synapse number.

FMRP has different developmental effects

A particularly interesting finding is that FMRP fails to induce synapse loss when expressed in very young neurons (equivalent day p6-7, as opposed to equivalent day p12-16). In young *Fmr1*-KO neurons, FMRP expression actually resulted in an increase of synaptic function, which was at least partially mediated by increased pre-synaptic release probability. Thus, FMRP appears to play a bi-directional role on synapse number depending on the developmental state of the neuron.

In older, p12-16 cultures, my data suggests that FMRP mediates the translation of one or more critical mRNAs which result in decreased synapse number. It is unknown whether FMRP-dependent increases in synaptic function in younger cultures rely upon the same mechanism. It is possible, in fact, that FMRP may stimulate the translation of select mRNA targets in older neurons, but inhibit the translation of those same mRNAs in younger neurons. This altered function may arise from differential expression or activation of kinases, phosphatases, or methylases and various stages of development.

The preliminary work I describe in Chapter 4 implicates the miRNA pathway as critically important for FMRP-mediated synapse loss in older neurons. An alluring model that incorporates this finding with the developmental shift in FMRP function states that select, as-of-yet unidentified miRNAs may associate with FMRP, allowing it to alter its function from a translational suppressor to a translational activator (or vice versa). In older neurons, expression of this miRNA initiates FMRP-dependent synapse loss. In younger neurons, however, the miRNA is not expressed, thus resulting in altered FMRP function. A promising target to examine in this respect may be the miRNA miR-134. miR-134 is first synthesized beginning around p7 and its levels increase until p19, a period of intense synapse elimination (Schratt et al., 2006). Importantly, miR-134 negatively regulates the development of dendritic spines through inhibition of a mRNA target, *Limk1* (Schratt et al., 2006). Additionally, miRNA expression may not alter FMRP function, *per se*, but instead may re-target FMRP to a different pool of mRNA, thus leading to altered synaptic effects following FMRP expression. Further work investigating the link between FMRP and miRNA pathway will be necessary to test this model.

Alternatively, the entire pool of mRNA targets may be different in young vs. older neurons, owing to different transcription factor activity. In Chapter 3, I describe a phenotypic interaction between the transcription factor MEF2 and FMRP. MEF2 induces synapse loss in WT neurons, but fails to do so in *Fmr1*-KO neurons. Furthermore, when MEF2 function is impaired with a dominant-negative construct, FMRP fails to elicit synapse loss in *Fmr1*-KO neurons. These data strongly implicate FMRP-dependent translation of MEF2-driven transcripts in synapse elimination in older cultures. It is unknown if MEF2 also drives synapse loss in younger cultures, but it is intriguing that MEF2 expression appears to be developmentally regulated. Indeed, MEF2A and -D expression is steadily increased from p7 to p14, coinciding with a period of intense synapse pruning (Flavell et al., 2006). Additionally, this data suggests that MEF2 may not be present in young neurons, thus altering the pool of mRNA targets for FMRP. It is possible that an unidentified transcription factor is highly active in young neurons, and that these mRNAs are translationally regulated by FMRP to increase synaptic function.

As the neuron matures, this transcription factor is downregulated and MEF2 is upregulated, leading to the production of FMRP-regulated mRNAs which now act to facilitate synapse elimination. This model is supported by the fact that complete inhibition of MEF2 with the dominant-negative form does not merely block FMRP-dependent synapse loss. Instead, it results in an FMRP-dependent increase in synaptic function, remarkably similar to what is observed following FMRP expression in young neurons. Thus, it would be expected that co-expression of FMRP and MEF2 in young neurons should lead to synapse elimination, whereas expression of MEF2 dominant negative forms in young neurons should have little or no effect.

Possible mechanisms of FMRP-dependent synapse loss

Signaling pathways regulating protein synthesis

What is known about the molecular mechanisms through which FMRP may alter synapse number or structure? Based upon its canonical function in translational regulation, FMRP likely governs synapse number through control of local protein synthesis. Furthermore, a phospho-mutant form of FMRP that is believed to inhibit translation of its mRNA targets fails to alter synapse number, indicating that FMRP-mediated translational stimulation is necessary to induce loss of synapses (Pfeiffer and Huber, 2007). Thus, factors that regulate FMRP-dependent translation or protein synthesis in general may affect synapse number. Indeed, many studies have investigated the role of translational regulation in both synapse structure and function and have revealed a link between protein synthesis and synapse number and structure.

Activation of the PI3K? Akt? mTOR pathway, a key mediator of group I mGluR signaling, induces protein synthesis and causes an increase in filopodia-like spines and a decrease in mushroom-shaped spines, a phenotype reminiscent of that seen in *Fmr1*-KO mice (Kumar et al., 2005). Likewise, inhibition of this pathway, presumably leading to reduced local protein synthesis, resulted in decreased total spine number (Kumar et al., 2005). Consistent with these findings, stimulation of group I metabotropic glutamate receptors (mGluRs), which induce local protein synthesis through the PI3K? Akt? mTOR pathway, caused a translation-dependent increase in spine length

(Vanderklish et al., 2002). Furthermore, repeated mGluR-LTD results in the elimination of synaptic connections, providing a further link between mGluR-mediated translation and synapse loss (Shinoda et al., 2005). Thus, it is possible that in the absence of FMRP, dendritic translation of critical mRNAs is altered, leading to an increase in spine length and number.

Interestingly, other factors that regulate protein synthesis have also been reported to affect spine number and/or morphology, indicating a common phenotype following changes in translation. The tumor suppressors TSC1 and TSC2 are thought to inhibit protein synthesis by decreasing mTOR activity; removal of these proteins increases spine length, but decreases overall spine number (Tavazoie et al., 2005). Several RNA-binding proteins are also known to regulate synaptic structure. Translocated-in-liposarcoma protein (TLS) is an RNA-binding protein that, like FMRP, is localized to dendrites and is trafficked at synapses in an mGluR-dependent manner (Fujii et al., 2005). *TLS*-KO mice display a reduction in mature spines and an increase in filopodia, similar to *Fmr1*-KO mice (Fujii et al., 2005). In addition, loss of the brain-specific RNA-binding protein Staufen2 results in an overall decrease in spine and synapse number (Goetze et al., 2006).

These data provide a compelling argument that alterations in many aspects of dendritic protein synthesis can affect the number and morphological structure of synapses in a complex manner. Thus, FMRP-dependent translation may not exclusively determine synapse number. Instead, it seems likely that the number of synaptic connections is regulated in a complicated manner by multiple independent processes. Indeed, if FMRP was solely responsible for synapse formation or elimination, one would expect FXS patients and *Fmr1*-KO mice to have so many excitatory synaptic connections that normal brain function would be virtually impossible. Thus, it is important to view FMRP as a key regulatory factor in controlling synapse number rather than a necessary component of the synapse machinery.

Cytoskeletal proteins as key factors in synapse number and structure

Given the above data that changes in translational regulatory pathways can cause synaptic abnormalities similar to what is observed in FXS and *Fmr1*-KO mice, it seems likely that the changes in synapse structure and function following loss of FMRP result from alterations in local protein synthesis. An obvious question, therefore, it what specific changes in the protein complement of the synapse might lead to the increased synapse number and the long, immature spine morphology observed in FXS and *Fmr1*-KO mice? Insight into this problem comes from multiple studies investigating the actin cytoskeleton.

Remodeling of the actin cytoskeleton is clearly important for changes in spine morphology (Sekino et al., 2007; Nakayama et al., 2000). A predominant molecular pathway coupling signaling events to actin dynamics is that of the Rho-family GTPases (Van Aelst et al., 1997). The Rho-GTPase family is comprised of many related members of the Ras superfamily of G-proteins, the most well-characterized of which are RhoA, Rac1, and Cdc42 (Linseman et al., 2008). Importantly, alterations in these genes are involved in nonspecific X-linked mental retardation (MRX) and changes in spine morphology (Chelly and Mandel, 2001; Frints et al., 2002, Ramakers et al., 2002). Like nearly all monomeric GTPases, the Rho-GTPases are inhibited or activated, respectively, by specific GTPase-activating proteins (GAPs) or guanine nucleotide exchange factors (GEFs). Despite being in the same family, RhoA and Rac1 appear to have opposing effects on dendritic spines, with Rac1 activity supporting spinogenesis and RhoA activity decreasing spine density (Luo et al., 1996; Tashiro et al., 2000; Tashiro et al., 2004). Both RhoA and Rac1 have additionally been shown to regulate spine length in a complex manner (Govek et al., 2004; Tashiro et al., 2000; Tashiro et al., 2004). Interestingly, in *Drosophila*, dRac mRNA is associated with dFmr1, and some synaptic phenotypes associated with dFmr1 loss were attributable to changes in dRac function (Lee et al., 2003). It is likely, therefore, that in the absence of FMRP, Rac protein levels are altered, leading to increased actin polymerization and an increase in spine formation and/or length. Indeed, Rac-induced remodeling of the actin cytoskeleton is enhanced in murine fibroblasts from *Fmr1*-KO mice (Castets et al., 2005).

Interestingly, despite the fact that Rho-GTPases are found throughout the entire dendritic tree and have a clear role in controlling dendritic spine morphology and number, the mRNA for both Rac1 and RhoA appears to be largely restricted to the soma in the mammalian hippocampus (Nakayama et al., 2000), suggesting that local regulation of Rho-GTPases likely occurs through control of upstream messengers (including Rho-GEFs or Rho-GAPs) or downstream effectors. Indeed, oligophrenin, a RhoA-GAP, is implicated in spine development, with siRNA-mediated knock-down of oligophrenin leading to decreased spine length which was rescued by concomitant inhibition of Rho-GTPase function (Govek et al., 2004). Another protein connected to the Rho-GTPase pathway that alters spine morphology is semaphorin3A, which is a member of a large family of neurite guidance cues and an upstream activator of Rac1. Semaphorin3A activation causes an increase in neurite formation and synapse formation, and Semaphorin3A-KO mice display a reduction in spine density, consistent with a reduction in Rac function (Morita et al., 2006). Several recent studies have shown association of FMRP with the mRNA for Semaphorin3F (Menon et al., 2007; Darnell et al., 2001), a close relative of Semaphorin3A that similarly regulates Rac1 signaling and axonal growth cone dynamics (for review, see Tran et al., 2007). Finally, a downstream effector of Rac signaling, p21-activated kinase (PAK), is also positively coupled with spine number, such that expression of a dominant-negative form of PAK (dnPAK) results in decreased spine density (Hayashi et al., 2004). Notably, it was recently reported that introduction of dnPAK into *Fmr1*-KO mice led to a complete negation of the *Fmr1*-KO spine phenotype (Hayashi et al., 2007), although it remains to be demonstrated that this is a direct rescue rather than two opposing forces acting independently on spine number. Thus the spine phenotype observed in *Fmr1*-KO mice bears a striking resemblance to that seen following increased Rac activity. Furthermore, FMRP has been shown to interact with the mRNAs encoding several proteins in the Rho-GTPase pathway, suggesting that this pathway may be particularly important for FMRP regulation of the spine number and morphology through control of the actin cytoskeleton. It is intriguing, therefore, to expect a link between FMRP-mediated synapse loss and Rho-GTPase activity. Indeed, the mRNAs encoding many regulators of G-protein signaling have been shown to be

associated with FMRP (Miyashiro et al., 2003; Chen et al., 2003; Darnell et al., 2001). Specific inhibitors of Rho-GTPase activity may therefore impair or facilitate FMRP-dependent synapse elimination.

AMPAR trafficking in regulation of synapse strength and number

There is also considerable evidence that FMRP may control spine morphology and synaptic function through regulation of AMPAR trafficking. In particular, recent work on activity-regulated cytoskeletal protein (Arc) suggests a promising mode of action for FMRP-mediated control of synaptic function. *Arc* mRNA is a target of FMRP and Arc protein levels are elevated in *Fmr1*-KO neurons and synaptoneurosomes (Zalfa et al., 2003). Arc is also rapidly translated at dendrites in response to mGluR activation and synaptic activity (Shepherd et al., 2006; Waung et al., 2008). Recent data strongly implicates Arc in AMPAR internalization. Acute knock-down of Arc increases AMPAR-mediated synaptic transmission (Shepherd et al., 2006; Waung et al., 2008), while overexpression of Arc causes rapid internalization of AMPARs and decreased synaptic strength (Waung et al., 2008). In addition, knock-down or genetic deletion of Arc blocks mGluR-mediated internalization of AMPARs, suggesting that Arc is a critical mediator of mGluR-LTD (Park et al., 2008; Waung et al., 2008). Indeed, Arc has been shown to interact with synaptic endocytic machinery to regulate surface AMPAR expression (Chowdhury et al., 2006). Furthermore, blocking Arc expression or genetically deleting Arc severely impairs mGluR-LTD (Park et al., 2008; Waung et al., 2008). These data strongly link FMRP-dependent Arc expression to AMPAR internalization and mGluR-LTD. It is likely that internalization of AMPARs is a critical first step in the dismantling of synapses. Furthermore, Arc is required for mGluR-LTD, which is capable of inducing synapse loss (Shinoda et al., 2005). It is possible, therefore, that Arc function may play a role in FMRP-mediated synapse loss.

Arc mRNA levels are increased following MEF2 stimulation. Therefore, Arc seems to form a convenient connection between FMRP and MEF2. In this model, MEF2 activation may lead (either directly or indirectly) to the transcription of *Arc*, which is bound by FMRP and translationally regulated. When the appropriate cellular signal is

received, FMRP mediates the synthesis of Arc, which in turn initiates synapse loss, likely in conjunction with additional newly synthesized proteins. This is an exciting model which can be readily tested by inhibiting Arc translation or synthesis. According to this model, Arc synthesis is required for both MEF2-dependent and FMRP-dependent synapse loss. Thus, in Arc-KO neurons or in neurons expression *Arc*-targeting siRNAs, neither of these mechanisms should function to regulate synapse number.

An additional protein that may be important in FMRP-mediated synapse loss is PSD-95. Like *Arc*, *PSD-95* mRNA is a target of FMRP and PSD-95 protein is known to be misregulated in the *Fmr1*-KO mouse (Todd et al., 2003; Zalfa et al., 2007; Muddashetty et al., 2007). PSD-95 is also normally synthesized following mGluR activation; however, PSD-95 synthesis fails to occur in *Fmr1*-KO neurons (Todd et al., 2003; Muddashetty et al., 2007). PSD-95 is a post-synaptic scaffolding protein believed to positively regulate synaptic strength by mediating AMPAR insertion into the post-synapse (Erlich et al., 2004). It is interesting that both PSD-95 and Arc are both regulated by FMRP considering that the proteins appear to have opposite effects on synaptic strength. Both proteins show elevated expression levels in *Fmr1*-KO neurons (Muddashetty et al., 2007; Zalfa et al., 2003), indicating that they are similarly regulated. FMRP-mediated translation of PSD-95 would be predicted to increase synaptic strength and possibly synapse number (Erlich et al., 2004). However, I would predict that PSD-95 protein levels would decrease following FMRP-mediated synapse loss. In fact, it is possible that even though loss of FMRP leads to increases in both Arc and PSD-95, that endogenous FMRP is capable of bi-directionally and differentially regulating the synthesis of these two proteins. Indeed, if FMRP expression increases Arc synthesis while simultaneously inhibiting PSD-95 synthesis, these changes alone may be sufficient to induce a reduction in synapse number. Furthermore, this may an example of a miRNA acting to shift FMRP association away from one mRNA target to another. In young neurons, perhaps, FMRP positively regulates PSD-95 translation, resulting in increased synaptic function. In older neurons, however, expression of select miRNAs may prevent FMRP from associating with PSD-95 or may confer an exclusively inhibitory role upon PSD-95 translation, allowing the translation of other mRNAs which lead to synapse loss.

Future experiments investigating a link between PSD-95 and FMRP-mediated synapse loss may prove interesting.

Finally, FMRP also appears to directly regulate the mRNA for the subunits of the AMPAR, GluR1 and GluR2 (Muddashetty et al., 2007; Li et al., 2001). Translational regulation of these mRNAs would be predicted to have a more direct impact on the ability of FMRP to regulate synaptic strength. However, I do not observe direct changes in post-synaptic strength (as measured by mEPSC amplitude) following FMRP expression, so I do not believe that the association between FMRP and *Glur1* and *Glur2* mRNA to be relevant to FMRP-dependent synapse loss. However, this interaction is likely important for other FMRP-mediated functions, such as synaptic plasticity.

Convergence of Synaptic Changes in FXS

Examination of the mGluR theory

A prevailing hypothesis regarding the underlying causes of FXS, termed the "mGluR theory of FXS" (Bear et al., 2004), argues that most of the phenotypes of FXS can be explained by increased and unregulated activity of group I mGluRs. This hypothesis is principally based upon the finding of enhanced mGluR-LTD in *Fmr1*-KO mice, coupled with multiple links between FXS symptoms and mGluR-mediated neural functions. The mGluR Theory also predicts that inhibition of mGluR activity should reduce or abolish phenotypes associated with the loss of FMRP. Several key studies have largely confirmed this prediction (as described in Chapter 1), strongly supporting the model.

However, the mGluR theory of FXS fails to adequately address all phenotypes of the *Fmr1*-KO mouse. In particular mGluR-dependent LTP is abolished in the cortex and amygdala of *Fmr1*-KO mice. The mGluR theory explains this fact by stating that mGluR-dependent LTP is saturated in these regions. However, mGluR-dependent LTD in the hippocampus is not saturated or abolished in *Fmr1*-KO mice – in fact, mGluR-LTD is enhanced in the absence of FMRP. In addition, mGluR stimulation leads to an elongation of dendritic spines and an elimination of synaptic connections. However, although dendritic spines are longer and thinner in *Fmr1*-KO mice, they are more, not

less, abundant. Thus, a more precise model of FMRP function is required to explain the many phenotypes of FXS.

Clearly, FMRP appears to act as a downstream mediator of mGluR-stimulated translation. Several lines of evidence support this view. Many proteins that are synthesized in response to mGluR activation have elevated basal expression levels in *Fmr1*-KO mice. In fact, basal expression of these proteins is so high that mGluR stimulation fails to further activate their synthesis (Ronesi et al., 2008; Lu et al., 2004; Hou et al., 2006; Zalfa et al., 2007). Thus, FMRP appears to act primarily as a key inhibitor of mGluR-mediated protein synthesis. However, this is likely too simplistic of a view.

Activation of dendritic protein synthesis is a complex procedure, requiring the activation of many initiation factors and elongation factors, as well as association of the appropriate mRNA and polyribosome. These mechanisms are activated by mGluR signaling, but are also modified by signaling cascades originating from other neurotransmitter receptors or second-messenger systems. These additional signal transduction pathways are likely differentially regulated in various regions of the brain. Therefore, mGluR stimulation should not be expected to have exactly the same effect on protein synthesis in the cortex, for example, as it does in the hippocampus.

Furthermore, phosphorylation, methylation, and association with co-factors or miRNAs may differentially regulate the effects of FMRP-mediated translation on select populations of mRNA. In the absence of FMRP, all FMRP-dependent regulation of synthesis is lost, such that all FMRP mRNA targets are upregulated, leading to the misinformed view that all FMRP targets are regulated identically. This does not necessarily mean, however, that mGluR activation leads to the synthesis of every one of these proteins in every brain region. It is possible, for example, that mGluR activation in the hippocampus might induce FMRP-dependent translation of *Arc* mRNA; however, in the cortex, expression of a particular miRNA or overactivation of PP2A might cause FMRP to act as an exclusive inhibitor of *Arc* translation, even after mGluR stimulation. This is an important point to keep in mind when considering the effects of FMRP on neuronal function in multiple brain regions.

Likewise, the expression of transcription factors plays an important role in regulating dendritic protein synthesis. Indeed, it is thought that the differences in shape, connectivity, and overall function of different brain regions arise due to differential activation of transcription factors during both developing and adult neurons. Likewise, the precise pattern of transcription factor expression, activation, and inhibition is a key mechanism in controlling which mRNAs are available for translation. This is most clearly demonstrated by MEF2, which induces synapse loss and is preferentially upregulated during a period of intense synapse elimination.

Therefore, it may not be the case that FMRP expression results in synapse elimination in all brain regions. In fact, in just CA1 pyramidal neurons of the hippocampus, FMRP expression results in opposite effects in young vs. older neurons. Thus, it may be that FMRP expression will not have the same exact effect on synapse number in cortical *Fmr1*-KO neurons as it does in hippocampal neurons. It is therefore important to keep in mind that drawing wide-reaching conclusions about the role that FMRP may play in regulating synapse number across the brain is risky.

However, the fact that multiple studies have demonstrated rescue of *Fmr1*-KO phenotypes by decreasing mGluR activity suggests that the underlying conclusions of the mGluR theory may be fundamentally correct – namely, that mGluR activity is enhanced and unregulated in the absence of FMRP.

Relation of synaptic changes to FXS

The data presented in this manuscript demonstrate clear regulation of synapse number by FMRP. In addition, many other studies have revealed profound changes in synaptic structure, function, and plasticity in the absence of FMRP. The most consistent findings in the literature regarding synaptic alterations in animal models of FXS are a shift toward an increase in synapse number, an immature morphology of dendritic spines, an enhancement and misregulation of Gq-protein-dependent LTD, and an impairment in cortical, possibly mGluR-mediated LTP. An unresolved question in the field is whether these phenotypes are independent of one another; if they are related, which is the primary

phenotype? These questions are of critical importance for pharmaceutical and therapeutic designs aimed at targeting the root causes of FXS.

According to the mGluR theory of FXS, elevated basal levels of "LTD proteins" in the *Fmr1*-KO mouse should lead to increased LTD in response to low-level activation of Gq-coupled receptors, effectively lowering the threshold for this form of plasticity. Prolonged LTD, which is predominantly manifest as a long-term reduction in the number of AMPA receptors (AMPARs) expressed at the postsynaptic surface (Waung et al., 2008), can be a prelude to synapse elimination (Shinoda et al., 2005). In addition, the size of the postsynaptic area can be altered by synaptic plasticity and trafficking of AMPARs, with LTP and LTD resulting in larger and smaller post-synapses, respectively. Thus, an animal model with enhanced LTD and impaired LTP would be expected to have thinner postsynaptic regions, similar to the long, thin dendritic spines observed in FXS patients and *Fmr1* KO mice.

It is possible that the alterations in synaptic function and spine number observed in *Fmr1*-KO mice are a result of impaired early synaptic development and that a number of FXS phenotypes result from impairments in synaptogenesis or enhancements in synapse pruning. Proper neuronal function requires precise connection patterns throughout the brain. Development of neural circuitry is typically marked by the overgrowth of synaptic connections in immature neurons, followed by a period of synaptic pruning, when inappropriate synapses are eliminated and appropriate synapses are strengthened. The overgrowth of dendritic spines in FXS patients, coupled with evidence that acute FMRP expression in *Fmr1*-KO mice results in synapse loss, strongly suggests that FMRP plays a critical role in this early stage of synaptic modeling.

The phenotype of enhanced susceptibility to seizures and increased rates of autism in FXS suggest alterations in the relative balance of excitatory to inhibitory synapses. The data presented in this manuscript clearly point to a role for both FMRP and MEF2 in refining precise excitatory connection patterns in the brain. Impairments in refinement of connectivity could ostensibly lead to many of the phenotypes of FXS. Such alterations in the early development of neuronal connection patterns may further result in altered patterns of synaptic activity, leading to inappropriate synaptic plasticity

or homeostatic alterations that manifest themselves as the changes in LTP and LTD observed in the *Fmr1*-KO mouse.

Conclusions

The data presented in this work demonstrate a clear phenotypic link between FMRP and MEF2, both of which negatively and cooperatively regulate synapse number. These findings provide novel insight into the mechanism of FMRP function and also provide a working molecular model that explains the phenotype of increased dendritic spine number in FXS patients and *Fmr1*-KO mice. Alterations in synapse number may ostensibly result in many of the phenotypes of FXS and, thus, early reversal of these alterations may provide a novel therapeutic avenue for treatment of this disease.

APPENDIX

List of Pharmacological Reagents

Compound	Site of Action	Effect	Concentration Used
2-Chloroadenosine	Adenosine receptor	Agonist	2 µM
4-Hydroxytamoxifen (4OHT)	Plasmids expressing ER^{TM} domain	Induces nuclear localization	1 µM or 10 µM
AP5	NMDA receptor	Antagonist	100 µM
DNQX	AMPA receptor	Antagonist	20 µM
Glycine	NMDA receptor	Partial agonist	20 µM
KN-92	CaMKII	Inactive analog of KN-93	20 µM
KN-93	CaMKII	Inhibitor	20 µM
LY341495	Group I mGluRs	Antagonist	20 µM
Okadaic Acid	PP2A	Inhibitor	0.5 nM
Picrotoxin	GABA-A receptor	Antagonist	100 µM
RNAi-I	miRNA production machinery (precise mechanism is unknown)	Inhibitor	100 µM
Tetrodotoxin (TTX)	Na^+ channels	Antangonist	1 µM

List of Constructs

Construct Name	Expression/Notes
?RGG-FMRP-GFP-hpr	FMRP with RGG-box deleted and with GFP fused to N-terminal, driven by human *FMR1* promoter
CRE-GFP	CRE-GFP fusion, driven by CMV promoter
I304N-FMRP-GFP-hpr	FMRP with isoleucine-to-asparagine point mutation at residue 304 and with GFP fused to N-terminal, driven by human *FMR1* promoter
MEF2-Engrailed	MEF2 DNA binding region (MADS and MEF2 domains) fused to Engrailed transcriptional repressor, driven by CMV promoter
MEF2-VP16-ER^{TM}	MEF2 DNA binding region (MADS and MEF2 domains) fused to VP16 transcriptional activator, driven by CMV promoter. ER^{TM} is a mutated estrogen receptor transmembrane domain that restricts expression to the cytoplasmuntil bound by 4OHT and is fused to the N-terminal.
MEF2-VP16	MEF2 DNA binding region (MADS and MEF2 domains) fused to VP16 transcriptional activator, driven by CMV promoter.
MEF2?16-37-VP16-ER^{TM}	MEF2 DNA binding region (MADS and MEF2 domains) with critical DNA binding region of MADS domain (residues 16-37) deleted, fused to VP16 transcriptional activator, driven by CMV promoter. ER^{TM} is a mutated estrogen receptor transmembrane domain that restricts expression to the cytoplasm until bound by 4OHT and is fused to the N-terminal.
MRE-EGFP	EGFP, driven by MEF2 response element
pC3-EGFP	EGFP, driven by CMV promoter
p-mCherry	mCherry, driven by CMV promoter
pSuper-siRNA-aFMRP-#1	Hairpin miRNA that is cleaved to form siRNA a-FMRP #1 (see below), driven by U6 promoter (also called pSuper #8 in my original notes)
pSuper-siRNA-aFMRP-#2	Hairpin miRNA that is cleaved to form siRNA a-FMRP #2 (see below), driven by U6 promoter (also called pSuper #9 in my original notes)
S500A-FMRP-GFP-hpr	FMRP with serine-to-alanine point mutation at residue 500 and with GFP fused to N-terminal, driven by human *FMR1* promoter
S500D-FMRP-GFP-hpr	FMRP with serine-to-aspartic acid point mutation at residue 500 and with GFP fused to N-terminal, driven by human *FMR1* promoter
siRNA a-FMRP #1	Short stretch of RNA with the following sequence: UCGUAAAUCUUCUGGCACCtc (also called siRNA #8 in my original notes)
siRNA a-FMRP #2	Short stretch of RNA with the following sequence: AACUUCGGAAUUAUGUAGCtt (also called siRNA #9 in my original notes)
wtFMRP-GFP-hpr	Wild-type FMRP with GFP fused to N-terminal, driven by human *FMR1* promoter

BIBLIOGRAPHY

Adinolfi, S., Ramos, A., Martin, S. R., Dal Piaz, F., Pucci, P., Bardoni, B., Mandel, J. L., and Pastore, A. (2003). The N-terminus of the fragile X mental retardation protein contains a novel domain involved in dimerization and RNA binding. Biochemistry *42*, 10437-10444.

Aiba, A., Kano, M., Chen, C., Stanton, M. E., Fox, G. D., Herrup, K., Zwingman, T. A., and Tonegawa, S. (1994). Deficient cerebellar long-term depression and impaired motor learning in mGluR1 mutant mice. Cell *79*, 377-388.

Andres, V., Cervera, M., and Mahdavi, V. (1995). Determination of the consensus binding site for MEF2 expressed in muscle and brain reveals tissue-specific sequence constraints. J Biol Chem *270*, 23246-23249.

Antar, L. N., Afroz, R., Dictenberg, J. B., Carroll, R. C., and Bassell, G. J. (2004). Metabotropic glutamate receptor activation regulates fragile x mental retardation protein and FMR1 mRNA localization differentially in dendrites and at synapses. J Neurosci *24*, 2648-2655.

Antar, L. N., Dictenberg, J. B., Plociniak, M., Afroz, R., and Bassell, G. J. (2005). Localization of FMRP-associated mRNA granules and requirement of microtubules for activity-dependent trafficking in hippocampal neurons. Genes Brain Behav *4*, 350-359.

Antar, L. N., Li, C., Zhang, H., Carroll, R. C., and Bassell, G. J. (2006). Local functions for FMRP in axon growth cone motility and activity-dependent regulation of filopodia and spine synapses. Mol Cell Neurosci.

Arnold, M. A., Kim, Y., Czubryt, M. P., Phan, D., McAnally, J., Qi, X., Shelton, J. M., Richardson, J. A., Bassel-Duby, R., and Olson, E. N. (2007). MEF2C transcription factor controls chondrocyte hypertrophy and bone development. Dev Cell *12*, 377-389.

Ashley, C. T., Jr., Wilkinson, K. D., Reines, D., and Warren, S. T. (1993). FMR1 protein: conserved RNP family domains and selective RNA binding. Science *262*, 563-566.

Bagni, C., and Greenough, W. T. (2005). From mRNP trafficking to spine dysmorphogenesis: the roots of fragile X syndrome. Nat Rev Neurosci *6*, 376-387.

Bakker, C. E., de Diego Otero, Y., Bontekoe, C., Raghoe, P., Luteijn, T., Hoogeveen, A. T., Oostra, B. A., and Willemsen, R. (2000). Immunocytochemical and biochemical characterization of FMRP, FXR1P, and FXR2P in the mouse. Exp Cell Res *258*, 162-170.

Bakker, D. B. (1994). Fmr1 knockout mice: a model to study fragile X mental retardation. The Dutch-Belgian Fragile X Consortium. Cell *78*, 23-33.

Balschun, D., and Wetzel, W. (2002). Inhibition of mGluR5 blocks hippocampal LTP in vivo and spatial learning in rats. Pharmacol Biochem Behav *73*, 375-380.

Barbosa, A. C., Kim, M. S., Ertunc, M., Adachi, M., Nelson, E. D., McAnally, J., Richardson, J. A., Kavalali, E. T., Monteggia, L. M., Bassel-Duby, R., and Olson, E. N. (2008). MEF2C, a transcription factor that facilitates learning and memory by negative regulation of synapse numbers and function. Proc Natl Acad Sci U S A *105*, 9391-9396.

Bardoni, B., Sittler, A., Shen, Y., and Mandel, J. L. (1997). Analysis of domains affecting intracellular localization of the FMRP protein. Neurobiol Dis *4*, 329-336.

Bartel, D. P. (2004). MicroRNAs: genomics, biogenesis, mechanism, and function. Cell *116*, 281-297.

Bear, M. F., Huber, K. M., and Warren, S. T. (2004). The mGluR theory of fragile X mental retardation. Trends Neurosci *27*, 370-377.

Biederer, T., Sara, Y., Mozhayeva, M., Atasoy, D., Liu, X., Kavalali, E. T., and Sudhof, T. C. (2002). SynCAM, a synaptic adhesion molecule that drives synapse assembly. Science *297*, 1525-1531.

Black, B. L., and Olson, E. N. (1998). Transcriptional control of muscle development by myocyte enhancer factor-2 (MEF2) proteins. Annu Rev Cell Dev Biol *14*, 167-196.

Blaeser, F., Ho, N., Prywes, R., and Chatila, T. A. (2000). Ca(2+)-dependent gene expression mediated by MEF2 transcription factors. J Biol Chem *275*, 197-209.

Bramham, C. R., and Wells, D. G. (2007). Dendritic mRNA: transport, translation and function. Nat Rev Neurosci *8*, 776-789.

Brennan, F. X., Albeck, D. S., and Paylor, R. (2006). Fmr1 knockout mice are impaired in a leverpress escape/avoidance task. Genes Brain Behav *5*, 467-471.

Brewer, G. J., Torricelli, J. R., Evege, E. K., and Price, P. J. (1993). Optimized survival of hippocampal neurons in B27-supplemented Neurobasal, a new serum-free medium combination. J Neurosci Res *35*, 567-576.

Brown, V., Jin, P., Ceman, S., Darnell, J. C., O'Donnell, W. T., Tenenbaum, S. A., Jin, X., Feng, Y., Wilkinson, K. D., Keene, J. D., *et al.* (2001). Microarray identification of FMRP-associated brain mRNAs and altered mRNA translational profiles in fragile X syndrome. Cell *107*, 477-487.

Brown, V., Small, K., Lakkis, L., Feng, Y., Gunter, C., Wilkinson, K. D., and Warren, S. T. (1998). Purified recombinant Fmrp exhibits selective RNA binding as an intrinsic property of the fragile X mental retardation protein. J Biol Chem *273*, 15521-15527.

Castren, M., Paakkonen, A., Tarkka, I. M., Ryynanen, M., and Partanen, J. (2003). Augmentation of auditory N1 in children with fragile X syndrome. Brain Topogr *15*, 165-171.

Caudy, A. A., Myers, M., Hannon, G. J., and Hammond, S. M. (2002). Fragile X-related protein and VIG associate with the RNA interference machinery. Genes Dev *16*, 2491-2496.

Ceman, S., O'Donnell, W. T., Reed, M., Patton, S., Pohl, J., and Warren, S. T. (2003). Phosphorylation influences the translation state of FMRP-associated polyribosomes. Hum Mol Genet *12*, 3295-3305.

Centonze, D., Rossi, S., Mercaldo, V., Napoli, I., Ciotti, M. T., De Chiara, V., Musella, A., Prosperetti, C., Calabresi, P., Bernardi, G., and Bagni, C. (2008). Abnormal striatal GABA transmission in the mouse model for the fragile X syndrome. Biol Psychiatry *63*, 963-973.

Chahrour, M., Jung, S. Y., Shaw, C., Zhou, X., Wong, S. T., Qin, J., and Zoghbi, H. Y. (2008). MeCP2, a key contributor to neurological disease, activates and represses transcription. Science *320*, 1224-1229.

Chapman, A. G., Nanan, K., Williams, M., and Meldrum, B. S. (2000). Anticonvulsant activity of two metabotropic glutamate group I antagonists selective for the mGlu5 receptor: 2-methyl-6-(phenylethynyl)-pyridine (MPEP), and (E)-6-methyl-2-styryl-pyridine (SIB 1893). Neuropharmacology *39*, 1567-1574.

Chen, C., Kano, M., Abeliovich, A., Chen, L., Bao, S., Kim, J. J., Hashimoto, K., Thompson, R. F., and Tonegawa, S. (1995). Impaired motor coordination correlates with persistent multiple climbing fiber innervation in PKC gamma mutant mice. Cell *83*, 1233-1242.

Chen, L., and Toth, M. (2001). Fragile X mice develop sensory hyperreactivity to auditory stimuli. Neuroscience *103*, 1043-1050.

Chiamulera, C., Epping-Jordan, M. P., Zocchi, A., Marcon, C., Cottiny, C., Tacconi, S., Corsi, M., Orzi, F., and Conquet, F. (2001). Reinforcing and locomotor stimulant effects of cocaine are absent in mGluR5 null mutant mice. Nat Neurosci *4*, 873-874.

Chuang, S. C., Zhao, W., Bauchwitz, R., Yan, Q., Bianchi, R., and Wong, R. K. (2005). Prolonged epileptiform discharges induced by altered group I metabotropic glutamate receptor-mediated synaptic responses in hippocampal slices of a fragile X mouse model. J Neurosci *25*, 8048-8055.

Cline, H. T. (2001). Dendritic arbor development and synaptogenesis. Curr Opin Neurobiol *11*, 118-126.

Comery, T. A., Harris, J. B., Willems, P. J., Oostra, B. A., Irwin, S. A., Weiler, I. J., and Greenough, W. T. (1997). Abnormal dendritic spines in fragile X knockout mice: maturation and pruning deficits. Proc Natl Acad Sci U S A *94*, 5401-5404.

Conquet, F., Bashir, Z. I., Davies, C. H., Daniel, H., Ferraguti, F., Bordi, F., Franz-Bacon, K., Reggiani, A., Matarese, V., Conde, F., and et al. (1994). Motor deficit and impairment of synaptic plasticity in mice lacking mGluR1. Nature *372*, 237-243.

Corbin, F., Bouillon, M., Fortin, A., Morin, S., Rousseau, F., and Khandjian, E. W. (1997). The fragile X mental retardation protein is associated with poly(A)+ mRNA in actively translating polyribosomes. Hum Mol Genet *6*, 1465-1472.

Cull-Candy, S., Brickley, S., and Farrant, M. (2001). NMDA receptor subunits: diversity, development and disease. Curr Opin Neurobiol *11*, 327-335.

Darnell, J. C., Fraser, C. E., Mostovetsky, O., Stefani, G., Jones, T. A., Eddy, S. R., and Darnell, R. B. (2005). Kissing complex RNAs mediate interaction between the Fragile-X mental retardation protein KH2 domain and brain polyribosomes. Genes Dev.

Darnell, J. C., Jensen, K. B., Jin, P., Brown, V., Warren, S. T., and Darnell, R. B. (2001). Fragile X mental retardation protein targets G quartet mRNAs important for neuronal function. Cell *107*, 489-499.

De Boulle, K., Verkerk, A. J., Reyniers, E., Vits, L., Hendrickx, J., Van Roy, B., Van den Bos, F., de Graaff, E., Oostra, B. A., and Willems, P. J. (1993). A point mutation in the FMR-1 gene associated with fragile X mental retardation. Nat Genet *3*, 31-35.

De Diego Otero, Y., Severijnen, L. A., van Cappellen, G., Schrier, M., Oostra, B., and Willemsen, R. (2002). Transport of fragile X mental retardation protein via granules in neurites of PC12 cells. Mol Cell Biol *22*, 8332-8341.

Denman, R. B. (2002). Methylation of the arginine-glycine-rich region in the fragile X mental retardation protein FMRP differentially affects RNA binding. Cell Mol Biol Lett *7*, 877-883.

Denman, R. B., Dolzhanskaya, N., and Sung, Y. J. (2004). Regulating a translational regulator: mechanisms cells use to control the activity of the fragile X mental retardation protein. Cell Mol Life Sci *61*, 1714-1728.

Desai, N. S., Casimiro, T. M., Gruber, S. M., and Vanderklish, P. W. (2006). Early postnatal plasticity in neocortex of Fmr1 knockout mice. J Neurophysiol *96*, 1734-1745.

Dityatev, A. E., and Bolshakov, V. Y. (2005). Amygdala, long-term potentiation, and fear conditioning. Neuroscientist *11*, 75-88.

Dolen, G., Osterweil, E., Rao, B. S., Smith, G. B., Auerbach, B. D., Chattarji, S., and Bear, M. F. (2007). Correction of fragile X syndrome in mice. Neuron *56*, 955-962.

Dolzhanskaya, N., Merz, G., Aletta, J. M., and Denman, R. B. (2006). Methylation regulates the intracellular protein-protein and protein-RNA interactions of FMRP. J Cell Sci *119*, 1933-1946.

Dolzhanskaya, N., Sung, Y. J., Conti, J., Currie, J. R., and Denman, R. B. (2003). The fragile X mental retardation protein interacts with U-rich RNAs in a yeast three-hybrid system. Biochem Biophys Res Commun *305*, 434-441.

Durand, G. M., Kovalchuk, Y., and Konnerth, A. (1996). Long-term potentiation and functional synapse induction in developing hippocampus. Nature *381*, 71-75.

Eichler, E. E., Richards, S., Gibbs, R. A., and Nelson, D. L. (1993). Fine structure of the human FMR1 gene. Hum Mol Genet *2*, 1147-1153.

Feng, Y. (2002). Fragile X mental retardation: misregulation of protein synthesis in the developing brain? Microsc Res Tech *57*, 145-147.

Feng, Y., Absher, D., Eberhart, D. E., Brown, V., Malter, H. E., and Warren, S. T. (1997a). FMRP associates with polyribosomes as an mRNP, and the I304N mutation of severe fragile X syndrome abolishes this association. Mol Cell *1*, 109-118.

Feng, Y., Gutekunst, C. A., Eberhart, D. E., Yi, H., Warren, S. T., and Hersch, S. M. (1997b). Fragile X mental retardation protein: nucleocytoplasmic shuttling and association with somatodendritic ribosomes. J Neurosci *17*, 1539-1547.

Ferrari, F., Mercaldo, V., Piccoli, G., Sala, C., Cannata, S., Achsel, T., and Bagni, C. (2007). The fragile X mental retardation protein-RNP granules show an mGluR-dependent localization in the post-synaptic spines. Mol Cell Neurosci *34*, 343-354.

Fiala, J. C., Spacek, J., and Harris, K. M. (2002). Dendritic spine pathology: cause or consequence of neurological disorders? Brain Res Brain Res Rev *39*, 29-54.

Flavell, S. W., Cowan, C. W., Kim, T. K., Greer, P. L., Lin, Y., Paradis, S., Griffith, E. C., Hu, L. S., Chen, C., and Greenberg, M. E. (2006). Activity-dependent regulation of MEF2 transcription factors suppresses excitatory synapse number. Science *311*, 1008-1012.

Friedman, H. V., Bresler, T., Garner, C. C., and Ziv, N. E. (2000). Assembly of new individual excitatory synapses: time course and temporal order of synaptic molecule recruitment. Neuron *27*, 57-69.

Gabel, L. A., Won, S., Kawai, H., McKinney, M., Tartakoff, A. M., and Fallon, J. R. (2004). Visual experience regulates transient expression and dendritic localization of fragile X mental retardation protein. J Neurosci *24*, 10579-10583.

Galvez, R., Gopal, A. R., and Greenough, W. T. (2003). Somatosensory cortical barrel dendritic abnormalities in a mouse model of the fragile X mental retardation syndrome. Brain Res *971*, 83-89.

Galvez, R., and Greenough, W. T. (2005). Sequence of abnormal dendritic spine development in primary somatosensory cortex of a mouse model of the fragile X mental retardation syndrome. Am J Med Genet A *135*, 155-160.

Gao, F. B. (2002). Understanding fragile X syndrome: insights from retarded flies. Neuron *34*, 859-862.

Garber, K., Smith, K. T., Reines, D., and Warren, S. T. (2006). Transcription, translation and fragile X syndrome. Curr Opin Genet Dev *16*, 270-275.

Gibson, T. J., Rice, P. M., Thompson, J. D., and Heringa, J. (1993). KH domains within the FMR1 sequence suggest that fragile X syndrome stems from a defect in RNA metabolism. Trends Biochem Sci *18*, 331-333.

Giuffrida, R., Musumeci, S., D'Antoni, S., Bonaccorso, C. M., Giuffrida-Stella, A. M., Oostra, B. A., and Catania, M. V. (2005). A reduced number of metabotropic glutamate subtype 5 receptors are associated with constitutive homer proteins in a mouse model of fragile X syndrome. J Neurosci *25*, 8908-8916.

Goda, Y., and Davis, G. W. (2003). Mechanisms of synapse assembly and disassembly. Neuron *40*, 243-264.

Gong, X., Tang, X., Wiedmann, M., Wang, X., Peng, J., Zheng, D., Blair, L. A., Marshall, J., and Mao, Z. (2003). Cdk5-mediated inhibition of the protective effects of transcription factor MEF2 in neurotoxicity-induced apoptosis. Neuron *38*, 33-46.

Graybiel, A. M. (1998). The basal ganglia and chunking of action repertoires. Neurobiol Learn Mem *70*, 119-136.

Grossman, A. W., Elisseou, N. M., McKinney, B. C., and Greenough, W. T. (2006). Hippocampal pyramidal cells in adult Fmr1 knockout mice exhibit an immature-appearing profile of dendritic spines. Brain Res *1084*, 158-164.

Grozinger, C. M., and Schreiber, S. L. (2000). Regulation of histone deacetylase 4 and 5 and transcriptional activity by 14-3-3-dependent cellular localization. Proc Natl Acad Sci U S A *97*, 7835-7840.

Gubellini, P., Saulle, E., Centonze, D., Costa, C., Tropepi, D., Bernardi, G., Conquet, F., and Calabresi, P. (2003). Corticostriatal LTP requires combined mGluR1 and mGluR5 activation. Neuropharmacology *44*, 8-16.

Hagerman, R. (2002). The physical and behavioral phenotype. In Fragile X Syndrome: Diagnosis, Treatment, and Research, R. Hagerman, and P. Hagerman, eds. (Baltimore, The Johns Hopkins University Press), pp. 3-109.

Hagerman, R. J., Ono, M. Y., and Hagerman, P. J. (2005). Recent advances in fragile X: a model for autism and neurodegeneration. Curr Opin Psychiatry *18*, 490-496.

Han, T. H., and Prywes, R. (1995). Regulatory role of MEF2D in serum induction of the c-jun promoter. Mol Cell Biol *15*, 2907-2915.

Hanson, J. E., and Madison, D. V. (2007). Presynaptic FMR1 genotype influences the degree of synaptic connectivity in a mosaic mouse model of fragile X syndrome. J Neurosci *27*, 4014-4018.

Hashimoto, K., and Kano, M. (2005). Postnatal development and synapse elimination of climbing fiber to Purkinje cell projection in the cerebellum. Neurosci Res *53*, 221-228.

Hayashi, M. L., Rao, B. S., Seo, J. S., Choi, H. S., Dolan, B. M., Choi, S. Y., Chattarji, S., and Tonegawa, S. (2007). Inhibition of p21-activated kinase rescues symptoms of fragile X syndrome in mice. Proc Natl Acad Sci U S A *104*, 11489-11494.

Hessl, D., Rivera, S. M., and Reiss, A. L. (2004). The neuroanatomy and neuroendocrinology of fragile X syndrome. Ment Retard Dev Disabil Res Rev *10*, 17-24.

Hinton, V. J., Brown, W. T., Wisniewski, K., and Rudelli, R. D. (1991). Analysis of neocortex in three males with the fragile X syndrome. Am J Med Genet *41*, 289-294.

Honeycutt, A., Dunlap, L., Chen, H., al Homsi, G., Grosse, S., and Schendel, D. (2004). Economic costs associated with mental retardation, cerebral palsy, hearing loss, and vision impairment -- United States, 2003. MMWR Morb Mortal Wkly Rep *53*, 57-59.

Hou, L., Antion, M. D., Hu, D., Spencer, C. M., Paylor, R., and Klann, E. (2006). Dynamic translational and proteasomal regulation of fragile X mental retardation protein controls mGluR-dependent long-term depression. Neuron *51*, 441-454.

Huber, K. M., Gallagher, S. M., Warren, S. T., and Bear, M. F. (2002). Altered synaptic plasticity in a mouse model of fragile-X mental retardation. Proc Natl Acad Sci *99*, 7746-7750.

Huber, K. M., Kayser, M. S., and Bear, M. F. (2000). Role for rapid dendritic protein synthesis in hippocampal mGluR-dependent LTD. Science *288*, 1254-1257.

Huber, K. M., Roder, J. C., and Bear, M. F. (2001). Chemical induction of mGluR5- and protein synthesis--dependent long-term depression in hippocampal area CA1. J Neurophysiol *86*, 321-325.

Iacoangeli, A., Rozhdestvensky, T. S., Dolzhanskaya, N., Tournier, B., Schutt, J., Brosius, J., Denman, R. B., Khandjian, E. W., Kindler, S., and Tiedge, H.

(2008). On BC1 RNA and the fragile X mental retardation protein. Proc Natl Acad Sci U S A *105*, 734-739.

Ichise, T., Kano, M., Hashimoto, K., Yanagihara, D., Nakao, K., Shigemoto, R., Katsuki, M., and Aiba, A. (2000). mGluR1 in cerebellar Purkinje cells essential for long-term depression, synapse elimination, and motor coordination. Science *288*, 1832-1835.

Ikeshima, H., Imai, S., Shimoda, K., Hata, J., and Takano, T. (1995). Expression of a MADS box gene, MEF2D, in neurons of the mouse central nervous system: implication of its binary function in myogenic and neurogenic cell lineages. Neurosci Lett *200*, 117-120.

Irwin, S. A., Idupulapati, M., Gilbert, M. E., Harris, J. B., Chakravarti, A. B., Rogers, E. J., Crisostomo, R. A., Larsen, B. P., Mehta, A., Alcantara, C. J., *et al.* (2002). Dendritic spine and dendritic field characteristics of layer V pyramidal neurons in the visual cortex of fragile-X knockout mice. Am J Med Genet *111*, 140-146.

Irwin, S. A., Patel, B., Idupulapati, M., Harris, J. B., Crisostomo, R. A., Larsen, B. P., Kooy, F., Willems, P. J., Cras, P., Kozlowski, P. B., *et al.* (2001). Abnormal dendritic spine characteristics in the temporal and visual cortices of patients with fragile-X syndrome: a quantitative examination. Am J Med Genet *98*, 161-167.

Ishizuka, A., Siomi, M. C., and Siomi, H. (2002). A Drosophila fragile X protein interacts with components of RNAi and ribosomal proteins. Genes Dev *16*, 2497-2508.

Jin, P., Alisch, R. S., and Warren, S. T. (2004a). RNA and microRNAs in fragile X mental retardation. Nat Cell Biol *6*, 1048-1053.

Jin, P., Zarnescu, D. C., Ceman, S., Nakamoto, M., Mowrey, J., Jongens, T. A., Nelson, D. L., Moses, K., and Warren, S. T. (2004b). Biochemical and genetic interaction between the fragile X mental retardation protein and the microRNA pathway. Nat Neurosci *7*, 113-117.

Kanai, Y., Dohmae, N., and Hirokawa, N. (2004). Kinesin transports RNA: isolation and characterization of an RNA-transporting granule. Neuron *43*, 513-525.

Kano, M., Hashimoto, K., Chen, C., Abeliovich, A., Aiba, A., Kurihara, H., Watanabe, M., Inoue, Y., and Tonegawa, S. (1995). Impaired synapse elimination during cerebellar development in PKC gamma mutant mice. Cell *83*, 1223-1231.

Kashiwabuchi, N., Ikeda, K., Araki, K., Hirano, T., Shibuki, K., Takayama, C., Inoue, Y., Kutsuwada, T., Yagi, T., Kang, Y., and et al. (1995). Impairment of motor coordination, Purkinje cell synapse formation, and cerebellar long-term depression in GluR delta 2 mutant mice. Cell *81*, 245-252.

Kato, Y., Kravchenko, V. V., Tapping, R. I., Han, J., Ulevitch, R. J., and Lee, J. D. (1997). BMK1/ERK5 regulates serum-induced early gene expression through transcription factor MEF2C. Embo J *16*, 7054-7066.

Kaufmann, W. E., Cohen, S., Sun, H. T., and Ho, G. (2002). Molecular phenotype of Fragile X syndrome: FMRP, FXRPs, and protein targets. Microsc Res Tech *57*, 135-144.

Kaufmann, W. E., Cortell, R., Kau, A. S., Bukelis, I., Tierney, E., Gray, R. M., Cox, C., Capone, G. T., and Stanard, P. (2004). Autism spectrum disorder in fragile X syndrome: communication, social interaction, and specific behaviors. Am J Med Genet A *129*, 225-234.

Kaufmann, W. E., and Moser, H. W. (2000). Dendritic anomalies in disorders associated with mental retardation. Cereb Cortex *10*, 981-991.

Khandjian, E. W., Corbin, F., Woerly, S., and Rousseau, F. (1996). The fragile X mental retardation protein is associated with ribosomes. Nat Genet *12*, 91-93.

Khandjian, E. W., Huot, M. E., Tremblay, S., Davidovic, L., Mazroui, R., and Bardoni, B. (2004). Biochemical evidence for the association of fragile X mental retardation protein with brain polyribosomal ribonucleoparticles. Proc Natl Acad Sci U S A *101*, 13357-13362.

Kim, D., Jun, K. S., Lee, S. B., Kang, N. G., Min, D. S., Kim, Y. H., Ryu, S. H., Suh, P. G., and Shin, H. S. (1997). Phospholipase C isozymes selectively couple to specific neurotransmitter receptors. Nature *389*, 290-293.

Knott, G. W., Holtmaat, A., Wilbrecht, L., Welker, E., and Svoboda, K. (2006). Spine growth precedes synapse formation in the adult neocortex in vivo. Nat Neurosci *9*, 1117-1124.

Koekkoek, S. K., Yamaguchi, K., Milojkovic, B. A., Dortland, B. R., Ruigrok, T. J., Maex, R., De Graaf, W., Smit, A. E., VanderWerf, F., Bakker, C. E., *et al.* (2005). Deletion of FMR1 in Purkinje cells enhances parallel fiber LTD, enlarges spines, and attenuates cerebellar eyelid conditioning in Fragile X syndrome. Neuron *47*, 339-352.

Kraszewski, K., Mundigl, O., Daniell, L., Verderio, C., Matteoli, M., and De Camilli, P. (1995). Synaptic vesicle dynamics in living cultured hippocampal neurons visualized with CY3-conjugated antibodies directed against the lumenal domain of synaptotagmin. J Neurosci *15*, 4328-4342.

Laggerbauer, B., Ostareck, D., Keidel, E., Ostareck-Lederer, A., and Fischer, U. (2001). Evidence that fragile X mental retardation protein is a negative regulator of translation. Hum Mol Genet *10*, 329-338.

Lam, B. Y., and Chawla, S. (2007). MEF2D expression increases during neuronal differentiation of neural progenitor cells and correlates with neurite length. Neurosci Lett *427*, 153-158.

Larson, J., Jessen, R. E., Kim, D., Fine, A. K., and du Hoffmann, J. (2005). Age-dependent and selective impairment of long-term potentiation in the anterior piriform cortex of mice lacking the fragile X mental retardation protein. J Neurosci *25*, 9460-9469.

Larson, S. A., Lakin, K. C., Anderson, L., Kwak, N., Lee, J. H., and Anderson, D. (2001). Prevalence of mental retardation and developmental disabilities: estimates from the 1994/1995 National Health Interview Survey Disability Supplements. Am J Ment Retard *106*, 231-252.

Lauterborn, J. C., Rex, C. S., Kramar, E., Chen, L. Y., Pandyarajan, V., Lynch, G., and Gall, C. M. (2007). Brain-derived neurotrophic factor rescues synaptic plasticity in a mouse model of fragile X syndrome. J Neurosci *27*, 10685-10694.

Lee, A., Li, W., Xu, K., Bogert, B. A., Su, K., and Gao, F. B. (2003). Control of dendritic development by the Drosophila fragile X-related gene involves the small GTPase Rac1. Development *130*, 5543-5552.

Lee, A. C., Wong, R. K., Chuang, S. C., Shin, H. S., and Bianchi, R. (2002). Role of synaptic metabotropic glutamate receptors in epileptiform discharges in hippocampal slices. J Neurophysiol *88*, 1625-1633.

Leifer, D., Krainc, D., Yu, Y. T., McDermott, J., Breitbart, R. E., Heng, J., Neve, R. L., Kosofsky, B., Nadal-Ginard, B., and Lipton, S. A. (1993). MEF2C, a MADS/MEF2-family transcription factor expressed in a laminar distribution in cerebral cortex. Proc Natl Acad Sci U S A *90*, 1546-1550.

Li, H., Radford, J. C., Ragusa, M. J., Shea, K. L., McKercher, S. R., Zaremba, J. D., Soussou, W., Nie, Z., Kang, Y. J., Nakanishi, N., *et al.* (2008). Transcription factor MEF2C influences neural stem/progenitor cell differentiation and maturation in vivo. Proc Natl Acad Sci U S A *105*, 9397-9402.

Li, J., Pelletier, M. R., Perez Velazquez, J. L., and Carlen, P. L. (2002). Reduced cortical synaptic plasticity and GluR1 expression associated with fragile X mental retardation protein deficiency. Mol Cell Neurosci *19*, 138-151.

Li, Z., Zhang, Y., Ku, L., Wilkinson, K. D., Warren, S. T., and Feng, Y. (2001). The fragile X mental retardation protein inhibits translation via interacting with mRNA. Nucleic Acids Res *29*, 2276-2283.

Liao, D., Hessler, N. A., and Malinow, R. (1995). Activation of postsynaptically silent synapses during pairing-induced LTP in CA1 region of hippocampal slice. Nature *375*, 400-404.

Lin, W., Burgess, R. W., Dominguez, B., Pfaff, S. L., Sanes, J. R., and Lee, K. F. (2001). Distinct roles of nerve and muscle in postsynaptic differentiation of the neuromuscular synapse. Nature *410*, 1057-1064.

Lin, X., Shah, S., and Bulleit, R. F. (1996). The expression of MEF2 genes is implicated in CNS neuronal differentiation. Brain Res Mol Brain Res *42*, 307-316.

Loesch, D. Z., Huggins, R. M., Bui, Q. M., Epstein, J. L., Taylor, A. K., and Hagerman, R. J. (2002). Effect of the deficits of fragile X mental retardation protein on cognitive status of fragile x males and females assessed by robust pedigree analysis. J Dev Behav Pediatr *23*, 416-423.

Loesch, D. Z., Huggins, R. M., Bui, Q. M., Taylor, A. K., and Hagerman, R. J. (2003). Relationship of deficits of FMR1 gene specific protein with physical phenotype of fragile X males and females in pedigrees: a new perspective. Am J Med Genet A *118A*, 127-134.

Loesch, D. Z., Huggins, R. M., and Hagerman, R. J. (2004). Phenotypic variation and FMRP levels in fragile X. Ment Retard Dev Disabil Res Rev *10*, 31-41.

Lu, J., McKinsey, T. A., Zhang, C. L., and Olson, E. N. (2000). Regulation of skeletal myogenesis by association of the MEF2 transcription factor with class II histone deacetylases. Mol Cell *6*, 233-244.

Lu, R., Wang, H., Liang, Z., Ku, L., O'Donnell W, T., Li, W., Warren, S. T., and Feng, Y. (2004). The fragile X protein controls microtubule-associated protein 1B translation and microtubule stability in brain neuron development. Proc Natl Acad Sci U S A *101*, 15201-15206.

Lugenbeel, K. A., Peier, A. M., Carson, N. L., Chudley, A. E., and Nelson, D. L. (1995). Intragenic loss of function mutations demonstrate the primary role of FMR1 in fragile X syndrome. Nat Genet *10*, 483-485.

Lukong, K. E., and Richard, S. (2004). Arginine methylation signals mRNA export. Nat Struct Mol Biol *11*, 914-915.

Lyons, G. E., Micales, B. K., Schwarz, J., Martin, J. F., and Olson, E. N. (1995). Expression of mef2 genes in the mouse central nervous system suggests a role in neuronal maturation. J Neurosci *15*, 5727-5738.

Mao, Z., Bonni, A., Xia, F., Nadal-Vicens, M., and Greenberg, M. E. (1999). Neuronal activity-dependent cell survival mediated by transcription factor MEF2. Science *286*, 785-790.

Mao, Z., and Wiedmann, M. (1999). Calcineurin enhances MEF2 DNA binding activity in calcium-dependent survival of cerebellar granule neurons. J Biol Chem *274*, 31102-31107.

Marin-Padilla, M. (1972). Structural abnormalities of the cerebral cortex in human chromosomal aberrations: a Golgi study. Brain Res *44*, 625-629.

Martin, J. F., Miano, J. M., Hustad, C. M., Copeland, N. G., Jenkins, N. A., and Olson, E. N. (1994). A Mef2 gene that generates a muscle-specific isoform via alternative mRNA splicing. Mol Cell Biol *14*, 1647-1656.

Mazroui, R., Huot, M. E., Tremblay, S., Filion, C., Labelle, Y., and Khandjian, E. W. (2002). Trapping of messenger RNA by Fragile X Mental Retardation protein into cytoplasmic granules induces translation repression. Hum Mol Genet *11*, 3007-3017.

McBride, S. M., Choi, C. H., Wang, Y., Liebelt, D., Braunstein, E., Ferreiro, D., Sehgal, A., Siwicki, K. K., Dockendorff, T. C., Nguyen, H. T., *et al.* (2005). Pharmacological rescue of synaptic plasticity, courtship behavior, and mushroom body defects in a Drosophila model of fragile X syndrome. Neuron *45*, 753-764.

McGee, A. W., and Bredt, D. S. (2003). Assembly and plasticity of the glutamatergic postsynaptic specialization. Curr Opin Neurobiol *13*, 111-118.

McKinney, B. C., Grossman, A. W., Elisseou, N. M., and Greenough, W. T. (2005). Dendritic spine abnormalities in the occipital cortex of C57BL/6 Fmr1 knockout mice. Am J Med Genet B Neuropsychiatr Genet *136B*, 98-102.

McKinsey, T. A., Zhang, C. L., Lu, J., and Olson, E. N. (2000). Signal-dependent nuclear export of a histone deacetylase regulates muscle differentiation. Nature *408*, 106-111.

McKinsey, T. A., Zhang, C. L., and Olson, E. N. (2001). Control of muscle development by dueling HATs and HDACs. Curr Opin Genet Dev *11*, 497-504.

McKinsey, T. A., Zhang, C. L., and Olson, E. N. (2002). MEF2: a calcium-dependent regulator of cell division, differentiation and death. Trends Biochem Sci *27*, 40-47.

Meredith, R. M., Holmgren, C. D., Weidum, M., Burnashev, N., and Mansvelder, H. D. (2007). Increased threshold for spike-timing-dependent plasticity is caused by unreliable calcium signaling in mice lacking fragile X gene FMR1. Neuron *54*, 627-638.

Merlin, L. R., Bergold, P. J., and Wong, R. K. (1998). Requirement of protein synthesis for group I mGluR-mediated induction of epileptiform discharges. J Neurophysiol *80*, 989-993.

Michel, C. I., Kraft, R., and Restifo, L. L. (2004). Defective neuronal development in the mushroom bodies of Drosophila fragile X mental retardation 1 mutants. J Neurosci *24*, 5798-5809.

Mientjes, E. J., Willemsen, R., Kirkpatrick, L. L., Nieuwenhuizen, I. M., Hoogeveen-Westerveld, M., Verweij, M., Reis, S., Bardoni, B., Hoogeveen, A. T., Oostra, B. A., and Nelson, D. L. (2004). Fxr1 knockout mice show a striated muscle phenotype: implications for Fxr1p function in vivo. Hum Mol Genet *13*, 1291-1302.

Miska, E. A., Langley, E., Wolf, D., Karlsson, C., Pines, J., and Kouzarides, T. (2001). Differential localization of HDAC4 orchestrates muscle differentiation. Nucleic Acids Res *29*, 3439-3447.

Miyashiro, K. Y., Beckel-Mitchener, A., Purk, T. P., Becker, K. G., Barret, T., Liu, L., Carbonetto, S., Weiler, I. J., Greenough, W. T., and Eberwine, J. (2003). RNA cargoes associating with FMRP reveal deficits in cellular functioning in Fmr1 null mice. Neuron *37*, 417-431.

Molkentin, J. D., and Olson, E. N. (1996). Combinatorial control of muscle development by basic helix-loop-helix and MADS-box transcription factors. Proc Natl Acad Sci U S A *93*, 9366-9373.

Morales, J., Hiesinger, P. R., Schroeder, A. J., Kume, K., Verstreken, P., Jackson, F. R., Nelson, D. L., and Hassan, B. A. (2002). Drosophila fragile X protein, DFXR, regulates neuronal morphology and function in the brain. Neuron *34*, 961-972.

Morrow, E. M., Yoo, S. Y., Flavell, S. W., Kim, T. K., Lin, Y., Hill, R. S., Mukaddes, N. M., Balkhy, S., Gascon, G., Hashmi, A., *et al.* (2008). Identifying autism loci and genes by tracing recent shared ancestry. Science *321*, 218-223.

Muddashetty, R. S., Kelic, S., Gross, C., Xu, M., and Bassell, G. J. (2007). Dysregulated metabotropic glutamate receptor-dependent translation of AMPA receptor and postsynaptic density-95 mRNAs at synapses in a mouse model of fragile X syndrome. J Neurosci *27*, 5338-5348.

Musumeci, S. A., Bosco, P., Calabrese, G., Bakker, C., De Sarro, G. B., Elia, M., Ferri, R., and Oostra, B. A. (2000). Audiogenic seizures susceptibility in transgenic mice with fragile X syndrome. Epilepsia *41*, 19-23.

Musumeci, S. A., Hagerman, R. J., Ferri, R., Bosco, P., Dalla Bernardina, B., Tassinari, C. A., De Sarro, G. B., and Elia, M. (1999). Epilepsy and EEG findings in males with fragile X syndrome. Epilepsia *40*, 1092-1099.

Nagerl, U. V., Kostinger, G., Anderson, J. C., Martin, K. A., and Bonhoeffer, T. (2007). Protracted synaptogenesis after activity-dependent spinogenesis in hippocampal neurons. J Neurosci *27*, 8149-8156.

Narayanan, U., Nalavadi, V., Nakamoto, M., Pallas, D. C., Ceman, S., Bassell, G. J., and Warren, S. T. (2007). FMRP phosphorylation reveals an immediate-early signaling pathway triggered by group I mGluR and mediated by PP2A. J Neurosci *27*, 14349-14357.

Narayanan, U., Nalavadi, V., Nakamoto, M., Thomas, G., Ceman, S., Bassell, G. J., and Warren, S. T. (2008). S6K1 phosphorylates and regulates fragile X mental retardation protein (FMRP) with the neuronal protein synthesis-dependent mammalian target of rapamycin (mTOR) signaling cascade. J Biol Chem *283*, 18478-18482.

Nguyen, Q. T., Son, Y. J., Sanes, J. R., and Lichtman, J. W. (2000). Nerve terminals form but fail to mature when postsynaptic differentiation is blocked: in vivo analysis using mammalian nerve-muscle chimeras. J Neurosci *20*, 6077-6086.

Nimchinsky, E. A., Oberlander, A. M., and Svoboda, K. (2001). Abnormal development of dendritic spines in FMR1 knock-out mice. J Neurosci *21*, 5139-5146.

Nosyreva, E. D., and Huber, K. M. (2005). Developmental switch in synaptic mechanisms of hippocampal metabotropic glutamate receptor-dependent long-term depression. J Neurosci *25*, 2992-3001.

Nosyreva, E. D., and Huber, K. M. (2006). Metabotropic receptor-dependent long-term depression persists in the absence of protein synthesis in the mouse model of fragile x syndrome. J Neurophysiol *95*, 3291-3295.

O'Donnell, W. T., and Warren, S. T. (2002). A decade of molecular studies of fragile X syndrome. Annu Rev Neurosci *25*, 315-338.

Offermanns, S., Hashimoto, K., Watanabe, M., Sun, W., Kurihara, H., Thompson, R. F., Inoue, Y., Kano, M., and Simon, M. I. (1997). Impaired motor coordination and persistent multiple climbing fiber innervation of cerebellar Purkinje cells in mice lacking Galphaq. Proc Natl Acad Sci U S A *94*, 14089-14094.

Okamoto, S., Krainc, D., Sherman, K., and Lipton, S. A. (2000). Antiapoptotic role of the p38 mitogen-activated protein kinase-myocyte enhancer factor 2 transcription factor pathway during neuronal differentiation. Proc Natl Acad Sci U S A *97*, 7561-7566.

Pan, L., Zhang, Y. Q., Woodruff, E., and Broadie, K. (2004). The Drosophila fragile X gene negatively regulates neuronal elaboration and synaptic differentiation. Curr Biol *14*, 1863-1870.

Paradee, W., Melikian, H. E., Rasmussen, D. L., Kenneson, A., Conn, P. J., and Warren, S. T. (1999). Fragile X mouse: strain effects of knockout phenotype and evidence suggesting deficient amygdala function. Neuroscience *94*, 185-192.

Passier, R., Zeng, H., Frey, N., Naya, F. J., Nicol, R. L., McKinsey, T. A., Overbeek, P., Richardson, J. A., Grant, S. R., and Olson, E. N. (2000). CaM kinase signaling induces cardiac hypertrophy and activates the MEF2 transcription factor in vivo. J Clin Invest *105*, 1395-1406.

Persico, A. M., and Bourgeron, T. (2006). Searching for ways out of the autism maze: genetic, epigenetic and environmental clues. Trends Neurosci *29*, 349-358.

Petralia, R. S., Esteban, J. A., Wang, Y. X., Partridge, J. G., Zhao, H. M., Wenthold, R. J., and Malinow, R. (1999). Selective acquisition of AMPA

receptors over postnatal development suggests a molecular basis for silent synapses. Nat Neurosci *2*, 31-36.

Pfeiffer, B. E., and Huber, K. M. (2006). Current advances in local protein synthesis and synaptic plasticity. J Neurosci *26*, 7147-7150.

Pfeiffer, B. E., and Huber, K. M. (2007). Fragile X mental retardation protein induces synapse loss through acute postsynaptic translational regulation. J Neurosci *27*, 3120-3130.

Pickett, J., and London, E. (2005). The neuropathology of autism: a review. J Neuropathol Exp Neurol *64*, 925-935.

Potthoff, M. J., and Olson, E. N. (2007). MEF2: a central regulator of diverse developmental programs. Development *134*, 4131-4140.

Price, T. J., Flores, C. M., Cervero, F., and Hargreaves, K. M. (2006). The RNA binding and transport proteins staufen and fragile X mental retardation protein are expressed by rat primary afferent neurons and localize to peripheral and central axons. Neuroscience *141*, 2107-2116.

Purpura, D. P. (1975). Dendritic differentiation in human cerebral cortex: normal and aberrant developmental patterns. Adv Neurol *12*, 91-134.

Qin, M., Kang, J., Burlin, T. V., Jiang, C., and Smith, C. B. (2005). Postadolescent changes in regional cerebral protein synthesis: an in vivo study in the FMR1 null mouse. J Neurosci *25*, 5087-5095.

Restivo, L., Ferrari, F., Passino, E., Sgobio, C., Bock, J., Oostra, B. A., Bagni, C., and Ammassari-Teule, M. (2005). Enriched environment promotes behavioral and morphological recovery in a mouse model for the fragile X syndrome. Proc Natl Acad Sci U S A *102*, 11557-11562.

Rodrigues, S. M., Bauer, E. P., Farb, C. R., Schafe, G. E., and LeDoux, J. E. (2002). The group I metabotropic glutamate receptor mGluR5 is required for fear memory formation and long-term potentiation in the lateral amygdala. J Neurosci *22*, 5219-5229.

Rodrigues, S. M., Schafe, G. E., and LeDoux, J. E. (2004). Molecular mechanisms underlying emotional learning and memory in the lateral amygdala. Neuron *44*, 75-91.

Ronesi, J. A., and Huber, K. M. (2008a). Homer interactions are necessary for metabotropic glutamate receptor-induced long-term depression and translational activation. J Neurosci *28*, 543-547.

Ronesi, J. A., and Huber, K. M. (2008b). Metabotropic glutamate receptors and fragile x mental retardation protein: partners in translational regulation at the synapse. Sci Signal *1*, pe6.

Rozhdestvensky, T. S., Kopylov, A. M., Brosius, J., and Huttenhofer, A. (2001). Neuronal BC1 RNA structure: evolutionary conversion of a tRNA(Ala) domain into an extended stem-loop structure. Rna *7*, 722-730.

Sabaratnam, M., Vroegop, P. G., and Gangadharan, S. K. (2001). Epilepsy and EEG findings in 18 males with fragile X syndrome. Seizure *10*, 60-63.

Sanes, J. R., and Lichtman, J. W. (1999). Development of the vertebrate neuromuscular junction. Annu Rev Neurosci *22*, 389-442.

Sara, Y., Biederer, T., Atasoy, D., Chubykin, A., Mozhayeva, M. G., Sudhof, T. C., and Kavalali, E. T. (2005). Selective capability of SynCAM and neuroligin for functional synapse assembly. J Neurosci *25*, 260-270.

Schaeffer, C., Bardoni, B., Mandel, J. L., Ehresmann, B., Ehresmann, C., and Moine, H. (2001). The fragile X mental retardation protein binds specifically to its mRNA via a purine quartet motif. Embo J *20*, 4803-4813.

Scheiffele, P., Fan, J., Choih, J., Fetter, R., and Serafini, T. (2000). Neuroligin expressed in nonneuronal cells triggers presynaptic development in contacting axons. Cell *101*, 657-669.

Selby, L., Zhang, C., and Sun, Q. Q. (2007). Major defects in neocortical GABAergic inhibitory circuits in mice lacking the fragile X mental retardation protein. Neurosci Lett *412*, 227-232.

Shalizi, A., Gaudilliere, B., Yuan, Z., Stegmuller, J., Shirogane, T., Ge, Q., Tan, Y., Schulman, B., Harper, J. W., and Bonni, A. (2006). A calcium-regulated MEF2 sumoylation switch controls postsynaptic differentiation. Science *311*, 1012-1017.

Shinoda, Y., Kamikubo, Y., Egashira, Y., Tominaga-Yoshino, K., and Ogura, A. (2005). Repetition of mGluR-dependent LTD causes slowly developing persistent reduction in synaptic strength accompanied by synapse elimination. Brain Res *1042*, 99-107.

Siomi, H., Siomi, M. C., Nussbaum, R. L., and Dreyfuss, G. (1993). The protein product of the fragile X gene, FMR1, has characteristics of an RNA-binding protein. Cell *74*, 291-298.

Siomi, M. C., Higashijima, K., Ishizuka, A., and Siomi, H. (2002). Casein kinase II phosphorylates the fragile X mental retardation protein and modulates its biological properties. Mol Cell Biol *22*, 8438-8447.

Siomi, M. C., Zhang, Y., Siomi, H., and Dreyfuss, G. (1996). Specific sequences in the fragile X syndrome protein FMR1 and the FXR proteins mediate their binding to 60S ribosomal subunits and the interactions among them. Mol Cell Biol *16*, 3825-3832.

Sourdet, V., Russier, M., Daoudal, G., Ankri, N., and Debanne, D. (2003). Long-term enhancement of neuronal excitability and temporal fidelity mediated by metabotropic glutamate receptor subtype 5. J Neurosci *23*, 10238-10248.

Spencer, C. M., Alekseyenko, O., Serysheva, E., Yuva-Paylor, L. A., and Paylor, R. (2005). Altered anxiety-related and social behaviors in the Fmr1

knockout mouse model of fragile X syndrome. Genes Brain Behav *4*, 420-430.

Spencer, C. M., Graham, D. F., Yuva-Paylor, L. A., Nelson, D. L., and Paylor, R. (2008). Social behavior in Fmr1 knockout mice carrying a human FMR1 transgene. Behav Neurosci *122*, 710-715.

Spencer, C. M., Serysheva, E., Yuva-Paylor, L. A., Oostra, B. A., Nelson, D. L., and Paylor, R. (2006). Exaggerated behavioral phenotypes in Fmr1/Fxr2 double knockout mice reveal a functional genetic interaction between Fragile X-related proteins. Hum Mol Genet *15*, 1984-1994.

Stefani, G., Fraser, C. E., Darnell, J. C., and Darnell, R. B. (2004). Fragile X mental retardation protein is associated with translating polyribosomes in neuronal cells. J Neurosci *24*, 7272-7276.

Stetler, A., Winograd, C., Sayegh, J., Cheever, A., Patton, E., Zhang, X., Clarke, S., and Ceman, S. (2006). Identification and characterization of the methyl arginines in the fragile X mental retardation protein Fmrp. Hum Mol Genet *15*, 87-96.

Steward, O., Bakker, C. E., Willems, P. J., and Oostra, B. A. (1998). No evidence for disruption of normal patterns of mRNA localization in dendrites or dendritic transport of recently synthesized mRNA in FMR1 knockout mice, a model for human fragile-X mental retardation syndrome. Neuroreport *9*, 477-481.

Steward, O., and Levy, W. B. (1982). Preferential localization of polyribosomes under the base of dendritic spines in granule cells of the dentate gyrus. J Neurosci *2*, 284-291.

Stoppini, L., Buchs, P. A., and Muller, D. (1991). A simple method for organotypic cultures of nervous tissue. J Neurosci Methods *37*, 173-182.

Strahl, B. D., and Allis, C. D. (2000). The language of covalent histone modifications. Nature *403*, 41-45.

Sung, Y. J., Conti, J., Currie, J. R., Brown, W. T., and Denman, R. B. (2000). RNAs that interact with the fragile X syndrome RNA binding protein FMRP. Biochem Biophys Res Commun *275*, 973-980.

Sung, Y. J., Dolzhanskaya, N., Nolin, S. L., Brown, T., Currie, J. R., and Denman, R. B. (2003). The fragile X mental retardation protein FMRP binds elongation factor 1A mRNA and negatively regulates its translation in vivo. J Biol Chem *278*, 15669-15678.

Swanson, C. J., Bures, M., Johnson, M. P., Linden, A. M., Monn, J. A., and Schoepp, D. D. (2005). Metabotropic glutamate receptors as novel targets for anxiety and stress disorders. Nat Rev Drug Discov *4*, 131-144.

Tamanini, F., Bontekoe, C., Bakker, C. E., van Unen, L., Anar, B., Willemsen, R., Yoshida, M., Galjaard, H., Oostra, B. A., and Hoogeveen, A. T. (1999a).

Different targets for the fragile X-related proteins revealed by their distinct nuclear localizations. Hum Mol Genet *8*, 863-869.

Tamanini, F., Meijer, N., Verheij, C., Willems, P. J., Galjaard, H., Oostra, B. A., and Hoogeveen, A. T. (1996). FMRP is associated to the ribosomes via RNA. Hum Mol Genet *5*, 809-813.

Tamanini, F., Van Unen, L., Bakker, C., Sacchi, N., Galjaard, H., Oostra, B. A., and Hoogeveen, A. T. (1999b). Oligomerization properties of fragile-X mental-retardation protein (FMRP) and the fragile-X-related proteins FXR1P and FXR2P. Biochem J *343 Pt 3*, 517-523.

Tang, X., Wang, X., Gong, X., Tong, M., Park, D., Xia, Z., and Mao, Z. (2005). Cyclin-dependent kinase 5 mediates neurotoxin-induced degradation of the transcription factor myocyte enhancer factor 2. J Neurosci *25*, 4823-4834.

Tassone, F., Hagerman, R. J., Ikle, D. N., Dyer, P. N., Lampe, M., Willemsen, R., Oostra, B. A., and Taylor, A. K. (1999). FMRP expression as a potential prognostic indicator in fragile X syndrome. Am J Med Genet *84*, 250-261.

Tatarczynska, E., Klodzinska, A., Chojnacka-Wojcik, E., Palucha, A., Gasparini, F., Kuhn, R., and Pilc, A. (2001). Potential anxiolytic- and antidepressant-like effects of MPEP, a potent, selective and systemically active mGlu5 receptor antagonist. Br J Pharmacol *132*, 1423-1430.

Taylor, G. W., Merlin, L. R., and Wong, R. K. (1995). Synchronized oscillations in hippocampal CA3 neurons induced by metabotropic glutamate receptor activation. J Neurosci *15*, 8039-8052.

Todd, P. K., and Mack, K. J. (2000). Sensory stimulation increases cortical expression of the fragile X mental retardation protein in vivo. Brain Res Mol Brain Res *80*, 17-25.

Todd, P. K., Mack, K. J., and Malter, J. S. (2003a). The fragile X mental retardation protein is required for type-I metabotropic glutamate receptor-dependent translation of PSD-95. Proc Natl Acad Sci U S A *100*, 14374-14378.

Todd, P. K., Malter, J. S., and Mack, K. J. (2003b). Whisker stimulation-dependent translation of FMRP in the barrel cortex requires activation of type I metabotropic glutamate receptors. Brain Res Mol Brain Res *110*, 267-278.

Tucker, B., Richards, R. I., and Lardelli, M. (2006). Contribution of mGluR and Fmr1 functional pathways to neurite morphogenesis, craniofacial development and fragile X syndrome. Hum Mol Genet *15*, 3446-3458.

Turner, G., Webb, T., Wake, S., and Robinson, H. (1996). Prevalence of fragile X syndrome. Am J Med Genet *64*, 196-197.

Vasudevan, S., Tong, Y., and Steitz, J. A. (2007). Switching from repression to activation: microRNAs can up-regulate translation. Science *318*, 1931-1934.

Verkerk, A. J., de Graaff, E., De Boulle, K., Eichler, E. E., Konecki, D. S., Reyniers, E., Manca, A., Poustka, A., Willems, P. J., Nelson, D. L., and et al. (1993). Alternative splicing in the fragile X gene FMR1. Hum Mol Genet *2*, 399-404.

Verkerk, A. J., Pieretti, M., Sutcliffe, J. S., Fu, Y. H., Kuhl, D. P., Pizzuti, A., Reiner, O., Richards, S., Victoria, M. F., Zhang, F. P., and et al. (1991). Identification of a gene (FMR-1) containing a CGG repeat coincident with a breakpoint cluster region exhibiting length variation in fragile X syndrome. Cell *65*, 905-914.

Volk, L. J., Pfeiffer, B. E., Gibson, J. R., and Huber, K. M. (2007). Multiple Gq-coupled receptors converge on a common protein synthesis-dependent long-term depression that is affected in fragile X syndrome mental retardation. J Neurosci *27*, 11624-11634.

Walsh, M. K., and Lichtman, J. W. (2003). In vivo time-lapse imaging of synaptic takeover associated with naturally occurring synapse elimination. Neuron *37*, 67-73.

Wang, H., Dictenberg, J. B., Ku, L., Li, W., Bassell, G. J., and Feng, Y. (2008). Dynamic Association of the Fragile X Mental Retardation Protein as a Messenger Ribonucleoprotein between Microtubules and Polyribosomes. Mol Biol Cell *19*, 105-114.

Wang, H., Iacoangeli, A., Lin, D., Williams, K., Denman, R. B., Hellen, C. U., and Tiedge, H. (2005a). Dendritic BC1 RNA in translational control mechanisms. J Cell Biol *171*, 811-821.

Wang, H., Iacoangeli, A., Popp, S., Muslimov, I. A., Imataka, H., Sonenberg, N., Lomakin, I. B., and Tiedge, H. (2002). Dendritic BC1 RNA: functional role in regulation of translation initiation. J Neurosci *22*, 10232-10241.

Wang, H., Ku, L., Osterhout, D. J., Li, W., Ahmadian, A., Liang, Z., and Feng, Y. (2004). Developmentally-programmed FMRP expression in oligodendrocytes: a potential role of FMRP in regulating translation in oligodendroglia progenitors. Hum Mol Genet *13*, 79-89.

Wang, X., Tang, X., Li, M., Marshall, J., and Mao, Z. (2005b). Regulation of neuroprotective activity of myocyte-enhancer factor 2 by cAMP-protein kinase A signaling pathway in neuronal survival. J Biol Chem *280*, 16705-16713.

Wang, X. F., and Daw, N. W. (2003). Long term potentiation varies with layer in rat visual cortex. Brain Res *989*, 26-34.

Weiler, I., Spangler, C., Klintsova, A., Grossman, A., SH, K., Bertaina-Anglade, V., Khaliq, H., de Vries, F., Lambers, F., Hatia, F., *et al.* (2004). Fragile X

mental retardation protein is necessary for neurotransmitter-activated protein translation at synapses. Proc Natl Acad Sci U S A *Early Edition*.

Weiler, I. J., Irwin, S. A., Klintsova, A. Y., Spencer, C. M., Brazelton, A. D., Miyashiro, K., Comery, T. A., Patel, B., Eberwine, J., and Greenough, W. T. (1997). Fragile X mental retardation protein is translated near synapses in response to neurotransmitter activation. Proc Natl Acad Sci U S A *94*, 5395-5400.

Wiedmann, M., Wang, X., Tang, X., Han, M., Li, M., and Mao, Z. (2005). PI3K/Akt-dependent regulation of the transcription factor myocyte enhancer factor-2 in insulin-like growth factor-1- and membrane depolarization-mediated survival of cerebellar granule neurons. J Neurosci Res *81*, 226-234.

Wilson, B. M., and Cox, C. L. (2007). Absence of metabotropic glutamate receptor-mediated plasticity in the neocortex of fragile X mice. Proc Natl Acad Sci U S A *104*, 2454-2459.

Wirth, M. J., and Wahle, P. (2003). Biolistic transfection of organotypic cultures of rat visual cortex using a handheld device. J Neurosci Methods *125*, 45-54.

Woronicz, J. D., Lina, A., Calnan, B. J., Szychowski, S., Cheng, L., and Winoto, A. (1995). Regulation of the Nur77 orphan steroid receptor in activation-induced apoptosis. Mol Cell Biol *15*, 6364-6376.

Wu, G., Malinow, R., and Cline, H. T. (1996). Maturation of a central glutamatergic synapse. Science *274*, 972-976.

Wu, H., Naya, F. J., McKinsey, T. A., Mercer, B., Shelton, J. M., Chin, E. R., Simard, A. R., Michel, R. N., Bassel-Duby, R., Olson, E. N., and Williams, R. S. (2000). MEF2 responds to multiple calcium-regulated signals in the control of skeletal muscle fiber type. Embo J *19*, 1963-1973.

Yan, Q. J., Asafo-Adjei, P. K., Arnold, H. M., Brown, R. E., and Bauchwitz, R. P. (2004). A phenotypic and molecular characterization of the fmr1-tm1Cgr fragile X mouse. Genes Brain Behav *3*, 337-359.

Yan, Q. J., Rammal, M., Tranfaglia, M., and Bauchwitz, R. P. (2005). Suppression of two major Fragile X Syndrome mouse model phenotypes by the mGluR5 antagonist MPEP. Neuropharmacology *49*, 1053-1066.

Yang, C. C., Ornatsky, O. I., McDermott, J. C., Cruz, T. F., and Prody, C. A. (1998). Interaction of myocyte enhancer factor 2 (MEF2) with a mitogen-activated protein kinase, ERK5/BMK1. Nucleic Acids Res *26*, 4771-4777.

Youn, H. D., Chatila, T. A., and Liu, J. O. (2000). Integration of calcineurin and MEF2 signals by the coactivator p300 during T-cell apoptosis. Embo J *19*, 4323-4331.

Zalfa, F., Adinolfi, S., Napoli, I., Kuhn-Holsken, E., Urlaub, H., Achsel, T., Pastore, A., and Bagni, C. (2005). Fragile X mental retardation protein

(FMRP) binds specifically to the brain cytoplasmic RNAs BC1/BC200 via a novel RNA-binding motif. J Biol Chem *280*, 33403-33410.

Zalfa, F., Eleuteri, B., Dickson, K. S., Mercaldo, V., De Rubeis, S., di Penta, A., Tabolacci, E., Chiurazzi, P., Neri, G., Grant, S. G., and Bagni, C. (2007). A new function for the fragile X mental retardation protein in regulation of PSD-95 mRNA stability. Nat Neurosci *10*, 578-587.

Zalfa, F., Giorgi, M., Primerano, B., Moro, A., Di Penta, A., Reis, S., Oostra, B., and Bagni, C. (2003). The fragile X syndrome protein FMRP associates with BC1 RNA and regulates the translation of specific mRNAs at synapses. Cell *112*, 317-327.

Zarnescu, D. C., Shan, G., Warren, S. T., and Jin, P. (2005). Come FLY with us: toward understanding fragile X syndrome. Genes Brain Behav *4*, 385-392.

Zhang, W., and Linden, D. J. (2003). The other side of the engram: experience-driven changes in neuronal intrinsic excitability. Nat Rev Neurosci *4*, 885-900.

Zhang, Y. Q., Bailey, A. M., Matthies, H. J., Renden, R. B., Smith, M. A., Speese, S. D., Rubin, G. M., and Broadie, K. (2001). Drosophila fragile X-related gene regulates the MAP1B homolog Futsch to control synaptic structure and function. Cell *107*, 591-603.

Zhao, J. (2007). Sumoylation regulates diverse biological processes. Cell Mol Life Sci *64*, 3017-3033.

Zhao, M. G., Toyoda, H., Ko, S. W., Ding, H. K., Wu, L. J., and Zhuo, M. (2005). Deficits in trace fear memory and long-term potentiation in a mouse model for fragile X syndrome. J Neurosci *25*, 7385-7392.

Zhu, B., Ramachandran, B., and Gulick, T. (2005). Alternative pre-mRNA splicing governs expression of a conserved acidic transactivation domain in myocyte enhancer factor 2 factors of striated muscle and brain. J Biol Chem *280*, 28749-28760.

Ziv, N. E., and Garner, C. C. (2004). Cellular and molecular mechanisms of presynaptic assembly. Nat Rev Neurosci *5*, 385-399.